

EPA

U.S. Environmental Protection Agency
Office of Research and Development

Industrial Environmental Research
Laboratory

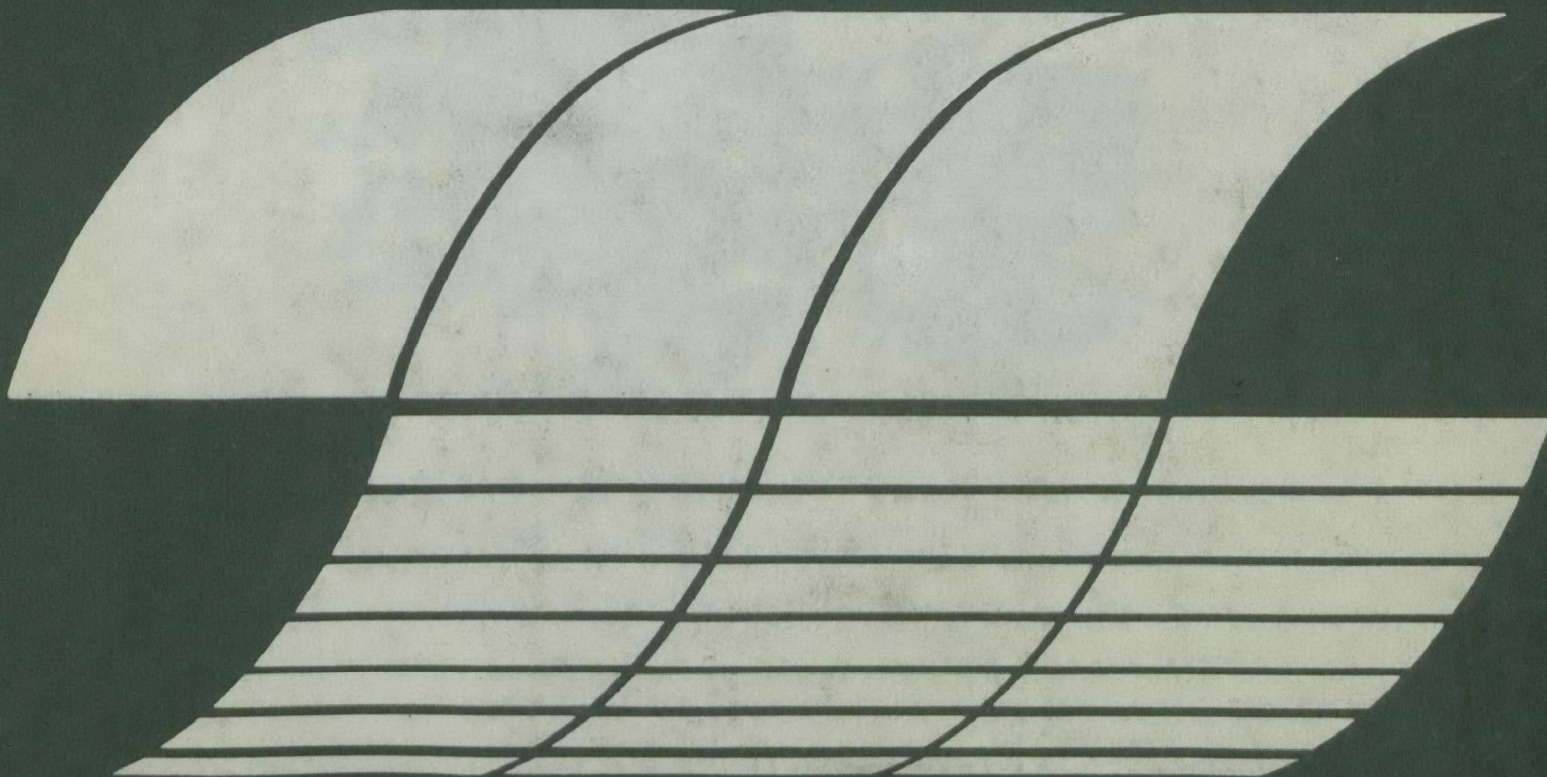
Research Triangle Park, North Carolina 27711

EPA-600/7-77-109

September 1977

PRECIPITATION CHEMISTRY OF MAGNESIUM SULFITE HYDRATES IN MAGNESIUM OXIDE SCRUBBING

Interagency
Energy-Environment
Research and Development
Program Report



RESEARCH REPORTING SERIES

Research reports of the Office of Research and Development, U.S. Environmental Protection Agency, have been grouped into seven series. These seven broad categories were established to facilitate further development and application of environmental technology. Elimination of traditional grouping was consciously planned to foster technology transfer and a maximum interface in related fields. The seven series are:

1. Environmental Health Effects Research
2. Environmental Protection Technology
3. Ecological Research
4. Environmental Monitoring
5. Socioeconomic Environmental Studies
6. Scientific and Technical Assessment Reports (STAR)
7. Interagency Energy-Environment Research and Development

This report has been assigned to the INTERAGENCY ENERGY-ENVIRONMENT RESEARCH AND DEVELOPMENT series. Reports in this series result from the effort funded under the 17-agency Federal Energy/Environment Research and Development Program. These studies relate to EPA's mission to protect the public health and welfare from adverse effects of pollutants associated with energy systems. The goal of the Program is to assure the rapid development of domestic energy supplies in an environmentally-compatible manner by providing the necessary environmental data and control technology. Investigations include analyses of the transport of energy-related pollutants and their health and ecological effects; assessments of, and development of, control technologies for energy systems; and integrated assessments of a wide range of energy-related environmental issues.

REVIEW NOTICE

This report has been reviewed by the participating Federal Agencies, and approved for publication. Approval does not signify that the contents necessarily reflect the views and policies of the Government, nor does mention of trade names or commercial products constitute endorsement or recommendation for use.

This document is available to the public through the National Technical Information Service, Springfield, Virginia 22161.

PRECIPITATION CHEMISTRY OF MAGNESIUM SULFITE HYDRATES IN MAGNESIUM OXIDE SCRUBBING

by

Philip S. Lowell, Frank B. Meserole, and Terry B. Parsons

Radian Corporation
8500 Shoal Creek Boulevard
Austin, Texas 78766

Contract No. 68-02-1319
Task Nos. 36 and 54
Program Element No. EHE528

EPA Task Officer: Charles J. Chatlynnne

Industrial Environmental Research Laboratory
Office of Energy, Minerals, and Industry
Research Triangle Park, North Carolina 27711

Prepared for

U.S. ENVIRONMENTAL PROTECTION AGENCY
Office of Research and Development
Washington, D.C. 20460

ABSTRACT

Laboratory studies were done to define the precipitation chemistry of magnesium sulfite hydrates. The results are applicable to the design of magnesium-based scrubbing processes for SO_2 removal from combustion flue gas. In magnesium-based scrubbing processes, magnesium sulfite precipitates as either the trihydrate or the hexahydrate. Equipment design and conditions depend on which hydrate is formed. Theoretical predictions that were verified experimentally indicated that MgSO_3 trihydrate is the thermodynamically stable hydrate formed at scrubbing process conditions. MgSO_3 hexahydrate is formed as a metastable solid due to kinetic phenomena. Nucleation and crystal growth rates are much faster for hexahydrate than for trihydrate.

The time scales observed in kinetic experiments at scrubbing process conditions are: hexahydrate precipitation (tens of minutes), hexahydrate dissolution and trihydrate precipitation (hundreds of minutes), and attainment of trihydrate equilibrium (thousands of minutes). Nucleation plays a dominant role in the formation of trihydrate solids. These results indicate that magnesium-based scrubbing processes can be designed to precipitate a majority of either hydrate form. Important design variables include scrubbing liquor composition and temperature, seed crystal composition, slurry volume, equipment residence times, and energy inputs to the slurry that influence nucleation.

CONTENTS

	<u>Page</u>
Abstract	ii
List of Figures	iv
List of Tables.	v
1. Summary.	1
2. Introduction.	3
Background.	3
Goals of the Study.	4
3. Conclusions.	5
4. Technical Approach and Results of the Study.	8
Technical Approach	8
Results.	9
 Bibliography	 61
 Appendices	
Technical Note 200-045-36-01, "Literature Survey of Information Available on Magnesium Sulfite Hydrate Formation Mechanisms"	 63
Technical Note 200-045-36-02, "Theoretical Predictions of Transition Temperature Lowering for the MgSO ₃ ·3H ₂ O - MgSO ₃ ·6H ₂ O System"	 109
Technical Note 200-045-36-03, "Experimental Veri- fication of the MgSO ₃ Trihydrate-Hexahydrate Transitions at 37.5°C in MgSO ₃ Solutions"	 123
Technical Note 200-045-36-04, "Experimental Results for the Equilibrium Studies on MgSO ₃ Hydrates"	 139
Technical Note 200-045-36-05, "Experimental Results for Precipitation Kinetics Studies on MgSO ₃ Hydrates"	 172
Technical Note 200-045-54-01, "Transition of MgSO ₃ Hydrates in 3M MgCl ₂ Solution"	 204
Technical Note 200-045-54-02, "MgSO ₃ Hexahydrate and Trihydrate Preparation, Handling and Characterization"	 209
Technical Note 200-045-54-03a, "Precipitation Kinetics of MgSO ₃ Hydrates in Scrubber-Like Media"	 232
Technical Note 200-045-54-04, "Homogeneous Nucleation of MgSO ₃ Hydrates in Scrubber-Like Media"	 309
Technical Note 200-045-54-05, "Secondary Nucleation of MgSO ₃ Hydrates in Scrubber-Like Media"	 336
Technical Note 200-045-54-06, "Additive Experiments on Trihydrate Kinetics"	 357

FIGURES

<u>Number</u>	<u>Page</u>
4-1 Weight Loss vs. Percent Composition for $\text{MgSO}_3 \cdot 6\text{H}_2\text{O}$ in a Self-Generated Atmosphere	14
4-2 Solubility vs. Temperature for MgSO_3 Hydrates.	20
4-3 Solubility Product Constant of $\text{MgSO}_3 \cdot 3\text{H}_2\text{O}$	25
4-4 Intersection of Solubility Product Constants of MgSO_3 Tri- and Hexahydrates Indicating the Phase Transition Temperature in Solutions of Different Compositions	26
4-5 Activity Products for MgSO_3 Hydrates in Solutions in which Homogeneous Nucleation Occurred (20 wt % MgSO_4 , pH 6).	34
4-6 Change in Sulfite Concentration in Slurry Liquor - due to Nucleation and Crystal Growth of $\text{MgSO}_3 \cdot 6\text{H}_2\text{O}$	37
4-7 Activity Products for MgSO_3 Hydrates in Solutions in which Primary and Secondary Nucleation Occurred (20 wt % MgSO_4 and pH 6).	41
4-8 $\text{MgSO}_3 \cdot 6\text{H}_2\text{O}$ Precipitation Rate vs Relative Saturation at Various Temperatures.	45
4-9 $\text{MgSO}_3 \cdot 3\text{H}_2\text{O}$ Precipitation Rate vs Relative Saturation at 55°C	46
4-10 $\text{MgSO}_3 \cdot 3\text{H}_2\text{O}$ Precipitation Rate vs Relative Saturation at 70°C	47
4-11 $\text{MgSO}_3 \cdot 3\text{H}_2\text{O}$ Precipitation Rate vs Relative Saturation at 85°C	48
4-12 Results of MgSO_3 Hydrate Precipitation Rate Experiment 3-2 Employing Trihydrate Seed Crystals	53
4-13 Results of MgSO_3 Hydrate Precipitation Rate Experiment 3-4 Employing Trihydrate Seed Crystals. .	54
4-14 Results of MgSO_3 Hydrate Precipitation Rate Experiment 3-3 Employing Hexahydrate Seed Crystals .	55

FIGURES (Cont'd)

<u>Number</u>	<u>Page</u>
4-15 Results of MgSO_3 Hydrate Precipitation Rate Experiment 3-5 Employing Hexahydrate Seed Crystals	56
4-16 Results of MgSO_3 Hydrate Precipitation Rate Experiment 3-6 Employing a Mixture of Tri- and Hexahydrate Seed Crystals.	58
4-17 Results of MgSO_3 Hydrate Precipitation Rate Experiment 3-7 Employing a Mixture of Tri- and Hexahydrate Seed Crystals.	59

TABLES

<u>Number</u>	<u>Page</u>
4-1 Results of Weight-Loss Experiments for MgSO_3 Hydrates	15
4-2 Results of Measurements of Ion-Pair Dissociation Constants using Two Methods.	18
4-3 Measured and Published Solubility Data for Magnesium Sulfate Hydrates	19
4-4 MgSO_3 Solubility Product Constants (K_{sp}) Calculated from Activities of Ions in Solubility Experiments. .	22
4-5 Equilibrium Composition of MgSO_3 Solids in 2.3M MgSO_4 Solution at 37°C	28
4-6 Temperature and Composition of Solutions which Produced Homogeneous Nucleation of MgSO_3 Hydrates. .	33
4-7 Results of Secondary Nucleation Experiments using $\text{MgSO}_3 \cdot 6\text{H}_2\text{O}$ Seed Crystals	39
4-8 Activities and Activity Products Calculated using Solution Data from Tests of Secondary Nucleation of $\text{MgSO}_3 \cdot 6\text{H}_2\text{O}$	40
4-9 Summary of Experimental Conditions in Tests of Magnesium Sulfite Hydrate Precipitation from Scrubber-Like Media	50

ACKNOWLEDGEMENTS

The authors wish to express their gratitude to the following people for their contributions: Dr. C. J. Chatlynne, EPA Project Officer, for his understanding of the value of this work; Dr. R. E. Pyle for directing the experimental portion of the project; Messrs. R. E. Sawyer, J. L. Skloss and K. R. Williams for performing the majority of the analytical chemistry; and our secretaries, Mrs. Jacquie Alberstadt, Karin Weidemann, and Dianne Sethness for typing and assembling this manuscript.

SECTION 1

SUMMARY

This report describes the results of work done by Radian Corporation for EPA under Contract 68-02-1319, Tasks 36 and 54. The work was an investigation of the physical chemistry of the precipitation of magnesium sulfite hydrates. The study was done to explain phenomena observed during the operation of magnesium based SO_2 scrubbing processes. In these processes SO_2 is removed from flue gas by absorption in magnesium oxide/sulfite slurries. Magnesium sulfite is precipitated as a hydrate. Thermal decomposition of the hydrate produces magnesium oxide for recycle. Operating experience indicates that both magnesium sulfite trihydrate and hexahydrate precipitate in magnesium-based SO_2 scrubbing processes.

From theoretical predictions, which were verified experimentally, this study shows that the trihydrate is the thermodynamically stable form at scrubbing process conditions. Precipitation of the hexahydrate occurs as the result of kinetic phenomena. Precipitation may take place by two mechanisms: nucleation and growth on existing crystals (crystallization). Both nucleation and crystallization were studied. The nucleation and crystal growth rates of the hexahydrate are much faster than the nucleation and crystal growth rates of the trihydrate at conditions encountered in the magnesium oxide wet scrubbing process.

The results of this study provide a useful design basis for magnesium based SO_2 scrubbing processes. Information is provided which defines operating conditions at which precipitation of either hydrate would be expected to occur. Guidelines are provided which indicate how equipment design and

selection might influence the composition of the solid hydrate product. By controlling design variables such as slurry density and volume, seed crystal size and composition, solution composition, and temperature, a process can be designed to produce more or less of either hydrate as the solid product.

SECTION 2

INTRODUCTION

This report describes the results of a study of the physical chemistry of the precipitation of magnesium sulfite hydrates. The work was done to explain phenomena observed during operation of magnesium oxide scrubbing processes for removing SO_2 from combustion flue gases. This explanation improves the design basis for the SO_2 scrubbing system. The work was conducted by Radian Corporation from August 1975 to October 1976 under EPA Contract No. 68-02-1319, Tasks 36 and 54.

BACKGROUND

The technical feasibility of the magnesium oxide wet scrubbing process for flue gas desulfurization has been demonstrated. The process employs a slurry of MgSO_3 and MgO to scrub SO_2 from flue gas. Sulfur is removed from the scrubbing slurry by precipitation of hydrated MgSO_3 . The hydrated MgSO_3 is dried and calcined to produce SO_2 and regenerated MgO for recycle to the scrubbing system. Two hydrates of MgSO_3 are involved, the trihydrate and the hexahydrate. Formation of both hydrates has been observed during operation of full scale magnesium oxide SO_2 scrubbing processes.

It is important for a number of reasons to be able to predict and thus control which hydrate is precipitated from the scrubbing liquor. First, the physical properties of the two hydrates differ. The trihydrate crystals are smaller than the more granular hexahydrate crystals. Design of solids separation and handling equipment depends on these physical properties. Second, the drying temperatures and heat requirements depend on how much water has to be removed to form anhydrous

magnesium sulfite. Finally, the properties of the anhydrous MgSO_3 depend on whether it was formed from the tri- or the hexahydrate. Again, solids handling equipment design is affected.

GOALS OF THE STUDY

The purpose of this study was to define the physical chemistry of MgSO_3 hydrate precipitation to explain why specific hydrates are formed at various conditions. Thermodynamic properties were used to identify the stable hydrate at equilibrium. Kinetic studies were done to define nucleation and crystallization rates. A further goal of the study was to show how these physical chemistry data apply to the design of magnesium-based SO_2 scrubbing systems.

SECTION 3

CONCLUSIONS

The results of this study of the physical chemistry of precipitation of magnesium sulfite hydrates are described in Section 4. The following conclusions are evident from the results:

- The theoretical description and analytical tools developed and used in this investigation provided an accurate set of results and a sound basis for the conclusions. The physical chemistry phenomena under investigation were first described theoretically and then confirmed experimentally.
- Magnesium sulfite trihydrate is the thermodynamically stable phase at the conditions encountered in magnesium based scrubbing processes. This result was predicted theoretically and confirmed experimentally.
- Operating experience for magnesium oxide scrubbing processes indicates that formation of magnesium sulfite hexahydrate occurs at conditions for which the trihydrate is the thermodynamically stable form. Formation of the metastable hexahydrate occurs due to kinetic phenomena which are described in this work.
- The system under investigation is complex and a number of phenomena can occur simultaneously. These include trihydrate nucleation, hexahydrate nucleation, trihydrate crystal growth, hexahydrate crystal growth, and hexahydrate dissolution. These phenomena were investigated in dilute solution experiments in

which the rates of the processes were accurately described. The dilute solutions were not representative of actual scrubbing solutions.

- Experiments were also done to study precipitation rates in systems characteristic of magnesium oxide scrubbing processes. In these systems the phenomena described above occurred simultaneously. The results obtained in scrubber-like systems were consistent with the results for tests of the individual phenomena.
- The following observations about the relative rates of the individual processes are important for design considerations. The rate of trihydrate nucleation at magnesium oxide operating temperatures of 55°C appears to be very slow compared to the rate of hexahydrate nucleations. Although hexahydrate nucleation was observed, evidence of trihydrate nucleation in scrubber-like media was not obtained. In addition, the rate of hexahydrate crystal growth is much faster than the rate of trihydrate crystal growth.
- The following sequence of events was observed in scrubber-like systems and the time frame was characterized: hexahydrate precipitation (tens of minutes), simultaneous hexahydrate dissolution and trihydrate precipitation (hundreds of minutes), trihydrate precipitation and attainment of equilibrium (thousands of minutes).
- The results of this study are directly applicable to the design of magnesium oxide scrubbing systems. They can provide a logical design basis for the process by

defining the conditions under which either hydrate may be formed.

- By specifying the composition and particle size of seed crystals, the solution composition (driving force), and the reactor volume (residence time) it is possible to design a system to produce either hydrate as the solid product.
- Design tools used in other SO₂ slurry scrubbing processes such as the particle balance concept are applicable to this system.
- Since nucleation rate is an important factor, equipment that causes high energy changes in solution will have an effect on precipitation phenomena. Turbulence effects of nozzles, pumping, agitator speed, and control valve throttling will be important.
- Hold tank and reactor volumes and slurry density determine the solid residence times. Solid residence time in the system will be an important design criteria.
- Temperature and solution composition can be used to control seed crystal composition.

SECTION 4

TECHNICAL APPROACH AND RESULTS OF THE STUDY

This section of the report describes the technical approach and the results of the work to define the physical chemistry of MgSO_3 hydrate precipitation. First the technical approach is broadly summarized; then the results are described. A complete description of results is included in the appendix. Each work package is described in detail in a Technical Note. Please refer to the Notes for details on methods of data collection and analysis.

TECHNICAL APPROACH

The investigation of the physical chemistry of MgSO_3 hydrate precipitation included three parts. The first was to develop analytical tools for use in data collection and analysis. There were two kinds of analytical tools necessary. One was methods for preparation, sample handling and qualitative and quantitative analysis of MgSO_3 tri- and hexahydrate. The other was a description of solution equilibria, a theoretical framework from which to predict which species are stable under equilibrium conditions. The description of solution equilibria provides a means of calculating the activities of species in solution. Activity data are used to correlate precipitation rate data, since the driving force for precipitation is expressed as the difference between actual conditions and equilibrium.

The second part of the technical approach was to use thermodynamic data to predict the conditions at which the hexahydrate or the trihydrate would be expected to precipitate. In

solutions containing only magnesium sulfite in water, the hexahydrate is the stable form at temperatures up to the transition temperature of 41°C. At higher temperatures the trihydrate is the form that precipitates from pure solutions. The analysis done in the second part of the technical approach showed that the trihydrate is the thermodynamically stable species at solution compositions and temperatures characteristic of the scrubbing process. Thus, the formation of hexahydrate crystals had to be explained on the basis of kinetic factors.

The third part of the technical approach was an experimental study of the precipitation rates of the tri- and hexahydrates. Nucleation and crystal growth rates were measured for each hydrate separately in dilute solutions. Then tests were done on more complex systems using solutions which more closely approximated scrubber conditions (scrubber-like media). Additional experiments were done to investigate the rates of primary and secondary nucleation of the hydrates and the effects of additives on nucleation rates.

RESULTS

This section gives an overview of the work done and the results obtained. The following subjects are discussed in separate subsections:

- Summary of background information
- Methods for hydrate preparation and solids handling and characterization
- Description of equilibria and measurement of equilibrium constants

- Prediction and verification of the stable hydrate form at scrubbing process conditions
- Precipitation Rate Studies
 - Homogeneous nucleation of individual hydrates
 - Secondary nucleation of individual hydrates
 - Precipitation rates of individual hydrates in dilute solutions
 - Precipitation experiments in scrubber-like solutions

Results are summarized in the following sections and are presented in more detail in Technical Notes appended to the report.

Summary of Background Information

Technical Note 200-045-36-01 provides a compilation of background material pertinent to this study. It presents information available from the literature on magnesium sulfite hydrate solubilities; transition temperatures; thermal decomposition; and methods for hydrate preparation, solids handling, and chemical analysis. The Note also summarizes results from operating magnesium oxide scrubbing systems. Equipment employed, chemical analyses performed, operating history, and observations of hydrates formed are described.

Methods for Hydrate Preparation, Solids Handling, and Characterization

In order to conduct experimental investigations of the magnesium sulfite hydrate system, reliable methods of sample

handling and characterization are required. Reliable, accurate methods preserve the chemical integrity of the sample. Such methods assure that the material actually analyzed is representative of the solutions or slurries from which it was obtained. Technical Note 200-045-54-02 describes these methods in detail. The results are briefly summarized in the following paragraphs.

Pure magnesium sulfite hexahydrate is prepared by nucleation of the crystals from a magnesium sulfate solution at 30°C. Concentrated sodium sulfite solution is added and $\text{MgSO}_3 \cdot 6\text{H}_2\text{O}$ nucleation occurs at a sulfite concentration of approximately 0.5 moles/liter. After about thirty minutes, 10-100 μm sized $\text{MgSO}_3 \cdot 6\text{H}_2\text{O}$ crystals are produced.

Pure magnesium sulfite trihydrate is produced by nucleation and crystal growth from a magnesium sulfate solution at 65°C. The addition of sodium sulfite produces 1-5 μm crystals. Larger crystals, up to 50 μm in size, can be grown overnight. Alternatively, the pure hydrates can be formed by adjusting the temperature of a slurry of magnesium sulfite solids. The trihydrate phase is obtained by overnight stirring of a slurry maintained at 55°C. The solution can be either pure MgSO_3 or 20 wt % MgSO_4 . The hexahydrate may be obtained by overnight stirring at room temperature.

The pure hydrate crystals are separated from liquids by vacuum filtration and alcohol washing. Fifty percent solutions of ethanol or methanol are employed, since the solubility of MgSO_3 in the alcohol solution is 1/30 of that in pure water. Several alcohol washings are required for complete removal of magnesium sulfate, sulfite, or chloride solution from the crystals. The solids are dried in an oven at 40-50°C. Higher temperatures will cause dehydration. Thirty minutes is adequate drying time for samples of one-gram or less. Dried

solids can be stored without deterioration in a closed glass or plastic container under nitrogen or in air of relative humidity less than 90%.

Solids characterization methods include differential scanning calorimetry (DSC), differential thermal analysis (DTA), infrared spectroscopy (IR), and analysis of X-ray diffraction patterns. DSC analyses measure the difference in rate of energy absorption or evolution between a sample and a reference material. The materials are subjected to a programmed rate of heating in a closed system. A DuPont 990 Thermal Analyzing System was used to develop the DSC method. A Perkin-Elmer DSC-2 was used for analysis of the samples from precipitation experiments. Both tri- and hexahydrates of MgSO_4 had only one endothermic transition. The trihydrate transition began at about 120°C with the maximum at about 170°C . The hexahydrate transition began at about 70°C with the maximum at about 100°C . The exact starting and maximum transition temperatures varied slightly from sample to sample and between the DuPont and Perkin-Elmer instruments, but the peaks are so widely separated that they can be identified without ambiguity.

A DuPont 951 Thermogravimetric Analyzer was also used to determine the composition of the hydrate mixture. The procedure involves heating a sample at a constant rate and recording weight loss or gain as a function of temperature. At 100°C the hexahydrate loses three moles of water to form trihydrate. At 180°C dehydration of the trihydrate to the anhydrous salt occurs. The percent weight loss of a mixture of hydrates at these temperatures can be used to calculate the weight percent of each hydrate and the magnesium sulfite content.

A method for characterization of solids in field applications was also developed. The procedure employs a large glass vacuum dessicator containing a thermometer with a Variac-controlled heating mantle. The temperature inside the dessicator is adjusted to 100-110°C. At that temperature in a self-generated water atmosphere the hexahydrate is converted to the trihydrate. Hydrate samples are weighed and placed in the dessicator in loosely stoppered closed containers for four hours. The samples are weighed again. The average weight loss for pure hexahydrate samples is about 25% (theoretical weight loss is 25.6%). For trihydrate samples, the average loss is about one percent (theoretical is zero). Results are shown in Figure 4-1 and Table 4-1.

Description of Equilibria and Measurement of Equilibrium Constants

A theoretical model of equilibrium in aqueous ionic solutions is used to calculate activities of the ions and ion pairs. Activities are used in calculating equilibrium as well as in the driving force term in rate data correlations. A computer program for calculating activities based on a model of equilibrium has been developed by Radian Corporation. The equilibrium model is described in the literature (LO-R-007) and was used for data analysis in this study.

In order to apply the equilibrium model to solutions employed in the magnesium oxide process, some equilibrium constants had to be added. Thermodynamic data for reactions involving magnesium and sodium ions were needed to extend the model. The reactions and equilibrium constants of interest are listed below.

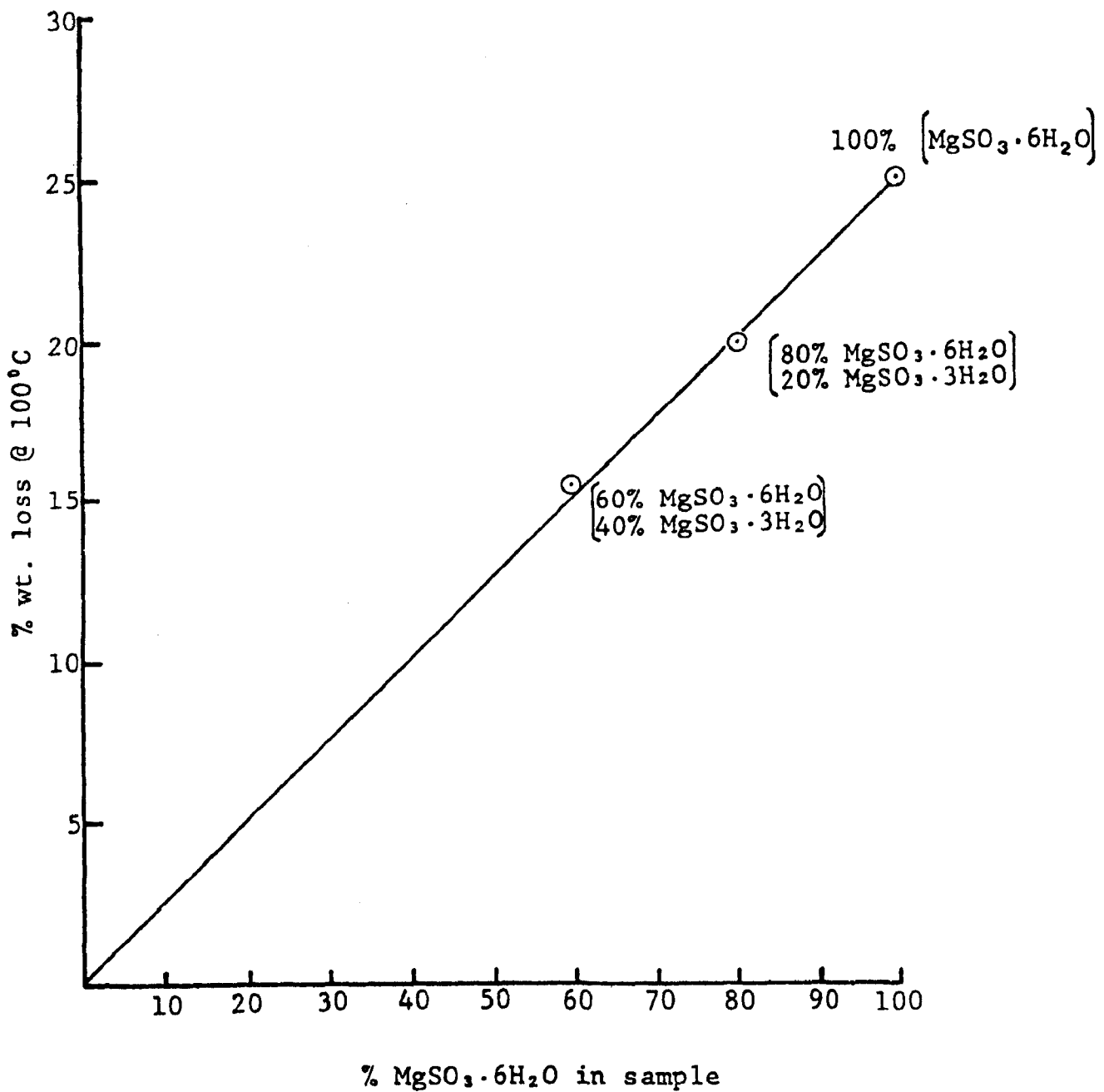
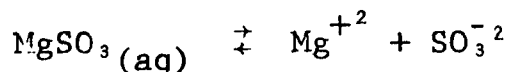


Figure 4-1. Weight Loss vs. Percent Composition for $\text{MgSO}_3 \cdot 6\text{H}_2\text{O}$ in a Self-Generated Atmosphere

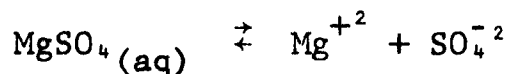
TABLE 4-1. RESULTS OF WEIGHT-LOSS EXPERIMENTS FOR MgSO_3 HYDRATES
AT 100°C IN A SELF-GENERATED ATMOSPHERE

Sample Composition (wt%)		Weight (Grams)		Wt. Loss, %	
Hexa	Tri	Sample Wt.	Wt. Loss	Observed	Theoretical
100	0	0.599	0.152	25.4	25.4
100	0	0.602	0.153	25.4	25.4
0	100	0.602	0.0018	0.29	0.0
0	100	0.600	0.0005	0.08	0.0
60	40	0.600	0.093	15.4	15.2
60	40	0.603	0.092	15.3	15.2
80	20	0.602	0.120	19.8	20.3
80	20	0.535	0.105	17.5	20.3

Magnesium sulfite ion pair dissociation constant



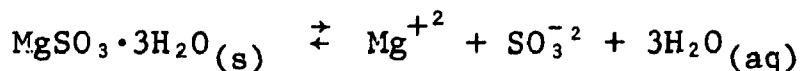
Magnesium sulfate ion pair dissociation constant



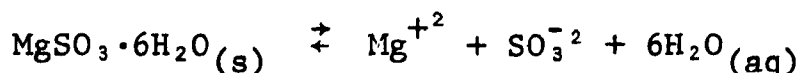
Sodium sulfite ion pair dissociation constant



Magnesium Sulfite trihydrate solubility product constant



Magnesium Sulfite hexahydrate solubility product constant



Technical Note 200-045-36-04 describes the experimental approach and the procedures and analytical methods employed. Two methods were used to measure ion-pair dissociation constants. One was to measure the free cation response of a solution with ion selective electrodes. These values were compared with the free cation responses of standard solutions with negligible ion pairing. The second method was to determine the influence of ion-pair formation on the solubility of a sparingly-soluble reference compound. The solubility of the reference compound is increased by the addition of an electrolyte which can form ion pairs with ions of the reference compound. Ion-pair dissociation constants determined by the second method were more accurate. It was found that selective cation

response measurements were influenced by an electrode junction potential inherent in each measurement. The magnitude of the electrode junction potential, which is a function of solution composition and temperature, is unknown but not negligible.

In the solubility influence experiments the ion-pair dissociation constants were measured at temperatures of 30°C and 50°C. $\text{CaSO}_3 \cdot \frac{1}{2}\text{H}_2\text{O}$ and $\text{CaSO}_4 \cdot 2\text{H}_2\text{O}$ were used as the sparingly-soluble reference compounds. The salts equilibrated with each solid in individual tests were MgCl_2 , NaCl , and CaCl_2 . Chloride salts were used because the chloride anion does not form ion pairs to an appreciable extent with cations of the above salts.

Data collection and analysis procedures for both methods are described in Technical Note 200-045-36-04. The resulting ion-pair dissociation constants are listed in Table 4-2. There were no reported values for these constants in the literature.

Solubility product constants for the tri- and hexahydrates were calculated from the results of solubility studies for the salts. Crystals of the pure tri- or hexahydrate were dissolved in de-ionized water in a vessel contained in a constant temperature bath and continuously purged with dry nitrogen. Hexahydrate crystals were dissolved at temperatures below 40°C and trihydrate crystals at higher temperatures. The solution was analyzed for Mg^{+2} , SO_3^{-2} , SO_4^{-2} , and pH as the crystals dissolved to monitor the approach to equilibrium. Solubilities were calculated from the analytical results. Measured solubilities are compared with literature values in Table 4-3 and Figure 4-2.

Solubility product constants at temperatures from 25 to 65°C were calculated from the activities of the ions in solution as shown in equations 4-1 and 4-2.

TABLE 4-2. RESULTS OF MEASUREMENTS OF ION-PAIR DISSOCIATION CONSTANTS
USING TWO METHODS

Ion-Pair	Temperature ($^{\circ}\text{C}$)	<u>K dissociation</u>	
		Ion-Specific Electrode Method	Sparingly-Soluble Reference Compound Method
$\text{MgSO}_3(\text{aq})$	25	0.00173	0.00136
	35	0.00140	0.00110
	45	0.00113	0.000896
	55	0.00091	0.000747
$\text{MgSO}_4(\text{aq})$	25	0.00347	0.00569
	35	0.00287	0.00533
	45	0.00238	0.00501
	55	0.00196	0.00473
$\text{NaSO}_3^-(\text{aq})$	25	0.055	0.06611
	35	0.055	0.05760
	45	0.055	0.05063
	55	0.055	0.04484

TABLE 4-3. MEASURED AND PUBLISHED SOLUBILITY DATA FOR MAGNESIUM SULFATE HYDRATES

Temperature (°C)	Stable Solid Phase	Measured Solubility (g MgSO ₃ /100 g)	Reported Solubility (g MgSO ₃ /100 g)
25.0	MgSO ₃ ·6H ₂ O	0.668	0.625
30.0	MgSO ₃ ·6H ₂ O	0.723	0.721
35.0	MgSO ₃ ·6H ₂ O	0.861	0.835
45.0	MgSO ₃ ·3H ₂ O	0.906	0.904
55.0	MgSO ₃ ·3H ₂ O	0.814	0.790
65.0	MgSO ₃ ·3H ₂ O	0.713	0.710

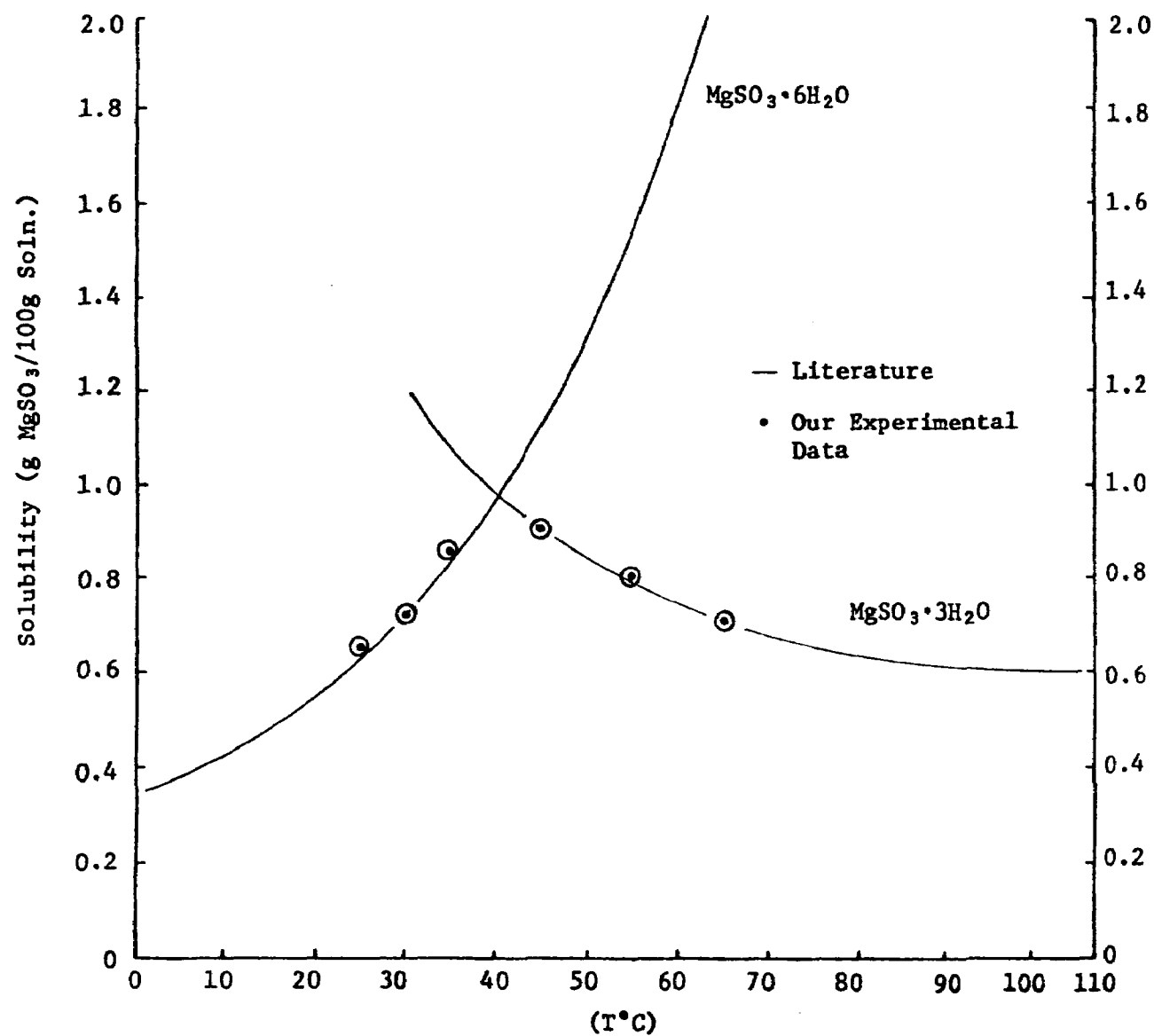


Figure 4-2. Solubility vs. Temperature for MgSO_3 Hydrates

$$K_{sp6}(T) = \frac{a_{Mg^{+2}} a_{SO_3^{-2}} a_{H_2O}^6}{a_{MgSO_3 \cdot 6H_2O(s)}} \quad (4-1)$$

$$K_{sp3}(T) = \frac{a_{Mg^{+2}} a_{SO_3^{-2}} a_{H_2O}^3}{a_{MgSO_3 \cdot 3H_2O(s)}} \quad (4-2)$$

The activities were calculated with the equilibrium model using the analytical data from the solubility experiments. Input data included concentrations of magnesium, sulfite, and sulfate; temperature; and pH. The results are shown in Table 4-4.

Prediction and Verification of the Thermodynamically Stable Hydrate Form at Scrubbing Process Conditions

Depending on solution composition and temperature, one of the magnesium sulfite hydrates is stable at equilibrium and would eventually be produced as the solid product. For a given solution composition, the hexahydrate is the stable hydrate form over the lower range of temperature. A transition to trihydrate as the stable form occurs at a temperature called the transition temperature. At temperatures above the transition temperature, the trihydrate is the stable form at equilibrium. In pure solutions containing only water and magnesium sulfite, the transition temperature is 41°C. The hexahydrate is the thermodynamically stable form below 41°; however, the precipitation of hexahydrate crystals occurs at temperatures higher than 41°C in some magnesium oxide scrubbing systems.

It has been suggested that at the solution compositions characteristic of the magnesium oxide process, the transition temperature might be higher than 41°C and the hexahydrate might be the thermodynamically stable hydrate form. The validity of this explanation for hexahydrate formation was examined using a two-step approach. First, thermodynamic properties

TABLE 4-4. MgSO_3 SOLUBILITY PRODUCT CONSTANTS (K_{sp}) CALCULATED FROM ACTIVITIES OF IONS IN SOLUBILITY EXPERIMENTS

Temperature (°C)	Stable Solid Phase	K_{sp}
0	$\text{MgSO}_3 \cdot 6\text{H}_2\text{O}$	4.537×10^{-5}
10	$\text{MgSO}_3 \cdot 6\text{H}_2\text{O}$	4.797×10^{-5}
20	$\text{MgSO}_3 \cdot 6\text{H}_2\text{O}$	5.368×10^{-5}
25	$\text{MgSO}_3 \cdot 6\text{H}_2\text{O}$	5.720×10^{-5}
30	$\text{MgSO}_3 \cdot 6\text{H}_2\text{O}$	6.124×10^{-5}
35	$\text{MgSO}_3 \cdot 6\text{H}_2\text{O}$	6.579×10^{-5}
40	$\text{MgSO}_3 \cdot 6\text{H}_2\text{O}$	7.120×10^{-5}
45	$\text{MgSO}_3 \cdot 6\text{H}_2\text{O}$ (metastable)	7.735×10^{-5}
50	$\text{MgSO}_3 \cdot 6\text{H}_2\text{O}$ (metastable)	8.375×10^{-5}
55	$\text{MgSO}_3 \cdot 6\text{H}_2\text{O}$ (metastable)	9.060×10^{-5}
60	$\text{MgSO}_3 \cdot 6\text{H}_2\text{O}$ (metastable)	9.786×10^{-5}
62.5	$\text{MgSO}_3 \cdot 6\text{H}_2\text{O}$ (metastable)	1.013×10^{-4}
30	$\text{MgSO}_3 \cdot 3\text{H}_2\text{O}$ (metastable)	1.074×10^{-4}
35	$\text{MgSO}_3 \cdot 3\text{H}_2\text{O}$ (metastable)	8.662×10^{-5}
40	$\text{MgSO}_3 \cdot 3\text{H}_2\text{O}$ (stable)	7.120×10^{-5}
45	$\text{MgSO}_3 \cdot 3\text{H}_2\text{O}$ (stable)	6.074×10^{-5}
50	$\text{MgSO}_3 \cdot 3\text{H}_2\text{O}$ (stable)	5.191×10^{-5}
55	$\text{MgSO}_3 \cdot 3\text{H}_2\text{O}$ (stable)	4.466×10^{-5}
60	$\text{MgSO}_3 \cdot 3\text{H}_2\text{O}$ (stable)	3.894×10^{-5}
70	$\text{MgSO}_3 \cdot 3\text{H}_2\text{O}$ (stable)	3.020×10^{-5}
80	$\text{MgSO}_3 \cdot 3\text{H}_2\text{O}$ (stable)	2.457×10^{-5}
90	$\text{MgSO}_3 \cdot 3\text{H}_2\text{O}$ (stable)	2.059×10^{-5}
100	$\text{MgSO}_3 \cdot 3\text{H}_2\text{O}$ (stable)	1.771×10^{-5}

were used to predict the stable hydrate form at equilibrium for specific temperatures and solution compositions. Then experiments were done in which solutions of appropriate composition were brought to equilibrium at controlled temperatures. The hydrate crystals were separated and characterized. The results are described in Technical Notes 200-045-36-02, -36-03, and -54-01.

Equation 4-3 describes the transition from magnesium sulfite hexahydrate to the trihydrate.



In Technical Note 200-045-36-02 it is shown that this equilibrium can be described in terms of the solubility product constants, K_{sp} , of the hydrates as shown in equation 4-4.

$$K_{\text{trans}} = \frac{a_{\text{MgSO}_3 \cdot 3\text{H}_2\text{O}} a_{\text{H}_2\text{O}}^3}{a_{\text{MgSO}_3 \cdot 6\text{H}_2\text{O}}} = \frac{K_{sp6}}{K_{sp3}} \quad (4-4)$$

At a given temperature for a saturated solution the solubility product constant is numerically equal to the value of the activity product (ap). The activity products for the tri- and hexahydrates are shown in equations 4-5 and 4-6.

$$ap_3 \equiv a_{\text{Mg}^{+2}} a_{\text{SO}_3^{-2}} a_{\text{H}_2\text{O}}^3 \quad (4-5)$$

$$\begin{aligned} ap_6 &\equiv a_{\text{Mg}^{+2}} a_{\text{SO}_3^{-2}} a_{\text{H}_2\text{O}}^6 \quad (4-6) \\ &= ap_3 a_{\text{H}_2\text{O}}^3 \end{aligned}$$

Thus the hydrate transition can be expressed in terms of saturated solution activity products.

$$K_{\text{trans}} = ap_6/ap_3 = a_{\text{H}_2\text{O}}^3 \quad (4-7)$$

Solutions in which the activity product ap_3 is greater than K_{sp_3} are supersaturated with respect to $\text{MgSO}_3 \cdot 3\text{H}_2\text{O}$ precipitation. Subsaturated solutions have an activity product less than the solubility product constant. Figure 4-3 shows the solubility product constant for the trihydrate as a function of temperature. The ordinate in Figure 4-3 is ap_3 .

The hexahydrate solubility properties can be plotted on the same graph since

$$ap_3 = ap_6/a_{\text{H}_2\text{O}}^3 \quad (4-8)$$

The lines representing the two solubility product constants on the ap_3 plot intersect at the hydrate transition temperature.

Figure 4-4 shows the two hydrate solubility product constants in terms of ap_3 in solutions of varying composition. The figure shows that the trihydrate-hexahydrate phase transition temperature decreases with increasing dissolved salt content or decreasing activity of water. In 2M MgSO_4 solutions, which are characteristic of the magnesium oxide scrubbing process, the transition temperature is predicted to be 37.5°C. At 37.5°C the hexahydrate should be the stable MgSO_3 phase in 1.5M MgSO_4 solution, and the trihydrate phase should be stable in 2.3M MgSO_4 solution.

Such predictions were verified experimentally as described in Technical Notes 200-045-36-03 and 200-045-54-01.

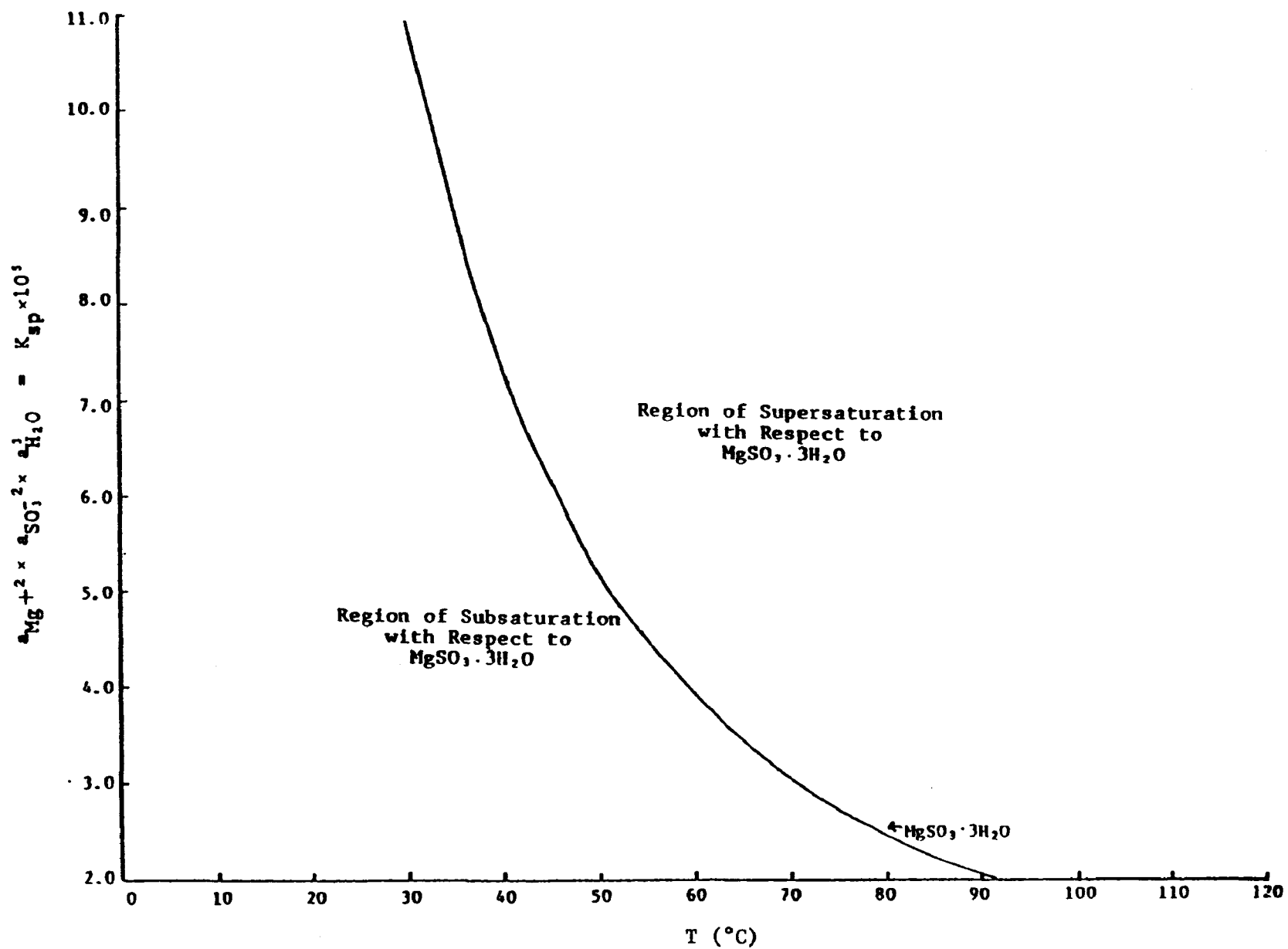


Figure 4-3. Solubility Product Constant of $\text{MgSO}_3 \cdot 3\text{H}_2\text{O}$

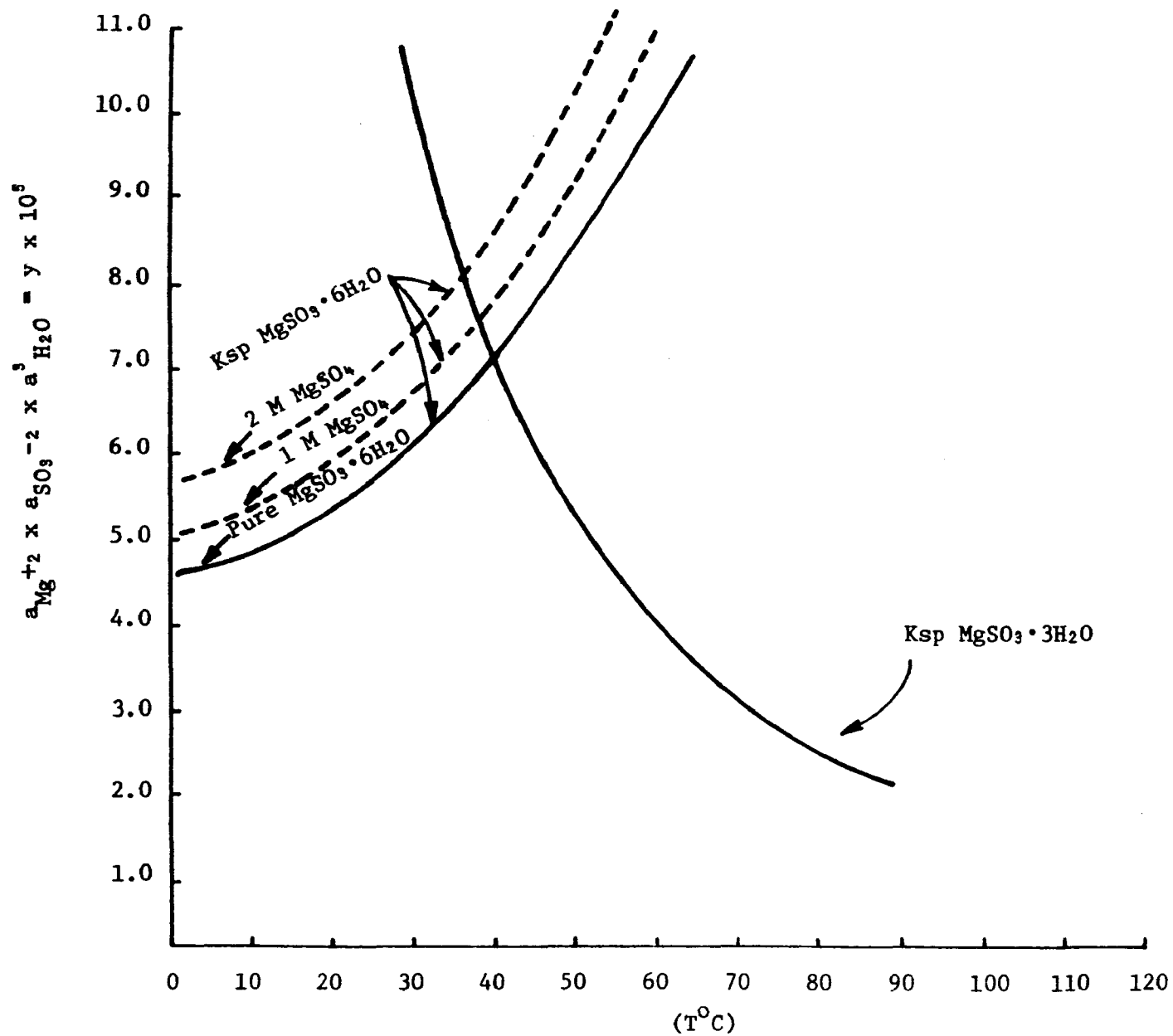


Figure 4-4. Intersection of Solubility Product Constants of MgSO_3 Tri- and Hexahydrates Indicating the Phase Transition Temperature in Solutions of Different Compositions

A 1.5M MgSO_4 solution at 37.5°C was saturated with MgSO_3 by adding excess $\text{MgSO}_3 \cdot 6\text{H}_2\text{O}$. The slurry, containing 25g undissolved solids, was maintained at 37.5°C in a stoppered flask and stirred continuously with a magnetic stirrer for one week. Chemical analysis of the solids confirmed that the hexahydrate phase remained stable. Then 7g $\text{MgSO}_3 \cdot 3\text{H}_2\text{O}$ were added. After another week of stirring at 37.5°C the solids were again analyzed and found to be pure $\text{MgSO}_3 \cdot 6\text{H}_2\text{O}$. All of the trihydrate had dissolved and reprecipitated as hexahydrate.

Identical tests were also done in 2.3M MgSO_4 solution at 37.5°C . The trihydrate phase was predicted to be the stable one in these solutions. The MgSO_4 solution was saturated with $\text{MgSO}_3 \cdot 6\text{H}_2\text{O}$, the solution was filtered and 11g of $\text{MgSO}_3 \cdot 3\text{H}_2\text{O}$ were added. Solids were sampled and analyzed after 4 days of stirring. Only trihydrate was found. Ten grams of $\text{MgSO}_3 \cdot 6\text{H}_2\text{O}$ were added and solids were sampled again after 9, 15, and 16 days of stirring at 37.5°C . The results are shown in Table 4-5. Chemical, microscopic, DSC, and IR analyses confirmed that the stable phase from the 2.3M MgSO_4 solution was $\text{MgSO}_3 \cdot 3\text{H}_2\text{O}$.

Additional tests were done to confirm the prediction that $\text{MgSO}_3 \cdot 3\text{H}_2\text{O}$ is the stable phase at 25°C in 3M MgCl_2 solution. These tests are described in Technical Note 200-045-54-01.

These results indicate that in magnesium oxide scrubber liquors the hexa- to trihydrate transition temperature will be lower than the pure solution value of 41°C . Therefore, magnesium sulfite trihydrate is the thermodynamically stable form, and production of hexahydrate crystals as a metastable intermediate must be the result of a kinetic phenomenon.

TABLE 4-5. EQUILIBRIUM COMPOSITION OF MgSO_3 SOLIDS IN 2.3M MgSO_4 SOLUTION AT 37°C

Elapsed Time Days	Filtrate Analyses (mole/l)		Solids Analyses (mmole/g)		Results of Microscopic Analysis	Conclusions
	Mg^{++}	$\text{SO}_3^{=}$	Mg^{++}	$\text{SO}_3^{=}$		
0	2.26	--	6.30	6.30	Trihydrate Crystals	Started with trihydrate
4	2.33	0.14	6.28	6.31	Trihydrate	Trihydrate unchanged
Added hexahydrate						
9	2.31	0.12	5.62	5.60	Mixture of tri- hexahydrate	Mixture of tri- and hexahydrate
15	--	--	--	--	Mostly tri- with some hexahydrate	—
16	2.25	0.12	6.22	6.25	All trihydrate	All hexahydrate converted to trihydrate

Precipitation Rate Studies

The investigation of kinetic phenomena involved in the precipitation of MgSO_4 hydrates is based on a model of crystallization. The model is useful because it describes precipitation processes in terms of some elementary steps. Each step has a rate that is dependent on some specific solution variables. The model helps explain what happens during hydrate precipitation and provides a basis for data correlation. The model defines precipitation, the formation of solids from a solution of ions, in terms of the following processes:

- Nucleation - the formation of a discrete solid particle where none existed before
- Primary homogeneous nucleation - nucleation in a homogeneous solution with no other crystals present
- Secondary homogeneous nucleation - nucleation in a homogeneous solution containing seed crystals of precipitating solid
- Heterogeneous nucleation - nucleation in a solution containing foreign particles
- Crystal growth or crystallization - deposition of solid material from a solution on the surface of an existing crystal.

According to the precipitation model, the following processes can occur during the precipitation of magnesium sulfite hydrates from magnesium oxide scrubbing liquors:

- secondary nucleation of $\text{MgSO}_3 \cdot 3\text{H}_2\text{O}$
- secondary nucleation of $\text{MgSO}_3 \cdot 6\text{H}_2\text{O}$
- crystallization of $\text{MgSO}_3 \cdot 3\text{H}_2\text{O}$
- crystallization of $\text{MgSO}_3 \cdot 6\text{H}_2\text{O}$
- dissolution of $\text{MgSO}_3 \cdot 6\text{H}_2\text{O}$ crystals

Each of these processes occurs at a characteristic rate. The rate of secondary nucleation depends on the solution temperature, composition, relative saturation, and energy input to the solution. In laboratory experiments energy is imparted to solutions by stirring. In industrial applications, pumps, nozzles and agitators are mechanical means of energy input. The rate of crystal growth depends on the incorporation of magnesium and sulfite ions into the surface of the solid. The rate is a function of temperature and solution composition. Because the surface growth rate is slow, diffusion from the bulk solution to the solid surface is not a significant factor.

The approach to investigating the kinetics of the magnesium sulfite hydrate precipitation process was first to examine the individual processes separately. These experiments provided an understanding of the individual processes. Then the overall precipitation process for each hydrate was examined in dilute solutions. Rate data correlation is straightforward in dilute solutions, since the non-ideality is accurately described. Finally, precipitation rates were studied in solutions containing higher levels of dissolved salts (highly non-ideal solutions). These solutions are characteristic of magnesium oxide scrubbing liquors so they are termed scrubber-like media. Data analysis for precipitation rate studies in scrubber-like media is more difficult because all the processes listed above

can occur simultaneously. In addition, the model for calculating ionic activities does not yield accurate results in solutions of high ionic strength since the parameters were determined primarily at low ionic strengths.

The kinetics studies are described in detail in Technical Notes 200-045-36-05, -54-03, -54-04, -54-05, and -54-06 contained in the appendix. The results are summarized in four sections: Primary nucleation, Secondary nucleation, Dilute solution precipitation rates, and Precipitation rates in scrubber-like media.

Primary Nucleation of Magnesium Sulfite Hydrates--

Precipitation occurs when the solubility product constant, K_{sp} , is exceeded in a solution containing seed crystals. If there are no nuclei present, metastable supersaturated solutions exist. Supersaturation in a clear solution can increase to some limit at which solids precipitate spontaneously. This induced precipitation is called primary nucleation. Experiments were done to determine solution compositions and temperatures at which spontaneous nucleation of magnesium sulfite solids occurs. Another goal of the experiments was to observe which hydrate is nucleated and whether hydrate mixtures are obtained.

The experiments are described in Technical Note 200-045-54-04. The procedures involved the addition of concentrated sodium sulfite solution to concentrated magnesium sulfate solution until nucleation was visually observed. Solutions were stirred at a constant rate and the desired temperature was maintained by using a water bath. The composition of solutions from which nucleation occurred was comparable to that of magnesium

oxide scrubber liquors, 2.08 molal (20 wt %) MgSO_4 at pH 6. The temperature range investigated was 28 to 80°C.

When nucleation occurred, the slurry was immediately filtered. The solids were washed with 50% ethanol and oven-dried at 45°C for 30 minutes. Oxidation of sulfite was negligible. The solutions were analyzed to determine pH and the concentrations of Mg^{+2} , SO_3^{-2} , and SO_4^{-2} . The solids were analyzed by DSC, chemical analysis, microscopic examination, and X-ray diffraction. Detailed results of these analyses are given in Technical Note 200-045-54-04.

The results of primary nucleation experiments are summarized in Table 4-6. Table 4-6 shows that pure $\text{MgSO}_3 \cdot 6\text{H}_2\text{O}$ is nucleated between 28 and 60°C and pure $\text{MgSO}_3 \cdot 3\text{H}_2\text{O}$ is nucleated at 69 and 80°C. No hydrate mixtures were observed.

From the solution composition data given in Table 4-6, the activities of Mg^{+2} , SO_4^{-2} and H_2O were calculated using the Radian equilibrium model. These activities were used to calculate the activity products ap_3 and ap_6 defined previously in Equations 4-5 and 4-6. Values for ap_3 and $ap_6/a_{\text{H}_2\text{O}}^3$ are shown in Figure 4-5 as a function of temperature for the solutions in which homogeneous nucleation occurred. The curves drawn in the figure indicate the conditions at the onset of primary nucleation for the two hydrate phases. The lower set of curves in the figure shows the same activity products for saturated solutions of $\text{MgSO}_3 \cdot 6\text{H}_2\text{O}$ and $\text{MgSO}_3 \cdot 3\text{H}_2\text{O}$.

The ratio of the activity product, ap_3 or ap_6 , to the appropriate solubility product constant is defined as the relative saturation, RS_3 or RS_6 . The relative saturation at which nucleation occurs is a way of describing the driving force for

TABLE 4-6. TEMPERATURE AND COMPOSITION OF SOLUTIONS WHICH PRODUCED
HOMOGENEOUS NUCLEATION OF MgSO_3 HYDRATES

Temperature $^{\circ}\text{C} \pm 1$	pH	Concentration of Ions (gmole/kg soln) ¹			Species Nucleated	$a_p \times 10^5$
		Mg^{++}	Na_2SO_3	SO_4		
28	5.7	2.220	0.381	2.240	$\text{MgSO}_3 \cdot 6\text{H}_2\text{O}^*$	30.5
40	6.0	2.190	0.393	2.206	$\text{MgSO}_3 \cdot 6\text{H}_2\text{O}^{**}$	31.6
50	6.1	2.028	0.519	2.053	$\text{MgSO}_3 \cdot 6\text{H}_2\text{O}^{**}$	35.9
60	6.2	2.091	0.602	2.112	$\text{MgSO}_3 \cdot 6\text{H}_2\text{O}^{**}$	37.1
69	6.2	2.040	0.678	2.065	$\text{MgSO}_3 \cdot 3\text{H}_2\text{O}$	35.3
80	6.3	2.257	0.602	2.273	$\text{MgSO}_3 \cdot 3\text{H}_2\text{O}$	28.8

¹ Solution density was 1.260 g/ml at room temperature.

* Rhombic crystal habit

** Hexagonal crystal habit

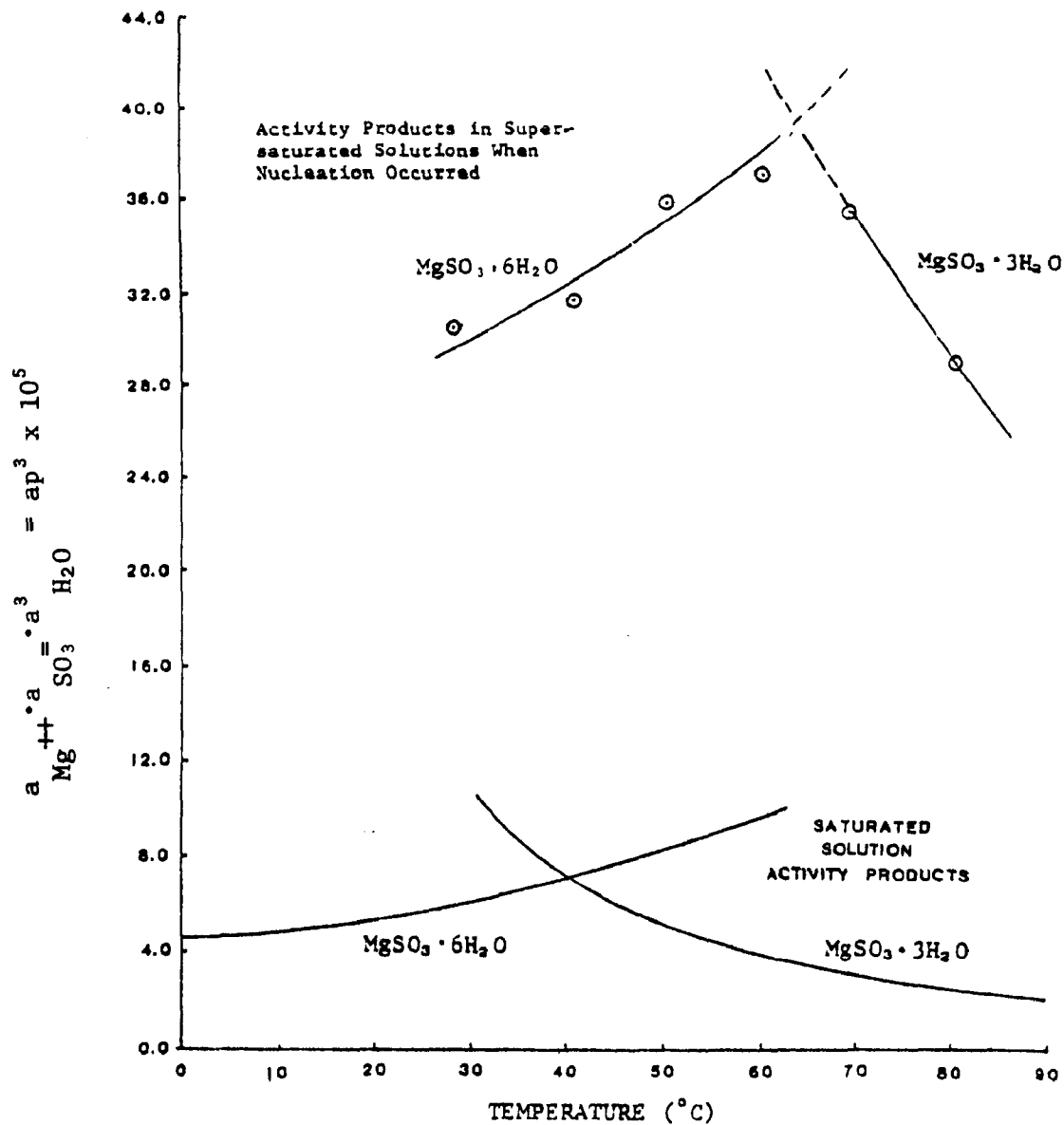


Figure 4-5. Activity Products for $MgSO_3$ Hydrates in Solutions in which Homogeneous Nucleation Occurred (20 wt % $MgSO_4$, pH 6)

precipitation. A relative saturation of 3 to 4 was required for primary nucleation of the hexahydrate. A relative saturation of about 12 was required for the trihydrate.

Although magnesium sulfite trihydrate is the thermodynamically stable phase in 20% MgSO_4 solutions at 40, 50 and 60°C, the hexahydrate is nucleated at these temperatures. Nucleation of the trihydrate phase was observed only at temperatures above 65°C. These results indicate that a kinetic effect is involved in the nucleation process. It was noted that the nucleation transition temperature is higher than the equilibrium transition temperature. The rate of primary nucleation of the hexahydrate is faster than that of the trihydrate. Further, primary nucleation occurs at lower values of relative saturation for the hexahydrate than for the trihydrate.

Secondary Nucleation of Magnesium Sulfite Hydrates--

As described above, secondary nucleation occurs in solutions containing seed crystals of the precipitating solid. Experiments done to investigate conditions at which secondary nucleation occurs for MgSO_3 hydrates are described in Technical Notes 200-045-54-05 and 06.

The experimental approach involved the use of a continuous liquid feed reactor with provisions for immediate mixing and thorough agitation of the reactant slurry. Batch addition of seed crystals was employed. The reactor was charged with 2M MgSO_4 - 1.1M Na_2SO_3 solution and a known quantity of seed crystals of either $\text{MgSO}_3 \cdot 3\text{H}_2\text{O}$ or $\text{MgSO}_3 \cdot 6\text{H}_2\text{O}$. Then Na_2SO_3 was added at a constant rate and the sulfite concentration and other variables in the reactor slurry were monitored. Secondary nucleation was investigated at temperatures from 30 to 60°C. Technical Note 200-045-54-05 describes detailed procedures and

equipment used for sampling, pH monitoring, chemical analysis, and variation of stirring speed and temperature.

In order to understand methods of data collection and analysis, it is useful to consider what happens in the precipitation process. Immediately after the onset of nucleation, an instantaneous process, the process of crystal growth begins. At first the solid particles are very small. They become larger as solid material is deposited on the surface of the particles. The crystal growth rate is partly a function of the particle surface area. At some point these changes are detectable as an increase in the weight percent solids. This increase in solids can be detected visually or by measuring the weight of solids in the slurry. Another indication of change is the sulfite concentration in the liquor. The sulfite concentration decreases as sulfite ions leave the solution in the MgSO_3 precipitate. The change in weight percent solids and sulfite concentration due solely to nuclei formation is probably imperceptibly small since the nuclei are very small. But the crystal growth which follows produces detectable changes in variables which can be measured. The approach to investigating secondary nucleation was to monitor the detectable changes produced due to crystal growth and to assume that nucleation occurred just prior to the point at which such changes were observed. Figure 4-6 illustrates the change in sulfite concentration in the reaction liquid during secondary nucleation and crystal growth of magnesium sulfite hexahydrate.

The onset of secondary nucleation for magnesium sulfite hexahydrate could be observed visually when an increase in the amount of solids in the slurry occurred. Nucleation in hexahydrate experiments was also indicated by a decrease in sulfite concentration in the reaction liquor. The onset of secondary nucleation for the hexahydrate system was taken to be the point

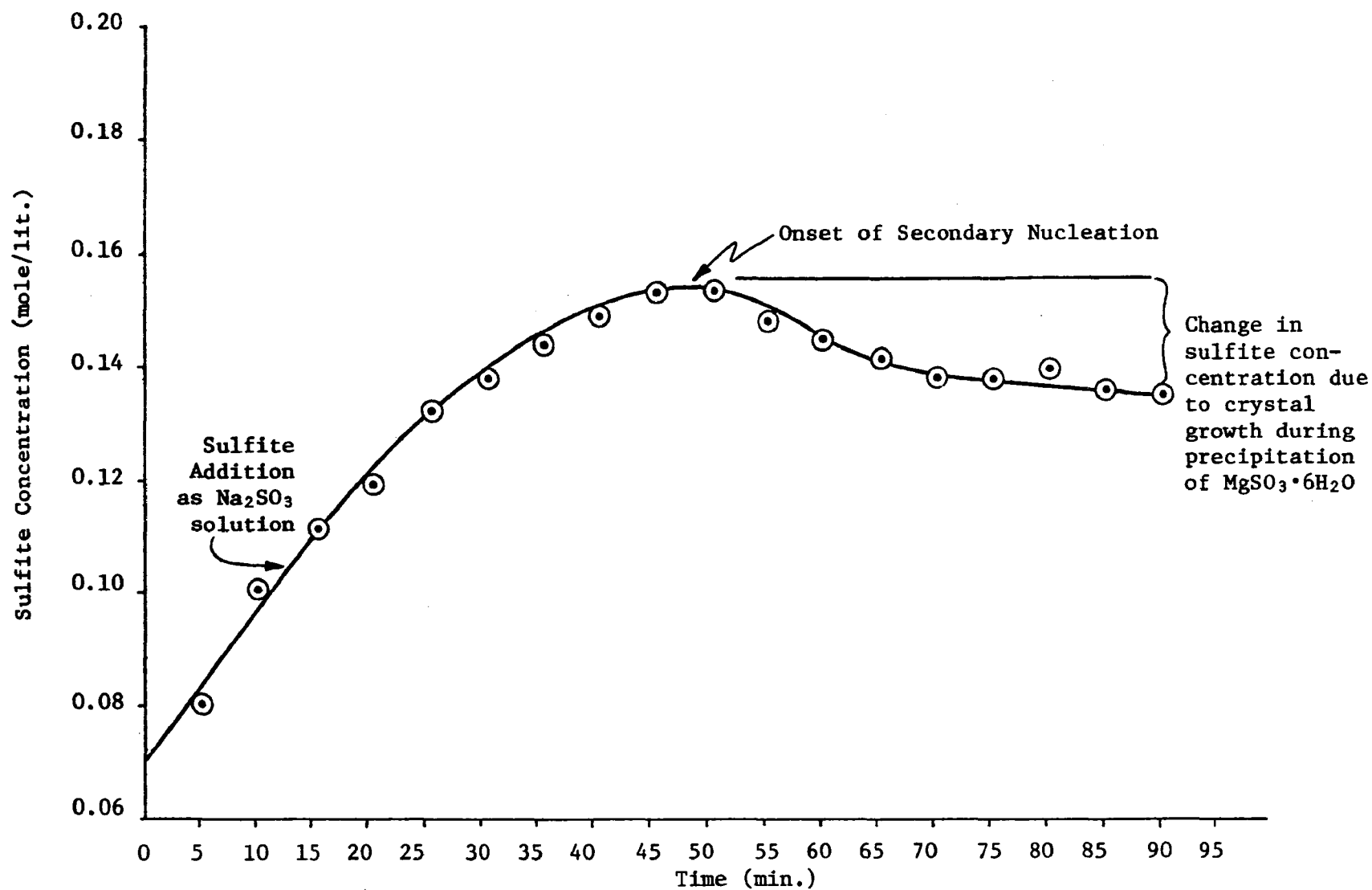


Figure 4-6. Change in Sulfite Concentration in Slurry Liquor - due to Nucleation and Crystal Growth of $\text{MgSO}_3 \cdot 6\text{H}_2\text{O}$

of maximum sulfite concentration. Data collected for the hexahydrate system are summarized in Table 4-7. Solution composition data were used in the Radian equilibrium program to calculate activities of the ions in solution at the onset of nucleation. The activity product ap_6 , the solubility product constant K_{sp_6} and the variable $ap_6/a_{H_2O}^3$ were calculated as described previously. These results are listed in Table 4-8. The results are plotted as a function of temperature and stirring speed in Figure 4-7.

It was not possible to detect the onset of secondary nucleation in experiments employing trihydrate seed crystals. A number of variations in experimental approach were employed in an effort to detect a change in weight percent solids in the system. These are described in Technical Note 200-045-54-05. The results indicate that the increase in trihydrate solids concentration caused by secondary nucleation and crystal growth was very small compared to the total solids concentration. Further, the growth rate of crystals after nucleation occurred was so slow that a decrease in sulfite concentration was difficult to detect.

An effect of stirrer speed on hexahydrate nucleation was observed as indicated in Figure 4-7. Stirring imparts energy to the system through crystal impact. The results indicate that at lower stirring speeds (lower energy input) a higher activity product (relative saturation) is required for the onset of secondary nucleation.

Batch experiments at 55°C were also done to investigate the effect of additives on nucleation and precipitation rates of magnesium sulfite trihydrate. These experiments are described in Technical Note 200-045-54-06. $MgSO_4$ solutions which

TABLE 4-7. RESULTS OF SECONDARY NUCLEATION EXPERIMENTS USING $\text{MgSO}_4 \cdot 6\text{H}_2\text{O}$ SEED CRYSTALS¹

Run	Stirring Speed (RPM)	Temp. (°C)	Solution Composition at Onset of Secondary Nucleation				
			pH	$[\text{Mg}^{++}]$ (gmole/kg)	$[\text{Na}^+]$ (gmole/kg)	$[\text{SO}_4^{--}]$ (gmole/kg)	$[\text{SO}_3^{--}]$ (gmole/kg)
4-3B	1200	30.0	6.03	2.07	.390	2.10	.195
4-4B	1200	44.4	6.03	2.11	.690	2.14	.345
4-7B	1200	46.0	6.0	2.04	.678	2.07	.339
4-8B	1200	45.0	5.96	1.97	.704	2.00	.352
4-9B	1200	33.6	5.75	1.96	.554	1.99	.277
4-10B	1000	32.6	6.10	1.93	.514	1.96	.257
4-11B	1000	32.5	6.13	1.97	.526	2.00	.263
4-12B	1200	60.5	6.25	1.91	1.136	1.94	.568
4-12B	1200	60.5	6.25	1.91	1.060	1.94	.530
4-12B	1200	60.5	6.25	2.07	1.154	2.10	.577
4-12B	1200	60.5	6.25	2.07	1.076	2.10	.538
4-13B	1200	59.2	6.27	2.02	1.038	2.05	.519
4-14B	1000	58.3	6.28	1.96	1.062	1.99	.531

¹ Tests were done by adding Na_2SO_3 to a slurry of 0.1M Na_2SO_3 -2.0M MgSO_4 containing 1g of $\text{MgSO}_4 \cdot 6\text{H}_2\text{O}$ seed crystals.

TABLE 4-8. ACTIVITIES AND ACTIVITY PRODUCTS CALCULATED USING SOLUTION DATA FROM TESTS OF SECONDARY NUCLEATION OF $\text{MgSO}_3 \cdot 6\text{H}_2\text{O}$

Run	$a_{\text{Mg}^{+2}}$	$a_{\text{SO}_3^{-2}}$	$a_{\text{H}_2\text{O}}$	K_{sp_6}	ap_6	Rel. Sat. ₆	$\frac{ap_6}{a_{\text{H}_2\text{O}}^3}$
4-3B	3.349-01	7.276-04	0.939	6.124-05	1.670-04	2.727	2.019-04
4-4B	3.182-01	1.012-03	0.9312	7.62-05	2.100-04	2.756	2.600-04
4-7B	2.955-01	1.322-03	0.9339	7.86-05	2.59-04	3.295	3.18-04
4-8B	2.900-01	1.021-03	0.9345	7.735-05	1.97-04	2.547	2.417-04
4-9B	3.034-01	7.898-04	0.9380	6.45-05	1.632-04	2.530	1.978-04
4-10B	2.935-01	1.053-03	0.9401	6.35-05	2.13-04	3.354	2.568-04
4-11B	3.006-01	1.087-03	0.9388	6.34-05	2.24-04	3.533	2.702-04
4-12B	2.498-01	1.754-03	0.9263	9.78-05	2.77-04	2.83	3.489-04
4-12B	2.531-01	1.612-03	0.9281	9.78-05	2.61-04	2.669	3.262-04
4-12B	2.798-01	1.657-03	0.9215	9.78-05	2.838-04	2.902	3.627-04
4-12B	2.833-01	1.521-03	0.9234	9.78-05	2.67-04	2.730	3.393-04
4-13B	2.749-01	1.544-03	0.9257	9.60-05	2.67-04	2.781	3.368-04
4-14B	2.621-01	1.670-03	0.9268	9.48-05	2.77-04	2.922	3.484-04

*. All analyses are reported in millimoles/liter.

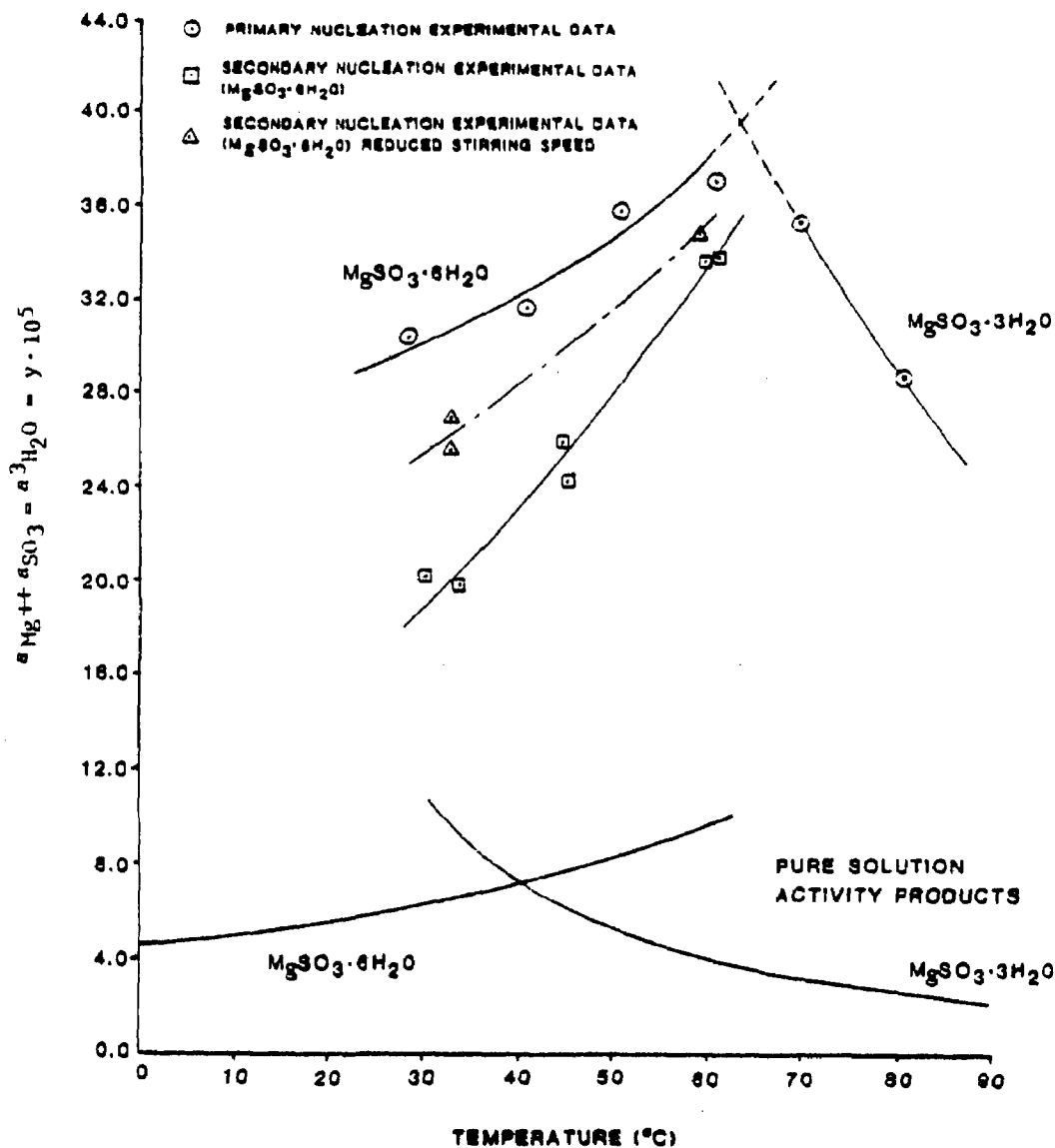


Figure 4-7. Activity Products for MgSO_3 Hydrates in Solutions in which Primary and Secondary Nucleation Occurred (20 wt % MgSO_4 and pH 6)

were supersaturated in Na_2SO_3 were stirred at a temperature of 55°C for 48 hours. Salts with metal cations of high ionic charge were added in an attempt to influence the nucleation or precipitation rate of $\text{MgSO}_3 \cdot 3\text{H}_2\text{O}$. Primary nucleation was studied in some systems and in other systems trihydrate seed crystals were added and secondary nucleation/crystal growth was studied. The change in solids concentration was determined after 48 hours for solutions containing additives. This was compared to the change in control solutions with no additives.

The results were that metal cation additives enhanced the primary nucleation rate, but no increase in precipitation rate was noted in solutions which contained seed crystals.

Precipitation Rates of Magnesium Sulfite Hydrates Measured Separately in Dilute Solutions--

Precipitation rate studies were first conducted separately for each hydrate in dilute solutions. Solution theory for these dilute solutions is adequate to provide accurate methods of calculating activities. Therefore, data correlation is fairly straightforward and it is possible to conduct accurate, meaningful rate measurements for precipitation of the individual hydrates. The conditions in these experiments, however, are not representative of those in actual scrubbing liquors.

The experimental procedure and data analysis methods are described in Technical Note 200-045-36-05. The rate of solids production and the rate of change of sulfite and magnesium concentrations in a batch-liquid, batch-solid stirred reactor were measured at 20 , 30 , and 40°C for the hexahydrate and 55 , 70 , and 85°C for the trihydrate. The procedure involved addition of seed crystals to a 0.2M mixture of MgCl_2 and Na_2SO_3 . The concentrations of Mg^{+2} , SO_3^{-2} , and total sulfur; pH; and weight percent solids were measured periodically thereafter.

The precipitation rate was calculated by plotting the amount of solid reaction product versus time and determining the slope of the curve at various times throughout the experiment. The amount of solids was determined in two ways. One was the measurement of weight percent solids in intermittent slurry samples. The other was from a liquid phase material balance calculation. The decrease in sulfite ion concentration was used to determine the number of moles of magnesium sulfite leaving the solution through formation of solid hydrates.

Rate data were correlated based on the form shown in equation 4-9.

$$R = kM\phi \quad (4-9)$$

where

R = precipitation rate, gmoles/min/gram solids

k = rate constant dependent on liquor temperature, composition, and transport parameters, gmoles/min/cm² solid surface

ϕ = driving force related to the difference between actual and equilibrium quantities of reacting species

M = term dependent on the amount of solid phase present, cm²/g

To attempt to account for the effect of solid surface area, seed material was prepared by sieving the seed crystals through a 400 mesh screen. The seed material had an average particle diameter less than or equal to 37 μ m. The measured

precipitation rates were normalized by dividing by the mass of crystals at the time of the measurement.

The driving force term is expressed as the difference between actual and equilibrium quantities of reacting species as shown by the general form in equation 4-10.

$$\phi = \frac{1}{K_{sp}} \left[(ap)^{1/n} - K_{sp}^{1/n} \right]^n \quad (4-10)$$

where

ap = activity product for the precipitating solid, ap_3 or ap_6 as previously defined

K_{sp} = solubility product constant, K_{sp_3} or K_{sp_6} as previously defined and

n = a parameter which, for this study, was set equal to the number of cations plus anions, i.e., 2.

The driving force term can also be expressed in terms of the relative saturation, RS, as shown in equation 4-11.

$$\phi = \left[RS^{1/n} - 1 \right]^n \quad (4-11)$$

Figures 4-8 through 4-11 show measured, normalized reaction rates in mmoles/gram/min versus relative saturation for the temperatures studied. The figures verify that precipitation rates for the hexahydrate are greater than those for the trihydrate. The hexahydrate rate at 30°C is nearly three orders of magnitude greater than trihydrate precipitation rate at 55°C.

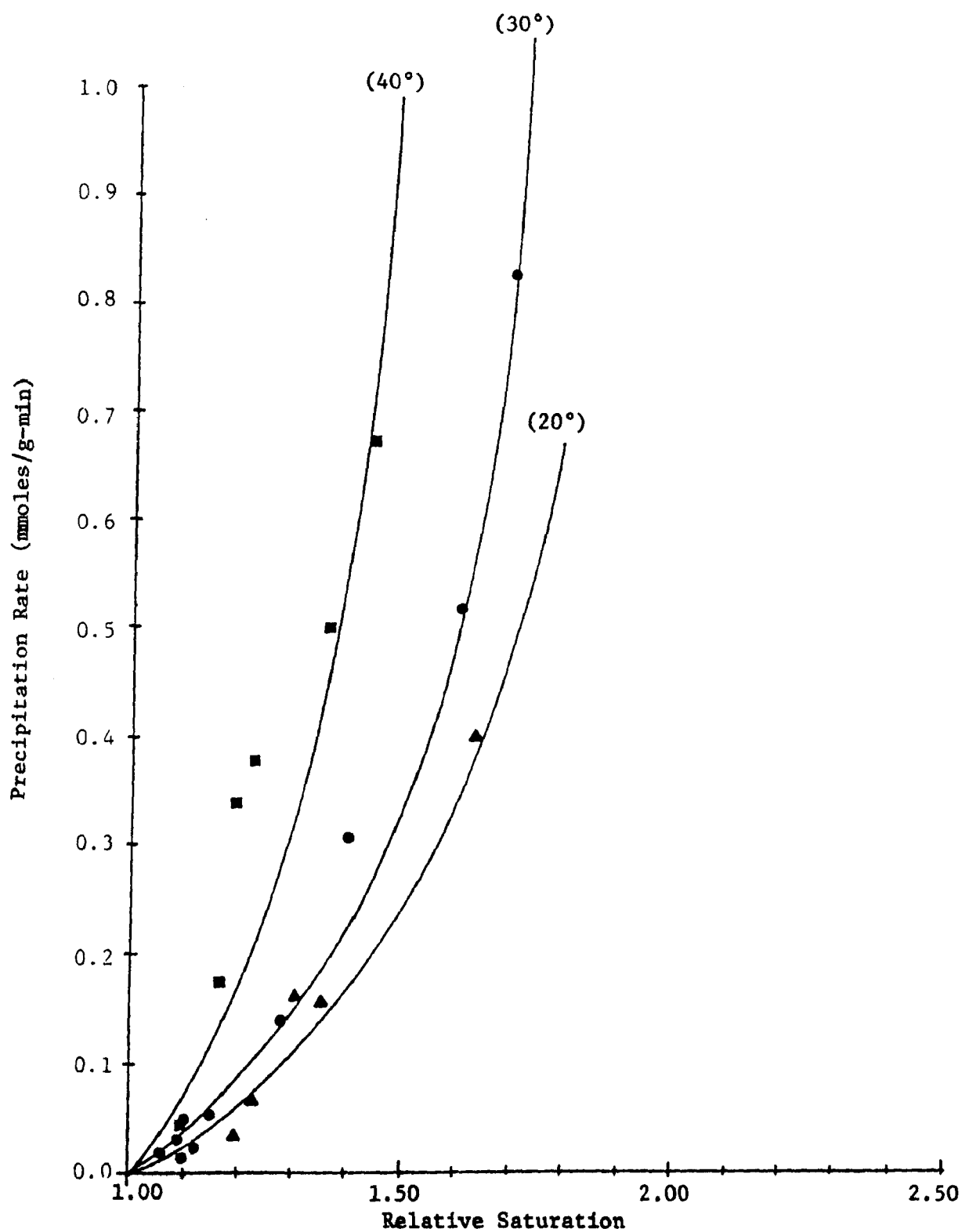


Figure 4-8. $\text{MgSO}_3 \cdot 6\text{H}_2\text{O}$ Precipitation Rate vs
Relative Saturation at Various Temperatures

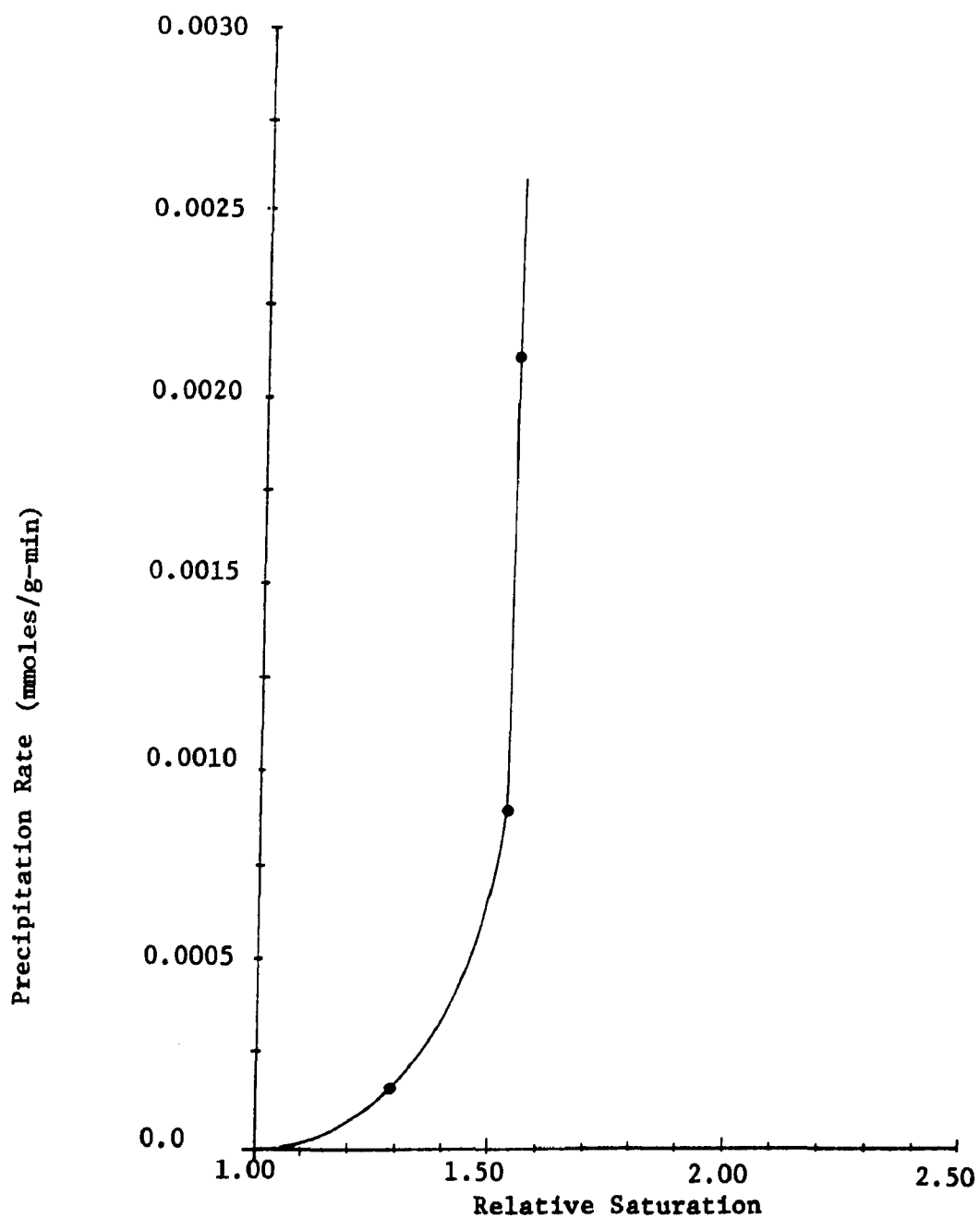


Figure 4-9. $\text{MgSO}_3 \cdot 3\text{H}_2\text{O}$ Precipitation Rate vs Relative Saturation at 55°C

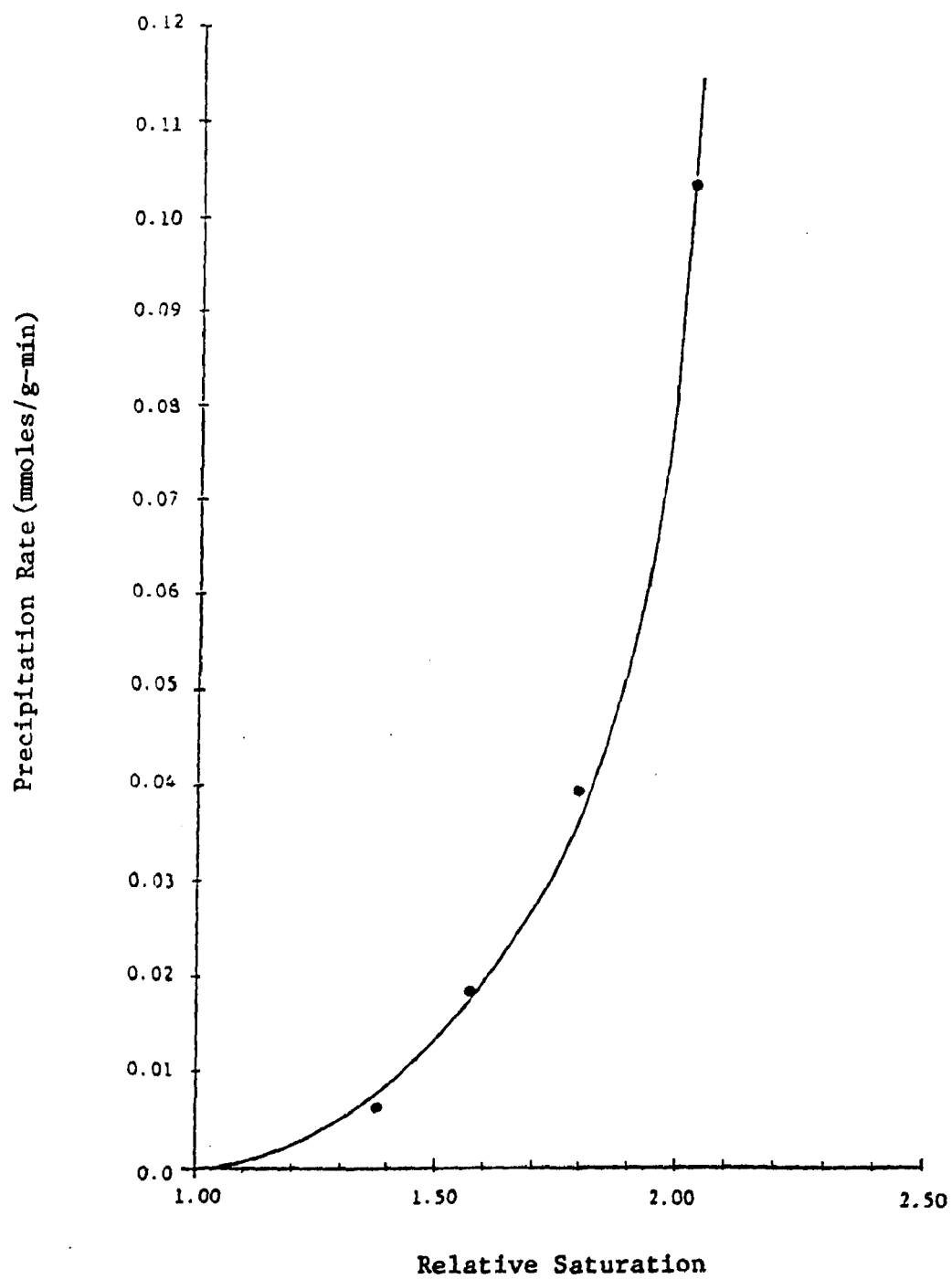


Figure 4-10. $\text{MgSO}_3 \cdot 3\text{H}_2\text{O}$ Precipitation Rate vs Relative Saturation at 70°C

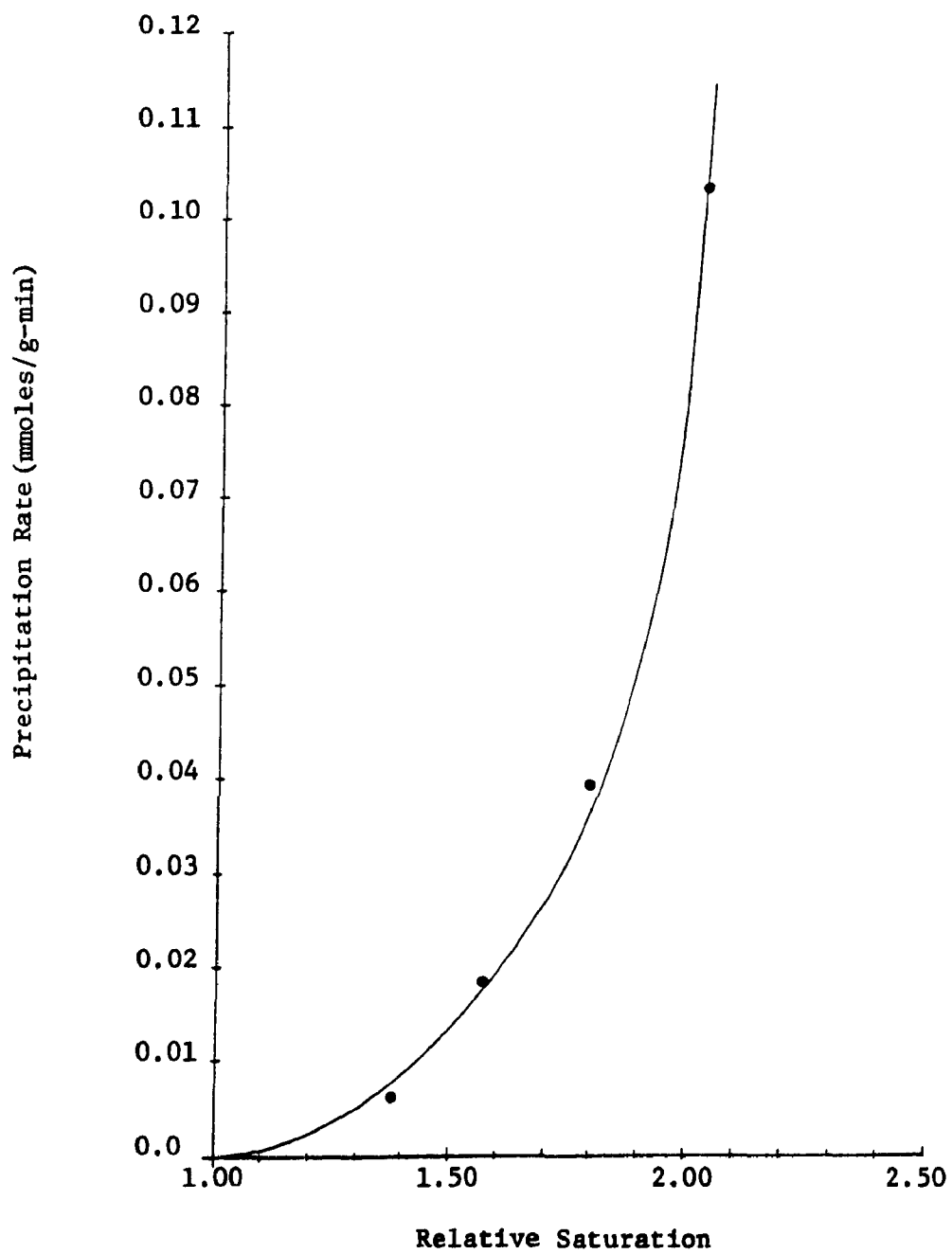


Figure 4-11. $\text{MgSO}_3 \cdot 3\text{H}_2\text{O}$ Precipitation Rate vs Relative Saturation at 85°C

Precipitation Rate Studies of Magnesium Sulfite Hydrates in Scrubber-Like Media--

The rate studies described in the preceding sections were done under conditions designed to allow the investigation of individual phenomena. The tests described in this section were done under conditions characteristic of those in magnesium oxide scrubbing processes in which these phenomena can occur simultaneously.

The equipment and procedures described previously for rate studies in dilute solutions were also employed in these experiments. Batch addition of MgSO_4 and Na_2SO_3 feedstock solutions and MgSO_3 seed crystals was employed. All tests were conducted at 55°C in approximately 20 wt% MgSO_4 solutions at pH 6. The initial sulfite concentration and the composition of the seed crystals were varied in each experiment. Tests were conducted for periods of 1,100 to 11,000 minutes with periodic sampling of the reactant slurry. Analyses performed on the slurry liquor and solids are summarized in Technical Note 200-045-54-03a. Table 4-9 summarizes the experimental conditions for each test.

The data analysis methods employed are essentially the same as those described for the rate studies in dilute solutions. The results of sulfite analysis of the slurry liquor were used to calculate the number of moles of MgSO_3 solids precipitating from solution. Solid samples were characterized using DSC analysis and microscopic examination.

The rate data correlation form shown in equation 4-12 is applicable to the results of these precipitation rate studies.

$$\text{Rate} = \{\text{Kinetic Factor}\} \{\text{Surface Area}\} \left\{ \begin{array}{c} \text{Driving} \\ \text{Force} \end{array} \right\} (4-12)$$

TABLE 4-9. SUMMARY OF EXPERIMENTAL CONDITIONS IN TESTS OF
MAGNESIUM SULFITE HYDRATE PRECIPITATION
FROM SCRUBBER-LIKE MEDIA¹

Test No.	Initial Sulfite Concentration (gmole/l)	Composition of 1 gram of Seed Crystals
3-2	0.316	MgSO ₃ ·3H ₂ O
3-3	0.475	MgSO ₃ ·6H ₂ O
3-4	0.316	MgSO ₃ ·3H ₂ O
3-5	0.367	MgSO ₃ ·6H ₂ O
3-6	0.374	MgSO ₃ ·3H ₂ O (0.5g) and MgSO ₃ ·6H ₂ O (0.5g)
3-7	0.358	MgSO ₃ ·3H ₂ O (0.5g) and MgSO ₃ ·6H ₂ O (0.5g)

¹ Tests were done at 55°C and pH 6 in solutions containing approximately 20 wt % MgSO₄. Initial magnesium concentration varied from 2.01 to 2.04 gmole/l.

The rate equation shown in equation 4-13 is derived in Technical Note 200-045-54-03a.

$$\frac{d(\psi^{1/3})}{dt} = \frac{1}{3}kf_d(r) \quad (4-13)$$

In equation 4-13, ψ is the amount of solid product at time, t , divided by the initial amount of solids; k is the kinetic factor which also takes into account initial crystal surface area, and f_d is the driving force which is described in terms of the activities of reactant species.

Precipitation rate data were plotted in the form of $\psi^{1/3}$ versus time. A logarithmic abscissa was employed due to the time scale of the reactions. The time variable used was θ which is equal to the logarithm of the sample time plus 10 minutes. The ten minute period was added to the sample time so that the first data point would not be zero.

Individual ion activities were calculated using the Radian equilibrium model in order to describe the driving force factor. The activities were used to calculate relative saturations. These calculations indicated that the system approached a steady state relative saturation of 2.5. Theoretically the steady state relative saturation at equilibrium should be equal to 1.0. In order to resolve this discrepancy, equilibrium experiments were done at ionic strengths of about 4 which are characteristic of this system. These equilibrium experiments confirmed the order of magnitude discrepancy in calculated relative saturations. These results indicate that the equilibrium model does not provide an accurate description of equilibrium for the system. While data correlation could be accomplished by going through the mechanics of calculating driving force terms, the results would be inaccurate and possibly misleading.

The results of the precipitation rate studies in scrubber-like media are summarized in the following paragraphs. Six experiments are described. Two were done using trihydrate seed crystals, two using hexahydrate seed crystals, and two using a mixture of the two hydrate crystals.

Figures 4-12 and 4-13 show the results of tests 3-2 and 3-4 done with 1 gram of trihydrate seed crystals both at an initial sulfite concentration of 0.316 gmole/l. The top parts of the graphs indicate the fraction of trihydrate solids in the product. Trihydrate was the only phase that precipitated in these experiments, so the fraction of trihydrate is constant at 1.0. The rate of production of trihydrate solids was fairly constant in both tests, although one rate was a little faster than the other. Since the solution compositions were the same, the driving forces would be expected to be equal in the two experiments. The difference in rates is probably due to crystal surface area effects. It appears that equilibrium was reached in test 3-4 as indicated by the constant value of $\psi^{1/3}$ at the end of the test.

Figures 4-14 and 4-15 show the results of tests done using hexahydrate seed crystals. The initial sulfite concentration was 0.475 g/mole/l in test 3-3, (Figure 4-14) and 0.367 gmole/l in test 3-5 (Figure 4-15). Hexahydrate nucleation was visually observed in the first 20 minutes of test 3-3. Nucleation is indicated in Figure 4-14 by the initial high rate of solids production. The results of DSC solids analysis indicate that trihydrate was not formed during the initial 200 minutes of this test.

Test 3-5 (Figure 4-15) was done with hexahydrate seed crystals at a lower initial sulfite concentration. Hexahydrate nucleation was not apparent. Solids analyses indicate the

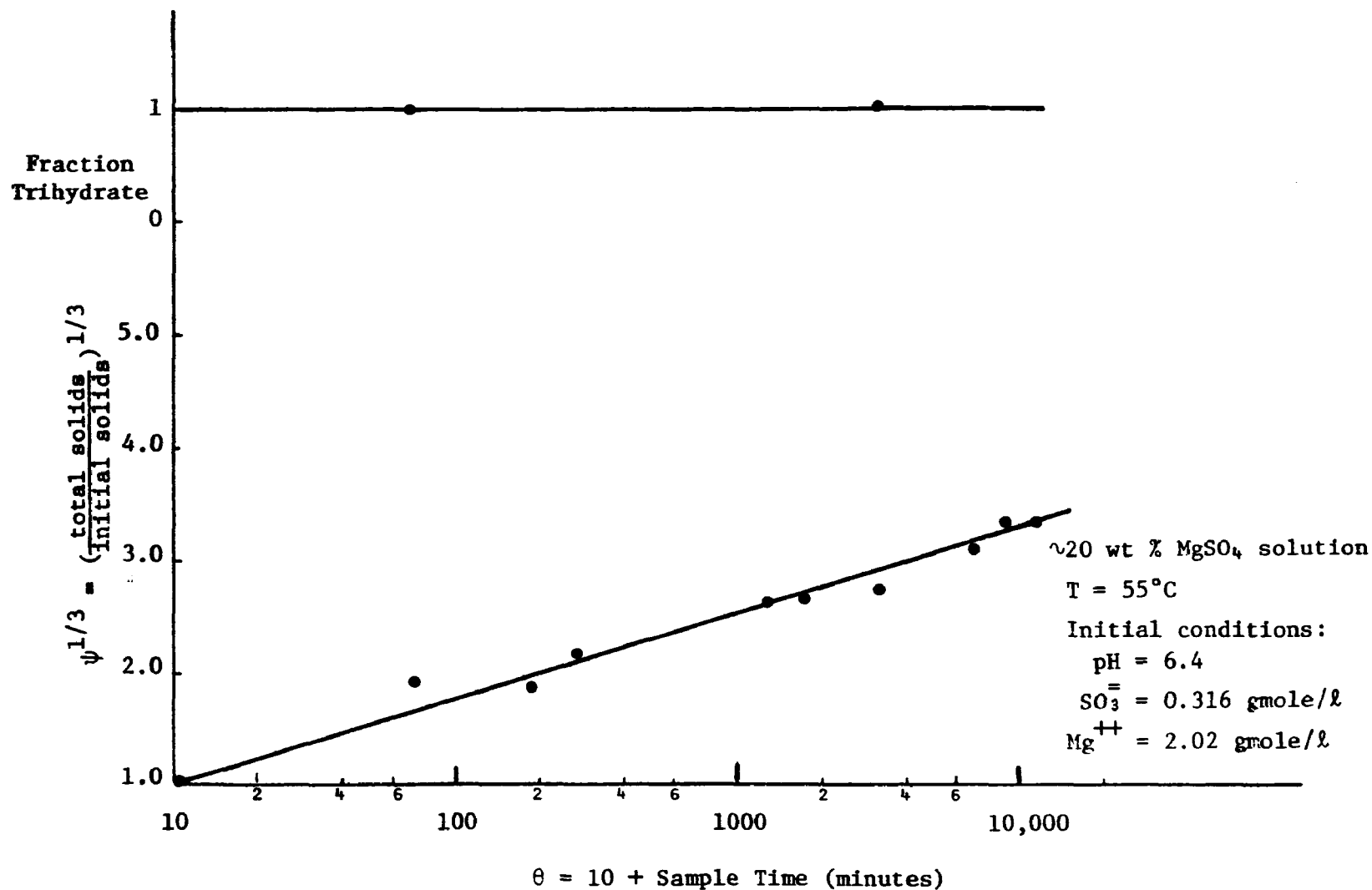


Figure 4-12. Results of MgSO_3 Hydrate Precipitation Rate
 Experiment 3-2 Employing Trihydrate Seed Crystals

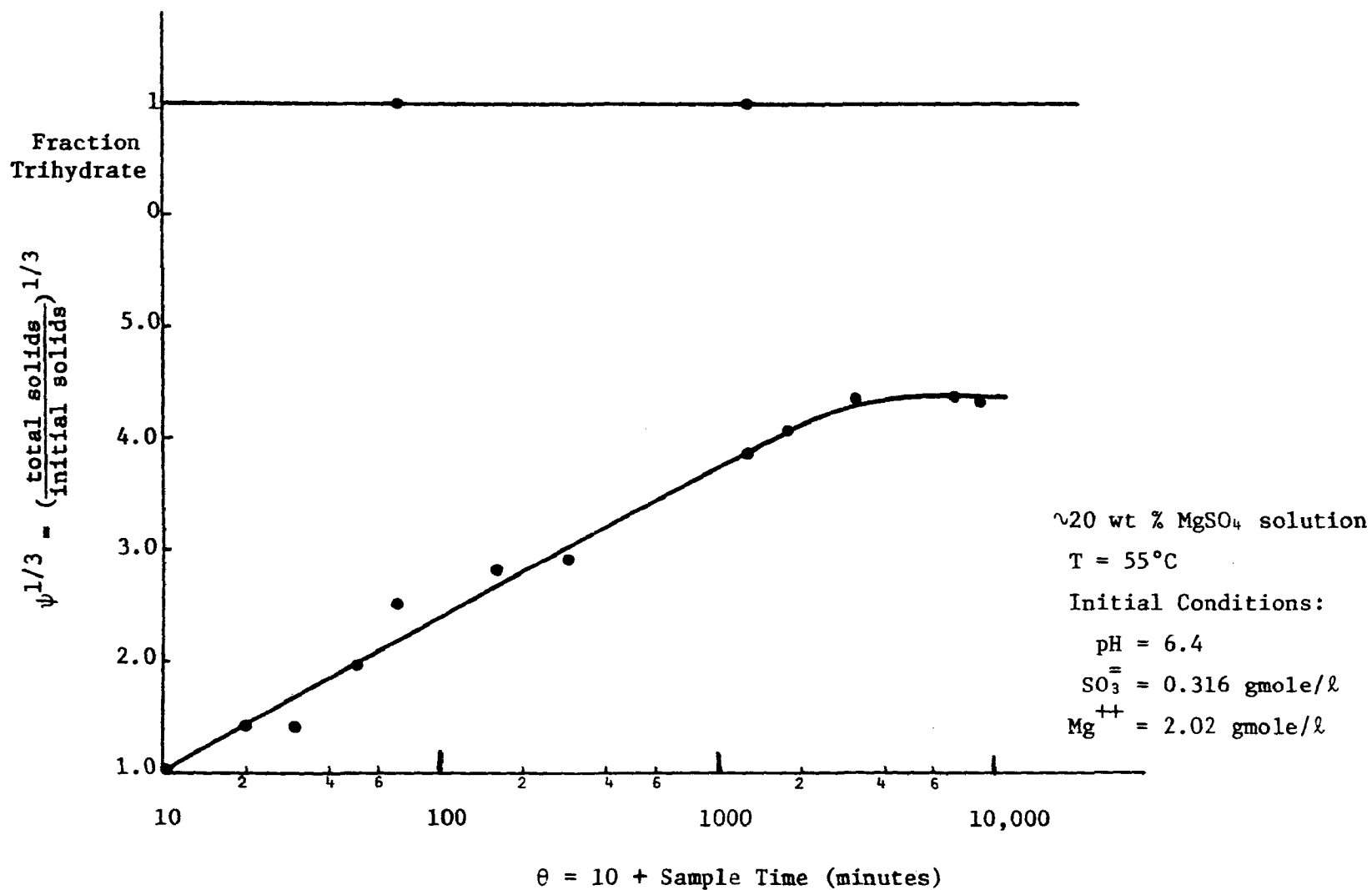


Figure 4-13. Results of MgSO_3 Hydrate Precipitation Rate Experiment 3-4
 Employing Trihydrate Seed Crystals

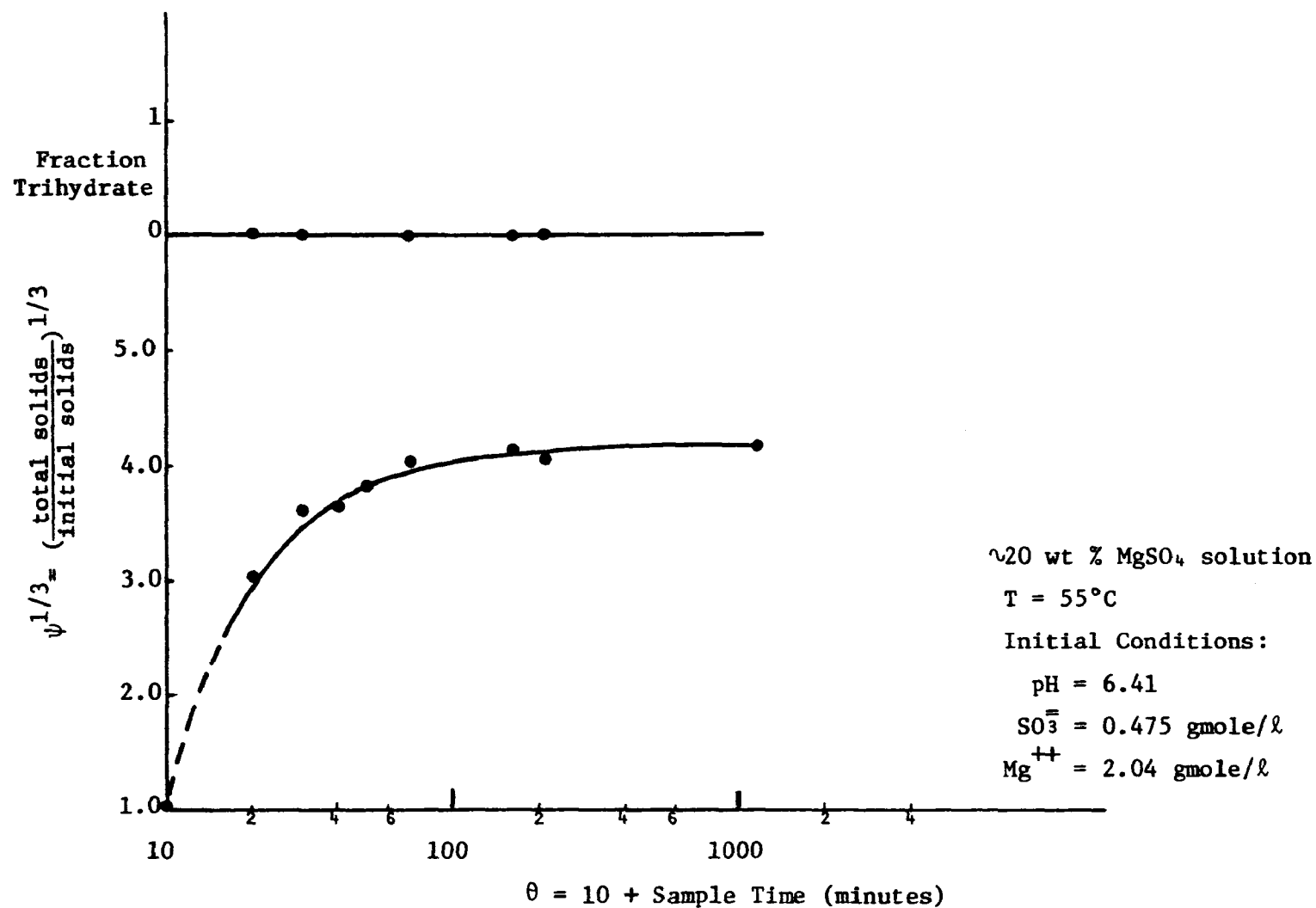


Figure 4-14. Results of MgSO_3 Hydrate Precipitation Rate Experiment 3-3
Employing Hexahydrate Seed Crystals

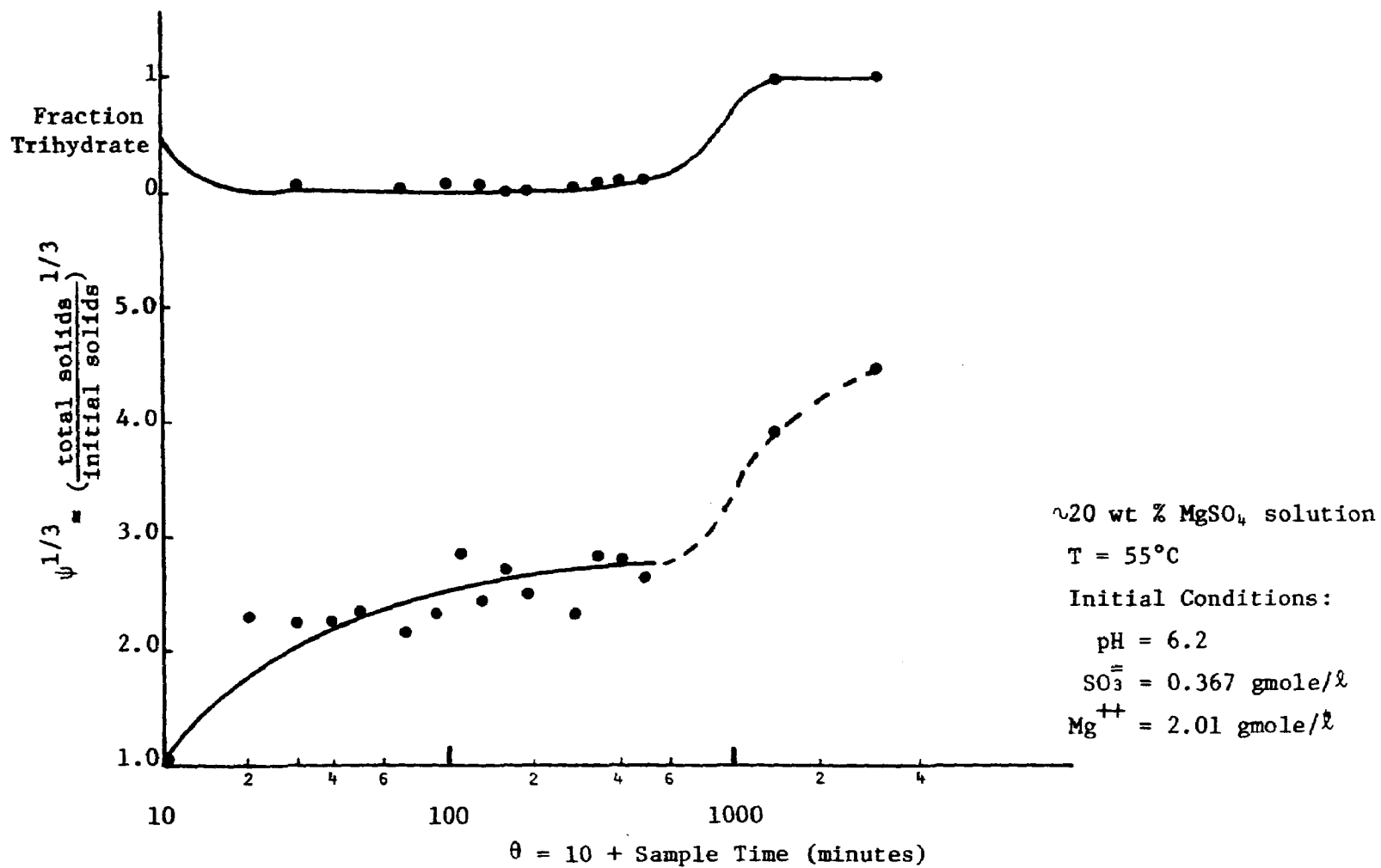


Figure 4-15. Results of MgSO_3 Hydrate Precipitation Rate Experiment 3-5
Employing Hexahydrate Seed Crystals

possibility of a very small amount of trihydrate in the seed crystals. The results of the liquid and solid analyses indicate that the following phenomena occurred during the 3,200 minute test. Hexahydrate precipitated during the first part of the test. This was followed by an intermediate period during which the amount of solids remained relatively constant. During this period the hexahydrate dissolved and the trihydrate precipitated. After all the hexahydrate dissolved, the amount of solids again increased due to further trihydrate precipitation. The trihydrate precipitation rate was dependent on the amount of trihydrate crystal surface area available. During the 930 minute period from 470 to 1,400 minutes the fraction of trihydrate increased from about 0.1 to about 1. At the end of 3,200 minutes the product was pure trihydrate.

The results of the tests 3-6 and 3-7 employing seed crystals composed of 0.5 grams of each hydrate are shown in Figures 4-16 and 4-17. The results of tests 3-6 and 3-7 can be explained on the same basis as those of test 3-5.

The results of tests of the precipitation rates of mixed hydrates in scrubber-like media provide an accurate qualitative explanation of what can occur during the operation of magnesium oxide scrubbing processes. Data are available for obtaining a quantitative rate correlation; however, some refinement of computational tools would be required in order to calculate accurate driving force terms.

The results for mixed hydrate precipitation in scrubber-like media are consistent with those for precipitation of individual hydrates in dilute solutions and tests of primary and

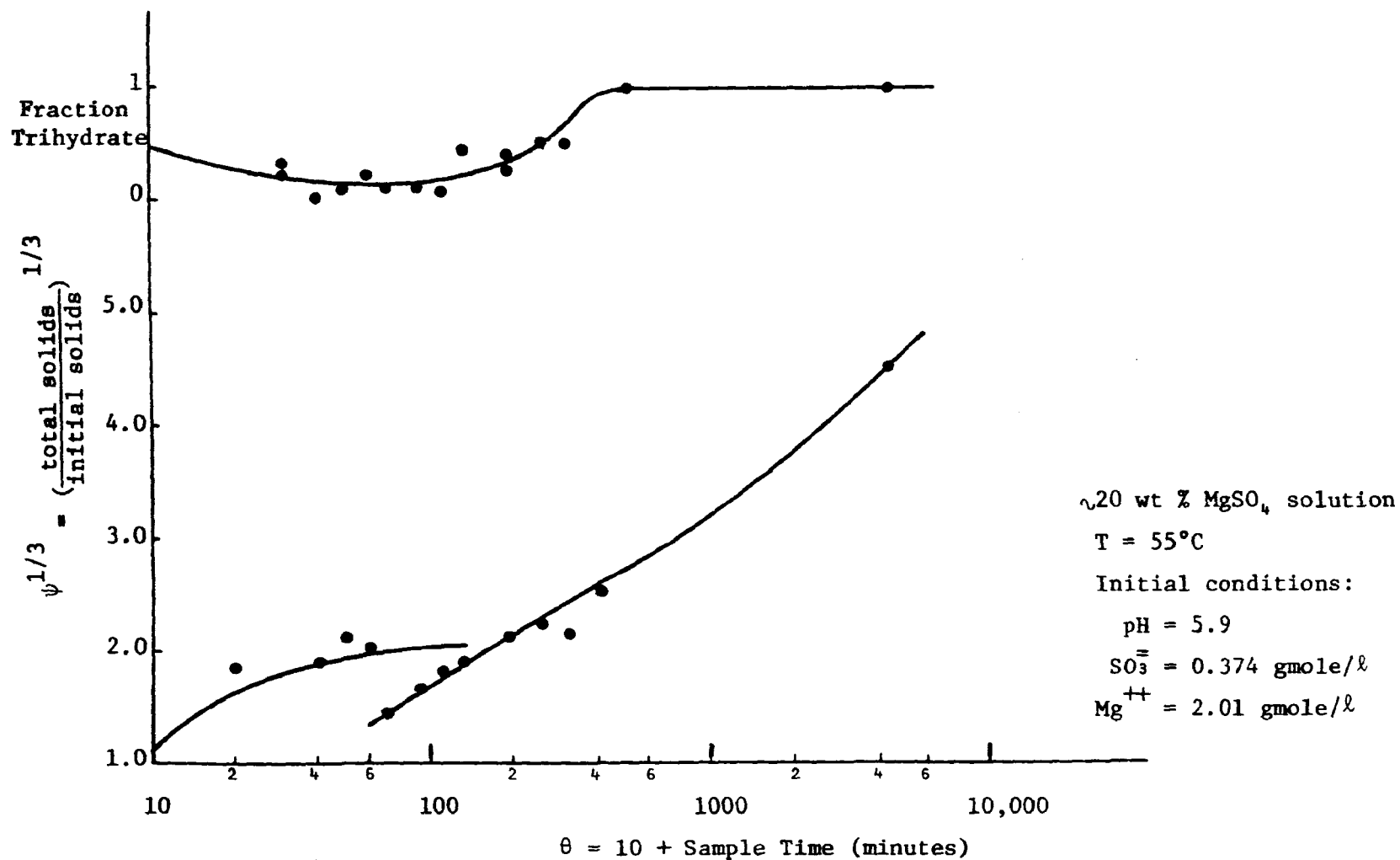


Figure 4-16. Results of MgSO_3 Hydrate Precipitation Rate Experiment 3-6 Employing a Mixture of Tri- and Hexahydrate Seed Crystals

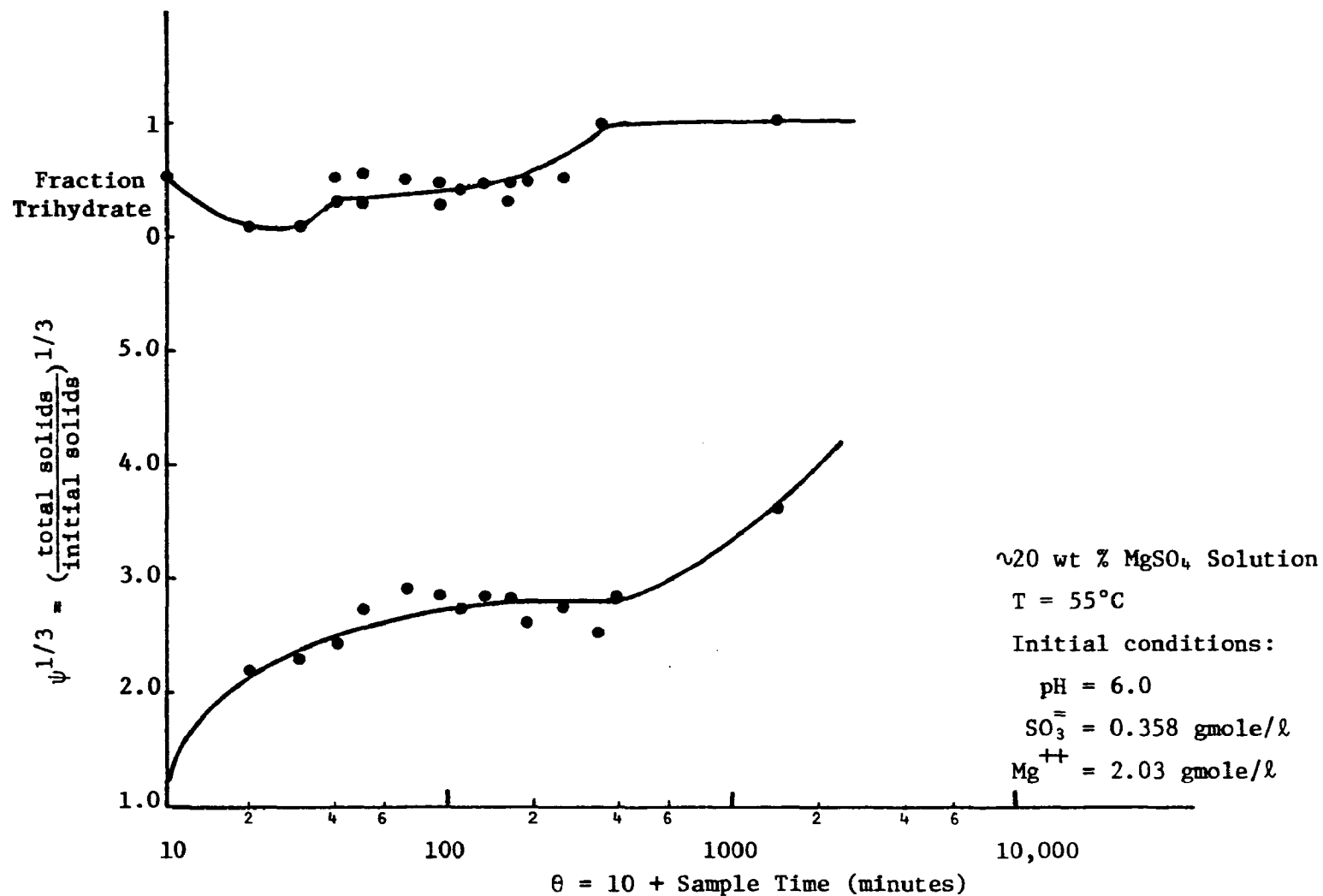


Figure 4-17. Results of MgSO_3 Hydrate Precipitation Rate Experiment 3-7
 Employing a Mixture of Tri- and Hexahydrate Seed Crystals

secondary nucleation in scrubber-like media. Hexahydrate nucleation and precipitation rates are faster than those of the trihydrate. The trihydrate is the thermodynamically stable phase. Clear evidence of trihydrate nucleation is not apparent. These results provide an adequate basis for the design of a magnesium oxide system to produce either hydrate as an intermediate solid product.

BIBLIOGRAPHY

- LO-R-007 Lowell, P.S., et al., A Theoretical Description of the Limestone Injection Wet Scrubbing Process, Final Report, 2 Vols., PB 193-029, PB 193-030, Contract No. CPA-22-69-138. Radian Project 200-002. Austin, Texas, Radian Corporation, June 1970.

APPENDICES

TECHNICAL NOTE 200-045-36-01
LITERATURE SURVEY OF
INFORMATION AVAILABLE ON
MAGNESIUM SULFITE HYDRATE
FORMATION MECHANISMS

Prepared by:
Ralph E. Sawyer

CONTENTS

1.	Introduction	66
	Background.	66
	Objectives.	67
2.	Basis of the Literature Survey	68
3.	Magnesium Sulfite Equilibrium and Kinetic Data for Aqueous Systems	70
	Solubility of Magnesium Sulfite	70
	Magnesium Sulfite in Scrubbing Liquors.	70
4.	Mag-Ox Plant Operating Characteristics	98
	References.	107

FIGURES

<u>Number</u>		<u>Page</u>
3-1	Effect of Temperature on Magnesium Sulfite Solubility	71
3-2	Mutual Solubility of Magnesium Sulfite-Bisulfite- and Sulfate at 40°, 50°, and 60°	74
3-3	Ternary Diagram of the MgO-SO ₂ -H ₂ O System (Liquid Phase)	77
3-4	System of Components Mg(HSO ₃) ₂ , MgSO ₃ , H ₂ SO ₃ , and H ₂ O.	77
3-5	Effect of Magnesium Sulfate on Magnesium Sulfite Solubility	79
3-6	Influence of Magnesium Sulfate Concentration on the Time of Recrystallization of Magnesium Sulfite Hexahydrate into the Trihydrate.	83
3-7	Time of Recrystallization of Magnesium Sulfite Trihydrate into the Hexahydrate.	85
3-8	Effect of Temperature and Slurry Concentration on Conversion Rate of MgSO ₃ ·6H ₂ O to MgSO ₃ ·3H ₂ O.	85

FIGURES (Cont'd)

<u>Number</u>		<u>Page</u>
3-9	DTA Thermogram of Dehydration of $\text{MgSO}_3 \cdot 3\text{H}_2\text{O}$ in a Self-Generated Atmosphere.	88
3-10	DTA Thermogram of Dehydration of $\text{MgSO}_3 \cdot 6\text{H}_2\text{O}$ in a Self-Generated Atmosphere.	89
3-11	DSC Thermogram of $\text{MgSO}_3 \cdot 3\text{H}_2\text{O}$ Dehydration in a Nitrogen Atmosphere.	90
3-12	DSC Thermogram of $\text{MgSO}_3 \cdot 6\text{H}_2\text{O}$ Dehydration in a Nitrogen Atmosphere.	91
3-13	TGA Thermogram of $\text{MgSO}_3 \cdot 3\text{H}_2\text{O}$ Dehydration in a Nitrogen Atmosphere.	93
3-14	TGA Thermogram of $\text{MgSO}_3 \cdot 6\text{H}_2\text{O}$ Dehydration in a Nitrogen Atmosphere.	95
3-15	TGA Thermogram of $\text{MgSO}_3 \cdot 3\text{H}_2\text{O}$ Dehydration in a Self-Generated Atmosphere	96
3-16	TGA Thermogram of $\text{MgSO}_3 \cdot 6\text{H}_2\text{O}$ Dehydration in a Self-Generated Atmosphere	97
4-1	Venturi Scrubber	104
4-2	Floating Bed Absorber.	104
4-3	Boston Edison Scrubber	105
4-4	Dickinson Station Scrubber	106

TABLES

<u>Number</u>		<u>Page</u>
3-1	Solubility of Magnesium Sulfite in Water (Hagisawa, 1934)	72
3-2	Magnesium Sulfite Hydrate Transition at Room Temperature.	80
3-3	Transition of $\text{MgSO}_3 \cdot 6\text{H}_2\text{O}$ pH Adjusted by Diluted H_2SO_4	82
4-1	Plant Operating Characteristics.	99

SECTION 1

INTRODUCTION

BACKGROUND

In an MgO scrubber system, a circulating slurry of MgO and hydrated MgSO_3 is used to absorb SO_2 from a flue gas stream. The SO_2 is removed from the scrubbing system as a precipitate of hydrate magnesium sulfite. Two hydrates have been identified, $\text{MgSO}_3 \cdot 3\text{H}_2\text{O}$ and $\text{MgSO}_3 \cdot 6\text{H}_2\text{O}$. The crystals formed in the installation which removes SO_2 from the flue gases of Boston Edison's oil fired boiler were found to be primarily trihydrate crystals. The installation at PEPCO's coal fired boiler produced primarily hexahydrate crystals.

The removal of SO_2 from flue gas streams by an MgO scrubbing system has proven to be technically feasible. The status of technology at the time the above units were designed was insufficient to predict which hydrated form would be favored. An understanding of the phenomena involved in the production of each hydrated form is important. The trihydrate crystals produced are small in size. In comparison, the hexahydrate crystals are large massive particles. Therefore, the settling and handling characteristics of these two hydrated states are markedly different. From a process point of view, the trihydrate may be the desirable crystalline form because it takes less energy to drive off the waters of hydration when the crystals are calcined to regenerate the MgO. The economics may depend, however, on the form of available heat. It is presently easier from an operating standpoint to produce hexahydrate crystals because of the ease with which the hexahydrate solids can be removed from the liquids in the scrubber.

OBJECTIVES

The objective of this literature survey is to present currently available information on $\text{MgSO}_3 \cdot 3\text{H}_2\text{O}$ and $\text{MgSO}_3 \cdot 6\text{H}_2\text{O}$ as pure solids, in aqueous solutions, and as binary mixtures. Information on thermodynamic and kinetic factors that would influence the system is also discussed. In addition, plant operating data concerning slurry mixtures of $\text{MgSO}_3 \cdot 6\text{H}_2\text{O}$ and $\text{MgSO}_3 \cdot 3\text{H}_2\text{O}$ are presented.

SECTION 2

BASIS OF THE LITERATURE SURVEY

The following sources were consulted for the present literature evaluation:

1. Chemical Abstracts - This source was consulted for the period of May 1975 - January 1977.
2. EPA Report R2-73-244, "Conceptual Design and Cost Study of SO₂ Removal from Power Plant Stack Gas."
3. Link, W. F., Solubilities of Inorganic and Metal Organic Compounds Volume II, Washington, D.C., American Chemical Society, p. 524.
4. Biannual Reviews on Analytical Chemistry Application - The reviews from the years 1971 and 1973 were considered.
5. Battelle Memorial Institute, "Fundamental Study of Sulfur Fixation by Lime and Magnesia," June 1966, NTIS Bulletin PB-176-843.
6. Report No. Y-8513, "Final Report for the Evaluation of the Magnesium Oxide Scrubbing System at Potomac Electric Power's Dickerson Station," York Research Corp., Stamford, Conn., January 1975.

7. Research Center Report 5153, "Magnesia Base Wet Scrubbing of Pulverized Coal Generated Flue Gas Pilot Demonstration," The Babcock and Wilcox Company, Research and Development Division, Alliance, Ohio, September 1970.
8. EPA-600/2-75-057, "The Magnesia Scrubbing Process as Applied to an Oil-Fired Power Plant," Chemical Construction Corporation, New York, New York, October 1975.
9. Other miscellaneous sources.

SECTION 3

MAGNESIUM SULFITE EQUILIBRIUM AND KINETIC DATA FOR AQUEOUS SYSTEMS

SOLUBILITY OF MAGNESIUM SULFITE

Pinaev (PI-070), Link (LI-068), Markant (MA-089) and others present solubility data for pure MgSO_3 in deionized water as a function of temperature and hydrate state. A plot of the solubility of MgSO_3 as a function of temperature, using these data points, is presented in Figure 3-1. The complete data set of Hakisawa is also illustrated in Table 3-1.

MAGNESIUM SULFITE IN SCRUBBING LIQUORS

The transition temperature between $\text{MgSO}_3 \cdot 6\text{H}_2\text{O}$ and $\text{MgSO}_3 \cdot 3\text{H}_2\text{O}$ is quoted as being between 40-50°C (KU-083, PI-073) in a binary system. There is some disagreement as to where the transition temperature in scrubbing liquors occurs. It is known that $\text{MgSO}_3 \cdot 6\text{H}_2\text{O}$ precipitates in the sulfur dioxide scrubber section even when the solution temperature exceeds 50°C (MC-076). There were at least two explanations offered for this phenomenon.

1. Since there is a solid phase of MgO-Mg(OH)_2 in the scrubber, the stable phase on the surface of an MgO particle may be $\text{MgSO}_3 \cdot 6\text{H}_2\text{O}$.
2. The stable phase at SO_2 scrubber operating temperatures may be $\text{MgSO}_3 \cdot 6\text{H}_2\text{O}$ and the temperature of transition exceeds 50°C.

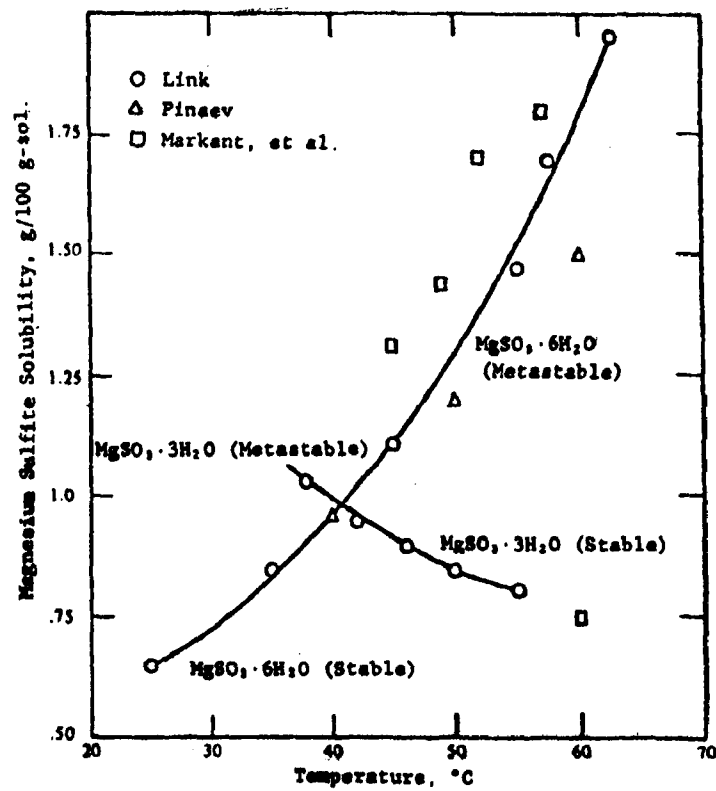


Figure 3-1. Effect of Temperature on Magnesium Sulfite Solubility

TABLE 3-1. SOLUBILITY OF MAGNESIUM SULFITE IN WATER (Hagisawa, 1934)

Temp. (°C)	Grams MgSO_3 /100 Grams Saturated Solution	Solid Phase	Temp. (°C)	Grams MgSO_3 /100 Grams Saturated Solution	Solid Phase
0	0.338	$\text{MgSO}_3 \cdot 6\text{H}_2\text{O}$	38	1.034*	$\text{MgSO}_3 \cdot 3\text{H}_2\text{O}$
15	.497	$\text{MgSO}_3 \cdot 6\text{H}_2\text{O}$	40	Transition Point	$\text{MgSO}_3 \cdot 6\text{H}_2\text{O} +$ $\text{MgSO}_3 \cdot 3\text{H}_2\text{O}$
25	.646	$\text{MgSO}_3 \cdot 6\text{H}_2\text{O}$	42	0.937	$\text{MgSO}_3 \cdot 3\text{H}_2\text{O}$
35	.846	$\text{MgSO}_3 \cdot 6\text{H}_2\text{O}$	46	.897	$\text{MgSO}_3 \cdot 3\text{H}_2\text{O}$
40	Transition Point	$\text{MgSO}_3 \cdot 6\text{H}_2\text{O} +$ $\text{MgSO}_3 \cdot 3\text{H}_2\text{O}$	50	.844	$\text{MgSO}_3 \cdot 3\text{H}_2\text{O}$
45	1.116*	$\text{MgSO}_3 \cdot 6\text{H}_2\text{O}$	55	.817	$\text{MgSO}_3 \cdot 3\text{H}_2\text{O}$
55	1.465*	$\text{MgSO}_3 \cdot 6\text{H}_2\text{O}$	65	.720	$\text{MgSO}_3 \cdot 3\text{H}_2\text{O}$
57.5	1.688*	$\text{MgSO}_3 \cdot 6\text{H}_2\text{O}$	75	.664	$\text{MgSO}_3 \cdot 3\text{H}_2\text{O}$
62.5	1.950*	$\text{MgSO}_3 \cdot 6\text{H}_2\text{O}$	85	.623	$\text{MgSO}_3 \cdot 3\text{H}_2\text{O}$
			98	.615	$\text{MgSO}_3 \cdot 3\text{H}_2\text{O}$

*Metastable

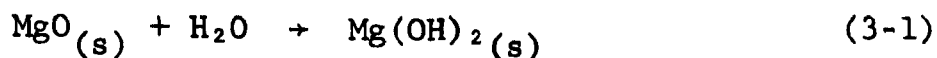
A third explanation put forth by P.S. Lowell, et al. (LO-153) argues that the transition temperature between $\text{MgSO}_3 \cdot 3\text{H}_2\text{O}$ and $\text{MgSO}_3 \cdot 6\text{H}_2\text{O}$ solids when precipitated in aqueous solution is dependent on the solution composition. Furthermore, the transition temperature is lowered from a maximum of 41°C as the dissolved solids content of the solution increases. Therefore, the precipitation of $\text{MgSO}_3 \cdot 6\text{H}_2\text{O}$ at scrubber conditions cannot be explained from an equilibrium standpoint but must be a kinetic phenomenon.

Information is also available on the chemistry of magnesium sulfite in a slurry solution with other species such as $\text{MgSO}_4 \cdot x\text{H}_2\text{O}$, MgO , and $\text{Mg}(\text{HSO}_3)_2$ (PI-072). The temperature dependence of the solubilities of magnesium sulfite and sulfate are summarized in Figure 3-2.

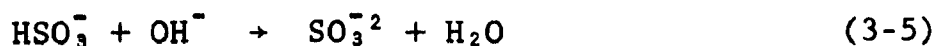
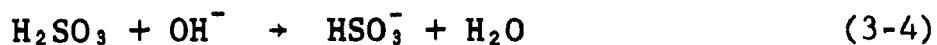
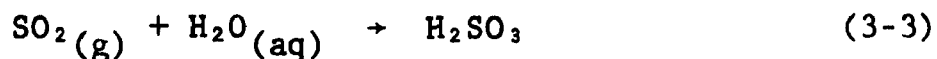
The chemistry of the magnesia base system plays an important role in the absorption of SO_2 . The overall reaction of the system is simply $\text{MgO} + \text{SO}_2 + \text{H}_2\text{O} \rightarrow \text{MgSO}_3 \cdot 6\text{H}_2\text{O} / \text{MgSO}_3 \cdot 3\text{H}_2\text{O}$.

This reaction can be viewed stepwise as:

Slaking Reactions:



SO_2 Absorption



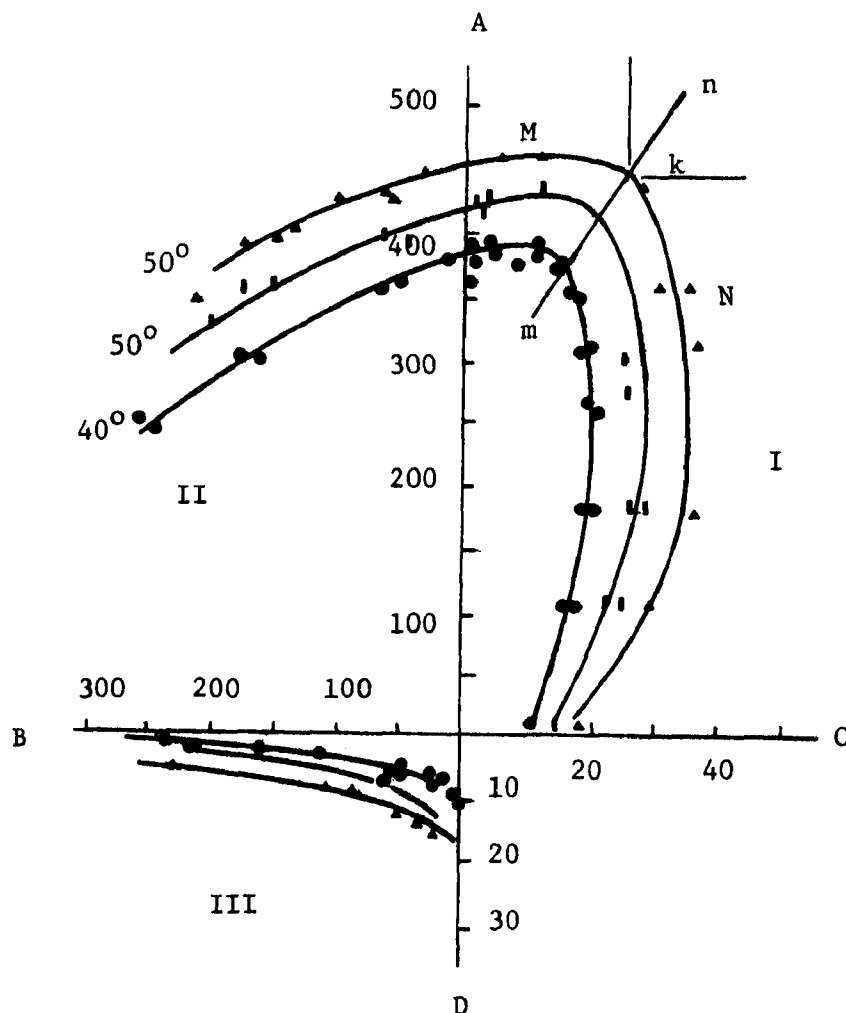


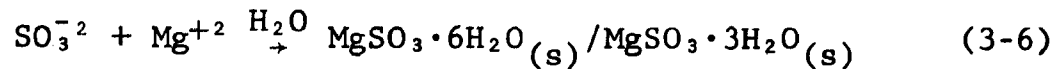
Figure 3-2. Mutual Solubility of Magnesium Sulfite-Bisulfite- and Sulfate at 40°, 50°, and 60°

- (A) MgSO_3 Content (g/liter)
- (B) $\text{Mg}(\text{HSO}_3)_2$ Content (g/liter)
- (C) MgSO_3 Content (g/liter)
- (D) MgSO_3 Content (g/liter)

SYSTEM ZONES

- (I) $\text{MgSO}_4\text{-MgSO}_3\text{-H}_2\text{O}$
- (II) $\text{MgSO}_4\text{-Mg}(\text{HSO}_3)_2\text{-H}_2\text{O}$
- (III) $\text{MgSO}_3\text{-Mg}(\text{HSO}_3)_2\text{-H}_2\text{O}$

Precipitation:



Under actual field conditions the composition of the absorbing slurry is usually controlled by the rate of MgO make-up. Three classes of the spray slurry are possible (DO-015).

Case 1: Excess sulfate, complete neutralization.

Composition: Mg^{+2} , HSO_3^- , SO_3^{-2} , $\text{MgSO}_3 \cdot 6\text{H}_2\text{O} / \text{MgSO}_3 \cdot 3\text{H}_2\text{O}$.

Case 2: Excess MgO {or $\text{Mg}(\text{OH})_2$ }, complete neutralization.

Composition: Mg^{+2} , SO_3^{-2} , $\text{MgSO}_3 \cdot 6\text{H}_2\text{O} / \text{MgSO}_3 \cdot 3\text{H}_2\text{O}$, OH^- , MgO {or $\text{Mg}(\text{OH})_2$ }.

Case 3: Incomplete neutralization (either excess bisulfite or MgO).

Composition: Mg^{+2} , SO_3^{-2} , $\text{MgSO}_3 \cdot 6\text{H}_2\text{O}$, MgO {or $\text{Mg}(\text{OH})_2$ }, HSO_3^- .

Case 3 is probably most prevalent because a small fraction of the MgO is slow to react even under strongly acidic conditions. On the other hand, Reactions 3-4 and 3-5 are ionic and therefore probably instantaneous.

In the calcium oxide and calcium carbonate absorption systems, the slurry concentration, or more explicitly, the specific surface of the limestone is a very important parameter and is possibly a controlling factor in SO_2 absorption. The magnesia-based system shows no corresponding dependence on slurry concentration because of the relatively high solubility of the magnesium sulfite. The ratio of the solubility of magnesium sulfite to calcium sulfite is 485 mole/mole at 78°C .

Since the sulfite ion acts as a buffer to maintain a nearly constant hydroxide ion concentration, the dissolution rate of magnesium hydroxide becomes less important. The calcium based system has no such buffering effect. Unfortunately, other than the developmental work done by TVA (TE-030) and several published reports by Chemico (QU-013), the most recent information is either considered proprietary in nature, or is as yet unpublished.

Some of the first chemical and physical data applicable to the magnesia process came from the pulp and paper industry, which has long used sulfite pulping with subsequent SO_2 recovery. Because of the nature of the pulping operation, much of this information applies to magnesium sulfite/bisulfite solutions and is, therefore, more related to the clear liquor process rather than the slurry process (MC-076). However, even in the pulp and paper industry, there are still many characteristics of magnesia-based solutions that have not been studied. H. P. Markant and Associates (MA-089) began an experimental program in the 1960's to gather data on the specific gravity, electrical conductivity, viscosity, surface tension, solubility and SO_2 vapor pressures of magnesia-based solutions over a wide range of compositions.

A summary of this work is exhibited in Figures 3-3 and 3-4. Figure 3-3 is a ternary diagram presentation of the experimental data in the form of isothermal lines of equilibrium composition of the saturated solutions.

A more usable form of this diagram is shown in Figure 3-4, which is plotted in terms of the combined and free SO_2 . The acid portion of the magnesium bisulfite, namely H_2SO_3 , is

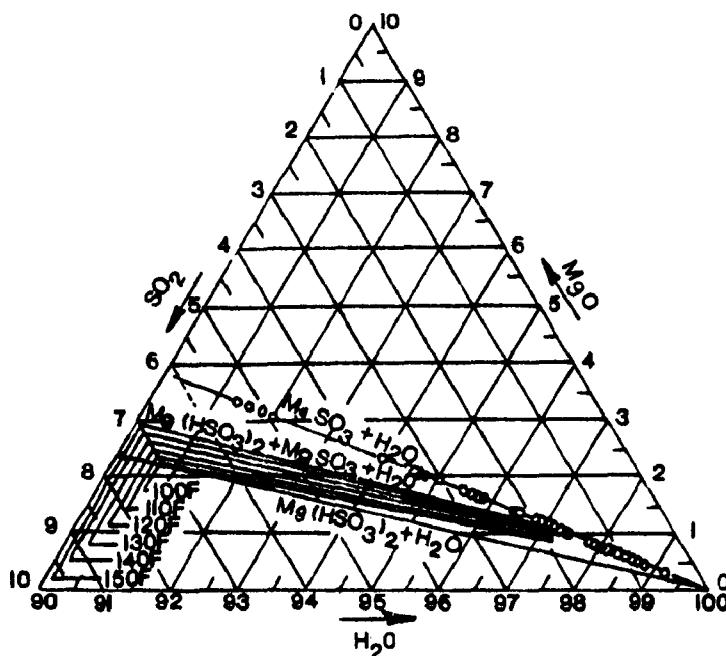


Figure 3-3. Ternary Diagram of the $\text{MgO-SO}_2\text{-H}_2\text{O}$ System (Liquid Phase)

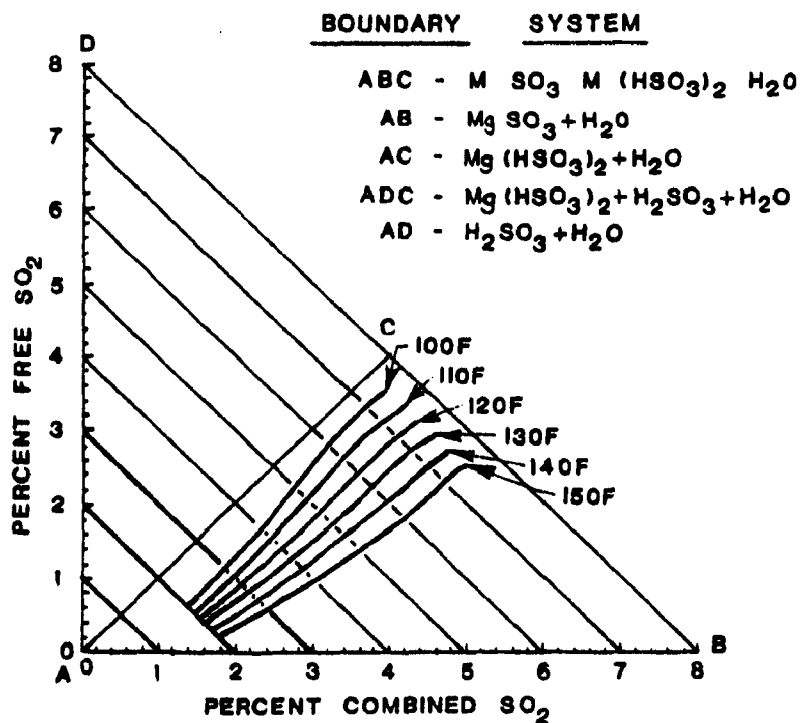


Figure 3-4. System of Components $\text{Mg(HSO}_3)_2$, MgSO_3 , H_2SO_3 , and H_2O

referred to as the free SO_2 concentration and is by convention considered to be one-half of the molar concentration of HSO_3^- expressed as SO_2 (DO-015).

Markant (MA-065), as early as 1965, reported the existence of $\text{MgSO}_3 \cdot x\text{H}_2\text{O}$, where x is less than 3, solids at temperatures of 59°C and 76°C in saturated solutions. However, these substances could not be isolated because they converted immediately to a more stable state.

Because the oxidation of sulfite can occur in a scrubbing medium, substantial amounts of MgSO_4 may be present in process solutions. Several authors have looked into the effects of MgSO_4 upon MgSO_3 characteristics in solution (PI-072; MC-076). In general, the addition of MgSO_4 up to concentrations of 200 grams per liter have been reported to increase the solubility of MgSO_3 over temperature ranges typically encountered in MgO scrubbing liquors (see Figure 3-5). The pH of the MgSO_4 solution was not reported in these studies.

One study noted that the concentration of MgSO_4 may have an influence on whether trihydrate or hexahydrate crystals will form in a scrubbing slurry. Slurries were prepared with a composition similar to conditions obtained during normal operations of MgO scrubbing systems. These bottles were then placed in a constant temperature bath. After a predetermined period of time the bottles were taken out and the contents filtered immediately, washed with methanol and dried in air at 40°C . The crystals were analyzed for sulfite, sulfate, and MgO content. The ratio of the two hydrates was determined using a chemical method developed at Chemico's laboratory. The results are shown in Table 3-2.

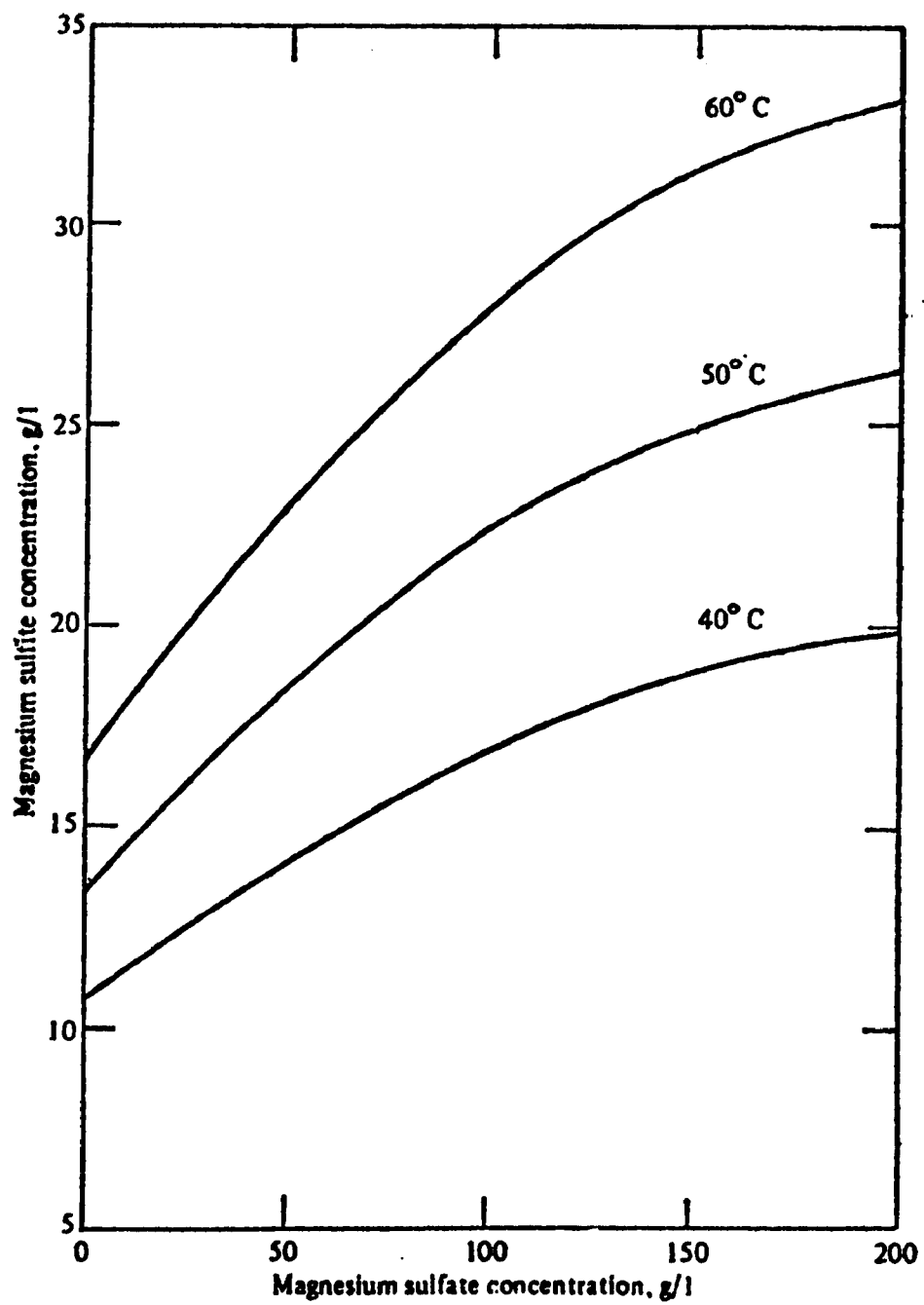


Figure 3-5. Effect of Magnesium Sulfate on Magnesium Sulfite Solubility

TABLE 3-2. MAGNESIUM SULFITE HYDRATE TRANSITION AT ROOM TEMPERATURE

<u>Conditions for Digestion</u>	<u>Trihydrate</u>	<u>Hexahydrate</u>
1. In 8% MgSO_4 solution for 24 hours.	All hexahydrate.	No change.
2. In 15% MgSO_4 solution:		
a. for 20 hours	No change.	Mostly hexa with some trihydrate..
b. for 64 hours	No change.	40% $6\text{H}_2\text{O}$ and 60% $3\text{H}_2\text{O}$.
c. for 97 hours		No change.
3. In 20% MgSO_4 solution:		
a. for 20 hours	No change.	80% $6\text{H}_2\text{O}$ and 20% $3\text{H}_2\text{O}$.
b. for 64 hours	No change.	40% $6\text{H}_2\text{O}$ and 60% $3\text{H}_2\text{O}$.
c. for 72 hours	-----	No change.
d. for 97 hours	-----	No change.

In another study the pH of saturated slurry varied while examination time was held constant. The results of that study are shown in Table 3-3. The pH of the medium seems to have had some effect on the rate of transition of the hydrates. It appears that alkaline pH retards, while acid pH favors the rate. However, the major factor in the transition of hexahydrate to trihydrate would appear to be temperature.

The Russian researcher Pinaev (PI-071) noted that concentrations above 3% of MgSO_4 in a MgO scrubbing liquor are undesirable particularly for the subsequent thermal decomposition of solids withdrawn from the system. The decomposition of MgSO_4 requires a higher temperature (1000-1200°C) than that required to decompose $\text{MgSO}_3 \cdot x\text{H}_2\text{O}$, which is associated with an additional consumption of heat. The MgSO_4 content of the sulfite crystals might reach values as high as 11-13% during storage of the removed crystals. He further noted that with the addition of 0.001-0.005 wt % of p-phenylenediamine (PPDA) to the scrubbing system, MgSO_3 crystals separated from the system were nearly free of MgSO_4 . The crystals were also stable during subsequent storage.

Pinaev (PI-073) also reports that the duration of transition of magnesium sulfite hexahydrate into trihydrate depends on the solution temperature and viscosity, which are determined mainly by the soluble magnesium sulfate. His data (Figure 3-6) on recrystallization times in the 50-70°C range were obtained at a solid to liquid ratio of 1:10 with 100 and 200 grams MgSO_4 per liter in solution at a pH of ~ 6.5 .

Reconversion of the trihydrate into hexahydrate can be induced by cooling the suspension from 40 to 30°C, but the rate of this process is several times slower than the forward process. He reports that the time for complete conversion of

TABLE 3-3. TRANSITION OF $\text{MgSO}_3 \cdot 6\text{H}_2\text{O}$, pH ADJUSTED BY DILUTED H_2SO_4

Conditions for Digestion	Results
1. pH 7.00: 59°C (45 minutes in water).	All trihydrate.
2. pH 7.00: 57°C (45 minutes in water).	Hexahydrate with few percent trihydrate.
3. pH 7.10: 60-63°C (45 minutes in water).	All trihydrate.
4. pH 7.00: 57-58°C (45 minutes in water).	All hexahydrate.
5. pH 7.00: 56-57°C (45 minutes in water).	All hexahydrate.
6. pH 7.15: 57-58°C (45 minutes in water).	All trihydrate.
7. pH 7.40: 59-61°C (45 minutes in water).	10% trihydrate and 90% hexahydrate.

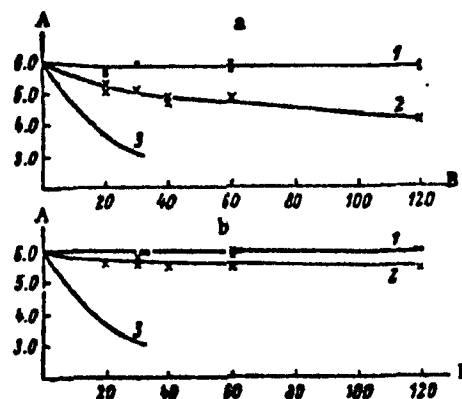


Figure 3-6. Influence of Magnesium Sulfate Concentration on the Time of Recrystallization of Magnesium Sulfite Hexahydrate into the Trihydrate.

- (A) Molecules of water of crystallization in the magnesium sulfite hydrates.
- (B) Time (minutes);
- Temperature (°C): (1) 50, (2) 60, (3) 70;
- MgSO₄ Contents (g/liter): (a) 100, (b) 200.

the crystalline trihydrate into hexahydrate is about 8-10 hours at 30°C and increases to 24-26 hours at 40°C (Figure 3-7).

As the hexahydrate is the stable form of crystalline magnesium sulfite at the normal temperatures (below 42°C), the trihydrate crystals cannot be stored for a long time because they absorb atmospheric moisture and adherent moisture and cake into a compact mass.

Since the commercialization of MgO scrubbing of SO₂ has begun, interest has been generated in the slurry conversion to MgSO₃·3H₂O prior to calcination. An example of the effect of temperature and slurry concentration on conversion from hexahydrate to trihydrate crystals is shown in Figure 3-8. Less energy would be required to dehydrate MgSO₃·3H₂O than MgSO₃·6H₂O. As early as 1940, Peisaklov and Chertkov had noted that the transition of MgSO₃·6H₂O slurry to MgSO₃·3H₂O occurred at reasonably low temperatures (MC-076).

More recently, studies of the thermal dehydration of the known stable hydrates of magnesium sulfite, MgSO₃·6H₂O and MgSO₃·3H₂O, have been conducted. However, the reported findings of the groups were apparently contradictory. Okabe and Hari (OK-015) used three different techniques to study the dehydration: differential thermal analysis (DTA), X-ray, and infrared (IR). From the DTA and X-ray results they concluded that MgSO₃·6H₂O loses three water molecules between 60 and 100°C to form MgSO₃·3H₂O. The latter, at 200°C, completely dehydrates to yield amorphous anhydrous MgSO₃. But, in the infrared investigation, they reported that the spectrum does not change when the trihydrate goes to the anhydrous state at 200°C. It does not seem plausible that the transformation suggested could have occurred without any change in the infrared

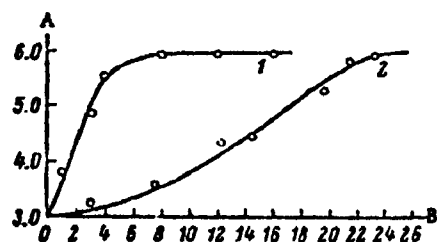


Figure 3-7. Time of Recrystallization of Magnesium Sulfite Trihydrate into the Hexahydrate.

(A) Molecules of water of crystallization in the Magnesium sulfite hydrates;

(B) Time (h);

Temperature (°C): (1) 30, (2) 40.

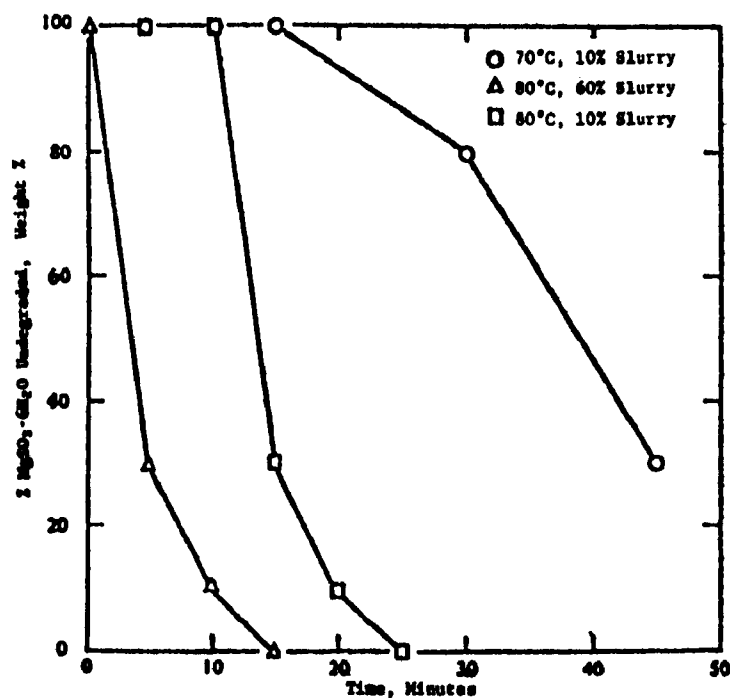


Figure 3-8. Effect of Temperature and Slurry Concentration on Conversion Rate of $\text{MgSO}_3 \cdot 6\text{H}_2\text{O}$ to $\text{MgSO}_3 \cdot 3\text{H}_2\text{O}$.

spectra. The band in the 3500 cm^{-1} region is obviously an O-H stretching band, therefore, if the salt is dehydrated it would be expected that this band should disappear.

Two other investigations using DTA were carried out by groups at the Tennessee Valley Authority (TVA). These studies were not published, but are presented, in part, in an EPA-sponsored critical analysis of the magnesia process prepared by TVA. In the above cited report, Jordan's work based upon DTA leads to the conclusion that the thermal dehydration of $\text{MgSO}_3 \cdot 6\text{H}_2\text{O}$ takes place in one step starting at 100°C and that $\text{MgSO}_3 \cdot 3\text{H}_2\text{O}$ dehydrates in one step, starting at 160°C .

In the other study, Hatfield and co-workers reported that $\text{MgSO}_3 \cdot 6\text{H}_2\text{O}$ loses nearly all its water when heated in a stream of argon or air at 104°C for 16 hours. This, too, supports the inference that the thermal dehydration of the hexahydrate occurs in one step. It is also reported that $\text{MgSO}_3 \cdot 3\text{H}_2\text{O}$ is partially dehydrated when heated in air for 16 hrs at 160°C .

In the above cited EPA report, it is suggested that the apparently contradictory results may be due to differences in experimental conditions. It was speculated that the samples were heated in sealed tubes in the work of Okabe and Hori, although such information was not provided in that paper. Without presenting a critical analysis of the effects of having the samples open or closed to the atmosphere, the TVA report concludes that the results of the TVA groups, in which the samples are open to the atmosphere, are valid and that $\text{MgSO}_3 \cdot 6\text{H}_2\text{O}$ dehydrates in one step to MgSO_3 at 100°C as long as the vapor pressure of water in the atmosphere in contact with the solids is sufficiently low, that is, lower than the equilibrium water vapor pressure of $\text{MgSO}_3 \cdot 3\text{H}_2\text{O}$ at 100°C .

First, the DTA results will be considered (DA-195). A typical thermogram for the dehydration of $\text{MgSO}_3 \cdot 3\text{H}_2\text{O}$ is shown in Figure 3-9. Only one endothermic transition is observed starting at 190°C . On the other hand, in the thermogram of $\text{MgSO}_3 \cdot 6\text{H}_2\text{O}$ shown in Figure 3-10, two endothermic transitions are observed. One starts at 90°C and the other coinciding with the endotherm observed for the trihydrate starts at 190°C . The inference to be drawn from these data is that the hexahydrate does degrade in two steps and that the two steps involve a transition from the hexahydrate phase to the trihydrate phase.

In the DSC studies heat input rather than the temperature is measured. The DSC thermogram of $\text{MgSO}_3 \cdot 3\text{H}_2\text{O}$ is shown in Figure 3-11. Only one endothermic transition was observed starting at 100°C with a peak maximum at 160°C . Both DTA and DSC analyses indicate that the thermal dehydration of $\text{MgSO}_3 \cdot 3\text{H}_2\text{O}$ is a one step process. The DSC data indicates that the dehydration of $\text{MgSO}_3 \cdot 3\text{H}_2\text{O}$ starts at a low temperature, 100°C , whereas the DTA data infers that 190°C is the starting temperature.

The DSC thermogram of $\text{MgSO}_3 \cdot 6\text{H}_2\text{O}$ is shown in Figure 3-12. It is significant to note that only one endothermic transition was observed starting at 45°C with a peak maximum at 90°C . DSC results suggest that the thermal dehydration of $\text{MgSO}_3 \cdot 6\text{H}_2\text{O}$ takes place in one step starting at 45°C , in contrast to the two-step mechanism starting at 90°C suggested by the DTA results. Again, this is most probably a water vapor pressure effect.

Since the phenomenon measured by DTA and DSC is the same, it was expected that the results would be consistent. Surprisingly, this was not the case. From the DSC data, it appears that the dehydration of both hydrates starts at a lower temperature and the hexa form dehydrates in one step and not in two steps as was inferred from the DTA results.

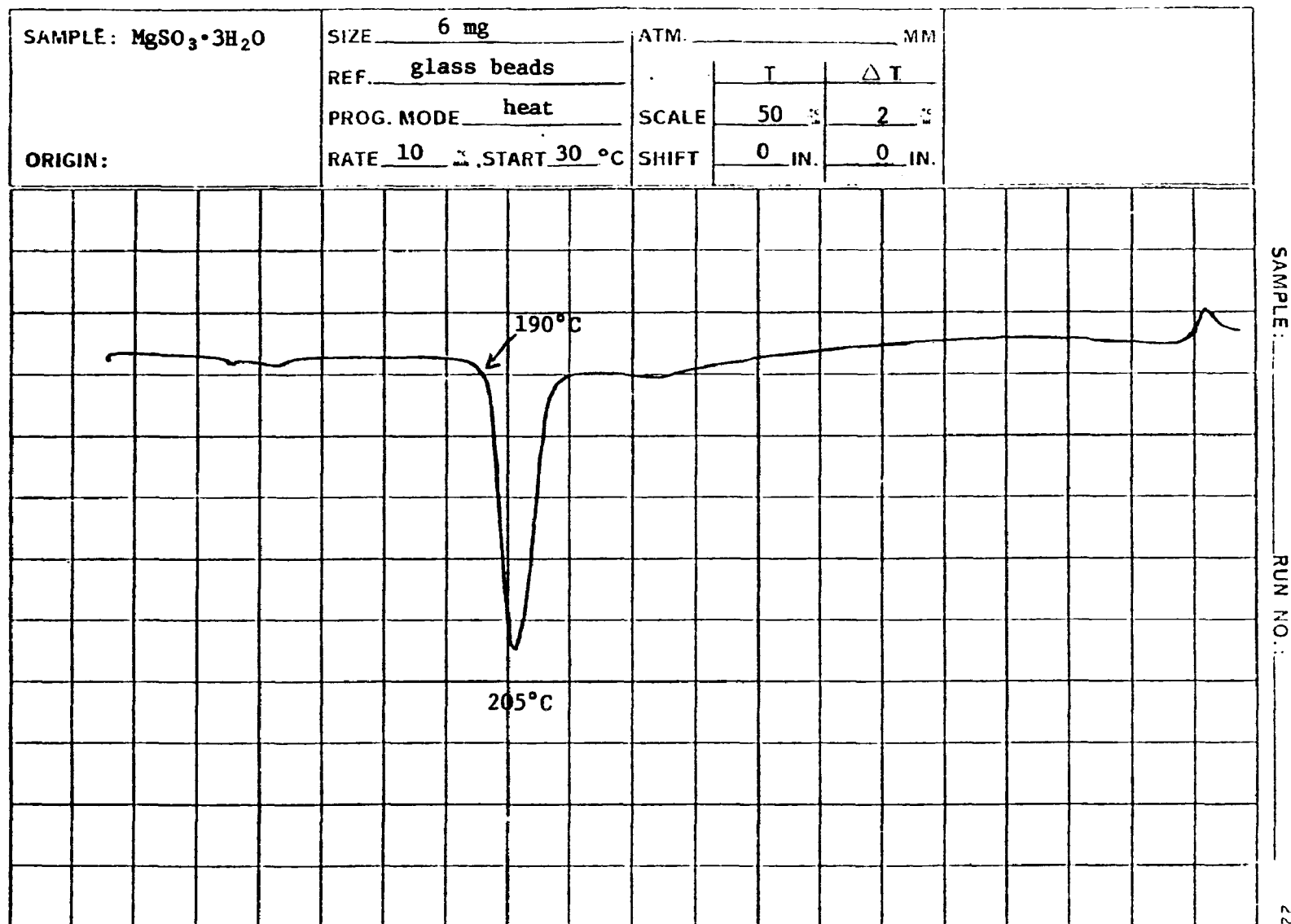


Figure 3-9. DTA Thermogram of Dehydration of $\text{MgSO}_3 \cdot 3\text{H}_2\text{O}$ in a Self-Generated Atmosphere

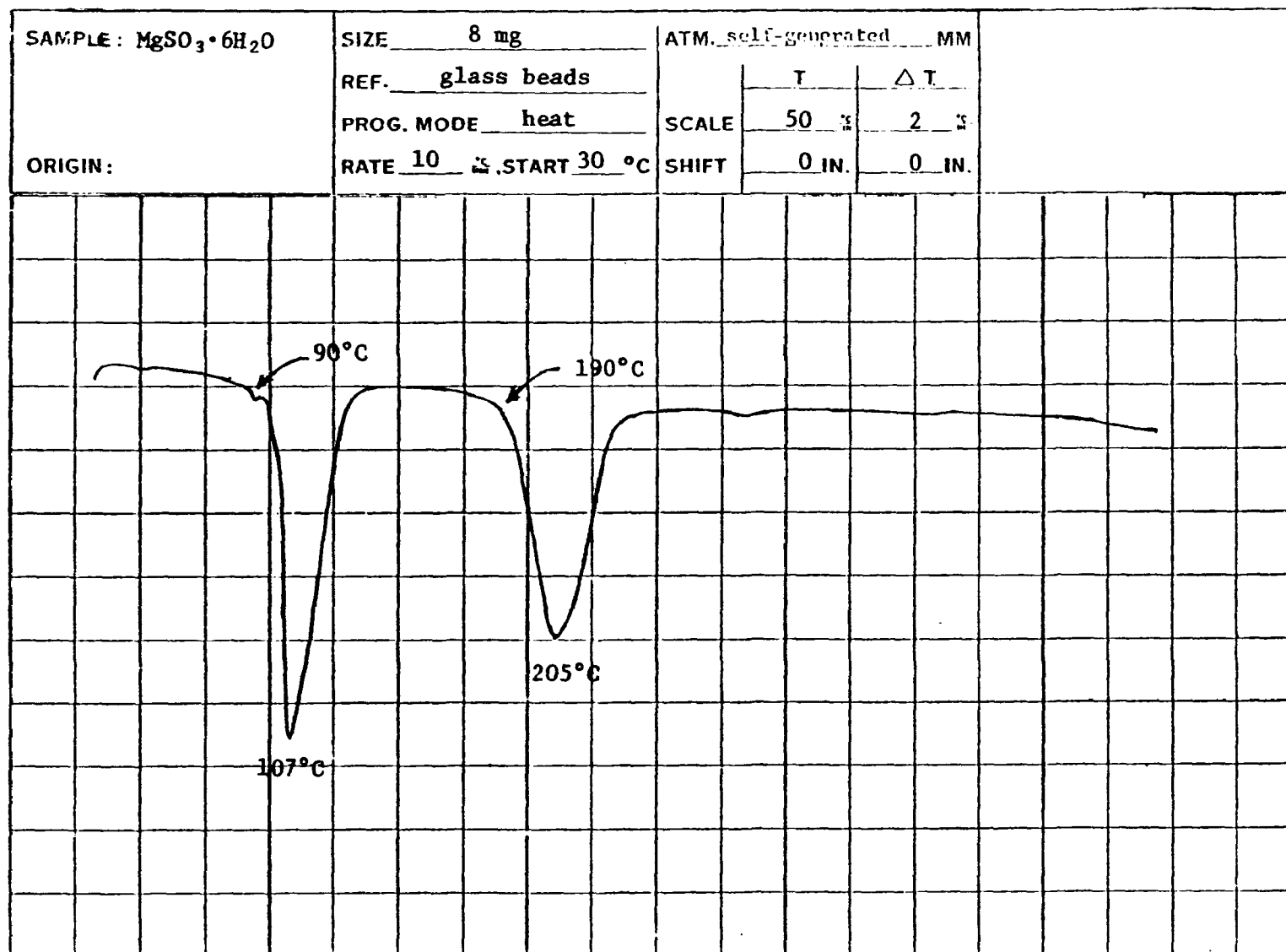


Figure 3-10. DTA Thermogram of Dehydration of $\text{MgSO}_3 \cdot 6\text{H}_2\text{O}$ in a Self-Generated Atmosphere

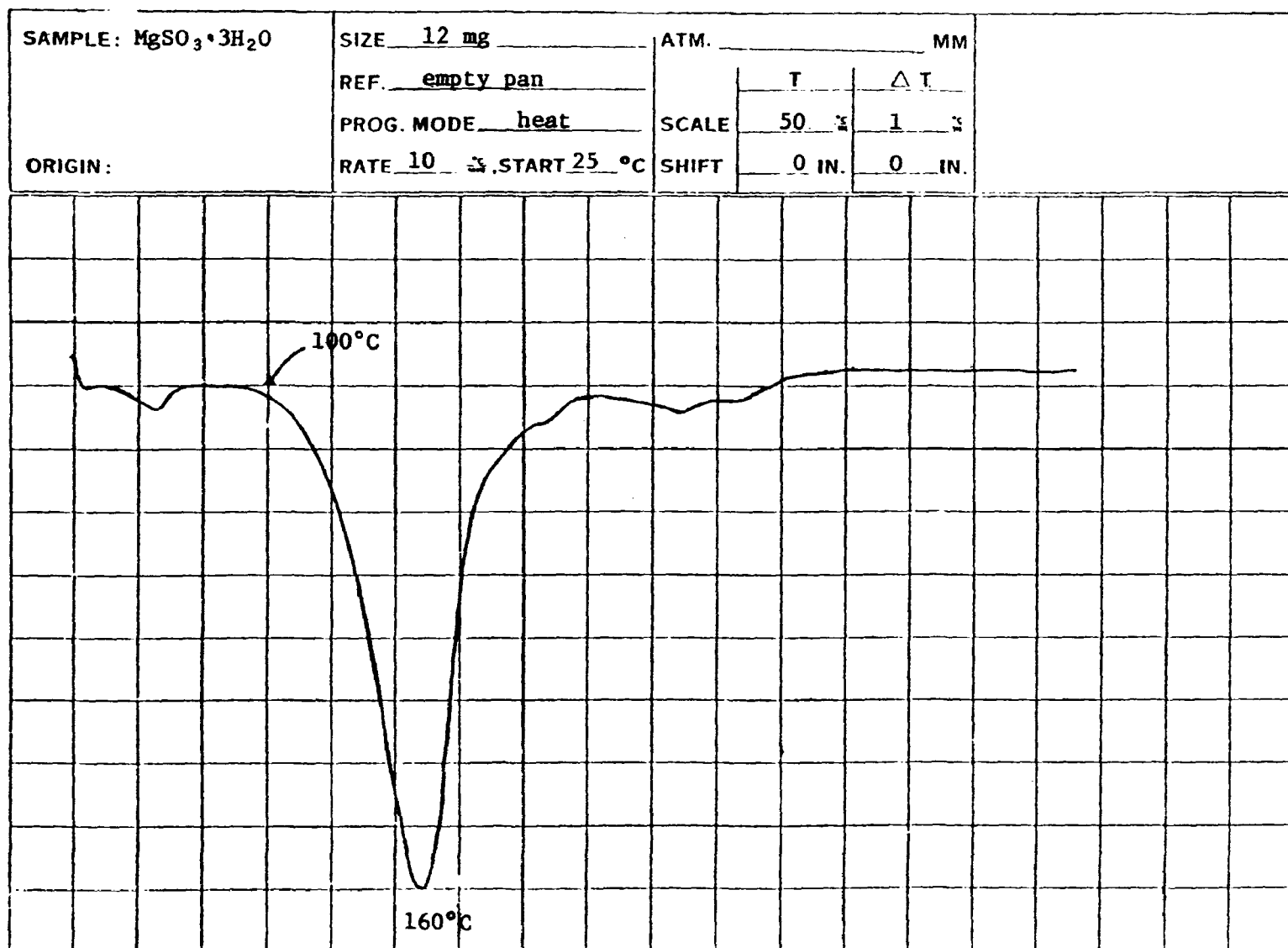


Figure 3-11. DSC Thermogram of $\text{MgSO}_3 \cdot 3\text{H}_2\text{O}$ Dehydration in a Nitrogen Atmosphere

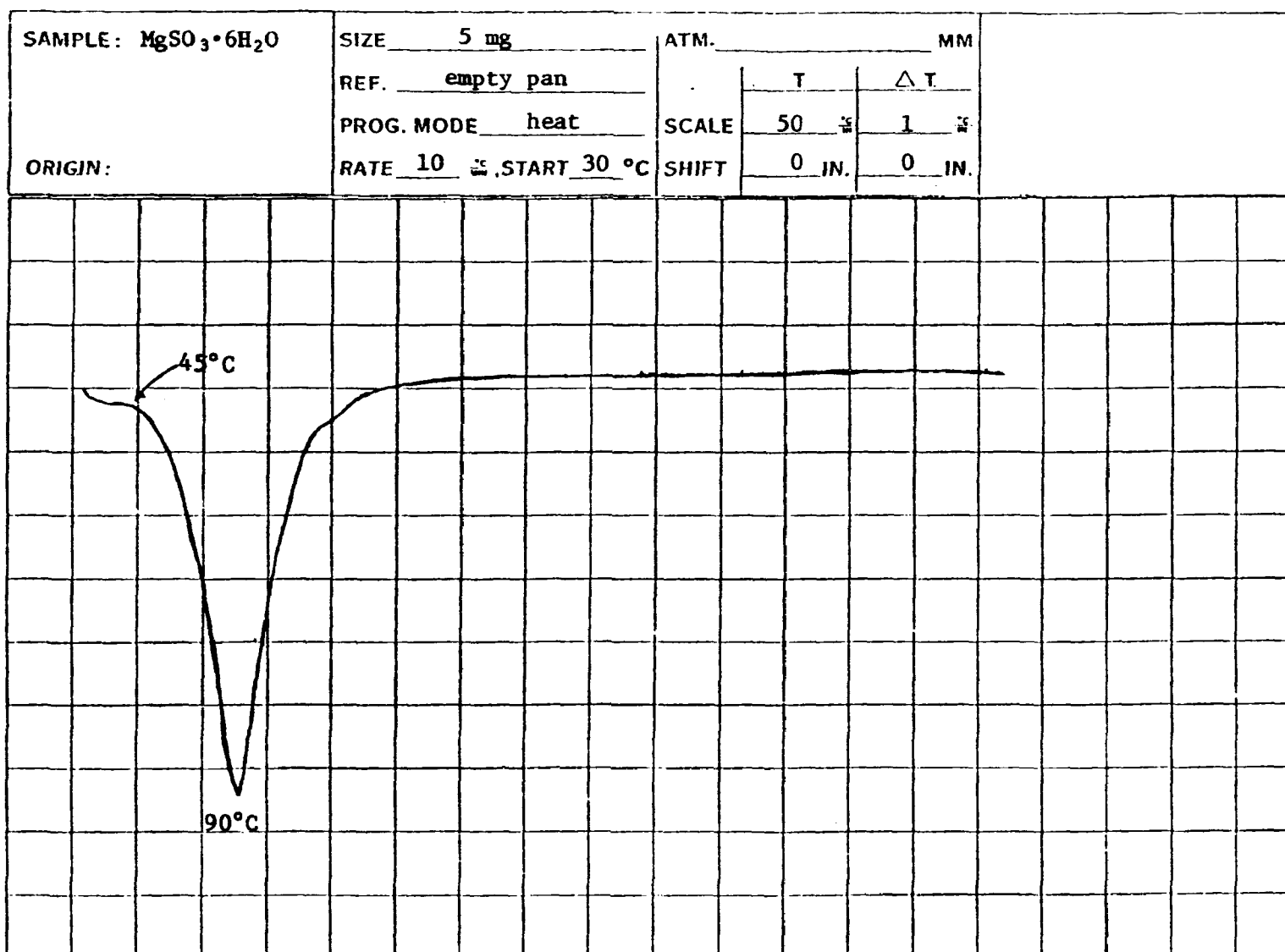


Figure 3-12. DSC Thermogram of $\text{MgSO}_3 \cdot 6\text{H}_2\text{O}$ Dehydration in a Nitrogen Atmosphere

The apparent contradiction between the DTA and the DSC results can be rationalized by considering the relationship between the dehydration reaction and the sample environmental conditions. In any dehydration reaction, water is liberated; if the latter is continuously removed from the reaction atmosphere two consequences are observed. First, the dehydration starts at a lower temperature, and, secondly, equilibrium is not attained.

In the DSC studies, the sample is placed in an open dish and is heated under a sweeping stream of nitrogen. Under these conditions the liberated water is continuously removed from the reaction environment. In the DTA studies, however, the sample is heated in a self-generated atmosphere in a closed capillary tube. Under the open conditions thermal dehydration starts at a lower temperature, 45°C versus 90°C, and only one endothermic transition is observed for the hexahydrate, whereas in the DTA studies two transitions were observed.

To confirm the above rationalization of the differences between the DTA and the DSC studies, the thermal dehydration was studied by another independent technique, TGA, in which it was possible to heat the samples either in an open condition or in a self-generated atmosphere. TGA thermograms under open conditions were obtained by the conventional procedure in which the sample is placed in an open platinum dish under a sweeping blanket of nitrogen. TGA under self-generated atmosphere was achieved by placing the sample in a capillary tube with a thermocouple inside. Then, the whole tube was placed in the platinum dish.

The TGA of $\text{MgSO}_3 \cdot 3\text{H}_2\text{O}$ under open conditions is shown in Figure 3-13. Thermal dehydration starts at 100°C and takes

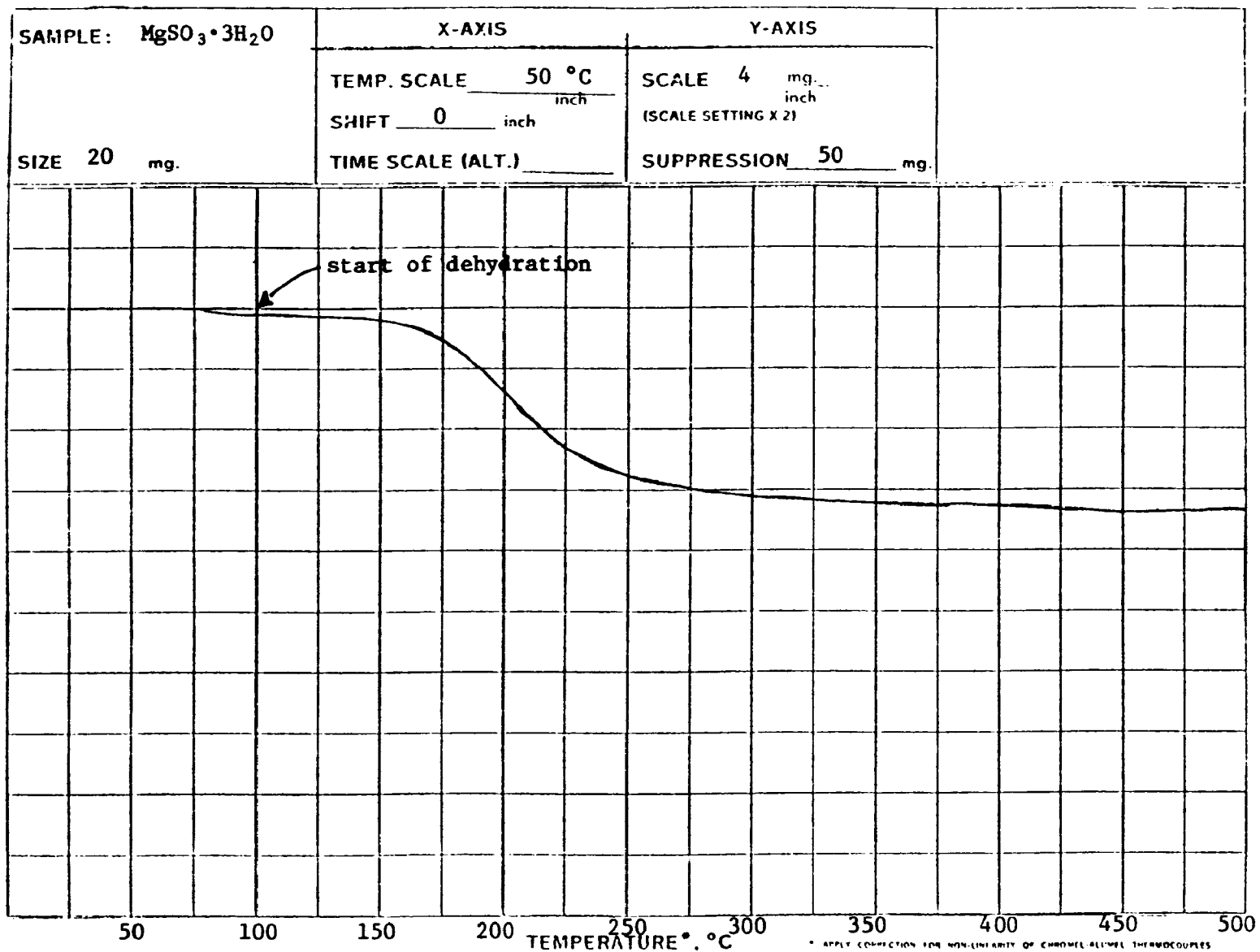


Figure 3-13. TGA Thermogram of $\text{MgSO}_3 \cdot 3\text{H}_2\text{O}$ Dehydration in a Nitrogen Atmosphere

place in one step. The weight loss of the sample is 34.0%, which corresponds to the loss of 3 moles of water. TGA of $\text{MgSO}_3 \cdot 6\text{H}_2\text{O}$ under open conditions is shown in Figure 3-14. Thermal dehydration of the hexaform starts at 70°C and takes place in one step. The weight loss of the sample is 51%, which corresponds to the loss of 6 moles of water.

The thermograms for the trihydrate and the hexahydrate, respectively, under the conditions of a self-generated atmosphere are shown in Figures 3-15 and 3-16. $\text{MgSO}_3 \cdot 3\text{H}_2\text{O}$, as shown in Figure 3-15, loses 34.5% of its weight in one step. This is a very good agreement with TGA under open conditions, but thermal dehydration starts at 220°C, i.e., at a higher temperature, because of the self-generated atmosphere conditions. The weight loss for the hexahydrate under a self-generated atmosphere, as shown in Figure 3-16, is 51%, which corresponds to the loss of 6 moles of water. It is significant to note that the thermal dehydration of the hexa form starts at a higher temperature and takes place in two steps, with a weight loss of 25.5% in each step. In other words, $\text{MgSO}_3 \cdot 6\text{H}_2\text{O}$ loses 3 moles of water in each dehydration step.

Thus, when the TGA study of the hexaform is carried under a sweeping nitrogen atmosphere, equilibrium is not attained due to the continuous removal of the liberated water. As a result, thermal dehydration starts at a lower temperature and takes place in one step. On the other hand, if equilibrium is approached by heating the sample in a self-generated atmosphere, the TGA results show that thermal dehydration starts at a higher temperature and takes place in two steps. The first dehydration step yields $\text{MgSO}_3 \cdot 3\text{H}_2\text{O}$ and anhydrous MgSO_3 is formed in the second. These TGA observations are consistent with the explanation of the differences observed in the DTA and the DSC studies.

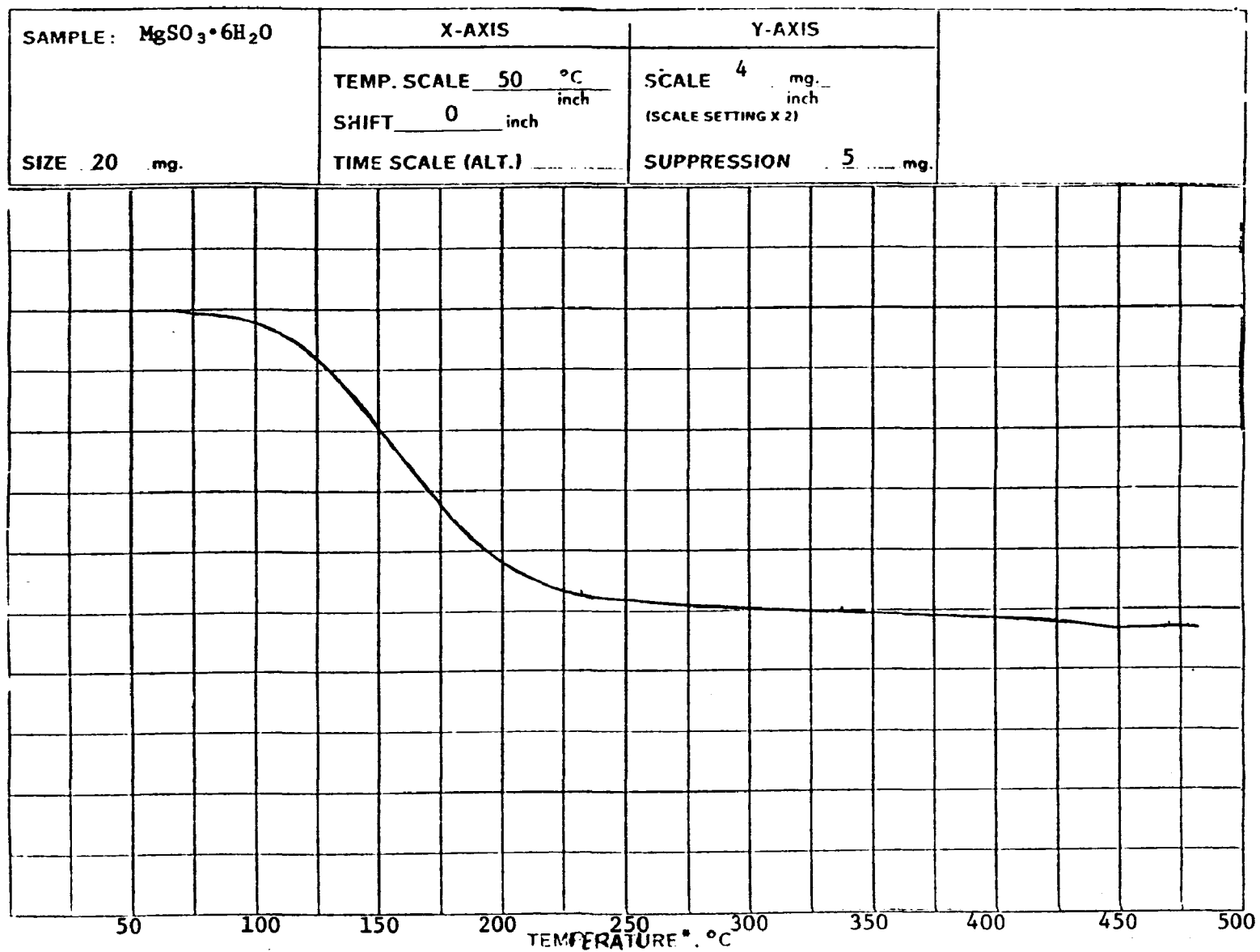


Figure 3-14. TGA Thermogram of $\text{MgSO}_3 \cdot 6\text{H}_2\text{O}$ Dehydration in a Nitrogen Atmosphere

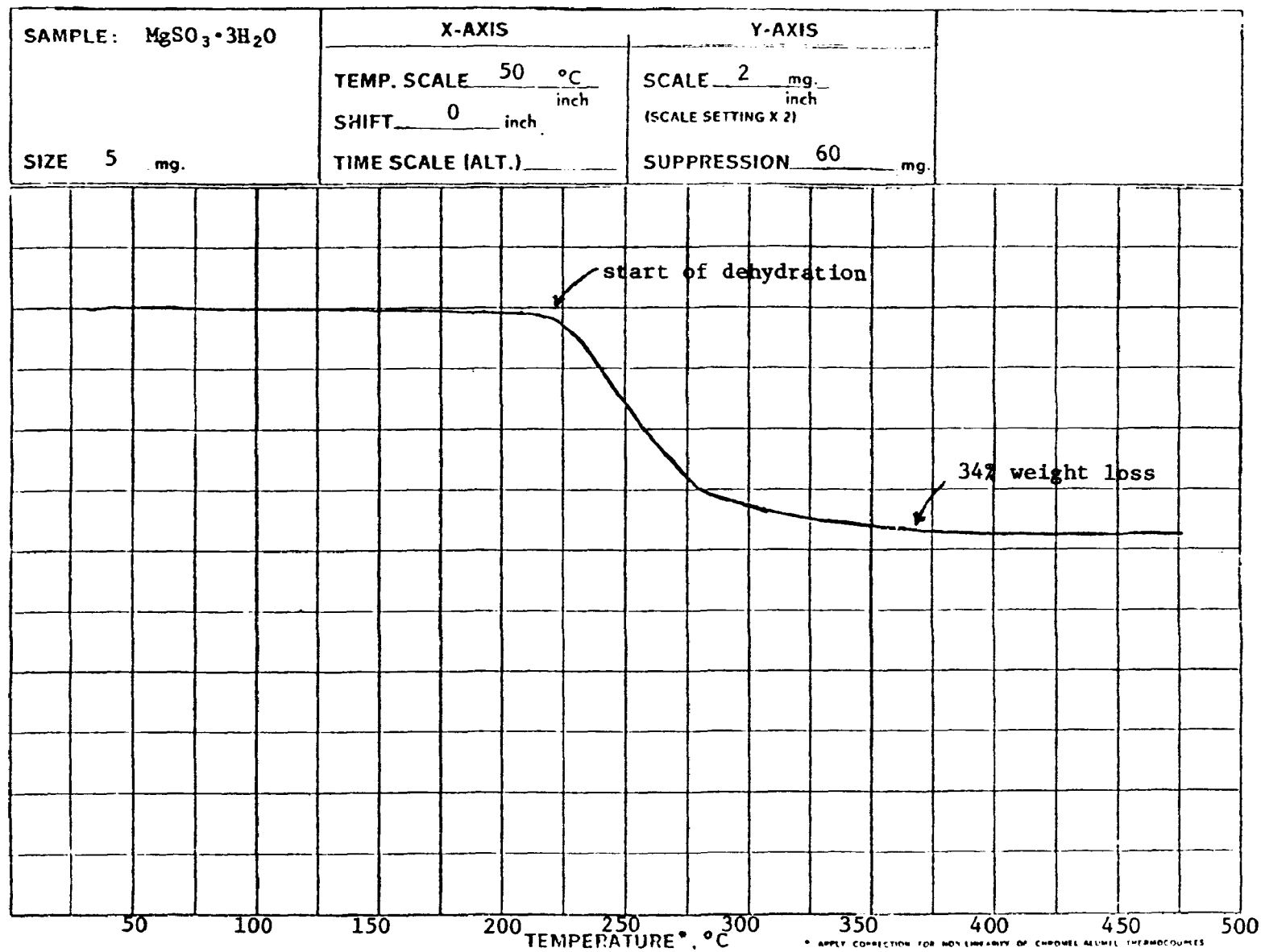


Figure 3-15. TGA Thermogram of $\text{MgSO}_3 \cdot 3\text{H}_2\text{O}$ Dehydration in a Self-Generated Atmosphere

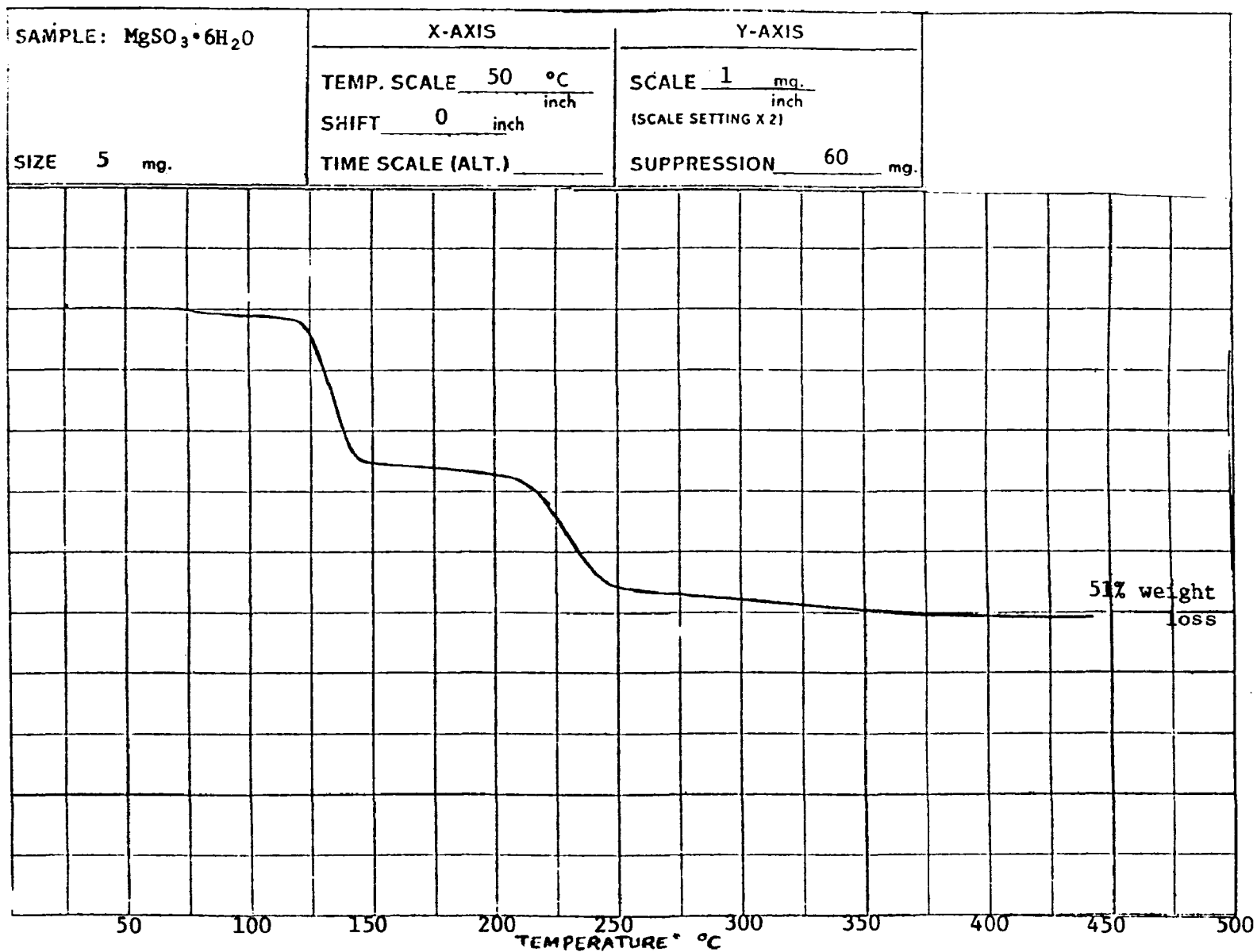


Figure 3-16. TGA Thermogram of $\text{MgSO}_3 \cdot 6\text{H}_2\text{O}$ Dehydration in a Self-Generated Atmosphere

SECTION 4

MAG-OX PLANT OPERATING CHARACTERISTICS

In this section plant operating characteristics with existing Mag-Ox scrubber systems are presented in detail. The location of the plant and a description of both plant and scrubber are included. In addition, the major analytical studies performed on the scrubber system and the major problems encountered in the analyses are also discussed.

TABLE 4-1. PLANT OPERATING CHARACTERISTICS

Plant	Contractors	Plant Description	Scrubber Description	Analytical Studies	Major Problems
Special Pilot Plant	Babcock and Wilcox, National Air Pollution Control Administration.	One-half MW pulverized coal burning furnace used to generate flue gas. A water tube section was used to cool the gases to a temperature typical of a boiler	<p><u>Venturi Scrubber</u> - The absorbant slurry spray nozzle enters just ahead of the venturi throat. The venturi promotes gas absorption by providing a zone with a high liquid to gas specific surface. The gases enter a cyclone separator where the absorbant slurry is removed from the gas stream. The slurry flows by gravity to the sump located immediately under the cyclone. The liquid level in the sump is controlled by a level controller which maintains a constant level with treated make-up water. The slurry composition is maintained indirectly by adjustment of the product flow rate which in turn controls the water make-up rate via the level controller.</p> <p>(See Figure 4-1)</p>	<p>In this special pilot plant project a number of different analytical studies were conducted. The gaseous sulfur dioxide concentrations were determined by colorimetric titration using a Barton analyzer and by Reich test using an iodometric determination. Sulfur trioxide was determined by condensation of sulfur trioxide vapor into condensers followed by analysis of the condensate. The NO_x sampling was done by converting NO_x to nitric acid and then reacting the acid with phenol disulfonic acid to produce a yellow complex which was measured colorimetrically. The magnesium sulfite and magnesium bisulfite were determined by a modified Palmrose analysis.</p> <p>The sulfate analysis was done by titration with barium chloride after cation removal.</p>	<p>In a detailed analysis of the methods used in the program, it was determined that although the NO_x sampling and analysis was an ASTM standard method, the procedure was tedious, time consuming, and contained a number of opportunities for experimental error which were difficult to subject to a numerical analysis. Error analysis studies and a spinning syringe check on the Barton titrator led to the conclusion that the maximum error varied from 16% at 10 ppm to 1.6% at 1000 ppm. The sulfur trioxide analysis did have problems with the condensation, but the maximum probable error was 17%.</p>

(cont.)

TABLE 4-1 (cont.)

Plant	Contractors	Plant Description	Scrubber Description	Analytical Studies	Major Problems
Special Pilot Plant (cont.)			<u>Floating Bed Absorber</u> - The floating bed absorber includes a sump, two contact stages, and a liquid disengagement section. Above the sump, the FBA consists of two stages. Each stage is packed with 6-8 inches of "wiffle balls." The spray nozzles located above the top tray directs the spray of absorbing slurry onto the top tray. Since the gas rises through the slurry it comes into intimate contact with the slurry. Flow to the spray nozzle is controlled and the slurry composition in the sump is controlled by the product nozzle flow. (See Figure 4-2)	The sulfate analysis was done by titration with barium chloride after cation removal.	The modified Palmrose analysis of the magnesium sulfite species had errors arising from volume errors in the syringe, titration errors, and errors in the chemical reagents. The sulfate analysis suffered from a vague end point when done titrimetrically. When they were performed gravimetrically, sample loss was a major problem.
Boston Edison, Mystic Station Facility.	Chemico, (York Research Corporation. Test Contractor)	Scrubber located at Unit 6 at Mystic Station on a 156 MW oil-fired boiler. New ducting was installed at the stack with dampers in the breaching to divert the flow gas to the scrubber and then back to the stack. During most of the period when the scrubber was operating, it was treated all the flue gas, about 40% over design flow at full boiler loads.	The scrubber is a single venturi scrubbing system. The MgO slurry enters the upper part of the absorber with the untreated flue gas. The gas and slurry mixture pass through the throat area into the diverging section, then into a central downcomer to exit the vessel. The flow of cleaned flue gas turns 180° upward. A bleed stream of slurry is centrifuged to remove the solids, and the mother liquor is sent back to the absorber. (See Figure 4-3)	The analytical studies performed the determinations of MgO by acid base titration; the determination of SO_2 in MgSO_3 iodometrically; the determination of SO_4 in MgSO_4 nephelometrically; the determination of carbon in a Leco combustion furnace; and several types of moisture analysis of the free and combined water. Other analyses performed included iron by colorimetric determination; nickel determination by dimethyl glyoxime method; vanadium determination spectrophotometrically; chloride	A thorough analysis of analytical problems encountered in the program was made by York Research personnel. It appeared that the determination of % MgO by acid base titration had few sources of experimental error. In the determination of SO_2 in MgSO_3 by the iodine sodium thiosulfate method the greatest source of error is undissolved sample not reacting with the iodine in solution. In the determination of SO_4 in MgSO_4 by nephelometry the greatest source of error revolves around experimental and individual error;

(cont.)

TABLE 4-1 (cont.)

Plant	Contractors	Plant Description	Scrubber Description	Analytical Studies	Major Problems
Boston Edison, Mystic Station Facility. (cont.)				determined by silver titration, and magnesium and calcium determined by EDTA titration.	<p>however, some blame was with the colorimeter itself. Past experiments had shown that readings below 20 ppm on the scale are highly inaccurate and that even readings between 20 and 60 ppm in the scale were subject to error.</p> <p>The % combined water analysis on the dryer product seemed to be more influenced by environmen- tal factors such as humid- ity and temperature than any other test. The % solids in the recycle slur- ry which was determined gravimetrically had as its greatest source of error loss of sample during prepa- ration. This was also true for the gravimetric deter- mination of the % solids in the centrifuge cake.</p> <p>The other major problem encountered in long term tests was that $\text{MgSO}_3 \cdot 3\text{H}_2\text{O}$ was the major solid formed in the recirculating slurry whereas $\text{MgSO}_3 \cdot 6\text{H}_2\text{O}$ had been expected. This caused solids handling problems with the equipment which had been designed to handle the larger $\text{MgSO}_3 \cdot 6\text{H}_2\text{O}$ crystals.</p>

(cont.)

TABLE 4-1 (cont.)

Plant	Contractors	Plant Description	Scrubber Description	Analytical Studies	Major Problems
Potomac Electric Power Company, Dickinson Station	Chemico, (York Research Corporation. Test Contractor)	Scrubber located at Unit 3 at Dickinson Station is 185 MW pulverized coal boiler. The system was arranged so that gases entering the scrubber can pass through an electrostatic precipitator or bypass it and go directly to the scrubber.	The scrubber is a two-stage venturi scrubbing system which had a design capacity of handling about 50% of the flue gas from Unit 3. In the first stage the flue gas is contacted with recycle liquor in a wet venturi to remove particulate. The wet gas is passed through a series of mist eliminators and they enter the second stage in a fixed throat venturi. The MgO in the second stage recycle liquor reacts with the SO ₂ and forms a MgSO ₃ slurry. A bleed stream is sent to the centrifuge where the solids are removed and the mother liquor sent back to Stage 2 for recycling. (See Figure 4-4)	The chemical analyses were similar to the study performed by Chemico on magnesia based SO ₂ scrubber systems at Boston Edison's Mystic Station. There were a few exceptions: (1) the acid concentrations used in the % MgO determination were increased; (2) the penetration analysis on the centrifuge cake was deleted; (3) the combined water analysis performed on the OHAUS moisture balance was now done at higher temperature of 160°C.	Several major problems that were encountered include the formation of MgSO ₃ ·6H ₂ O in the scrubber slurry after scrubber operations of 10-12 hours when MgSO ₃ ·3H ₂ O was the expected stable product. This created problems with solids handling in the system. In addition, the reactivity of regenerated MgO decreased when it was added to the system.
Severo-Donetsk Power Plant.	NIIOGAZ (USSR)- State Scientific Research Institute on Industrial and Sanitary Purification of Gases.	(Not Known)	(Not Known)	A number of analytical studies were performed. These analyses included: 1. concentration of SO ₂ in gas; 2. ratio of solid portion of suspension to its liquid phase; 3. solid-liquid (wt) of working suspension; 4. content of solid phase in suspension; 5. acidity of working suspension (pH) of solution; 6. density of working suspension and solution.	The analyses outlined appeared to be well developed and effective. The crystallization moisture of MgSO ₃ is determined by a weight loss method on drying of the crystals, but some details were lost in translation. Further work proposed at the power plant include: (1) determination of the efficiency of additives of oxidation inhibitors in tests of absorbers with replaceable spherical packing on the pilot equipment, (2) further studies of low (cont.)

TABLE 4-1 (cont.)

Plant	Contractors	Plant Description	Scrubber Description	Analytical Studies	Major Problems
Severo-Donetsk Power Plant (cont.)				7. viscosity of working suspension and solu- tion. 8. moisture of solid phase (MgSO_4 crys- tals): hygroscopic and crystalline, 9. chemical composition of liquid phase, 10. chemical composition of solid phase, 11. chemical composition of magnesite.	temperature magnesite scrubbing with $\text{MgSO}_4 \cdot 6\text{H}_2\text{O}$ precipitation, (3) further studies of high temperature magnesite scrubbing with $\text{MgSO}_4 \cdot$ $3\text{H}_2\text{O}$.

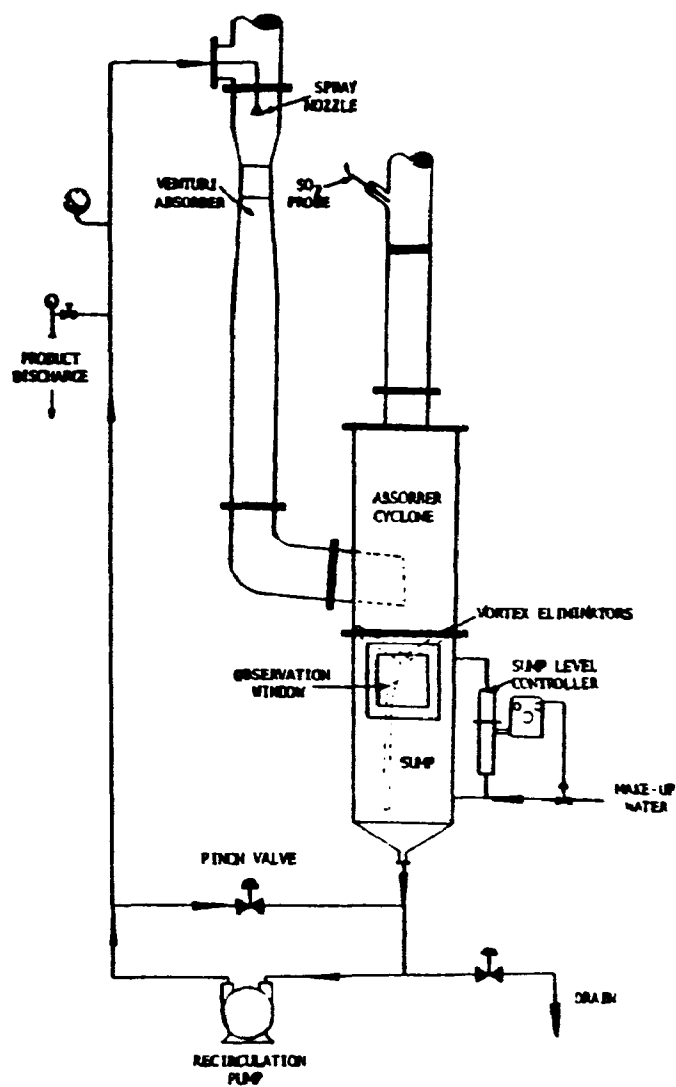


Figure 4-1. Venturi Scrubber

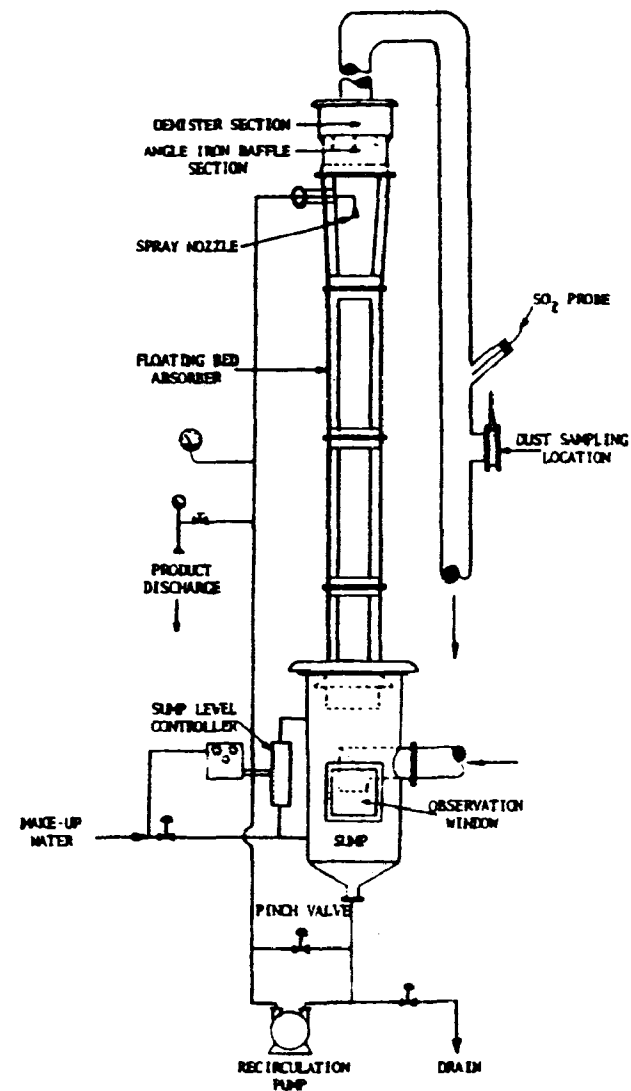


Figure 4-2. Floating Bed Absorber

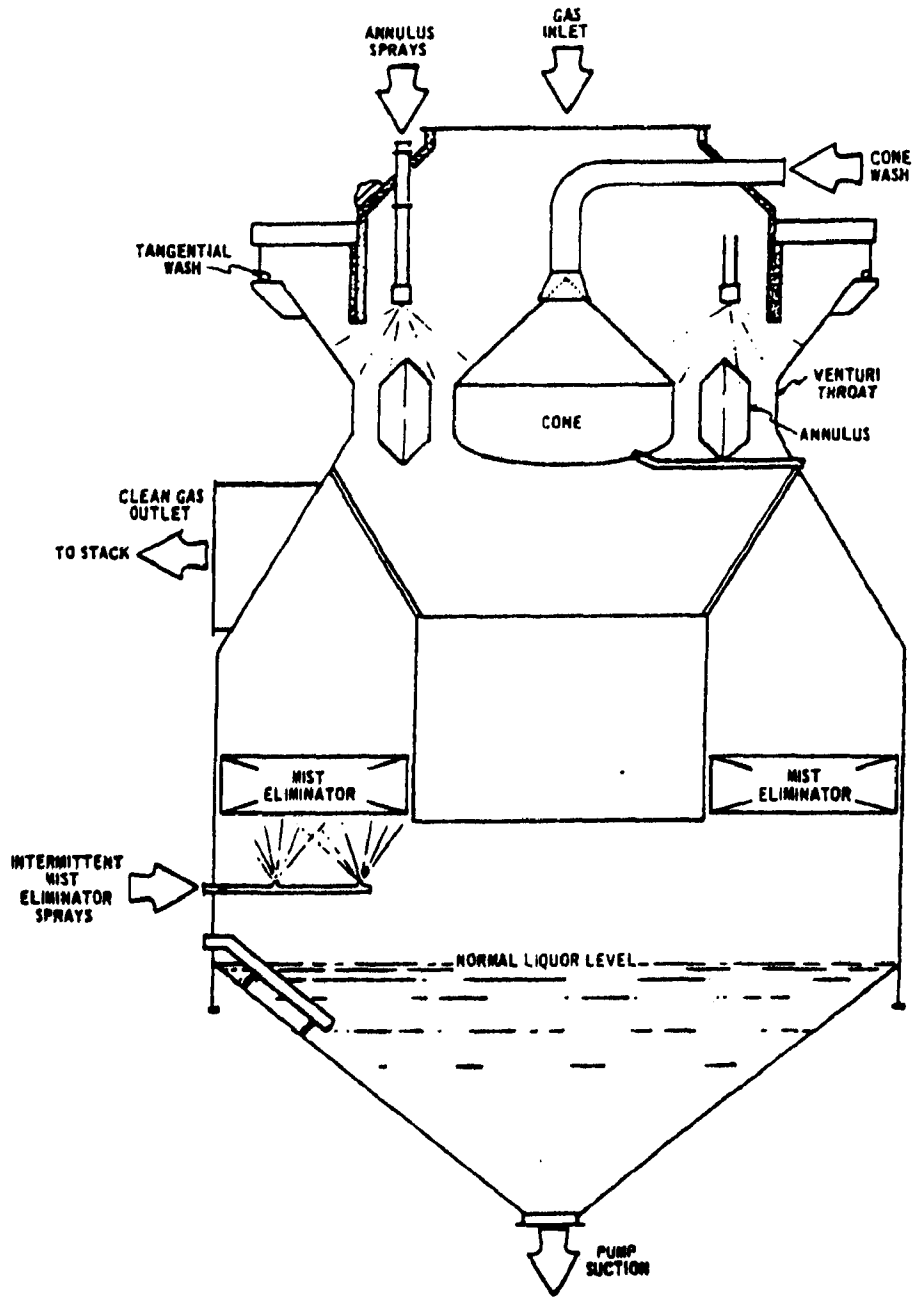


Figure 4-3. Boston Edison Scrubber

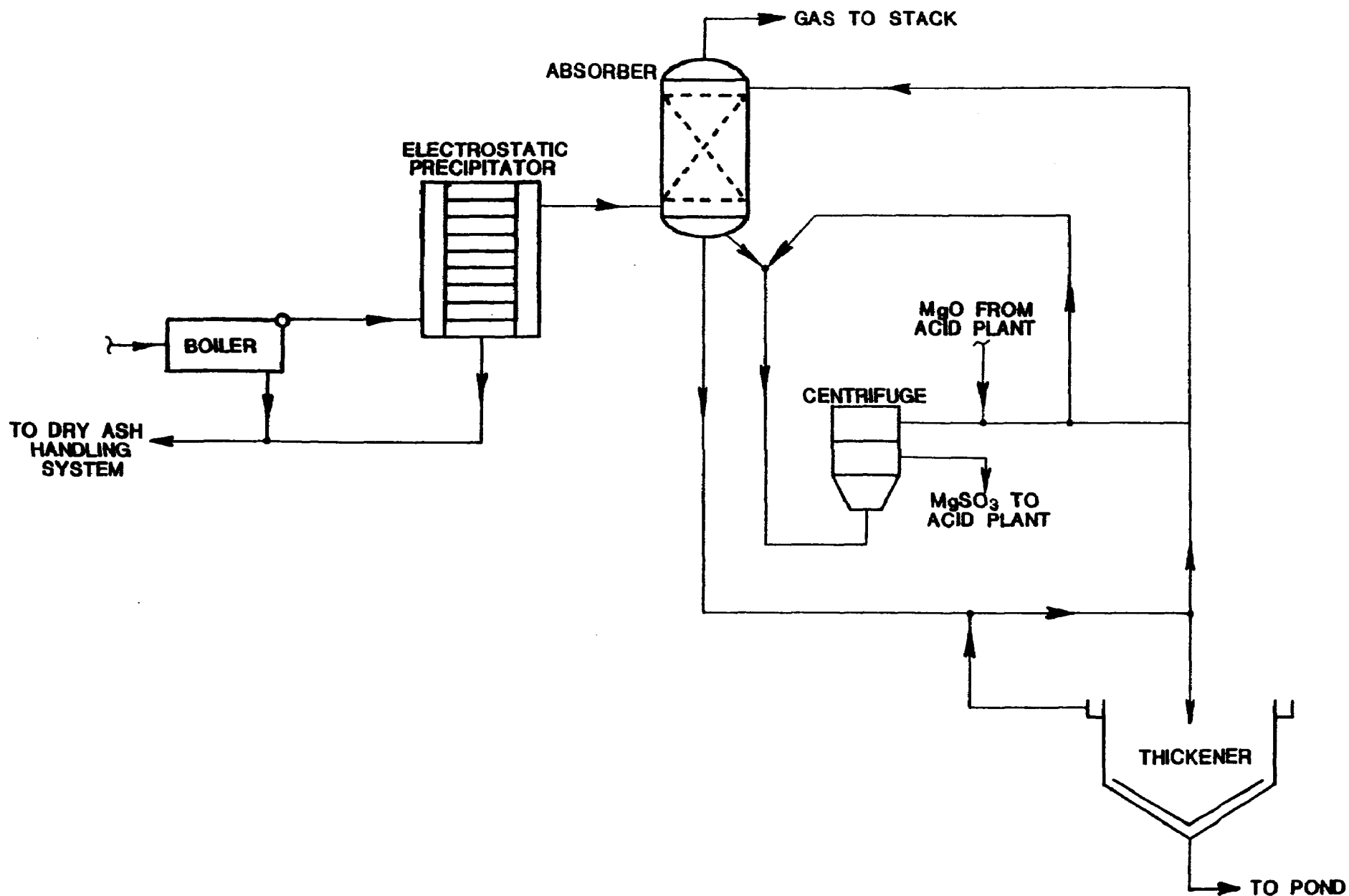


Figure 4-4. Dickerson Station Scrubber

REFERENCES

- DA-195 Dauerman, Leonard, Sulfur Oxide Removal from Power Plant Stack Gas. Magnesia Scrubbing Regeneration: Production of Sulfuric Acid, Newark, N.J., Inst. of Technology, Feb. 1975.
- DO-015 Downs, W., and A. J. Kubasco, Magnesia Base Wet Scrubbing of Pulverized Coal Generated Flue Gas--Pilot Demonstration, Alliance, Ohio, Babcock and Wilcox Co., 1970; PB 198-074.
- KU-083 Kuzminykh, I. N., and M. D. Babushkina, "Equilibrium Between Sulfur Dioxide and Magnesium Bisulfite Solutions," J. Appl. Chem. USSR 30(3), 495-98 (1957).
- LI-068 Linke, William F., Comp., Seidell's Solubilities; Inorganic and Metal-Organic Compounds, 4th ed., 2 vols., Princeton, N.J., D. Van Nostrand, 1958 (Volume 1) and 1965 (Volume 2).
- LO-153 Lowell, P. S., Formation of Tri- and Hexahydrates of Magnesium Sulfite, Technical Note 500-403-03, Austin, Texas, Radian Corporation, December 1974.
- MC-076 McGlamery, G. G., Tarstrick, R. L.; Simpson, J. P., and Phillips, J. F., Conceptual Design and Cost Study. Sulfur Oxide Removal from Power Plant Stack Gas. Magnesia Scrubbing - Regeneration: Production of Concentrated Sulfuric Acid, EPA-R2-73-244. Muscle Shoals, Ala., TVA, 1973.

- MA-089 Markant, H. P., N. D. Phillips, and I. S. Shah, "Physical and Chemical Properties of Magnesia-Base Pulping Solutions," Tappi 48(11), 648-53 (1965).
- OK-015 Okabe, Taijiro, and Shoichiro Hori, "Thermal Decomposition of Magnesium Sulfite and Magnesium Thiosulfate," Technol. Repts. Tohoku Univ. 23(2), 85-9 (1959).
- PI-070 Pinaev, V. A., "The Viscosity and Density of Magnesium Sulfite-Bisulfite-Sulfate Solutions," J. Appl. Chem. USSR 36(10), 2253-55 (1963).
- PI-072 Pinaev, V. A., "Mutual Solubility of Magnesium Sulfite, Bisulfite and Sulfate," J. Appl. Chem. USSR 37(6), 1353-55 (1964).
- PI-073 Pinaev, V. A., "Recrystallization of Magnesium Sulfite Hydrates," J. Appl. Chem. USSR 43(4), 869-70, (1970).
- QU-013 Quigley, Christopher P., "Operational Performance of the Chemico Magnesium Oxide System at the Boston Edison Co., Part II," Presented at the Flue Gas Desulfurization Symposium, New Orleans, 14-17 May 1973.
- TE-030 Tennessee Valley Authority, Removal of Sulfur Dioxide from Stack Gases. Thermal Decomposition of Magnesium Sulfite, Muscle Shoals, Ala., Feb. 1971, #38.
- WA-065 Walden Research Corp., Improved Chemical Methods for Sampling and Analysis of Gaseous Pollutants from the Combustion of Fossil Fuels; Vol. 1, Sulfur Oxides, by J. N. Driscoll and A. W. Berger, Final Report, Contract No. CPA 22-69-95. Cambridge, Mass., 1971.

TECHNICAL NOTE 200-045-36-02

THEORETICAL PREDICTION OF TRANSITION
TEMPERATURE LOWERING FOR THE
 $\text{MgSO}_3 \cdot 3\text{H}_2\text{O}$ - $\text{MgSO}_3 \cdot 6\text{H}_2\text{O}$ SYSTEM

Prepared by:

R. E. Pyle
P. S. Lowell

CONTENTS

1. Introduction and Summary	111
2. Theoretical Predictions.	112
3. Conclusions.	121
4. Nomenclature	122

FIGURES

<u>Number</u>	<u>Page</u>
2-1 Solubility Product Constant of $\text{MgSO}_3 \cdot 3\text{H}_2\text{O}$	113
2-2 Transition in MgSO_4 Solution	115
2-3 Transition in NaCl Solution.	120

TABLES

<u>Number</u>	<u>Page</u>
2-1 Saturated Conditions for $\text{MgSO}_3 \cdot 6\text{H}_2\text{O}$ in Pure Water. .	116
2-2 Influence of MgSO_4 Addition.	117
2-3 Influence of NaCl Addition	119

SECTION 1

INTRODUCTION AND SUMMARY

The magnesium oxide (Mag-Ox) process for removing SO_2 from flue gases has been applied to several power plants. While the results have generally been successful, there are still several areas of uncertainty. One is the inability to predict which hydrate of magnesium sulfite is precipitated at a given set of conditions.

There has been speculation that in the solutions encountered in actual operating scrubbers the transition temperature for $\text{MgSO}_3 \cdot 3\text{H}_2\text{O}$ and $\text{MgSO}_3 \cdot 6\text{H}_2\text{O}$ is raised. Mag-Ox units treating flue gases from oil-fired units tend to give trihydrate while coal-fired units give hexahydrate.

In this technical note the theoretical framework for predicting the transition temperature is developed and numerical results are calculated. Theory predicts that in all practical solutions the transition temperature is lowered from the $\sim 41^\circ\text{C}$ for pure solutions. In most actual scrubber liquors a transition temperature lowering of 3 to 10 degrees may be expected. Therefore, the effect of solution composition on the transition temperature cannot explain the existence of $\text{MgSO}_3 \cdot 6\text{H}_2\text{O}$ under scrubber operating conditions.

An experimental verification of the theoretical predictions is given in Technical Note 200-045-36-03.

SECTION 2

THEORETICAL PREDICTIONS

In Technical Note 500-403-03, it was shown that the transition equilibrium constant could be obtained from the solubility product constants of the hydrates. That is:

$$K_{sp_3} = a_{Mg^{+2}} a_{SO_3}^{-2} a_w^3 / a_{MgSO_3 \cdot 3H_2O} \quad (2-1a)$$

$$K_{sp_6} = a_{Mg^{+2}} a_{SO_3}^{-2} a_w^6 / a_{MgSO_3 \cdot 6H_2O} \quad (2-1b)$$

$$K_{trans} = K_{sp_6} / K_{sp_3} \quad (2-2a)$$

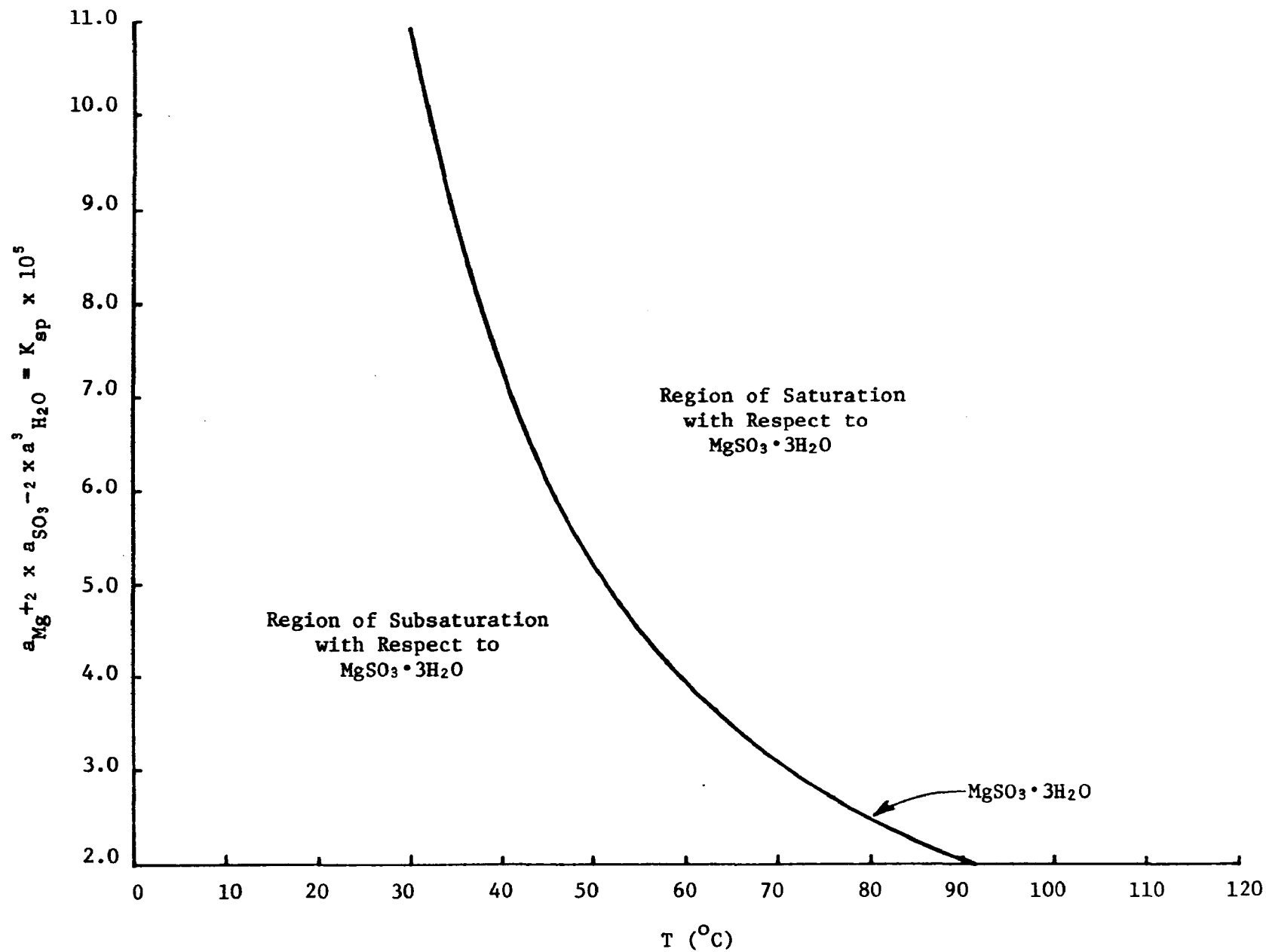
$$= a_w^3 a_{MgSO_3 \cdot 3H_2O} / a_{MgSO_3 \cdot 6H_2O} \quad (2-2b)$$

$$\approx a_w^3 \quad (2-2c)$$

It is convenient to plot solution properties versus temperature in a general fashion. A means of doing this for the trihydrate is to plot the activity product,

$$ap_3 \equiv a_{Mg^{+2}} a_{SO_3}^{-2} a_w^3 \quad (2-3)$$

At a given temperature, the saturated solution value of ap_3 is the solubility product constant, K_{sp_3} . This value is plotted in Figure 2-1. Solutions with values of ap_3 greater

Figure 2-1. Solubility Product Constant of $\text{MgSO}_3 \cdot 3\text{H}_2\text{O}$

than K_{sp_3} are supersaturated with respect to the trihydrate, and solutions with ap_3 less than K_{sp_3} are subsaturated.

It would also be convenient to plot the solubility tendencies of the hexahydrate on the same graph as the trihydrate species. The property of interest for the hexahydrate is its activity product, ap_6 . That is:

$$ap_6 \equiv a_{Mg}^{+2} a_{SO_3}^{-2} a_w^6, \quad (2-4a)$$

$$= ap_3 a_w^3. \quad (2-4b)$$

If we consider the ordinate on our ap_3 plot as y , then we can plot ap_6 values on our ap_3 graph by defining the y ordinate as:

$$ap_6 = y a_w^3, \text{ or} \quad (2-5a)$$

$$y = ap_6 / a_w^3. \quad (2-5b)$$

Different saturated solutions of hexahydrate will now be plotted as a single line on the ap_3 graph. For solutions composed of pure $MgSO_3$, the saturated condition for hexahydrate may be plotted on the ap_3 graph from the data given in Table 2-1. This is shown in Figure 2-2 as the solid line.

Also plotted on Figure 2-2 are values of K_{sp_6}/a_w^3 for $MgSO_3$ in 1.0 and 2.0 M $MgSO_4$ solutions. The data are taken from Table 2-2.

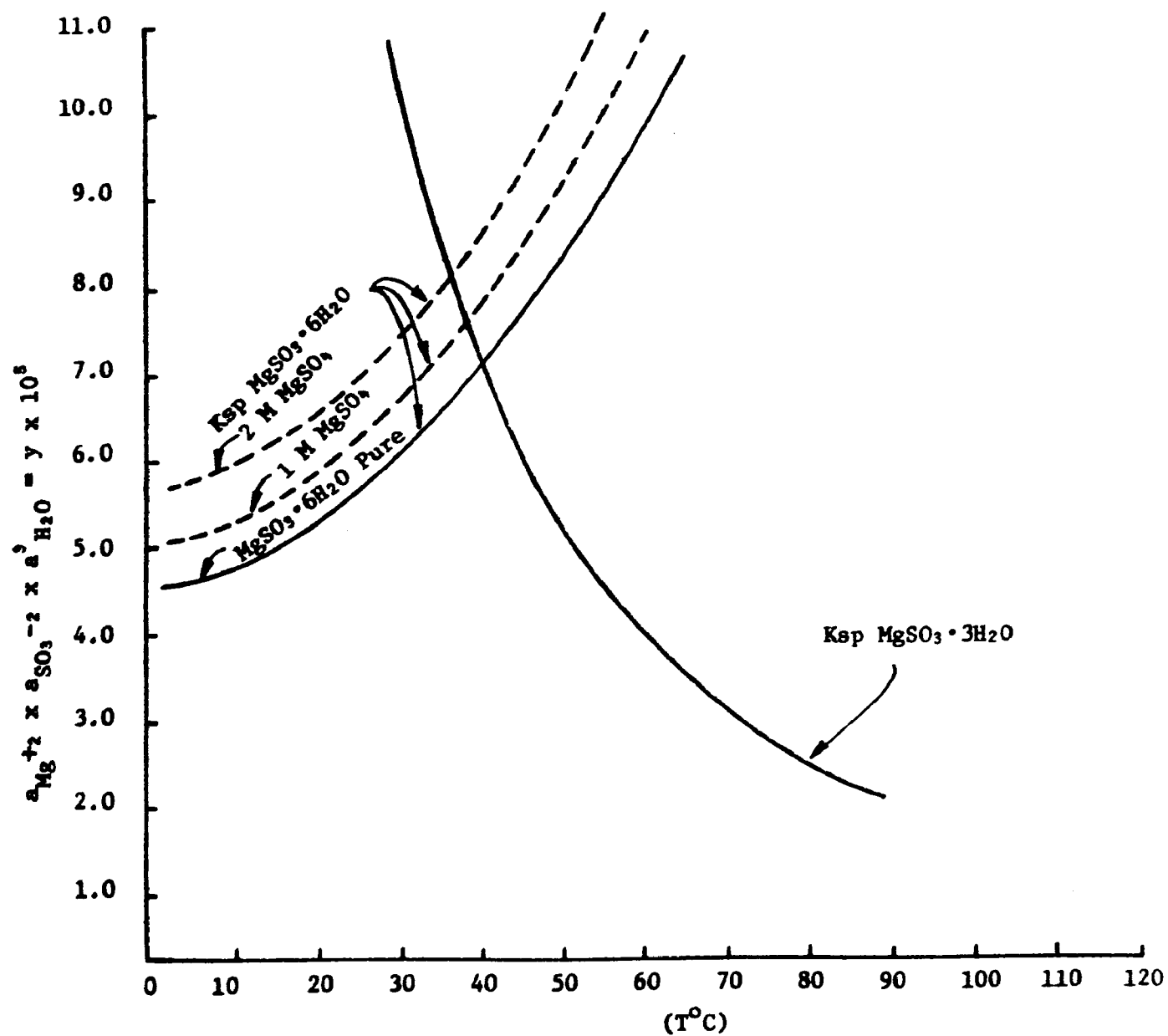
Figure 2-2. Transition in MgSO_4 Solution

TABLE 2-1. SATURATED CONDITIONS FOR $\text{MgSO}_3 \cdot 6\text{H}_2\text{O}$ IN PURE WATER

<u>Temperature (°C)</u>	<u>K_{sp_6}</u>	<u>a_w</u>	<u>$y = K_{sp_6}/a_w^3$</u>
25	5.720×10^{-5}	0.9987	5.742×10^{-5}
40	7.120×10^{-5}	0.9982	7.161×10^{-5}
45	7.735×10^{-5}	0.9978	7.786×10^{-5}
55	9.060×10^{-5}	0.9971	9.139×10^{-5}
62.5	10.13×10^{-5}	0.9964	10.24×10^{-5}

TABLE 2-2. INFLUENCE OF MgSO_4 ADDITION

Temp. (°C)	$K_{sp_6} \times 10^5$	a_w^3		$y = K_{sp_6}/a_w^3$	
		1 M	2 M	1 M	2 M
25	5.720	0.932	0.858	6.14×10^{-5}	6.67×10^{-5}
40	7.120	.932	.858	7.64×10^{-5}	8.30×10^{-5}
45	7.735	.932	.858	8.30×10^{-5}	9.02×10^{-5}
55	9.060	.932	.858	9.72×10^{-5}	10.56×10^{-5}
62.5	10.13	.932	.858	10.87×10^{-5}	11.81×10^{-5}

Note: 1 M MgSO_4 = 11 wt % MgSO_4

2 M MgSO_4 = 19 wt % MgSO_4

The intersection of these lines on the a_{p_3} plot (Figure 2-2) is the transition point. From this it is seen that the trihydrate-hexahydrate phase transition point continually decreased with increasing dissolved salt content or decreasing activity of water.

Sodium chloride has a more significant effect than magnesium sulfate as may be seen from the data in Table 2-3. These data are given graphically in Figure 2-3.

TABLE 2-3. INFLUENCE OF NaCl ADDITION

Temp. (°C)	$K_{sp_6} \times 10^5$	a_w^3		$y = K_{sp_6} / a_w^3$	
		1 M	2 M	1 M	2 M
25	5.720	0.905	0.815	6.32×10^{-5}	7.02×10^{-5}
40	7.120	.905	.815	7.87×10^{-5}	8.74×10^{-5}
45	7.735	.905	.815	8.55×10^{-5}	9.49×10^{-5}
55	9.060	.905	.815	10.01×10^{-5}	11.12×10^{-5}
62.5	10.13	.905	.815	11.19×10^{-5}	12.43×10^{-5}

Note: 1 M NaCl = 5.5 wt % NaCl
 2 M NaCl = 10.5 wt % NaCl

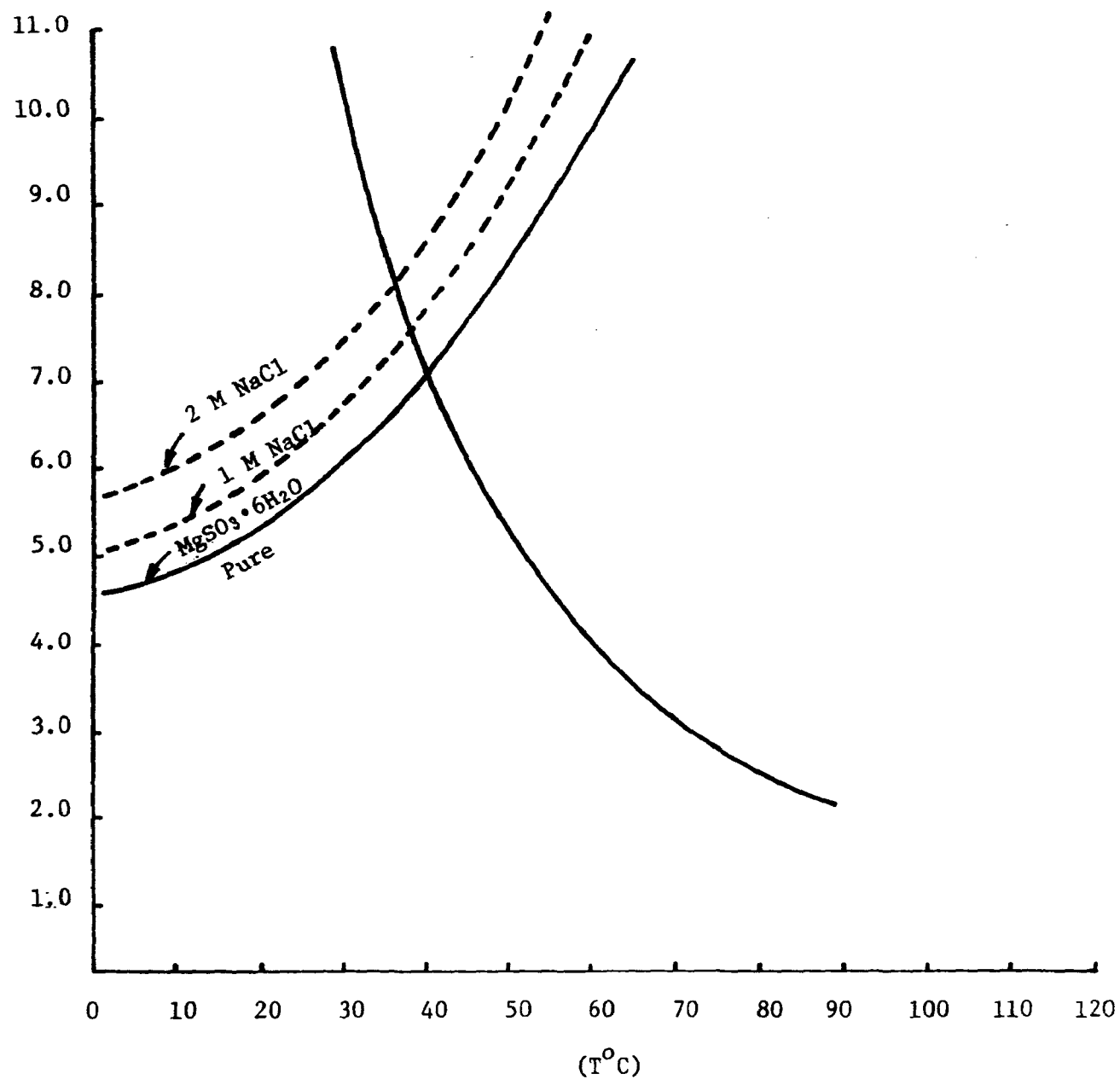


Figure 2-3. Transition in NaCl Solution

SECTION 3

CONCLUSIONS

From this description it can be seen that theory predicts a MgSO_3 hexahydrate-trihydrate phase transition temperature lowering with increasing solution dissolved solids content.

This indicates that for all operating units to date ($T > 37^\circ\text{C}$), the trihydrate is the stable form. Production of hexahydrate crystals as a metastable intermediate must be a kinetic phenomenon.

SECTION 4
NOMENCLATURE

a	activity
K	equilibrium constant
y	activity product ordinate defined in Equation 2-5b.

Subscripts

p	product
trans	transition, hexa to tri
w	water
3	trihydrate
6	hexahydrate

TECHNICAL NOTE 200-045-36-03

EXPERIMENTAL VERIFICATION OF THE MgSO_3
TRIHYDRATE-HEXAHYDRATE TRANSITIONS
AT 37.5°C IN MgSO_4 SOLUTIONS

Prepared by:

J. L. Skloss

CONTENTS

1. Introduction.	125
2. Experimental.	126
1.5M MgSO_4 Solution Test.	126
2.3M MgSO_4 Solution	127
3. Results	128
4. Conclusions	138

FIGURES

<u>Number</u>	<u>Page</u>
3-1 $\text{MgSO}_3 \cdot 6\text{H}_2\text{O}$ Crystals, 100X	129
3-2 $\text{MgSO}_3 \cdot 3\text{H}_2\text{O}$ Crystals, 200X	129
3-3 DSC Scan of the MgSO_3 Solids Present in the 2.3M MgSO_4 Solution.	132
3-4 DSC Scan of Pure $\text{MgSO}_3 \cdot 3\text{H}_2\text{O}$	133
3-5 DSC Scan of Pure $\text{MgSO}_3 \cdot 6\text{H}_2\text{O}$	134
3-6 DSC Scan of the Intermediate MgSO_3 Solids	135
3-7 IR Spectra of Pure $\text{MgSO}_3 \cdot 3\text{H}_2\text{O}$ and Pure $\text{MgSO}_3 \cdot 6\text{H}_2\text{O}$. . .	136
3-8 IR Spectra of the MgSO_3 Solids Present in the 2.3M MgSO_4 Solution and Pure $\text{MgSO}_3 \cdot 3\text{H}_2\text{O}$	137

TABLES

<u>Number</u>	<u>Page</u>
3-1 Transition of MgSO_3 Solids in 2.3M MgSO_4 Solution at 37°C	130

SECTION 1

INTRODUCTION

It has been shown theoretically that the transition temperature ($\sim 41^{\circ}\text{C}$ in pure solutions) of $\text{MgSO}_3 \cdot 3\text{H}_2\text{O}$ and $\text{MgSO}_3 \cdot 6\text{H}_2\text{O}$ can be lowered by increasing the ionic strength of the solution. In Technical Note 200-045-36-02 it was predicted that a 2.0M MgSO_4 solution could lower the transition temperature to 37.5°C . Therefore, the hexahydrate phase of magnesium sulfite is predicted to be stable in 1.5M magnesium sulfate solution at 37.5°C , whereas the trihydrate phase is predicted to be stable in 2.3M magnesium sulfate solution at the same temperature. It was desirable to verify these predictions by experiment.

SECTION 2

EXPERIMENTAL

Magnesium sulfate solutions (1.5 and 2.3M) were prepared and heated to 37.5°C. Excess hexa- and/or trihydrate magnesium sulfite crystals were added to these solutions and stirred continuously for several days. Sample aliquots were filtered, and the hydrate state of the magnesium sulfite solids was determined by chemical analyses and microscopic examination of the solids. In the case of the 2.3M magnesium sulfate solution test, differential scanning calorimetry (DSC) and infrared (IR) scans of the solids were also performed.

1.5M MgSO_4 SOLUTION TEST

A 1-liter solution of 1.5M magnesium sulfate was prepared and heated to 37.5°C. Excess $\text{MgSO}_3 \cdot 6\text{H}_2\text{O}$ solids were added to saturate the solution with respect to magnesium sulfite and to leave 25g of solids undissolved. The 1-liter erlenmeyer flask containing the slurry was stoppered and placed into a water bath maintained at 37.5°C. The slurry was stirred continuously with a magnetic stirrer. The hexahydrate phase remained stable during a one-week trial period as confirmed by chemical analyses.

Then 7g of $\text{MgSO}_3 \cdot 3\text{H}_2\text{O}$ solids were added. After one week of stirring at 37.5°C, a 100-ml portion of this slurry was filtered on Whatman No. 42 paper. The filtrate was saved for chemical analyses, and the solids were washed with 50% ethyl alcohol solution preheated to 37°C. The solids were oven dried at 45°C for 30 minutes, then analyzed and found to be pure $\text{MgSO}_3 \cdot 6\text{H}_2\text{O}$.

2.3M MgSO_4 SOLUTION

500 ml of 2.3M magnesium sulfate solution was prepared and heated to 37.5°C . Sufficient magnesium sulfite hexahydrate solids were added to saturate the solution. After filtration, 11g of $\text{MgSO}_3 \cdot 3\text{H}_2\text{O}$ were added. A nitrogen purge was used each time the erlenmeyer flask containing the slurry was opened.

The solids were allowed to equilibrate with the 2.3M magnesium sulfate solution for four days with gentle stirring in a water bath set at 37.5°C . A 50-ml sample was withdrawn and filtered by the same technique as described in the 1.5M MgSO_4 Solution Test Section. The solid sample was analyzed to be pure trihydrate.

Then, 10g of $\text{MgSO}_3 \cdot 6\text{H}_2\text{O}$ was added to the 2.3M magnesium sulfate solution (which contained the $\text{MgSO}_3 \cdot 3\text{H}_2\text{O}$ solids). The slurry was stirred continuously for five days at 37.5°C . A 50-ml sample was withdrawn and the slurry was allowed to equilibrate for another week under the same conditions. Finally, another sample was taken.

Chemical analyses of the filtrate and solids and microscopic examination of the solids were performed each time the slurry was sampled. The solids from the final sample were also analyzed by the DSC and the IR methods. The stable phase from this solution was found to be $\text{MgSO}_3 \cdot 3\text{H}_2\text{O}$.

SECTION 3

RESULTS

The chemical analyses of the final 1.5M magnesium sulfate solution containing the magnesium sulfite solids showed that the filtrate contained 1.5M magnesium and 0.13M sulfite. The solids contained 4.71 ± 0.20 mmole/g of magnesium and sulfite which indicated that the solids were pure $\text{MgSO}_3 \cdot 6\text{H}_2\text{O}$ and that all the $\text{MgSO}_3 \cdot 3\text{H}_2\text{O}$ solids were converted to the hexahydrate phase of magnesium sulfite. Microscopic examination also showed that the solid sample was $\text{MgSO}_3 \cdot 6\text{H}_2\text{O}$. The hexahydrate phase was observed to consist of relatively large hexagonal crystals (see Figure 3-1).

The chemical analyses of the 2.3M magnesium sulfate solution containing the magnesium sulfite solids are shown in Table 3-1. The magnesium and the sulfite concentrations of the filtrates were fairly consistent. The magnesium and the sulfite analyses of the solids showed that the trihydrate phase of magnesium sulfite remained stable during the four-day trial period.

After the addition of $\text{MgSO}_3 \cdot 6\text{H}_2\text{O}$ solids to the slurry, the magnesium and the sulfite content of the solids dropped. Analyses showed a mixture of phases was present in the slurry after five days of continuous stirring. Within the next 12 days, an increase in the magnesium and the sulfite content to near the theoretical value of 6.31 mmole/g indicated that the hexahydrate phase had converted to the trihydrate phase. Microscopic examination also showed that the final solids sample was $\text{MgSO}_3 \cdot 3\text{H}_2\text{O}$. The trihydrate phase was characterized as being relatively small bipyramid crystals (see Figure 3-2).

When the DSC scan of the final solids sample, shown in Figure 3-3, was compared with the DSC scans of the pure

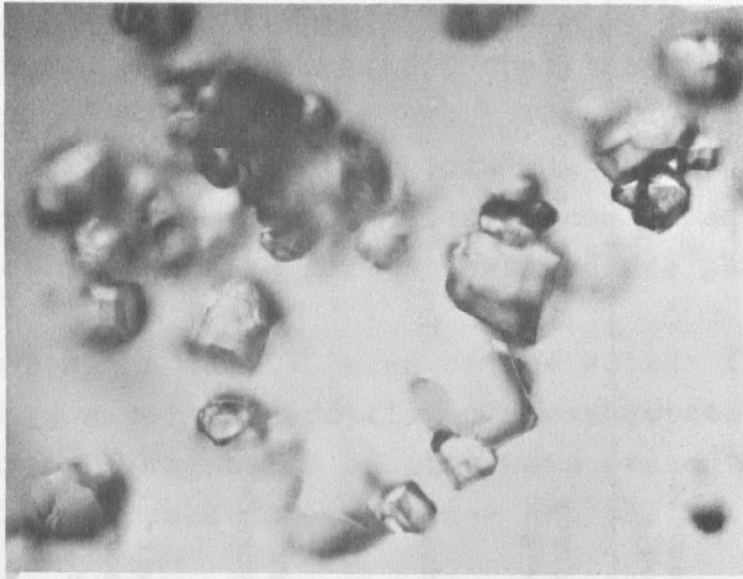


FIGURE 3-1. $\text{MgSO}_3 \cdot 6\text{H}_2\text{O}$ CRYSTALS, 100X

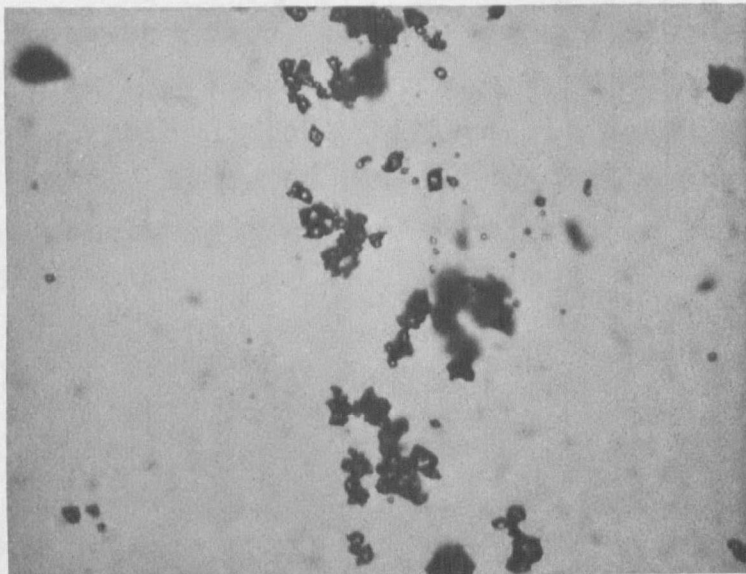


FIGURE 3-2. $\text{MgSO}_3 \cdot 3\text{H}_2\text{O}$ CRYSTALS, 200X

TABLE 3-1. TRANSITION OF MgSO_3 SOLIDS IN 2.3M MgSO_4 SOLUTION AT 37°C

Total Time Allowed, Days	Filtrate Analyses (mole/l)		Solids Analyses (mmole/g)		Microscopic Analysis	Conclusions
	Mg^{+2}	SO_3^{-2}	Mg	Sulfite		
0	2.26	--	6.30	6.30	Trihydrate Crystals	Started with trihy- drate
4	2.33	0.14	6.28	6.31	Trihydrate	Trihydrate unchanged
Added hexahydrate						
9	2.31	0.12	5.62	5.60	Mixture of tri- hexahydrate	Mixture of tri- and hexahydrate
15	--	--	--	--	Mostly tri- with some hexahydrate	--
16	2.25	0.12	6.22	6.25	All trihydrate	All hexahydrate converted to trihydrate

trihydrate and the pure hexahydrate solids (Figures 3-4 and 3-5, respectively), it was concluded that the final solids sample was the pure trihydrate phase. The loss of water (or the surge of energy required to maintain a steady temperature increase) started at 160°C and obviously continued well beyond the 80°C temperature needed for the hexahydrate phase.

Figure 3-6 shows the DSC scan of the solids from an earlier sample five days after the addition of hexahydrate crystals, when both phases of magnesium sulfite were present. Note the two characteristic peaks for the hexa- and the trihydrate phases.

IR spectra of pure magnesium sulfite trihydrate and hexahydrate were also made (see Figure 3-7). Small differences in these spectra can be noticed. The IR spectrum of the final solids sample from the 2.3M magnesium sulfate solution is shown in Figure 3-8 where it is compared with that of pure magnesium sulfite trihydrate standard. These spectra matched well and it was concluded that the solids from the 2.3M magnesium sulfate solution were all trihydrate. Sulfate, if present, would absorb at $1,100\text{ cm}^{-1}$. Since no absorbance was observed in this region, it was concluded that the equilibrated solids sample was sulfate free.

PART NO. 9909M

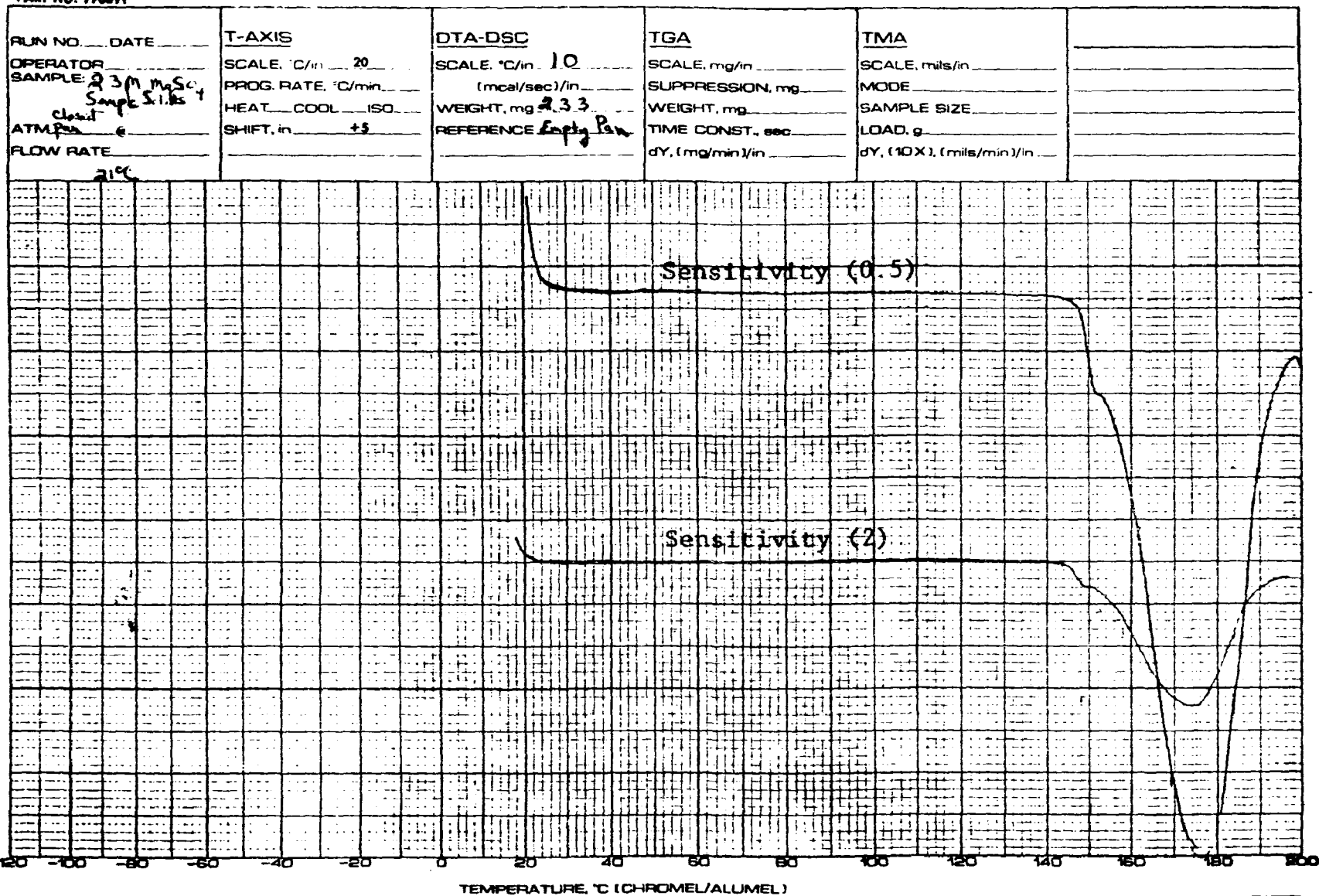


Figure 3-3. DSC Scan of the MgSO₃ Solids Present in the 2.3M MgSO₄ Solution

PART NO. 990091

RUN NO. 3 DATE 3-18-74
 OPERATOR RES
 SAMPLE: $MgSO_4 \cdot 3H_2O$
 Cooled Run
 ATM 6
 FLOW RATE
 Start 27°C

T-AXIS
 SCALE, °C/in 20
 PROG. RATE, °C/min
 HEAT COOL ISO
 SHIFT, in +5

DTA-OSC
 SCALE, °C/in 10
 (mcal/sec)/in
 WEIGHT, mg 0.63
 REFERENCE Empty Pan

TGA
 SCALE, mg/in
 SUPPRESSION, mg
 WEIGHT, mg
 TIME CONST., sec
 dY, (mg/min)/in

TMA
 SCALE, mils/in
 MODE
 SAMPLE SIZE
 LOAD, g
 dY, (10X), (mils/min)/in

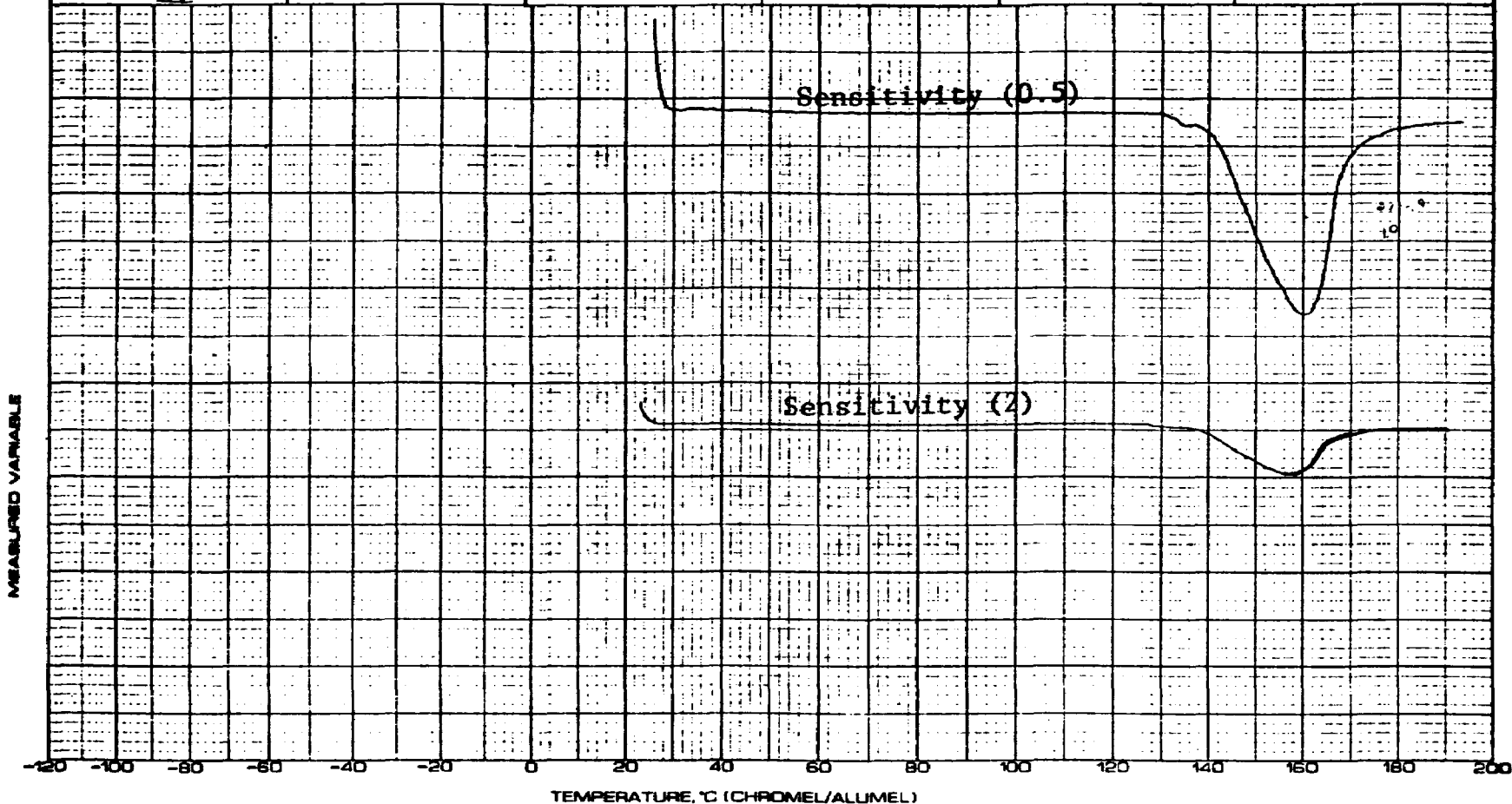
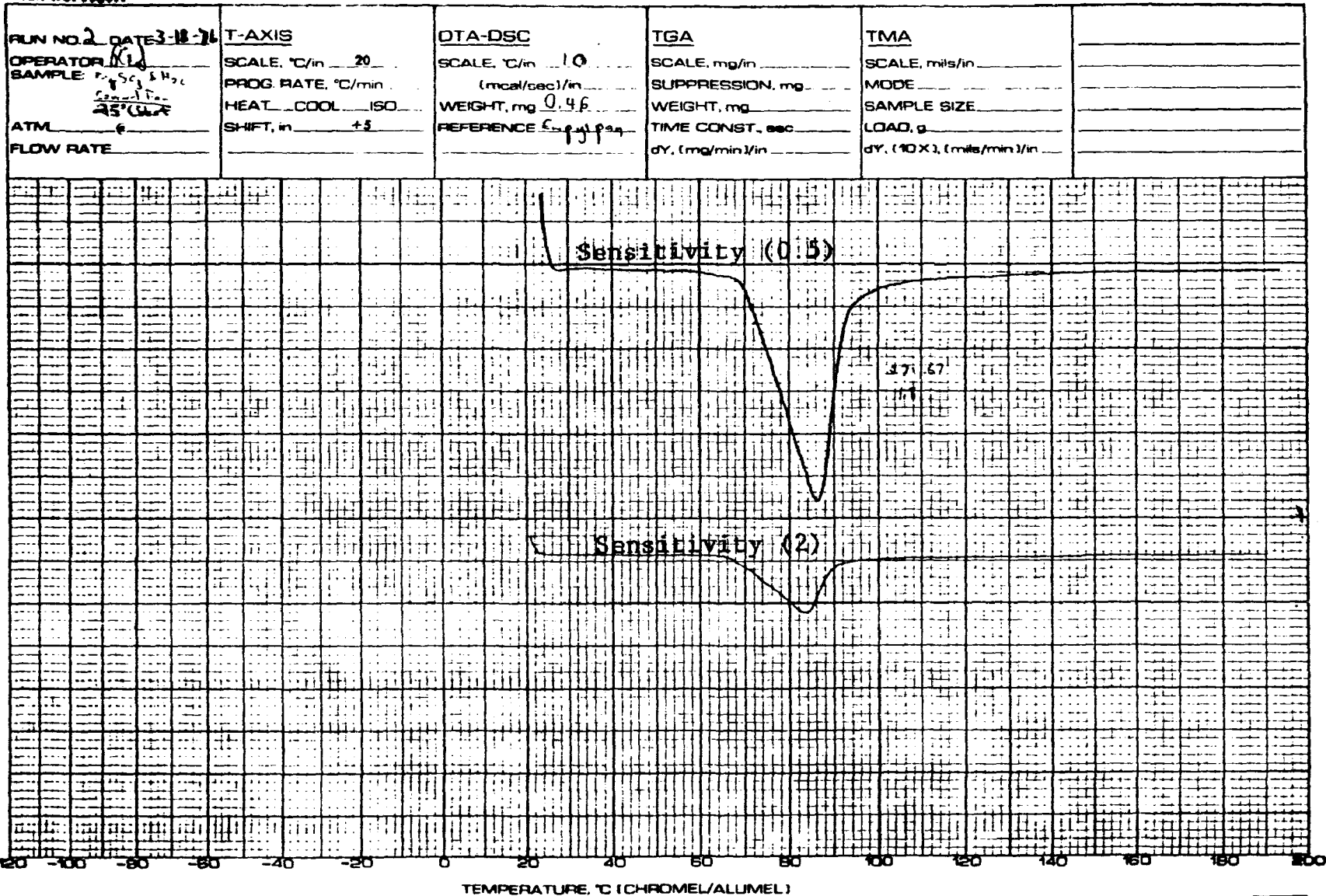


Figure 3-4. DSC Scan of Pure $MgSO_4 \cdot 3H_2O$

PART NO. 9900H

Figure 3-5. DSC Scan of Pure MgSO₃·6H₂O

PART NO. 990091

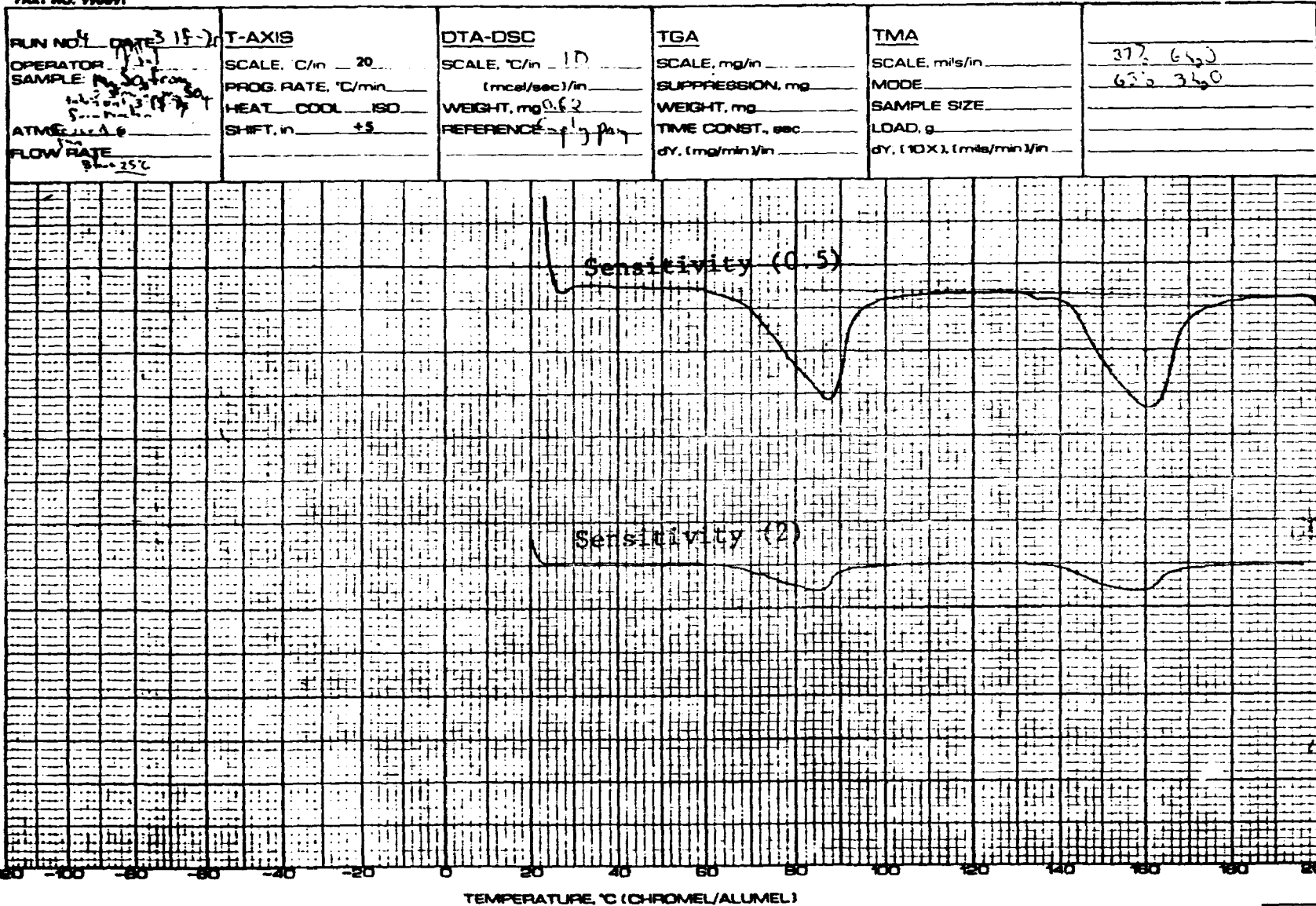


Figure 3-6. DSC Scan of the Intermediate MgSO₃ Solids

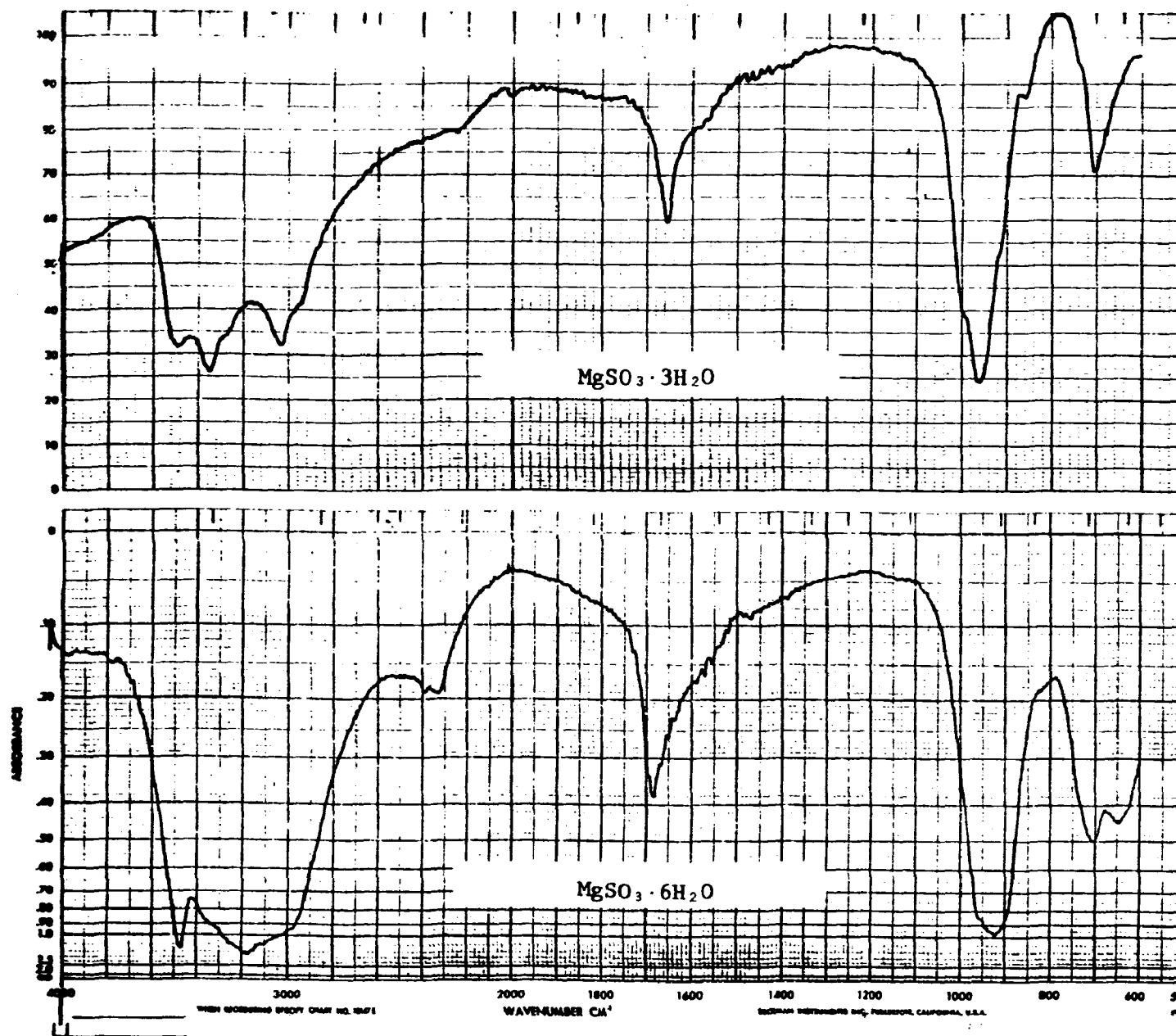


Figure 3-7. IR Spectra of Pure $\text{MgSO}_3 \cdot 3\text{H}_2\text{O}$ and Pure $\text{MgSO}_3 \cdot 6\text{H}_2\text{O}$

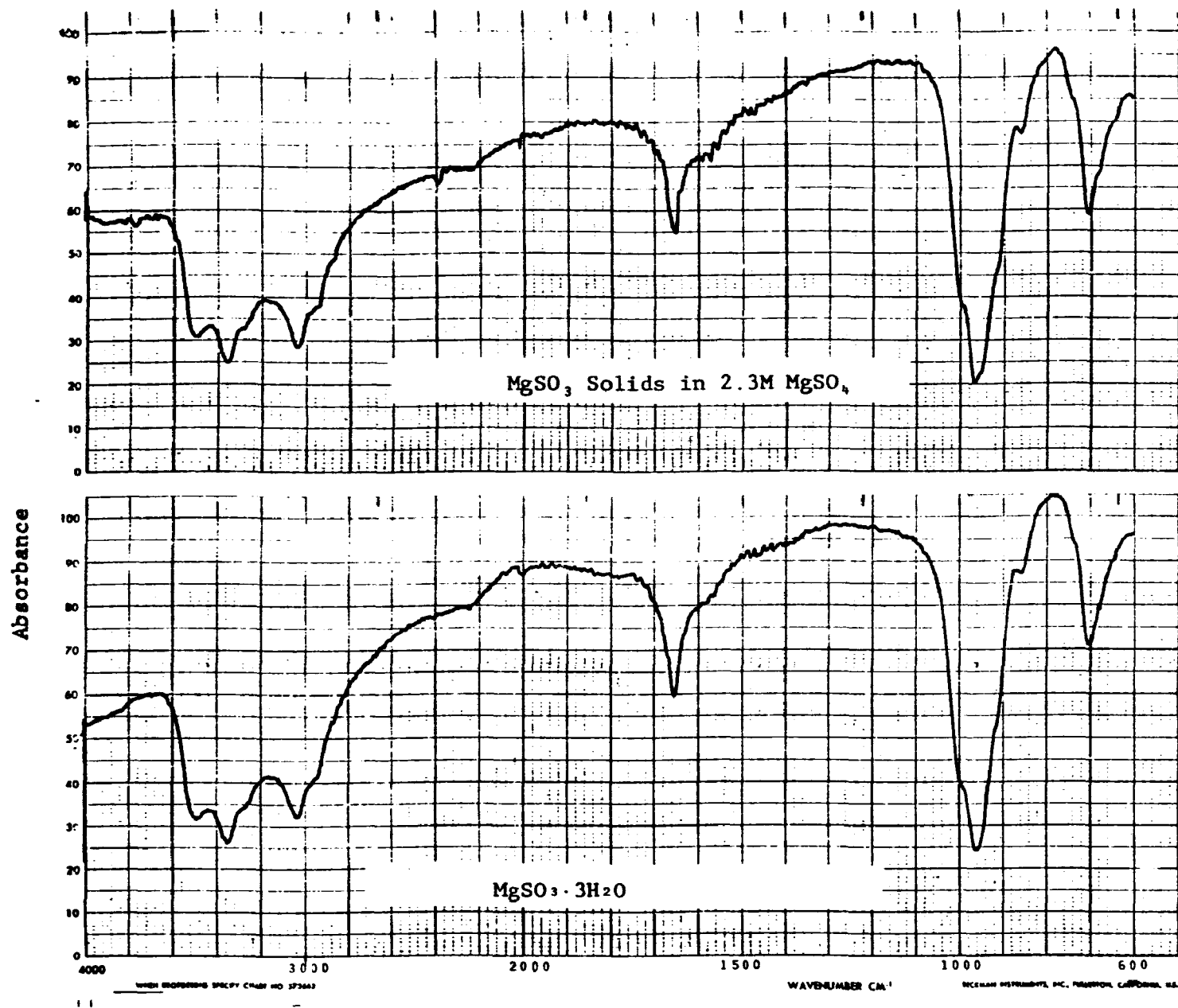


Figure 3-8. IR Spectra of the MgSO₃ Solids Present in the 2.3M MgSO₄ Solution and Pure MgSO₃ · 3H₂O

SECTION 4

CONCLUSIONS

The transition temperature of magnesium sulfite trihydrate and hexahydrate phases can be lowered by increasing the concentration of the magnesium sulfate solution. It was observed that at 37.5°C, $\text{MgSO}_3 \cdot 6\text{H}_2\text{O}$ is the stable phase in a 1.5M magnesium sulfate solution and $\text{MgSO}_3 \cdot 3\text{H}_2\text{O}$ is the stable phase in a 2.3M magnesium sulfate solution. The theoretically predicted equilibrium solution was approximately 2.0M MgSO_4 .

TECHNICAL NOTE 200-045-36-04

EXPERIMENTAL RESULTS FOR THE
EQUILIBRIUM STUDIES ON MgSO_3 HYDRATES

Prepared by:

R. E. Pyle

CONTENTS

1.	Introduction	143
2.	Experimental Approach for the Solubility and Solubility Product Constant Studies.	145
	Experimental Apparatus	145
	Experimental Procedures	146
	Analytical Methods.	147
3.	Experimental Results for the Solubility and Solubility Product Constant Studies.	148
	Equilibrium Data Processing	148
	Results for the Solubility and Solubility Product Constant Studies	149
4.	Experimental Approach for the Ion-Pair Dissociation Studies - Ion Selective Electrode Measurements	157
	Experimental Apparatus.	157
	Experimental Procedure	158
	Analytical Methods.	159
5.	Experimental Approach for the Ion-Pair Dissociation Studies - Method of Influence of Ion-Pair Formation on a Reference Compound Solubility.	161
	Experimental Apparatus and Procedures	161
	Analytical Methods.	162
6.	Experimental Results for the Ion-Pair Dissociation Studies	165

CONTENTS (Cont'd)

Equilibrium Data Processing - Ion Selective Electrode Measurements	165
Equilibrium Data Processing - Method of Influence of Ion-Pair Formation on a Reference Compound Solubility	166
Results for the Ion-Pair Dissociation Studies.	166
7. Conclusions	170
Bibliography	171

FIGURES

<u>Number</u>		<u>Page</u>
3-1	Solubility vs. Temperature for MgSO_3 Hydrates . .	153
3-2	Pure Solution Activity Product vs. Temperature. .	156
6-1	$\log_{10} K_d$ vs. $1/T(K) \times 10^3$	167

TABLES

<u>Number</u>		<u>Page</u>
3-1	Experimental Results for the MgSO_3 Solubility Measurements.	150
3-2	MgSO_3 Solubility Data	151
3-3	Experimental MgSO_3 Solubility Product Constants (K_{sp})	154
5-1	Results of Equilibrium Studies.	163
6-1	Ion-Pair Dissociation Constants	169

SECTION 1

INTRODUCTION

The magnesium oxide or "Mag-Ox" process for sulfur dioxide removal has proven to be technically feasible and is one of the most advanced regenerative processes. In this scrubbing process, the reaction of SO_2 from flue gases with the MgO scrubbing slurry yields the hydrated phases of MgSO_3 and other products. Experience has been that at a coal-fired unit with MgO scrubber the hexahydrate crystalline phase was produced; and at an oil-fired unit, the trihydrate crystalline phase was produced. From a process point of view, the trihydrate phase may be more desirable because less energy is required to drive off the waters of hydration in the regenerative cycle. However, the trihydrate crystals that are produced are very small, on the order of a few micrometers in size, while the hexahydrate crystals that are produced are large massive particles several hundred micrometers in size. Consequently, the settling and handling characteristics of the two phases are vastly different. Currently the hexahydrate phase is much easier to process in the solid separation equipment. In view of these process problems, it was the objective of this work to:

- 1) investigate the theoretical aspects of hydrate phase transitions,
- 2) determine the equilibrium solubilities and solubility product constants of the trihydrate and hexahydrate phases of MgSO_3 as a function of temperature,
- 3) investigate the influence of solution composition on the transition temperature of the hexahydrate-trihydrate phase change, and

- 4) investigate the influence of solution composition and temperature on the formation kinetics of the two solid phases.

This Technical Note presents in detail the experimental data that were derived from the equilibrium studies on the hexahydrate and trihydrate crystalline phases of MgSO_3 . The equilibrium studies are separated into two phases of experimental work:

- 1) the determination of the equilibrium solubilities and the solubility product constants of the trihydrate and hexahydrate phases of MgSO_3 as a function of temperature, and
- 2) the determination of ion-pair dissociation constants for the species: $\text{MgSO}_3(\text{aq})$, $\text{MgSO}_4(\text{aq})$, and $\text{NaSO}_3^-(\text{aq})$ as a function of temperature.

SECTION 2

EXPERIMENTAL APPROACH FOR THE SOLUBILITY AND SOLUBILITY PRODUCT CONSTANT STUDIES

EXPERIMENTAL APPARATUS

Solubility measurements for the MgSO_3 hydrates were performed as a function of temperature over the range 25-65°C. Excess magnesium sulfite hexahydrate or trihydrate crystals were allowed to dissolve into approximately 300 ml of deoxygenated deionized water. This slurry was continuously agitated by magnetic stirring in a closed reaction vessel specially designed for these studies. The reaction vessel consisted of a five-neck round-bottom flask of 500 ml capacity suspended in an insulated constant temperature bath. With this arrangement, the temperature of the reaction vessel could be held at the desired reaction temperature to within $\pm 0.1^\circ\text{C}$.

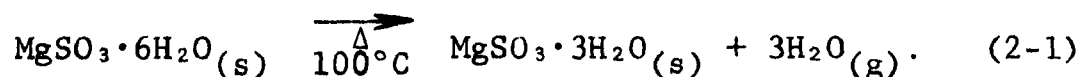
Two necks of the multiple-neck reaction flask were used as a continuous dry nitrogen purge gas inlet and outlet. The dry nitrogen gas from the cylinder was passed through a deoxygenating scrubbing train consisting of two fritted 4-liter bottles containing 1M Na_2SO_3 prior to entering the sealed reaction vessel. A fritted Na_2SO_3 scrubbing bottle was also located at the gas outlet. This nitrogen purge gas was used to minimize oxidation of the sulfite ion in the reaction medium.

Another neck of the reaction vessel supported a ground glass precision thermometer which penetrated the reaction solution. A fourth neck was used for periodic sampling which was performed by forcing the slurry out of the reaction flask through a 42mm, 0.8 micrometer Millipore filter membrane by

pressurizing the vessel with the dry nitrogen purge gas. The filtrate was then collected and the pertinent analyses performed.

EXPERIMENTAL PROCEDURES

The clean reaction vessel was first charged with the de-oxygenated deionized water and then heated to the desired reaction temperature in the constant temperature bath. After the continuous nitrogen purge gas stream was started, excess MgSO_3 hydrate solids were added to the reaction vessel. $\text{MgSO}_3 \cdot 6\text{H}_2\text{O}$ crystals were used for the solubility determinations below 40°C and $\text{MgSO}_3 \cdot 3\text{H}_2\text{O}$ crystals were used for the solubility determination above 40°C . The $\text{MgSO}_3 \cdot 6\text{H}_2\text{O}$ crystals, 99% pure, were obtained from Heico Laboratories. The $\text{MgSO}_3 \cdot 3\text{H}_2\text{O}$ crystals for these experiments were obtained by dehydrating $\text{MgSO}_3 \cdot 6\text{H}_2\text{O}$ crystals under their own atmosphere in a purged oven at 100°C after the method of Dauerman (DA-001). The equation for this reaction was:



The trihydrate product was then analyzed for purity before use.

The dissolution reaction was allowed to come to equilibrium while constant reaction temperature, continuous stirring and nitrogen gas purging were maintained. The approach to equilibrium was followed by periodically sampling the reaction solution as described earlier. The solution samples were analyzed for concentrations of magnesium, sulfite, and sulfate, solution pH, and reaction temperature (see Section 2.3 for Analytical Methods). The solubilities and solubility

product constants were calculated from the equilibrium analytical data obtained at each reaction temperature.

ANALYTICAL METHODS

In this section, a brief outline of the analytical methods used in the MgSO_3 hydrate equilibrium studies is given:

- 1) Magnesium - colorimetric titration with Na_2EDTA or dilution preparation and atomic absorption determination;
- 2) Sulfite - iodine-buffer preparation and back titration with standard arsenite or thiosulfate; and
- 3) Sulfate - peroxide oxidation of sulfite, hydrogen ion exchange, and titration with standard sodium hydroxide. Sulfate is calculated as the difference between total sulfur and sulfite sulfur.

SECTION 3

EXPERIMENTAL RESULTS FOR THE SOLUBILITY AND SOLUBILITY PRODUCT CONSTANT STUDIES

EQUILIBRIUM DATA PROCESSING

Solubilities for $\text{MgSO}_3 \cdot 6\text{H}_2\text{O}$ below 40°C and $\text{MgSO}_3 \cdot 3\text{H}_2\text{O}$ above 40°C are determined from the experimental dissolution analytical data. The solubilities in grams of MgSO_3 per 100 grams of saturated solution are calculated from the equilibrium concentrations of magnesium and/or sulfite in the saturated solution at each experimental reaction temperature. That is:

$$S(\text{g}/100\text{g}) = [\text{Ion}] \frac{\text{MW}}{10} \cdot \frac{1}{D} \quad (3-1)$$

where:

S = solubility of MgSO_3 at temperature, T ,

$[\text{Ion}]$ = equilibrium magnesium or sulfite ion
concentration in moles/liter,

MW = molecular weight of MgSO_3 , i.e. 104.37
grams/mole, and

D = density of MgSO_3 solution at the
particular reaction temperature in
grams/ml (from literature data).

The solubility product constants for $\text{MgSO}_3 \cdot 6\text{H}_2\text{O}$ and $\text{MgSO}_3 \cdot 3\text{H}_2\text{O}$ are also determined from the experimental dissolution analytical data. The solubility product constants can be expressed as:

$$K_{sp_6}(T) = a_{Mg^{+2}} \cdot a_{SO_3^{-2}} \cdot a_{H_2O}^6 \quad (3-2)$$

and,

$$K_{sp_3}(T) = a_{Mg^{+2}} \cdot a_{SO_3^{-2}} \cdot a_{H_2O}^3 \quad (3-3)$$

Equilibrium activities for these particular solution species are calculated by inputting pertinent reactor solution equilibrium information, such as concentrations of magnesium and sulfite, solution pH, and reaction temperature, to the Radian chemical equilibrium computer program. This program takes into account the important and complex solution equilibria, such as critical ion-pair formations, for each set of input reaction conditions.

Reliable and accurate temperature-dependent dissociation constant (K_d) information for pertinent ion-pair species is needed to calculate accurate solubility product constants from experimental solubility data. Therefore, temperature dependent ion-pair dissociation measurements for the species $MgSO_3(aq)$, $MgSO_4(aq)$, and $NaSO_3^-(aq)$ were performed using two different experimental approaches. These ion-pair dissociation studies are discussed in detail in Sections 4, 5 and 6.

RESULTS FOR THE SOLUBILITY AND SOLUBILITY PRODUCT CONSTANT STUDIES

Experimental results for the solubility measurements on the $MgSO_3$ system are summarized in Table 3-1. Experimental solubilities for $MgSO_3 \cdot 6H_2O$ and $MgSO_3 \cdot 3H_2O$, calculated from the results in Table 3-1, are presented in Table 3-2 along with solubility data taken from the literature (LI-001).

TABLE 3-1. EXPERIMENTAL RESULTS FOR THE MgSO_3 SOLUBILITY MEASUREMENTS

Run No.	Solution pH	Reactor Temp. (°C)	Conc. of Magnesium (mole/l)	Conc. of Sulfite (mole/l)	Conc. of Sulfate (mole/l)
1	9.54	25.0	0.0638	0.0631	0.00098
2	9.39	30.0	0.069	0.061	0.0094
3	9.30	35.0	0.082	0.075	0.0082
4	8.51	45.0	0.0816	0.086	0.000
5	8.47	55.0	0.0769	0.077	0.000
6	8.32	65.0	0.067	0.067	0.002

TABLE 3-2. MgSO_3 SOLUBILITY DATA

Temperature (°C)	Stable Solid Phase	Experimental Solubility (g MgSO_3 /100 g)	Literature Solubility (g MgSO_3 /100 g)
25.0	$\text{MgSO}_3 \cdot 6\text{H}_2\text{O}$	0.668	0.625
30.0	$\text{MgSO}_3 \cdot 6\text{H}_2\text{O}$	0.723	0.721
35.0	$\text{MgSO}_3 \cdot 6\text{H}_2\text{O}$	0.861	0.835
45.0	$\text{MgSO}_3 \cdot 3\text{H}_2\text{O}$	0.906	0.904
55.0	$\text{MgSO}_3 \cdot 3\text{H}_2\text{O}$	0.814	0.790
65.0	$\text{MgSO}_3 \cdot 3\text{H}_2\text{O}$	0.713	0.710

In Figure 3-1, a plot of the MgSO_3 solubility data from the literature (LI-100) versus temperature is presented along with our experimentally derived values for comparison.

Solubility product constants for $\text{MgSO}_3 \cdot 6\text{H}_2\text{O}$ and $\text{MgSO}_3 \cdot 3\text{H}_2\text{O}$ derived from the literature solubility data are presented in tabular form as a function of temperature in Table 3-3.

It is also convenient to plot the solubility tendencies of the hexahydrate species on the same graph as the trihydrate species. As defined earlier, the pure solution activity products or solubility product constants for the hydrate species can be written as:

$$K_{\text{sp}_6}(\text{T}) = a_{\text{Mg}^{+2}} \cdot a_{\text{SO}_3^{-2}} \cdot a^6_{\text{H}_2\text{O}} = \text{ap}_6 \quad (3-4)$$

and,

$$K_{\text{sp}_3}(\text{T}) = a_{\text{Mg}^{+2}} \cdot a_{\text{SO}_3^{-2}} \cdot a^3_{\text{H}_2\text{O}} = \text{ap}_3 \quad (3-5)$$

It is clear that the hexahydrate activity product has units that differ from the trihydrate activity product units. Therefore, if we consider the ordinate on our ap_3 plot as y , then we can plot ap_6 values as a function of temperature on our ap_3 graph by defining the y ordinate as:

$$\text{ap}_6 = y \cdot a^3_{\text{H}_2\text{O}} \quad (3-6)$$

or

$$y = \text{ap}_6 / a^3_{\text{H}_2\text{O}} \quad (3-7)$$

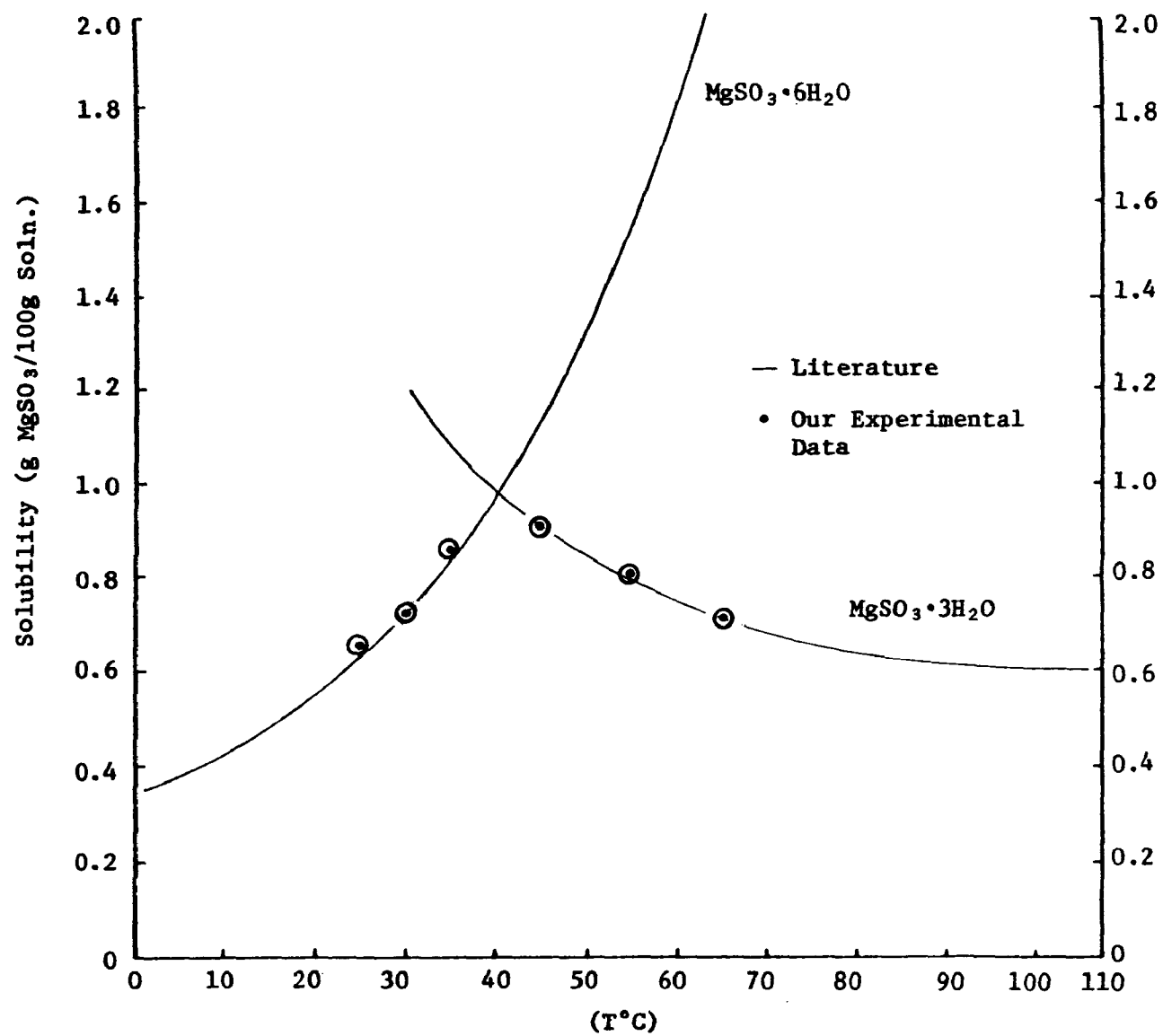


Figure 3-1. Solubility vs. Temperature for MgSO_3 Hydrates

TABLE 3-3. EXPERIMENTAL MgSO_3 SOLUBILITY PRODUCT CONSTANTS (K_{sp})

Temperature (°C)	Stable Solid Phase	K_{sp}
0	$\text{MgSO}_3 \cdot 6\text{H}_2\text{O}$	4.537×10^{-5}
10	$\text{MgSO}_3 \cdot 6\text{H}_2\text{O}$	4.797×10^{-5}
20	$\text{MgSO}_3 \cdot 6\text{H}_2\text{O}$	5.368×10^{-5}
25	$\text{MgSO}_3 \cdot 6\text{H}_2\text{O}$	5.720×10^{-5}
30	$\text{MgSO}_3 \cdot 6\text{H}_2\text{O}$	6.124×10^{-5}
35	$\text{MgSO}_3 \cdot 6\text{H}_2\text{O}$	6.579×10^{-5}
40	$\text{MgSO}_3 \cdot 6\text{H}_2\text{O}$	7.120×10^{-5}
45	$\text{MgSO}_3 \cdot 6\text{H}_2\text{O}$ (metastable)	7.735×10^{-5}
50	$\text{MgSO}_3 \cdot 6\text{H}_2\text{O}$ (metastable)	8.375×10^{-5}
55	$\text{MgSO}_3 \cdot 6\text{H}_2\text{O}$ (metastable)	9.060×10^{-5}
60	$\text{MgSO}_3 \cdot 6\text{H}_2\text{O}$ (metastable)	9.786×10^{-5}
62.5	$\text{MgSO}_3 \cdot 6\text{H}_2\text{O}$ (metastable)	1.013×10^{-4}
30	$\text{MgSO}_3 \cdot 3\text{H}_2\text{O}$ (metastable)	1.074×10^{-4}
35	$\text{MgSO}_3 \cdot 3\text{H}_2\text{O}$ (metastable)	8.662×10^{-5}
40	$\text{MgSO}_3 \cdot 3\text{H}_2\text{O}$ (stable)	7.120×10^{-5}
45	$\text{MgSO}_3 \cdot 3\text{H}_2\text{O}$ (stable)	6.074×10^{-5}
50	$\text{MgSO}_3 \cdot 3\text{H}_2\text{O}$ (stable)	5.191×10^{-5}
55	$\text{MgSO}_3 \cdot 3\text{H}_2\text{O}$ (stable)	4.466×10^{-5}
60	$\text{MgSO}_3 \cdot 3\text{H}_2\text{O}$ (stable)	3.894×10^{-5}
70	$\text{MgSO}_3 \cdot 3\text{H}_2\text{O}$ (stable)	3.020×10^{-5}
80	$\text{MgSO}_3 \cdot 3\text{H}_2\text{O}$ (stable)	2.457×10^{-5}
90	$\text{MgSO}_3 \cdot 3\text{H}_2\text{O}$ (stable)	2.059×10^{-5}
100	$\text{MgSO}_3 \cdot 3\text{H}_2\text{O}$ (stable)	1.771×10^{-5}

Therefore, in Figure 3-2, a plot of y versus temperature is presented. The activity products for the solubility product constants were calculated using the Radian chemical equilibrium computer program as described earlier. No solubility product constants for the MgSO_3 hydrates were found in the literature to compare with our experimentally derived values.

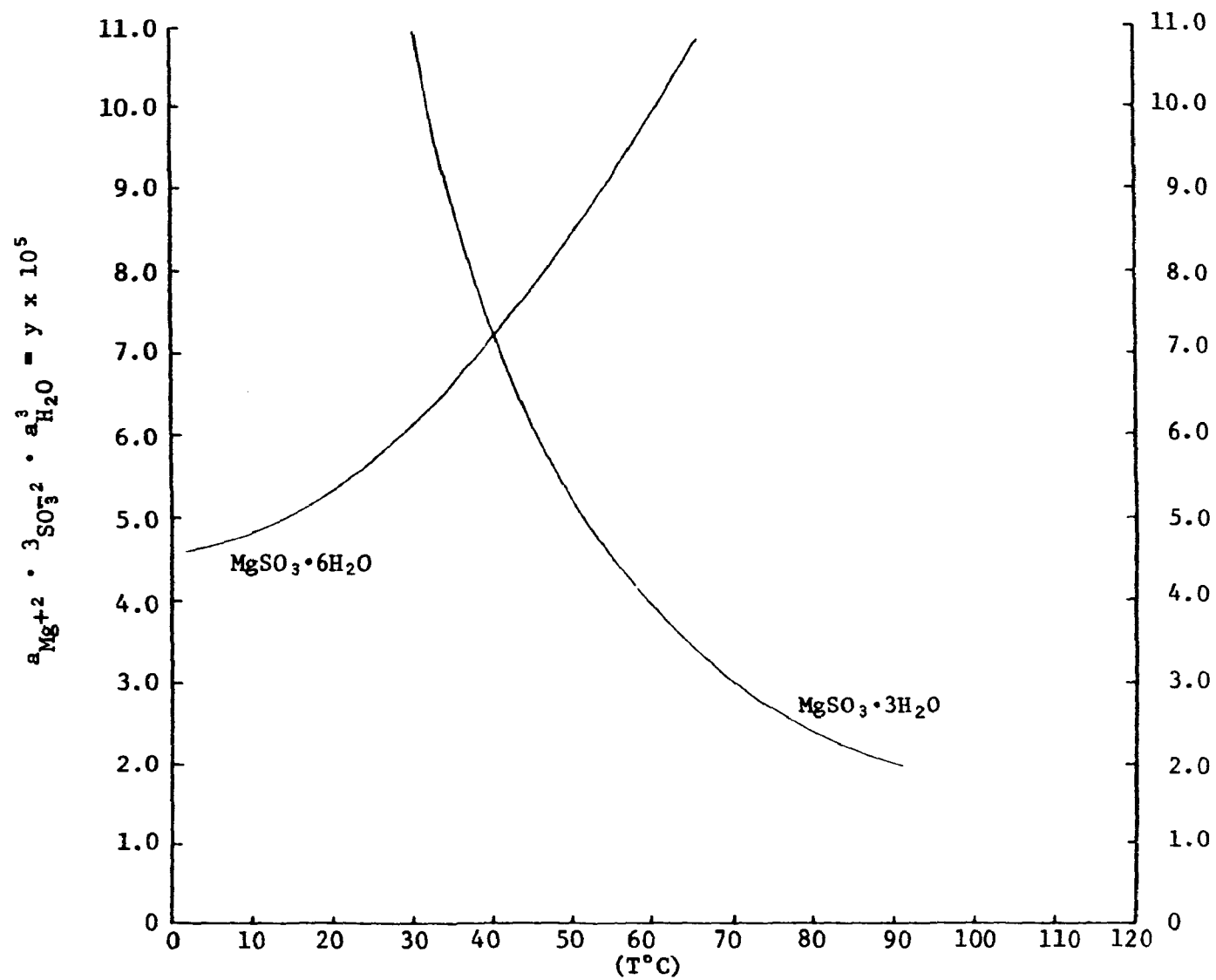


Figure 3-2. Pure Solution Activity Product vs. Temperature

SECTION 4

EXPERIMENTAL APPROACH FOR THE ION-PAIR DISSOCIATION STUDIES - ION SELECTIVE ELECTRODE MEASUREMENTS

EXPERIMENTAL APPARATUS

Ion-pair dissociation measurements for the species $\text{MgSO}_3(\text{aq})$, $\text{MgSO}_4(\text{aq})$, and $\text{NaSO}_3^-(\text{aq})$ were performed as a function of temperature over the range 25-55°C. Unsaturated test solutions of the species of interest were prepared and brought to the desired experimental temperature. The free cation response of the solution was then measured with special cation selective electrodes. This value was compared to the measured free cation response of standard solutions with negligible ion pairing.

Test solutions for the particular ion-pair species were prepared from either $\text{MgSO}_3 \cdot 6\text{H}_2\text{O}$, MgSO_4 , or Na_2SO_3 by dissolution of the respective pure solid in approximately 150 ml of deoxygenated deionized water to a predetermined unsaturated concentration with pH adjustment if necessary. The test solutions were continuously agitated by magnetic stirring in closed reaction vessels used specifically for these equilibrium studies. These vessels were Nalge high temperature, wide-mouth, flat-bottom plastic bottles with sealable tops and of 250-ml capacity. The sealed reaction vessels containing the appropriate test and cation standard solutions for each experiment were supported in an insulated constant temperature bath that maintained the desired reaction temperature to within $\pm 0.1^\circ\text{C}$.

A 4-holed rubber stopper was used to support a precision thermometer for accurate solution temperature measurements,

an input divalent or sodium cation electrode for free cation activity measurements, an Orion single junction or Beckman standard saturated calomel reference electrode, and a standard pH electrode for solution pH measurements. The thermometer-electrode assembly was inserted consecutively in the appropriate standard and test solutions maintained at the desired experimental temperature. The rubber stopper provided an airtight seal with the Nalge reaction vessels to minimize oxidation of sulfite during the measurements. In addition, a nitrogen blanket for the solutions was also provided. The solution pH and free cation response measurements were taken with a calibrated Model 701 Orion Digital Meter.

EXPERIMENTAL PROCEDURE

A series of standard solutions of different concentrations with negligible ion pairing were prepared quantitatively. Unsaturated magnesium ion standard solutions were prepared from pure $\text{MgCl}_2 \cdot 6\text{H}_2\text{O}$, and sodium ion standard solutions from pure NaCl . Sodium and magnesium concentrations of the standard solutions were determined accurately with dilution preparation and atomic absorption spectroscopy. Concentrations of the standard solutions ranged over approximately two decades of molarity with the extremes bracketing the concentrations of the particular ion-pair test solutions under investigation.

The sodium or magnesium standard solutions contained in the sealed Nalge reaction vessels were then placed in the constant temperature bath maintained at 25°C and allowed to thermally equilibrate. The solution temperature, pH, and free cation response of each standard solution was then measured in duplicate by the technique described in Section 4.1.

Equilibrium activities for the particular standard solution species were calculated by inputting the ion concentrations, solution pH, and temperature for each standard solution into the Radian chemical equilibrium computer program. Calibration curves for the cation selective electrodes were prepared by plotting the logarithm of the sodium or magnesium free-cation calculated activity versus the measured electrode response in millivolts for each standard solution.

Test solutions of different concentrations and of the desired ion-pairs were then prepared in duplicate for each experimental measurement and analyzed for magnesium, sulfite, sulfate, or sodium before and after the response measurement at each experimental temperature. The thermal and drift corrected free-cation response derived from the measurements of these test solutions at the various experimental temperatures were then compared to the free-cation electrode response from the calibration curve for the particular standard solutions. Activities for the particular test solution species were calculated, as before, by using the Radian chemical equilibrium computer program. From these experimental measurements and computer calculations, temperature-dependent dissociation constants (K_d) for the particular ion-pairs were calculated (see Section 6).

ANALYTICAL METHODS

The following analytical methods were used in the ion-selective electrode ion-pair dissociation studies:

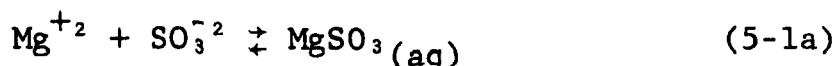
- 1) Magnesium - colorimetric titration with Na_2EDTA or dilution preparation and atomic absorption determination.

- 2) Sodium - dilution preparation and atomic absorption determination.
- 3) Sulfite - iodine-buffer preparation and back titration with standard arsenite or thio-sulfate.
- 4) Sulfate - peroxide oxidation of sulfite, hydrogen ion exchange, and titration with standard sodium hydroxide. Sulfate is calculated as the difference between total sulfur and sulfite sulfur.

SECTION 5

EXPERIMENTAL APPROACH FOR THE ION-PAIR DISSOCIATION STUDIES - METHOD OF INFLUENCE OF ION-PAIR FORMATION ON A REFERENCE COMPOUND SOLUBILITY

The measurement of the solubility of a sparingly soluble reference compound in the presence of another electrolyte may also be used to derive dissociation constants if the equilibrium constants for the reference compounds are known. The solubility of the reference compound is increased by an electrolyte containing ions which can form ion-pairs with the saturating salt. For example, the solubility of $\text{CaSO}_3 \cdot \frac{1}{2}\text{H}_2\text{O}$ is increased in the presence of MgCl_2 , primarily due to the following reaction:



with

$$K_d = a_{\text{Mg}^{+2}} \cdot a_{\text{SO}_3^{-2}} / a_{\text{MgSO}_3(\text{aq})}. \quad (5-1b)$$

The equilibrium constant of reaction 5-1b can be derived from a complete chemical analysis of the equilibrium solution and calculations which consider other pertinent reactions and activity coefficient effects. For these calculations, the Radian chemical equilibrium computer program is used.

EXPERIMENTAL APPARATUS AND PROCEDURE

In this work $\text{CaSO}_3 \cdot \frac{1}{2}\text{H}_2\text{O}$ and $\text{CaSO}_4 \cdot 2\text{H}_2\text{O}$ were used as the sparingly soluble reference compounds. The salts equilibrated with each solid in individual runs were MgCl_2 , NaCl , and CaCl_2 . Chloride salts were used since the chloride anion does not form ion-pairs with Mg^{+2} , Ca^{+2} , or Na^{+} to any appreciable

extent. Experiments with CaCl_2 were done in order to check the reference compound equilibrium constants.

The added electrolyte concentration was varied from 0.01 M to 0.6 M depending on the particular salt used and selected run condition. Controlled experimental reaction temperatures of 30°C and 50°C were used. The equilibrium experiments using freshly prepared solid were carried out in sealed, cylindrical tumblers with reaction times varying from 3-5 days. At the end of each run, solution pH was measured and samples were withdrawn for analysis. The results of these analyses are presented in Table 5-1.

ANALYTICAL METHODS

The following analytical methods were used in the ion-pair dissociation studies:

- 1) Magnesium and calcium - colorimetric titration with Na_2EDTA or dilution preparation and atomic absorption determination.
- 2) Sodium - dilution preparation and atomic absorption determination.
- 3) Sulfite - iodine-buffer preparation and back titration with standard arsenite or thiosulfate.
- 4) Sulfate - peroxide oxidation of sulfite, hydrogen ion exchange, and titration with standard sodium hydroxide. Sulfate is calculated as the difference between total sulfur and sulfite sulfur.

TABLE 5-1. RESULTS OF EQUILIBRIUM STUDIES

Date	Run No.	Run Conditions		Analytical Results (mmoles/liter)								
		Temp. (°C)	Solids	Liquor	pH	Temp. (°C)	Ca ⁺⁺	Mg ⁺⁺	Na ⁺	Cl ⁻	SO ₄ ⁼⁼	SO ₄ ⁼⁼
2/19/76	13	50	CaSO ₄ · $\frac{1}{2}$ H ₂ O	D.I. H ₂ O	8.20	48.0	1.09	---	---	---	0.39	0.42
"	14	"	"	0.2 M MgCl ₂	8.63	48.6	5.13	198	---	399	3.89	1.57
"	15	"	"	0.6 M NaCl	9.81	46.8	2.26	---	588	588	2.26	.57
"	16	"	CaSO ₄ ·2H ₂ O	D.I. H ₂ O	5.50	48.5	14.9	---	---	---	---	15.1
"	17	"	"	0.2 M MgCl ₂	8.49	48.0	43.4	193	---	395	---	43.2
"	18	"	"	0.6 M NaCl	9.34	48.0	37.9	---	572	580	---	37.4
2/24/76	19	30	CaSO ₄ · $\frac{1}{2}$ H ₂ O	D.I. H ₂ O	7.90	30.0	1.01	---	---	---	0.67	0.17
"	20	"	"	0.2 M MgCl ₂	8.58	30.5	5.11	183	---	375	4.54	.50
"	21	"	"	0.6 M NaCl	8.49	30.8	3.08	---	529	524	2.39	.64
"	22	"	"	0.1 M MgCl ₂	8.05	30.0	4.04	108	---	213	3.33	.76
"	23	"	"	0.3 M NaCl	8.72	30.0	2.45	---	285	292	1.94	.75
"	24	"	"	0.2 M CaCl ₂	8.85	30.0	177.	---	---	354	0.25	.28
3/04/76	25	30	CaSO ₄ ·2H ₂ O	D.I. H ₂ O	7.51	33.0	14.6	---	---	---	---	14.5
"	26	"	"	0.2 M MgCl ₂	7.97	33.4	40.5	223	---	402	---	41.3
"	27	"	"	0.6 M NaCl	8.20	33.0	34.5	---	569	581	---	35.4
"	28	"	"	0.1 M MgCl ₂	8.02	33.0	31.6	135	---	217	---	33.7
"	29	"	"	0.3 M NaCl	8.38	33.0	27.4	---	278	286	---	29.2
"	30	"	"	0.2 M CaCl ₂	8.81	33.0	200.	---	---	364	---	8.31
3/09/76	31	30	CaSO ₄ · $\frac{1}{2}$ H ₂ O	D.I. H ₂ O	7.51	32.0	1.11	---	---	---	0.60	0.85
"	32	"	"	0.01 M CaCl ₂	7.10	32.0	11.5	---	---	20.4	0.26	0.67
"	33	"	"	0.1 M CaCl ₂	7.09	31.5	92.8	---	---	186	0.18	0.49
3/15/76	34*	50	CaSO ₄ · $\frac{1}{2}$ H ₂ O	D.I. H ₂ O	6.23	50.5	0.99	---	---	---	0.54	0.63
"	35*	"	"	0.6 M NaCl	6.14	50.3	2.52	---	600	580	2.08	2.21
"	36*	"	"	0.2 M MgCl ₂	6.16	50.5	4.73	208	---	405	4.09	4.10
"	37*	"	"	0.2 M CaCl ₂	6.08	50.3	200.	---	---	400.	0.25	0.32

* pH adjusted to 6 with HCl.

- 5) Chloride - potentiometric titration with standard silver nitrate.

SECTION 6

EXPERIMENTAL RESULTS FOR THE ION-PAIR DISSOCIATION STUDIES

EQUILIBRIUM DATA PROCESSING - ION SELECTIVE ELECTRODE MEASUREMENTS

Given an ion pair such as $MA_{(aq)}$ with the following equilibrium dissociation in solution:



an equilibrium dissociation constant for this reaction can be written as:

$$K_d = \frac{a_{M^{+2}} \cdot a_{A^{-2}}}{a_{MA_{(aq)}}} \quad (6-2)$$

where a is the activity for the particular solution species and K_d is a function of temperature. The activity of a particular solution species is related to its solution concentration by the relationship:

$$a = \gamma \cdot M \quad (6-3)$$

where

γ = the activity coefficient, and

M = the molality of the species.

At temperature T the dissociation constant for a particular ion-pair is calculated by an iterative trial and error procedure using the measured experimental data (LO-001). A trial value for K_d and the experimentally determined total

concentrations of all solution species are input to the Radian chemical equilibrium computer program. The computer-calculated free cation activity is then compared to the value derived from the cation selective electrode measurements of the appropriate test solutions. The accepted value of K_d at temperature T is the value that minimizes the difference between the experimentally and theoretically derived values of activity for the free cation of interest.

EQUILIBRIUM DATA PROCESSING - METHOD OF INFLUENCE OF ION-PAIR FORMATION ON A REFERENCE COMPOUND SOLUBILITY

The pH, temperature, and chemical analysis results from these equilibrium experiments are input to the Radian chemical equilibrium computer program. For each run a series of equilibrium distributions and relative saturations are calculated as a function of the input dissociation constants for the reaction considered. The actual dissociation constant is then obtained graphically as that value which yields a calculated relative saturation of 1.00 for the particular sparingly soluble reference compound. Effects of probable errors in the chemical analyses are estimated by varying the input concentrations over the expected range and noting the change in calculated dissociation constant.

RESULTS FOR THE ION-PAIR DISSOCIATION STUDIES

The dissociation constants for $\text{MgSO}_3(\text{aq})$, $\text{MgSO}_4(\text{aq})$, and $\text{NaSO}_3^-(\text{aq})$ were determined at 25, 35, 45 and 55°C by the ion specific electrode method. The same constants were also determined at 30 and 50°C by the sparingly soluble salt method. The sparingly soluble salt data are plotted as $\log_{10} K_d$ versus $1/T(\text{K})$ in Figure 6-1. This figure is used to

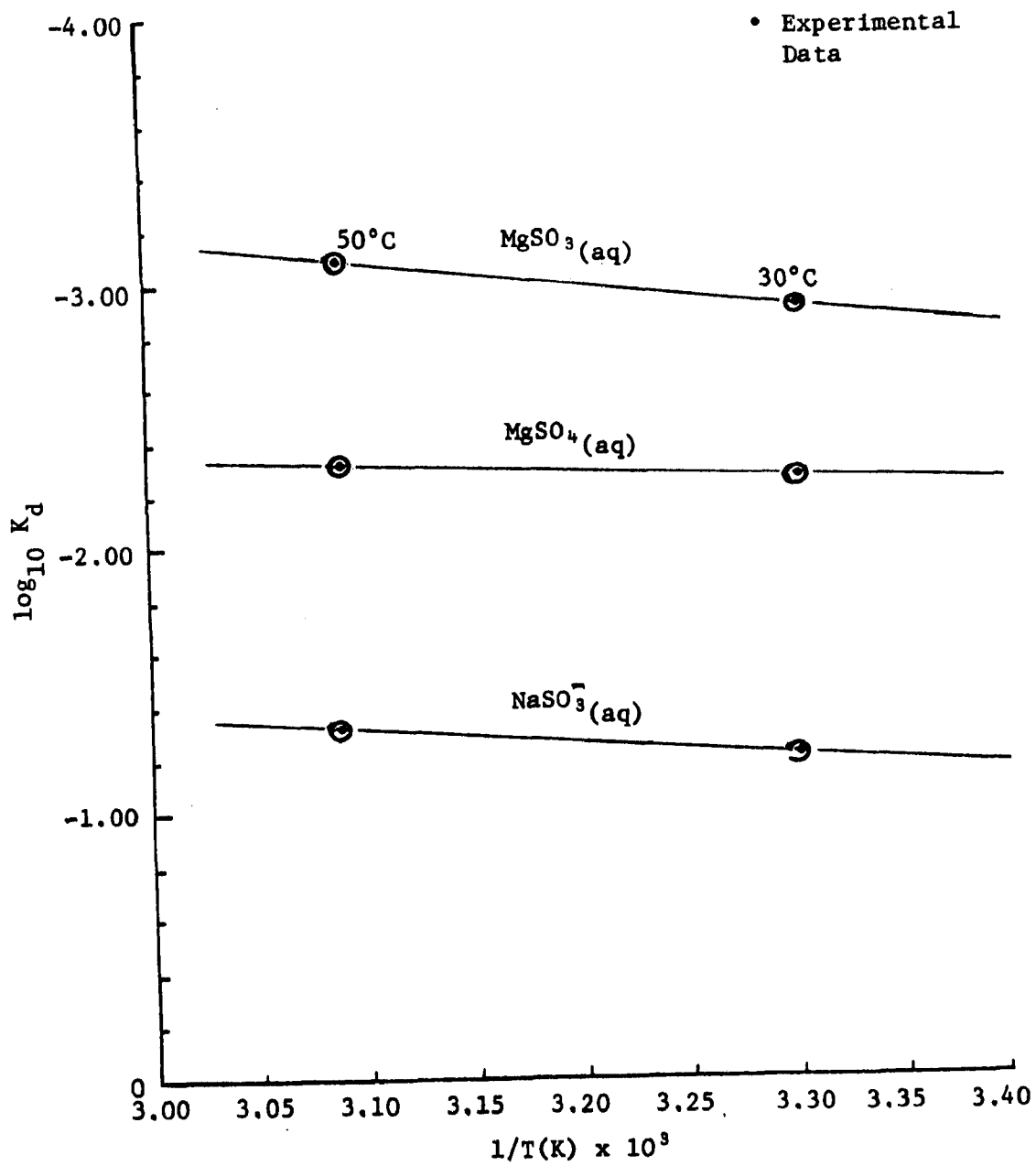


Figure 6-1. $\log_{10} K_d$ vs. $1/T(\text{K}) \times 10^3$

extrapolate and interpolate points at 25, 35, 45, and 55°C. These points and the experimental points for the ion specific electrode method are given in Table 6-1.

TABLE 6-1. ION-PAIR DISSOCIATION CONSTANTS

Ion-Pair	Temperature (°C)	<u>K dissociation</u>	
		Ion-Specific Electrode	Sparingly Soluble Compound
$\text{MgSO}_3(\text{aq})$	25	0.00173	0.00136
	35	0.00140	0.00110
	45	0.00113	0.000896
	55	0.00091	0.000747
$\text{MgSO}_4(\text{aq})$	25	0.00347	0.00569
	35	0.00287	0.00533
	45	0.00238	0.00501
	55	0.00196	0.00473
$\text{NaSO}_3^-(\text{aq})$	25	0.055	0.06611
	35	0.055	0.05760
	45	0.055	0.05063
	55	0.055	0.04484

SECTION 7

CONCLUSIONS

It was found that the experimental solubilities of the MgSO_3 hydrate solids determined by Radian agree quite well with the literature values (LI-001). From these temperature-dependent solubilities accurate solubility product constants were calculated by using the Radian experimentally determined dissociation constants. It was felt that in order to arrive at accurate temperature-dependent solubility product constants, an update of critical equilibrium dissociation constants was needed. Therefore, a great deal of effort was spent in determining accurate temperature-dependent dissociation constants for $\text{MgSO}_3(\text{aq})$, $\text{MgSO}_4(\text{aq})$ and $\text{NaSO}_3^-(\text{aq})$ ion-pairs.

It was found that the method of influence of ion-pair formation on the solubility of a sparingly soluble reference compound to determine ion-pair dissociation constants yielded generally more reliable results than the ion-selective electrode experiments. This was because the selective cation response measurements were found to be offset by a non-negligible electrode junction potential. This electrode junction potential, inherent in every measurement, is a function of test solution composition and temperature and is of unknown magnitude. Therefore, the temperature-dependent dissociation constants from Table 6-2 (specifically $\text{MgSO}_3(\text{aq})$) were used in calculating accurate temperature-dependent solubility product constants for the MgSO_3 hydrate solids.

BIBLIOGRAPHY

- DA-001 Dauerman, Leonard, The Thermal Dehydration of $\text{MgSO}_3 \cdot 6\text{H}_2\text{O}$ and $\text{MgSO}_3 \cdot 3\text{H}_2\text{O}$, Chemical Construction Company, 1975.
- LI-001 Link, W. F., Solubilities of Inorganic and Metal Organic Compounds - Vol. II, Washington, D. C., American Chemical Society, p. 985.
- LO-001 Lowell, P. S., et al., A Theoretical Description of the Limestone Injection-Wet Scrubbing Process, Contract No. CPA-22-69-138, Austin, Texas; Radian Corporation, 1970.

TECHNICAL NOTE 200-045-36-05

EXPERIMENTAL RESULTS FOR PRECIPITATION
KINETICS STUDIES ON MgSO_3 HYDRATES

Prepared by:

R. E. Pyle

CONTENTS

1. Introduction	174
2. Experimental Approach.	176
Experimental Apparatus and Procedure.	176
Experimental Sampling Procedure	176
Analytical Methods.	177
3. Experimental Results	
Kinetics Data Processing.	179
Results	184
4. Discussion of Results.	189
Bibliography	
Appendix	

FIGURES

<u>Number</u>	<u>Page</u>
3-1 $\text{MgSO}_3 \cdot 6\text{H}_2\text{O}$ Precipitation Rate vs. Relative Saturation at Various Temperatures	185
3-2 $\text{MgSO}_3 \cdot 3\text{H}_2\text{O}$ Precipitation Rate vs. Relative Saturation at 55°C	186
3-3 $\text{MgSO}_3 \cdot 3\text{H}_2\text{O}$ Precipitation Rate vs. Relative Saturation at 70°C	187
3-4 $\text{MgSO}_3 \cdot 3\text{H}_2\text{O}$ Precipitation Rate vs. Relative Saturation at 85°C	188

TABLES

<u>Number</u>	<u>Page</u>
3-1	193

SECTION 1

INTRODUCTION

In an MgO scrubber system, a circulating slurry of MgO and hydrated MgSO_3 is used to absorb SO_2 from a flue gas stream. The SO_2 is removed from the scrubber system as a precipitate of hydrated magnesium sulfite. Two hydrates have been identified, $\text{MgSO}_3 \cdot 3\text{H}_2\text{O}$ and $\text{MgSO}_3 \cdot 6\text{H}_2\text{O}$. The crystals formed in the installation removing SO_2 from the flue gases of Boston Edison's oil-fired boiler were found to be primarily trihydrate crystals. The installation at PEPCO's coal-fired boiler produced primarily hexahydrate crystals.

The removal of SO_2 from flue gas streams by an MgO regenerative scrubbing system has proven to be technically feasible. The status of technology at the time the above units were designed was insufficient to predict which hydrates form would be favored. An understanding of the phenomena involved in the production of either hydrated form is important. The trihydrate crystals that are produced are very small in size. In comparison, the settling and handling characteristics of these two hydrated phases are markedly different. From a process point of view, the trihydrate may be the more desirable crystalline form because it takes less energy to drive off the waters of hydration when the crystals are calcined to regenerate the MgO. The economics may depend, however, on the form of available heat. It is presently easier from an operating standpoint to produce hexahydrate crystals because of the ease with which the hexahydrate solids can be removed from the liquids in the scrubber.

In view of these process problems, it is clear that the chemistry involved in the preferential production of either hydrated phase of MgSO_3 must be characterized. It was, therefore, the objectives of this work to:

- (1) investigate the theoretical aspects of hydrate phase transitions,
- (2) to determine the equilibrium solubilities and solubility product constants of the trihydrate and hexahydrate phases of MgSO_3 as a function of temperature,
- (3) investigate the influence of solution composition on the transition temperature of the hexahydrate-trihydrate phase change, and
- (4) investigate the influence of solution composition and temperature on the formation kinetics of the two solid phases.

This Technical Note presents in detail the experimental results that were derived from the precipitation kinetics studies on the hexahydrate and trihydrate crystalline phases of MgSO_3 . Experimental details of the equilibrium studies may be found in Technical Note No. 200-045-36-04, and results of the transition temperature lowering studies may be found in Technical Notes No. 200-045-36-02 and No. 200-045-36-03.

SECTION 2

EXPERIMENTAL APPROACH

EXPERIMENTAL APPARATUS AND PROCEDURE

The precipitation kinetics experiments on $\text{MgSO}_3 \cdot 6\text{H}_2\text{O}$ and $\text{MgSO}_3 \cdot 3\text{H}_2\text{O}$ were performed by using batch-solid/batch-liquid reaction techniques. It was found that this experimental technique works well for these more soluble salts although data analysis is generally more difficult. For low reaction temperatures ($<50^\circ\text{C}$), a batch-solid/batch-liquid crystallizer of plexiglass construction and an external stirring motor were used for the kinetics experiments. For higher reaction temperatures, a pyrex reactor of approximately 3-liter capacity was used.

Supersaturated solutions were produced in the well-stirred reactors by introducing equal volumes of the two separate feedstock solutions, especially MgCl_2 and Na_2SO_3 of predetermined concentrations. The reactor was situated in a constant temperature bath held at the desired experimental reaction temperature. Within the reactor, precipitation from the supersaturated solution was initiated by the addition of $\text{MgSO}_3 \cdot 6\text{H}_2\text{O}$ or $\text{MgSO}_3 \cdot 3\text{H}_2\text{O}$ seed crystals. From this point, the reactor contents could be sampled and the various analytical determinations performed.

EXPERIMENTAL SAMPLING PROCEDURES

Initial samples of the mixed feedstock solutions, specifically MgCl_2 and Na_2SO_3 , were taken from the reactor contents just prior to adding seed crystals. Determination of magnesium and sulfite was performed on these samples to establish the initial concentrations of the reacting species. In addition, solution pH and temperature were taken.

At predetermined intervals during an experimental run, samples of the reactor contents were taken until the crystal growth reaction was complete. Determinations of magnesium, sulfite and total sulfur were performed on the liquid phase samples. Total sulfur determinations were used to determine the extent of sulfite oxidation to sulfate. (It was found that sulfite oxidation was negligible in these high sulfite concentration solutions.) In addition, weight percent solids, solution pH, and temperature were taken. In this way, the reaction progress could be monitored regularly throughout the experimental run.

The results of these analytical determinations were primarily used in quantifying the two principal experimental quantities of interest, namely: the rate of precipitation and the reaction solution relative supersaturation.

ANALYTICAL METHODS

In this section, a brief outline of the analytical methods used in the MgSO_3 hexahydrate and trihydrate precipitation kinetics studies is given.

- (1) Magnesium - colorimetric titration with Na EDTA or dilution preparation and atomic absorption determination;
- (2) Sodium - dilution preparation and atomic absorption determination;
- (3) Chloride - silver nitrate potentiometric titration;
- (4) Sulfite - iodine-buffer preparation and back titration with arsenite; and

- (5) Total Sulfur - peroxide oxidation of sulfite, hydrogen ion exchange, and titration with standard sodium hydroxide.

SECTION 3
EXPERIMENTAL RESULTS

KINETICS DATA PROCESSING

Precipitation Rate

For the batch-solid/batch-liquid kinetics experiments, a precipitation rate can be calculated from the amount of solid material produced as a function of the time. The slope of the total amount of solids versus reaction time curve is equal to the precipitation rate or rate of growth for the precipitating species. Therefore, the precipitation rate at time t_0 can be expressed as:

$$R = \lim_{\Delta t \rightarrow 0} (1/MW) \left(\frac{\Delta N}{\Delta t} \right) \Big|_{t=t_0} = (1/MW) \left(\frac{dN}{dt} \right) \Big|_{t=t_0} \quad (3-1)$$

where,

N = mass of solids produced in grams,

t = time duration of the run in min,

MW = molecular weight of the precipitating species
in grams/mMole, and

R = precipitation rate in mMoles/min at time t_0 .

The total mass of solids, N , was determined from the weight percent solids measurements or solution material balances at predetermined time intervals throughout the kinetics experiment.

Equation 3-1 expresses the precipitation rate at time t_o or the rate at which solid material is being produced in the reactor at time t_o . The experimental precipitation rate is determined then by approximating Equation 3-1 and manually calculating slopes of the amount of product versus reaction time curve at various times throughout the kinetics experiment.

The amount of precipitating material produced at time t_o can be determined not only through weight percent solids measurements, but also from material balance criteria. That is, the change in the solution magnesium or sulfite ion concentration with time determined by analytical means must be equivalent to the number of moles of magnesium or sulfite reacted to form the $MgSO_3$ hydrate product. Therefore, the amount of precipitated material produced at time t_o can be calculated from the following equation:

$$N(t_o) = ([Ion]_{t=0} - [Ion]_{t=t_o}) \cdot Vol_{Reactor} \cdot MW \quad (3-2)$$

where,

$N(t_o)$ = mass of $MgSO_3$ hydrate product material
at time t_o in grams,

$[Ion]_{t=0}$ = initial magnesium or sulfite ion concentration in solution in moles/l,

$[Ion]_{t=t_o}$ = magnesium or sulfite ion concentration in
solution at time t_o in moles/l,

$Vol_{Reactor}$ = total reaction solution volume in liters,
and

MW = molecular weight of precipitating MgSO_3
hydrate product in g/mole.

This determination provides an excellent method in addition to the weight percent solids measurements for calculating the precipitation rates.

Solution Relative Supersaturation

The MgSO_3 hydrate precipitation rate, R , at time t_0 determined in the manner previously described, is a function of the solution relative supersaturation. The relative supersaturation is defined as the ratio of the reaction solution activity product for the precipitating species to the equilibrium solubility product, K_{sp} , for the precipitating species. In this case:

$$\text{R.S.}_6 = a_{\text{Mg}^{+2}} \cdot a_{\text{SO}_3^{2-}} \cdot a_{\text{H}_2\text{O}}^6 / K_{sp} \text{MgSO}_3 \cdot 6\text{H}_2\text{O} \quad (3-3)$$

or

$$\text{R.S.}_3 = a_{\text{Mg}^{+2}} \cdot a_{\text{SO}_3^{2-}} \cdot a_{\text{H}_2\text{O}}^3 / K_{sp} \text{MgSO}_3 \cdot 3\text{H}_2\text{O} \quad (3-4)$$

Activities for the particular solution species are calculated by inputting pertinent reaction solution information for reaction time t_0 such as concentrations of magnesium, sodium, chloride, sulfate and sulfite, pH, and temperature, to the Radian chemical equilibrium computer program.

The Rate Equation

A suitable rate expression for the MgSO_3 hydrate solid precipitation from supersaturated liquor may be written in the

following form:

$$R = k \cdot M \cdot \phi \quad (3-5)$$

where,

R = rate of solid precipitation,

k = rate constant, which may vary with liquor temperature, composition, and transport parameters,

ϕ = driving force which is related to the degree of MgSO_3 supersaturation, and

M = term dependent on the amount of solid phase present.

The term M is often assumed to be proportional to the exposed surface area of the solid phase. This is difficult to quantify in experiments with suspensions of many fine particles of seed crystals. Consequently, no crystal surface area measurements were attempted. However, MgSO_3 hexahydrate crystals, previously grown from solution and analyzed for purity, were ground and then sieved through 400 mesh wire screen. The resulting sieved product, with an average particle diameter of less than or equal to 37 microns, was used as uniform seed material for all MgSO_3 hexahydrate kinetics experiments in order to facilitate rate data correlation. The measured precipitation rates were, subsequently, normalized by dividing by the mass of crystals at time t_0 .

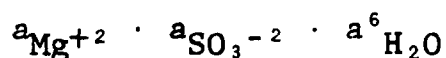
For dissolution and precipitation reactions, the driving force term, ϕ , is normally a function of the difference between

the actual and equilibrium quantities of the reacting species. A general form for the driving force function (NA-033) can therefore be written as:

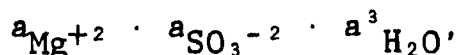
$$\phi = [(ap)^{1/n} - K_{sp}^{1/n}]^n \quad (3-6)$$

where

ap = the activity product for the precipitating species, i.e.



or



K_{sp} = the equilibrium solubility product constant for the precipitating species,

n = an exponent generally taken to be equal to the number of cations plus anions, in this case $n = 2$.

Equation 3-6 may also be written in the following form:

$$\phi = K_{sp} [R.S.^{1/n} - 1]^n \quad (3-7)$$

where

R.S. = the solution relative supersaturation for the precipitating species.

With this general form for the driving force, the expression for

the rate of precipitation (3-5) can now be written as:

$$R(\text{mMoles/min}) = k(\text{mMoles/gram-min}) \cdot M(\text{grams}) \cdot K_{sp} [R.S.^{1/n} - 1]^n \quad (3-8)$$

In this kinetics study, the precipitation rate normalized by dividing by the mass term, M, is analyzed as a function of the solution relative supersaturation.

RESULTS

Experimental results for the precipitation kinetics studies on the MgSO_3 system have been summarized in Table 3-1, and are presented in the Appendix. The relative saturations were calculated using the Radian chemical equilibrium computer program as described earlier. The precipitation rates for $\text{MgSO}_3 \cdot 6\text{H}_2\text{O}$ and $\text{MgSO}_3 \cdot 3\text{H}_2\text{O}$ (in mMoles/gram-min) at various experimental temperatures are plotted versus solution relative saturation in Figures 3-1 through 3-4. The reported precipitation rates were calculated by using the methods described in Kinetics Data Processing.

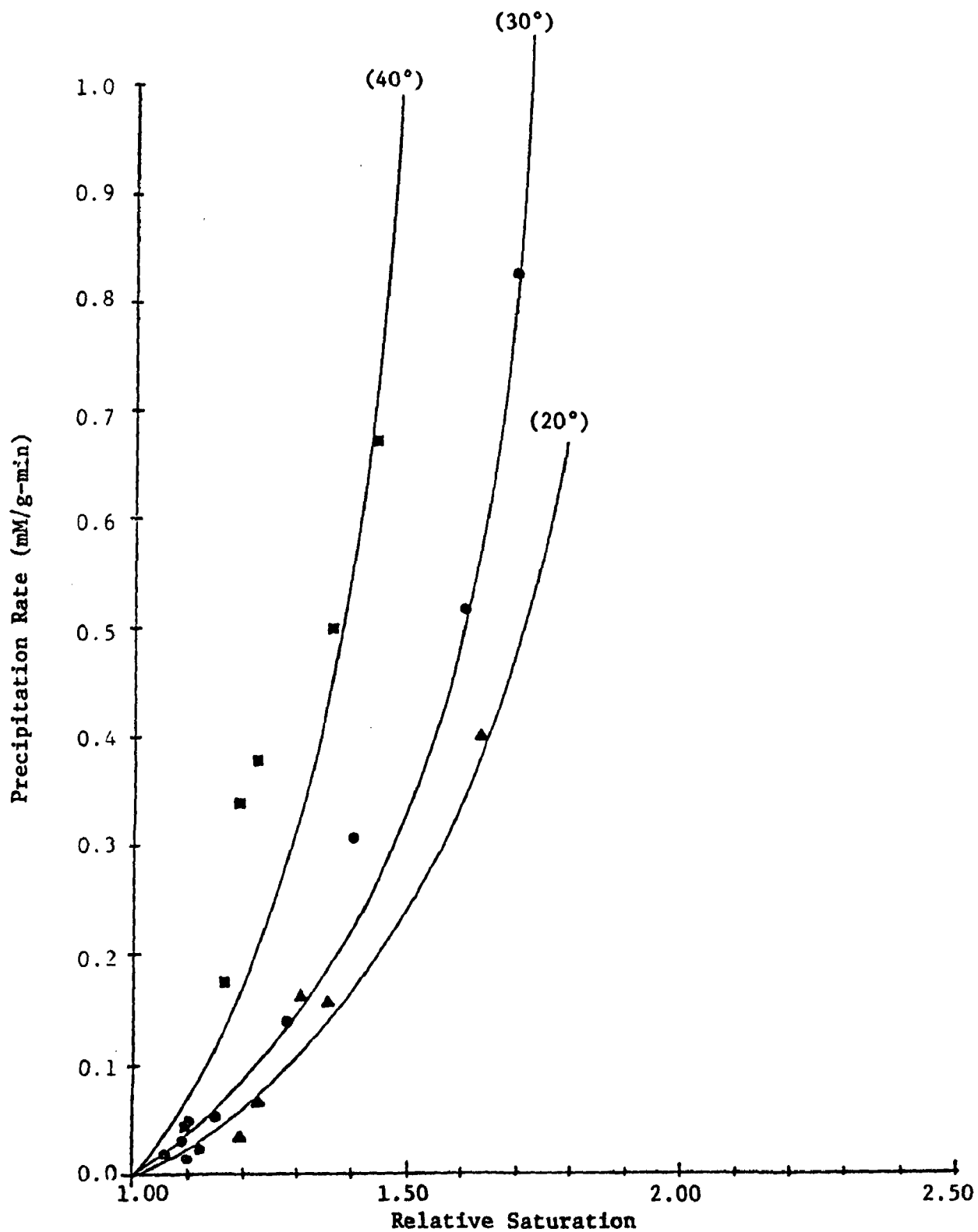


Figure 3-1. $\text{MgSO}_3 \cdot 6\text{H}_2\text{O}$ Precipitation Rate vs Relative Saturation at Various Temperatures

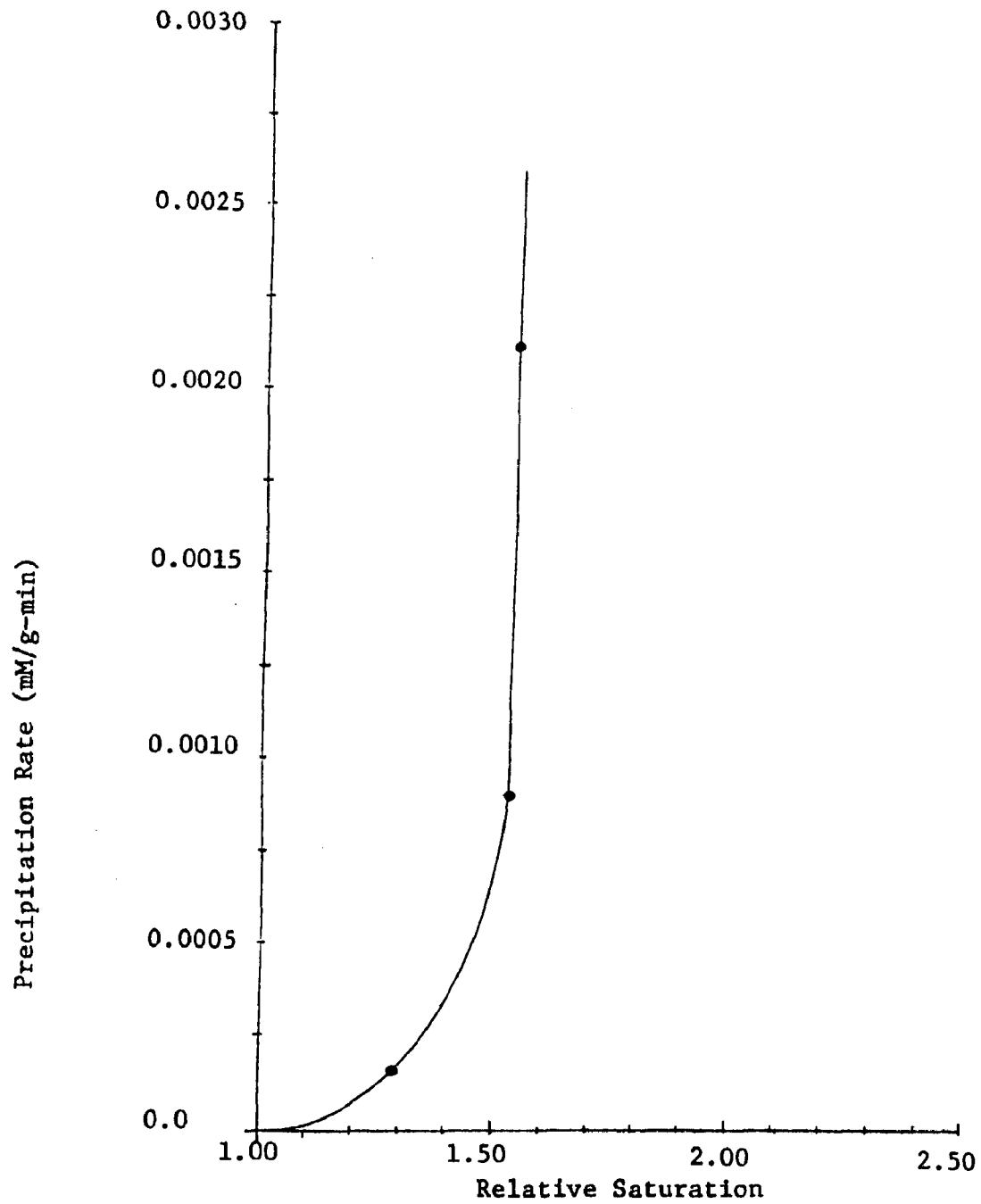


Figure 3-2. $\text{MgSO}_3 \cdot 3\text{H}_2\text{O}$ Precipitation Rate vs Relative Saturation at 55°C

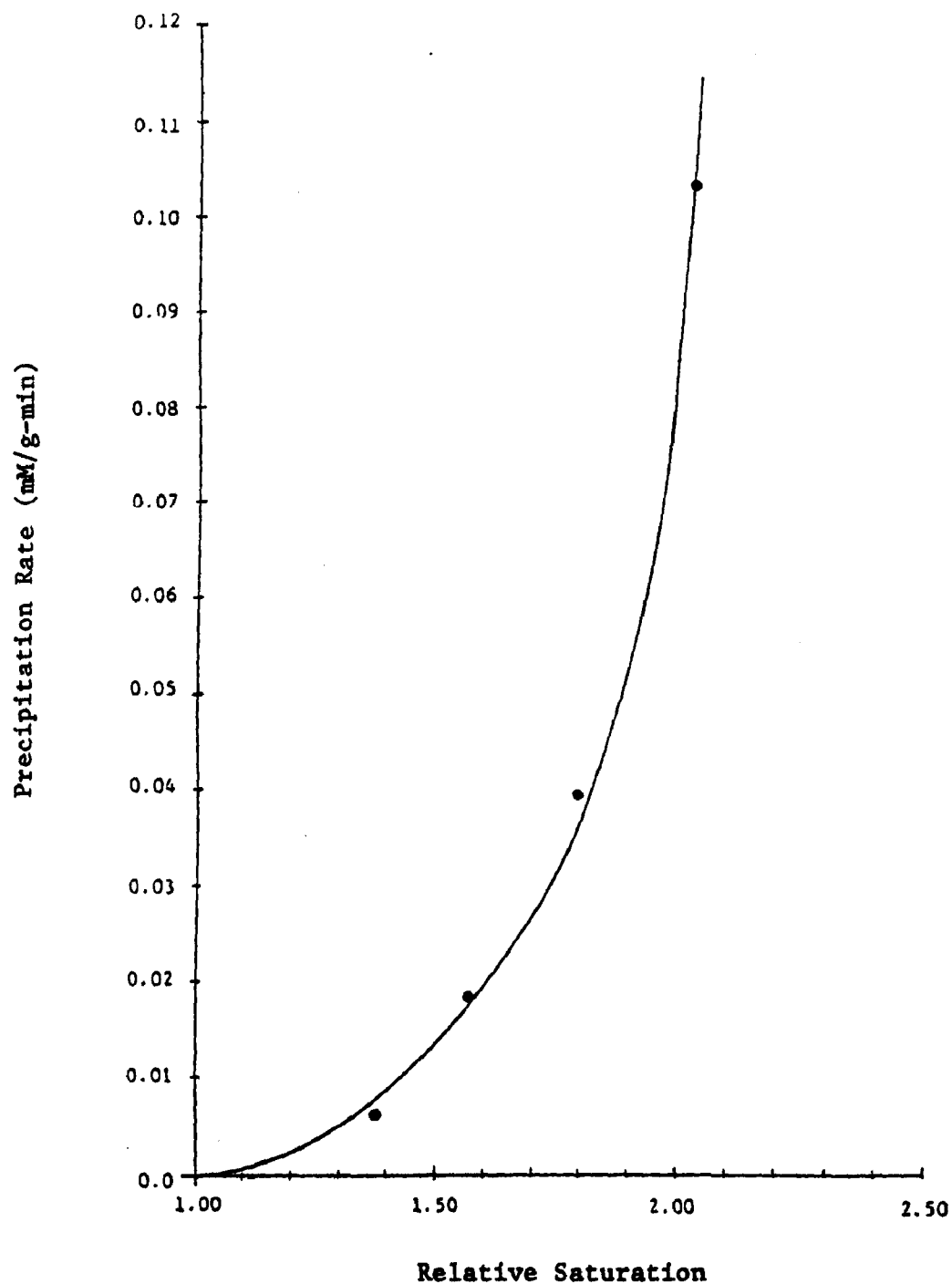


Figure 3-3. $\text{MgSO}_3 \cdot 3\text{H}_2\text{O}$ Precipitation Rate vs Relative Saturation at 70°C

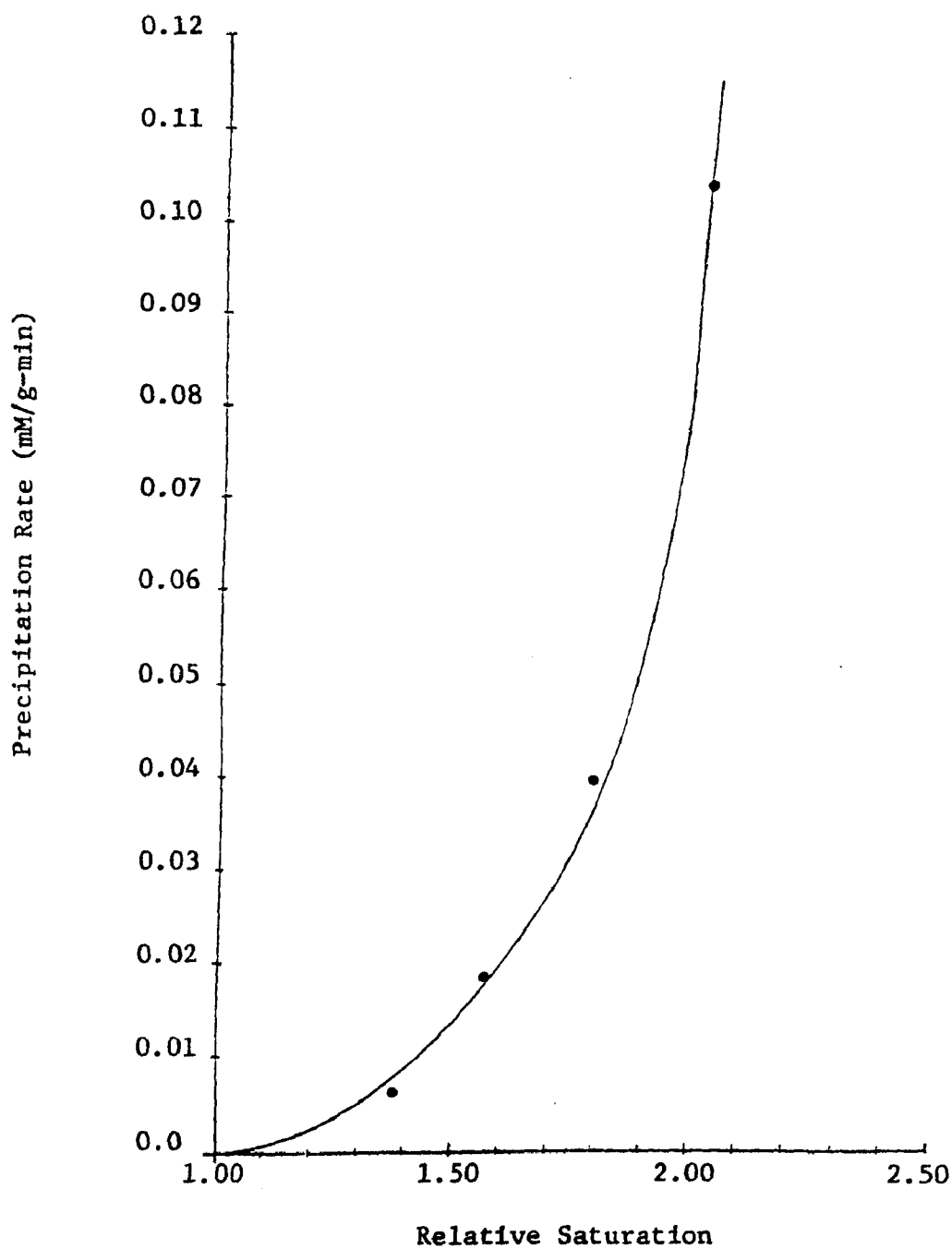


Figure 3-4. $\text{MgSO}_3 \cdot 3\text{H}_2\text{O}$ Precipitation Rate vs Relative Saturation at 85°C

SECTION 4

DISCUSSION OF RESULTS

As stated in Section 1.0, experience has been that at a coal-fired unit with MgO scrubber the hexahydrate crystalline phase was produced, although scrubber operating temperatures of near 55°C would suggest the thermodynamically favored trihydrate product. Also, Technical Notes 200-045-36-02 and 200-045-36-03 demonstrate both theoretically (Technical Note 200-045-36-02) and experimentally (Technical Note 200-045-36-03) that the phase transition temperature between $\text{MgSO}_3 \cdot 6\text{H}_2\text{O}$ and $\text{MgSO}_3 \cdot 3\text{H}_2\text{O}$ solid in aqueous solution is dependent upon the solution composition. Furthermore, the transition temperature is lowered from a maximum of 41°C as the dissolved solids content of the solution increases. Therefore, the precipitation of $\text{MgSO}_3 \cdot 6\text{H}_2\text{O}$ at scrubber conditions cannot be explained from an equilibrium point of view but must be the result of a kinetic phenomenon. Indeed, the experimental results of this Technical Note tend to verify this assumption.

As can be seen from Figures 3-1 through 3-4, there is a wide variation in growth rate magnitudes between the hexahydrate and trihydrate phases and over the range of temperature studied. For example, the hexahydrate precipitation rate at 30°C is nearly three orders of magnitude greater than the trihydrate precipitation rate at 55°C at the same relative saturation or driving force. In fact, the trihydrate precipitation rate only begins to approach magnitudes characteristics of hexahydrate growth near reaction temperatures of 85°C. This temperature enhancement of the rate is of course expected from the Arrhenius equation. Nevertheless, the growth rates of the two hydrate phases near scrubber operating temperatures are sufficiently disparate that hexahydrate precipitation under these conditions

must be the result of kinetic factors. Kinetic effects under conditions more typical of actual operating scrubber conditions are being investigated in Task 54.

BIBLIOGRAPHY

- NA-033 Nancollas, George H. and N. Purdie, "The Kinetics of Crystal Growth", Chem. Soc. Quarterly Rev., 18, 1-20 (1964).

APPENDIX
TO TECHNICAL NOTE
200-045-36-05

TABLE 3-1
 RUN NO. 1
 MgSO₃·6H₂O @ 20°C

(Min.) Time/Date	Temp °C	pH	(Mg ⁺⁺)	(Na ⁺)	(Cl ⁻)	(SO ₃ ⁼)	Precipitated Solids	Calculated Solids	(lg Seed) Rel. Saturation
t=0 11/18/75	22	9.10	.095	.188	.1872	.088	---	---	1.380
t=10 11/18/75	22	9.15	.090	.188	.1872	.084	2.41g	2.87g	1.296
t=20 11/18/75	22	9.20	.087	.188	.1872	.0817	2.80g	4.59g	1.247
t=30 11/18/75	22	9.40	.086	.188	.1872	.078	3.16g	5.16g	1.200
t=40 11/18/75	21.5	9.25	.084	.188	.1872	.077	3.12g	6.31g	1.191
t=50 11/18/75	21.5	9.20	.082	.188	.1872	.073	3.65g	7.45g	1.132
t=60 11/18/75	21	9.20	.083	.188	.1872	.074	3.29g	6.88g	1.169
t=120 11/18/75	20.9	9.23	.077	.188	.1872	.069	5.12	10.32g	1.069
t=240 11/18/75	20	9.20	.083	.188	.1872	.066	2.97g	---	1.109
t=300 11/18/75	20	9.10	.090	.188	.1872	.0622	1.36g	---	1.100

TABLE 3-1 (Cont'd)

 RUN NO. 2
 $\text{MgSO}_3 \cdot 6\text{H}_2\text{O}$ @ 20°C

(Min.) Time/Date	Temp °C	pH	(Mg ⁺⁺)	(Na ⁺)	(Cl ⁻)	(SO ₃ ⁻)	Precipitated Solids	Calculated Solids	(1.0g Seed) Rel. Saturation
t=0 11/20/75	21	9.1	.121	.235	.250	.115	---	---	1.864
t=10 11/20/75	21	9.1	.100	.235	.250	.093	8.58g	12.04g	1.441
t=20 11/20/75	21	9.1	.092	.235	.250	.081	11.75g	16.63g	1.245
t=30 11/20/75	21	9.1	.085	.235	.250	.079	11.73g	20.64g	1.203
t=40 11/20/75	21	9.1	.083	.235	.250	.077	12.59g	21.79g	1.164
t=50 11/20/75	20	9.1	.085	.235	.250	.074	12.66g	20.64g	1.148
t=60 11/20/75	20	9.1	.084	.235	.250	.072	12.67g	21.21g	1.118
t=120 11/20/75	20	9.1	.083	.235	.250	.070	12.47g	21.79g	1.087
t=240 11/20/75	20.5	9.1	.086	.235	.250	.0700	12.11g	20.07g	1.093
t=300 11/20/75	20.5	9.1	.089	.235	.250	.067	8.44g	---	1.078

TABLE 3-1 (Cont'd)

RUN NO. 3

 $\text{MgSO}_3 \cdot 6\text{H}_2\text{O}$ @ 30°C

(Min.) Time/Date	Temp °C	pH	(Mg ⁺⁺)	(Na ⁺)	(Cl ⁻)	(SO ₃ ⁼)	Precipitated Solids	Calculated Solids	(lg Seed) Rel. Saturation
t=0 10/15/75	32.5	9.04	.147	.232	.294	.116	--	---	1.434
t=31 10/15/75	32.8	9.00	.135	.232	.294	.107	5.77g	7.24g	1.283
t=82 10/15/75	32.5	8.97	.119	.232	.294	.091	22.18g	18.43g	1.077
t=130 10/15/75	32.1	8.98	.115	.232	.294	.089	20.44g	21.10g	1.055
t=191 10/15/75	32.1	8.90	.115	.232	.294	.089	15.48g	21.10g	1.055
t=251 10/15/75	32.1	9.00	.115	.232	.294	.089	22.75g	21.10g	1.055

TABLE 3-1 (Cont'd)

RUN NO. 4 $\text{MgSO}_3 \cdot 6\text{H}_2\text{O}$ @ 30°C

(Min.) Time/Date	Temp °C	pH	(Mg^{++})	(Na^+)	(Cl^-)	(SO_3^{*})	Precipitated Solids	Calculated Solids	(1g Seed) Rel. Saturation
t=0 10/21/75	32.7	9.00	.109	.216	.218	.108	--	---	1.179
t=40 10/21/75	32.7	9.02	.107	.216	.218	.105	1.35g	1.32g	1.145
t=120 10/21/75	31.9	9.05	.1045	.216	.218	.1035	4.31g	2.96g	1.145
t=215 10/21/75	31.5	9.10	.102	.216	.218	.101	4.77g	4.61g	1.128
t=275 10/21/75	31.5	9.05	.100	.216	.218	.0995	5.69g	5.60g	1.107
t=334 10/21/75	31.5	9.10	.100	.216	.218	.100	6.95g	5.92g	1.108

TABLE 3-1 (Cont'd)

RUN NO. 5 $\text{MgSO}_3 \cdot 6\text{H}_2\text{O}$ @ 30°C

(Min.) Time/Date	Temp °C	pH	(Mg^{++})	(Na^+)	(Cl^-)	(SO_3^-)	Precipitated Solids	Calculated Solids	(1.02g Seed) Rel. Saturation
t=0 10/30/75	31.1	9.15	.164	.307	.329	.1529	--	--	1.858
t=25 10/30/75	30.8	9.15	.113	.307	.329	.098	38.86g	33.90g	1.109
t=40 10/30/75	30.8	9.12	.1065	.307	.329	.0975	38.00g	38.50g	1.067
t=60 10/30/75	31.0	9.10	.1065	.307	.329	.096	39.39g	38.50g	1.049
t=120 10/30/75	30.9	9.15	.107	.307	.329	.0965	38.41g	38.50g	1.059
t=240 10/30/75	30.9	9.15	.1045	.307	.329	.096	38.43g	39.80g	1.040
t=280 10/30/75	30.6	9.16	.1045	.307	.329	.091	36.50g	39.80g	1.011
t=5700 11/3/75	30.6	9.12	.1085	.307	.329	.093	42.89g	--	1.050

TABLE 3-1 (Cont'd)

RUN NO. 6
 $\text{MgSO}_3 \cdot 6\text{H}_2\text{O}$ @ 40°C

(Min.) Time/Date	Temp $^\circ\text{C}$	pH	(Mg^{++})	(Na^+)	(Cl^-)	($\text{SO}_3^{=}$)	Precipitated Solids	Calculated Solids	(1.0 g Seed) Rel. Saturation
t=0 11/7/75	40.5	9.08	.200	.362	.400	.181	--	--	1.753
t=13 11/7/75	40.5	9.08	.147	.326	.400	.1275	32.269g	30.39g	1.156
t=26 11/7/75	40.5	9.08	.142	.326	.400	.119	37.03g	33.26g	1.079
t=39 11/7/75	40.5	9.08	.142	.326	.400	.118	36.46g	33.26g	1.072
t=60 11/7/75	40.5	9.08	.140	.326	.400	.117	31.80g	34.40g	1.057
t=120 11/7/75	40.5	9.08	.141	.326	.400	.1185	32.29g	33.83g	1.071
t=240 11/7/75	40.5	9.08	.145	.326	.400	.116	27.31g	31.54g	1.071

TABLE 3-1 (Cont'd)

RUN NO. 7 $\text{MgSO}_3 \cdot 6\text{H}_2\text{O}$ @ 40°C

(Min.) Time/Date	Temp °C	pH	(Mg ⁺⁺)	(Na ⁺)	(Cl ⁻)	(SO ₃ ⁼)	Precipitated Solids	Calculated Solids	(1.0g Seed) Rel. Saturation
t=0 11/19/75	41	9.40	.140	.278	.286	.136	---	--	1.239
t=10 11/19/75	41	9.20	.135	.278	.286	.129	3.70g	2.87g	1.173
t=20 11/19/75	41	9.15	.133	.278	.286	.128	4.90g	4.01g	1.157
t=30 11/19/75	41	9.36	.133	.278	.286	.124	5.77g	4.01g	1.131
t=40 11/19/75	41	9.30	.129	.278	.286	.123	6.16g	6.31g	1.106
t=50 11/19/75	41	9.30	.128	.278	.286	.123	6.47g	6.88g	1.101
t=60 11/19/75	41	9.30	.127	.278	.286	.123	6.48g	7.45g	1.096
t=120 11/19/75	41	9.20	.127	.278	.286	.123	6.56g	7.45g	1.096
t=240 11/19/75	41	9.30	.127	.278	.286	.122	6.19g	7.45g	1.090

TABLE 3-1 (Cont'd)
 RUN NO. 8
 $\text{MgSO}_4 \cdot 3\text{H}_2\text{O}$ @ 55°C

(Min.) Time/Date	Temp °C	pH	(Mg^{++})	(Na^+)	(Cl^-)	(SO_4^{--})	Precipitated Solids	Calculated Solids	(.125g Seed) Rel. Saturation
t=0 10/22/75	55	8.23	.1427	.2754	.2854	.1377	--	--	1.550
t=680 10/23/75	55	8.23	.142	.2754	.2854	.135	1.06g	0.34g	1.526
t=2880 10/24/75	55	8.23	.142	.2754	.2854	.135	1.30g	0.69g	1.522
t=4320 10/25/75	55	8.15	.141	.2754	.2854	.136	2.45g	0.84g	1.526
t=5700 10/26/75	46	8.00	.141	.2754	.2854	.133	2.49g	0.84g	1.358
t=7200 10/27/75	52	7.98	.141	.2754	.2854	.132	3.15g	0.84g	1.438

TABLE 3-1 (Cont'd)
 RUN NO. 9
 $\text{MgSO}_3 \cdot 3\text{H}_2\text{O}$ @55°C

(Min.) Time/Date	Temp °C	pH	(Mg ⁺⁺)	(Na ⁺)	(Cl ⁻)	(SO ₃ ⁼)	Precipitated Solids	Calculated Solids	(Seed Solution = 1.0362g/500ml) Rel. Saturation
t=0 11/3/75	54.9	8.18	.125	.244	.250	.122	--	--	1.351
t=1440 11/4/75	54.9	8.18	.125	.244	.250	.118	1.39g	--	1.322
t=2880 11/5/75	53.9	8.18	.125	.244	.250	.119	1.61g	--	1.313
t=4320 11/6/75	55.5	8.05	.130	.244	.250	.119	1.70g	--	1.366
t=5700 11/7/75	55	8.01	.130	.244	.250	.119	1.35g	--	1.357
t=11520 11/10/75	54.5	7.85	.123	.244	.250	.111	1.94g	--	1.243

TABLE 3-1 (Cont'd)

RUN NO. 10MgSO₃·3H₂O @ 70°C

(Min.) Time/Date	Temp °C	pH	(Mg ⁺⁺)	(Na ⁺)	(Cl ⁻)	(SO ₃ ⁼)	Precipitated Solids	Calculated Solids	(Seed Solution = 5.42g/500ml) Rel. Saturation
t=0 11/17/75	70.5	7.50	.172	.340	.344	.170	---	---	2.196
t=10 11/17/75	71	7.30	.170	.340	.344	.162	5.99g	1.11g	2.087
t=20 11/17/75	71	7.1	.165	.340	.344	.158	7.63g	3.88g	1.986
t=30 11/17/75	71	7.0	.163	.340	.344	.158	8.23g	4.99g	1.944
t=40 11/17/75	71	7.2	.160	.340	.344	.149	9.40g	6.65g	1.898
t=50 11/17/75	71	7.0	.157	.340	.344	.150	4.84g	8.32g	1.837
t=60 11/17/75	71	7.0	.157	.340	.344	.148	4.78g	8.32g	1.821
t=120 11/17/75	71	6.9	.151	.340	.344	.108	11.22g	11.64g	1.395
t=240 11/17/75	70.5	6.8	.140	.340	.344	.134	10.61g	17.74g	1.550
t=1680 11/18/75	70.1	6.75	.132	.340	.344	.145	14.85g	22.17g	1.297
t=3120 11/19/75	71	6.60	.139	.340	.344	.102	6.21g	18.29g	1.179
t=4560 11/20/75	71	6.90	.145	.340	.344	.096	9.61g	---	1.247
t=6000 11/21/75	71	6.80	.155	.340	.344	.0886	10.52g	---	1.180

TABLE 3-1 (Cont'd)

RUN NO. 11 $\text{MgSO}_3 \cdot 3\text{H}_2\text{O}$ @ 85°C

(Min.) Time/Date	Temp $^\circ\text{C}$	pH	(Mg^{++})	(Na^+)	(Cl^-)	(SO_3^-)	Precipitated Solids	Calculated Solids	(.69g/500ml seed) Rel. Saturation
t=0 12/15/75	86	8.1	.124	.240	.288	.118	---	---	1.733
t=10 12/15/75	86	8.0	.124	.240	.288	.120	2.46g	---	1.749
t=20 12/15/75	85	8.0	.117	.240	.288	.1145	2.63g	3.88g	1.630
t=30 12/15/75	84	7.8	.108	.240	.288	.1085	4.86g	8.87g	1.480
t=40 12/15/75	84	7.6	.100	.240	.288	.098	6.94g	13.30g	1.316
t=50 12/15/75	83	7.5	.097	.240	.288	.0945	9.10g	14.97g	1.245
t=60 12/15/75	84	7.5	.098	.240	.288	.094	9.24g	14.41g	1.258
t=120 12/15/75	84	7.3	.094	.240	.288	.0855	9.06g	16.63g	1.130
t=180 12/15/75	85	7.3	.091	.240	.288	.085	3.95g	18.29g	1.113
t=1620 12/16/75	85	7.3	.081	.240	.288	.0745	2.36g	23.83g	0.9503

TECHNICAL NOTE 200-045-54-01

TRANSITION OF MgSO_3 HYDRATES
IN 3M MgCl_2 SOLUTION

Prepared by:

J. L. Skloss

FIGURES

<u>Number</u>		<u>Page</u>
1	MgSO ₃ Solids Present in the 3M MgCl ₂ Solution, 200X	207
2	DSC Scan of the MgSO ₃ Solids Present in the 3M MgCl ₂ Solution	208

It has been found theoretically that the transition temperature of $\text{MgSO}_3 \cdot 3\text{H}_2\text{O}$ and $\text{MgSO}_3 \cdot 6\text{H}_2\text{O}$ can be lowered to room temperature in a medium of 3M magnesium chloride solution. The trihydrate phase of magnesium sulfite is predicted to be stable at 25°C in this medium. This prediction was verified by experiment.

A 1-liter solution of 3M magnesium chloride was prepared, and excess $\text{MgSO}_3 \cdot 6\text{H}_2\text{O}$ solids were added to saturate the solution with respect to magnesium sulfite at room temperature. After filtration, 10g of $\text{MgSO}_3 \cdot 6\text{H}_2\text{O}$ and 10g of $\text{MgSO}_3 \cdot 3\text{H}_2\text{O}$ solids were added. The solids were allowed to equilibrate with the 3M magnesium chloride solution at room temperature (25±2°C) with gentle stirring on a magnetic stirrer. A stoppered 1-liter Erlenmeyer flask was used to contain the system, and a nitrogen purge was used as necessary to prevent oxidation of sulfite ion.

After eight days of continuous stirring, a 50-ml portion of the slurry was filtered on Whatman No. 42 paper. The solids were washed with 50% ethanol and over-dried at 45°C for 30 minutes. The chemical analyses of the solids showed that the magnesium and the sulfite concentrations were 6.31±0.05 mmole/g, which was expected for $\text{MgSO}_3 \cdot 3\text{H}_2\text{O}$. The trihydrate phase of magnesium sulfite was identified in the microphotograph (see Figure 1). Also the DSC scan, Figure 2, indicated that the solids sample was $\text{MgSO}_3 \cdot 3\text{H}_2\text{O}$.

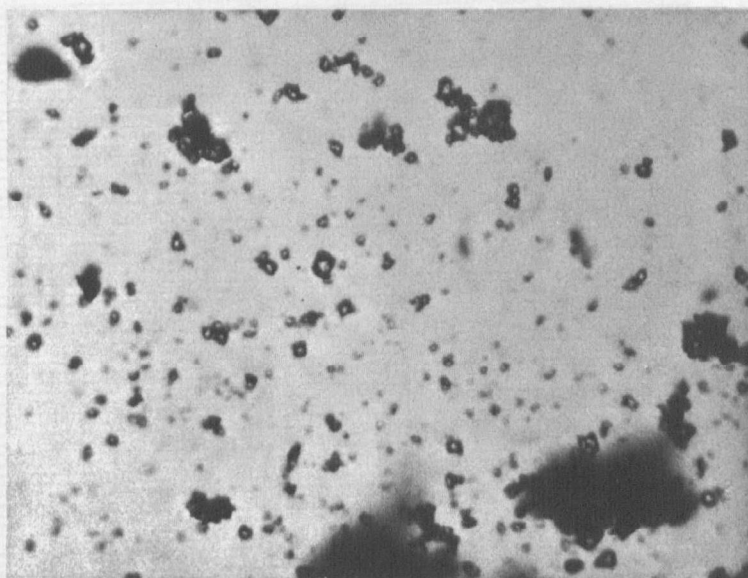


FIGURE 1 MgSO_3 SOLIDS PRESENT IN THE
3M MgCl_2 SOLUTION, 200X

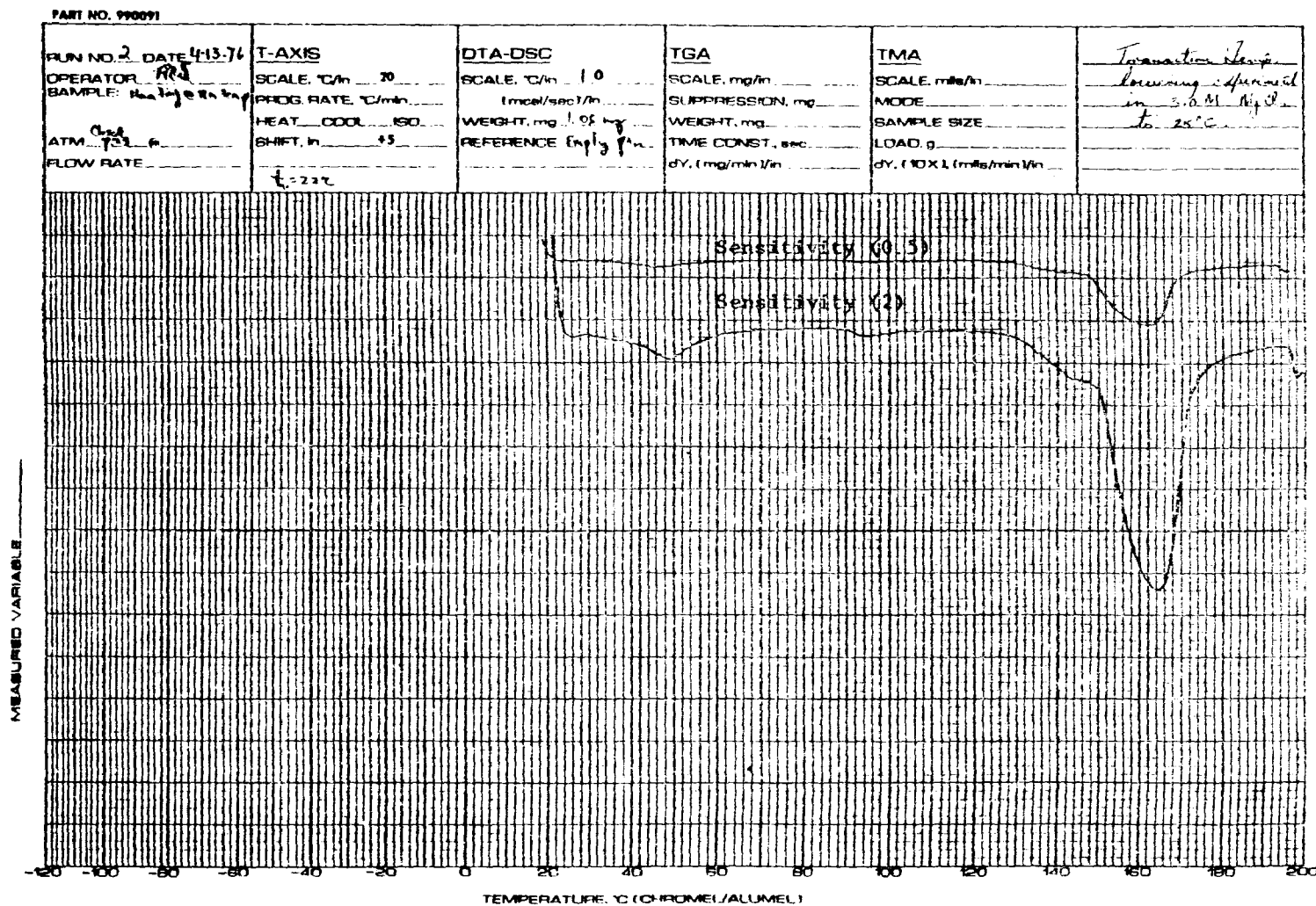


Figure 2. DSC Scan of the MgSO_4 Solids Present in the 3M MgCl_2 Solution

TECHNICAL NOTE 200-045-54-02

MgSO₃ HEXAHYDRATE AND TRIHYDRATE
PREPARATION, HANDLING
AND CHARACTERIZATION

Prepared by:

R. E. Sawyer
J. L. Skloss
R. E. Pyle

CONTENTS

1.	Introduction	212
2.	Preparation of Magnesium Sulfite Hexahydrate and Trihydrate	213
	Nucleation of $\text{MgSO}_3 \cdot \text{Hexahydrate}$	213
	Nucleation of $\text{MgSO}_3 \cdot \text{Trihydrate}$	213
	Conversion of Hydrates	214
3.	Solids Handling.	215
4.	Solids Characterization	217
	DSC Theory of Operation and Application	217
	Theory and Application of TGA Analysis	223
	Dessicator TGA	226
	Bibliography	231
<u>Number</u>	<u>FIGURES</u>	<u>Page</u>
4-1	DSC Scan of $\text{MgSO}_3 \cdot 3\text{H}_2\text{O}$	219
4-2	DSC Scan of $\text{MgSO}_3 \cdot 6\text{H}_2\text{O}$	220
4-3	DSC Scan of $\text{MgSO}_3 \cdot 6\text{H}_2\text{O}$ and $\text{MgSO}_3 \cdot 3\text{H}_2\text{O}$	222
4-4	TGA of $\text{MgSO}_3 \cdot 6\text{H}_2\text{O}$ and $\text{MgSO}_3 \cdot 3\text{H}_2\text{O}$ Mixture	224
4-5	$\text{MgSO}_3 \cdot 6\text{H}_2\text{O}$ Wt. Loss vs. % Composition @ 100°C (self generated atmosphere).	229

<u>Number</u>	TABLES	<u>Page</u>
4-1	221
4-2	Dessiccator TGA Results @ 100°C	228

SECTION 1

INTRODUCTION

The removal of SO_2 from flue gas streams by an MgO regenerative scrubbing system has proven to be technically feasible. The SO_2 is removed from the scrubbing system as a precipitate of hydrated magnesium sulfite. Two hydrates have been identified, $\text{MgO}_3 \cdot 6\text{H}_2\text{O}$ and $\text{MgSO}_3 \cdot 3\text{H}_2\text{O}$.

In order to make experimental measurements in support of the magnesium oxide process, it is necessary to have sample taking, handling and preparation methods such that the material actually analyzed is representative of the process from which it was sampled. This technical note describes such procedures developed for the tri- and hexahydrates of MgSO_3 .

SECTION 2

PREPARATION OF MAGNESIUM SULFITE HEXAHYDRATE AND TRIHYDRATE

Pure crystals of magnesium sulfite hexahydrate or trihydrate may be prepared by two methods: nucleation and hydrate conversion. Either hydrate of MgSO_3 may be prepared by nucleation, depending on temperature, from supersaturated solutions of magnesium sulfite. Once a particular hydrate phase is obtained, conversion to the other hydrate can be achieved by temperature adjustment and allowance for equilibration.

NUCLEATION OF MgSO_3 HEXAHYDRATE

Pure $\text{MgSO}_3 \cdot 6\text{H}_2\text{O}$ may be nucleated from magnesium sulfate solution by the addition of concentrated sodium sulfite solution. A solution temperature of 30°C is suitable. When sufficient sodium sulfite has been added ($\sim 0.5\text{m}$) nucleation occurs. After the onset of nucleation approximately 30 minutes is allowed for the precipitation of solids. 10-100 micrometer sized $\text{MgSO}_3 \cdot 6\text{H}_2\text{O}$ crystals are obtained by this method.

NUCLEATION OF MgSO_3 TRIHYDRATE

Pure $\text{MgSO}_3 \cdot 3\text{H}_2\text{O}$ may be nucleated by the addition of concentrated sodium sulfite solution to magnesium sulfate solution heated above 65°C . Extremely small (1-5 micrometer) crystals are obtained by homogeneous nucleation under these conditions. Larger crystals up to 50 micrometers may be obtained by overnight stirring of the slurry and subsequent precipitation of the solid.

CONVERSION OF HYDRATES

Magnesium sulfite hexahydrate may be converted to the trihydrate phase and vice versa by adjusting the temperature of the slurry containing an excess of magnesium sulfite solids. $\text{MgSO}_3 \cdot 6\text{H}_2\text{O}$ is stable in pure water slurries below 41°C whereas $\text{MgSO}_3 \cdot 3\text{H}_2\text{O}$ is stable above 41°C . Increasing the ionic strength of the solution decreases the transition temperature. The hexahydrate phase is converted completely to the trihydrate phase overnight by continually stirring the slurry maintained at approximately 55°C . This conversion takes place either in pure solutions of magnesium sulfite or in 20% magnesium sulfate medium. The trihydrate phase of magnesium sulfite is converted to the hexahydrate phase by overnight stirring at room temperatures.

SECTION 3

SOLIDS HANDLING

Once a pure hydrate form of magnesium sulfite is prepared in a slurry medium it is important to remove the solid phase from the solution without affecting the integrity of the crystals. The most applicable method is vacuum filtration followed by alcohol washings. Only a few seconds are required to filter 100 ml of slurry through a 47-mm filter membrane. Trihydrate slurries filter more slowly than hexahydrate slurries because of the smaller crystal size. The filter membranes may consist of glass fiber, paper, or other common filtering materials which are resistant to alcohol.

After all of the slurry sample has been filtered, the magnesium sulfite crystals are washed immediately with 50 vol.% methanol or ethanol in water solutions that have been preheated to the slurry temperature. Three 10-ml portions of alcohol solution are recommended for the complete washing of the crystals. Tests with barium chloride addition showed that all the sulfate ion from the 20% magnesium sulfate medium is removed from the crystals by these washings.

The 50% alcohol solution is a very suitable washing solvent. The solubility of magnesium sulfite in 50% ethanol is only 1/30 of that in pure water at the temperatures encountered in this study. Also, the removal of magnesium sulfate, sulfite or chloride solution from the magnesium sulfite crystals is easily and quickly accomplished by the alcohol solution washings.

After washing, the crystals present on the filter membrane are placed in an oven set at 40-50°C. Solid samples less than 1 gm dry within 30 minutes. More time is required for larger

samples, and overnight drying may be necessary in some instances. Caution should be used not to exceed 50°C; otherwise, some of the waters of hydration may be lost. The dried solids are generally stored in a desiccator (without desiccant) purged with nitrogen or other inert gas. The magnesium sulfite solids may also be stored in air without problem provided the relative humidity does not exceed 90%. No crystal deterioration of either hydrate phase was observed during four months storage time in plastic bottles.

SECTION 4

SOLIDS CHARACTERIZATION

The Radian Literature Survey Technical Note 200-045-36-01 reported that there have been several methods used to characterize magnesium sulfite hexahydrate and trihydrate solids. Such characterization techniques as infrared (IR), X-ray, differential thermal analysis (DTA) and differential scanning calorimetry (DSC) have been used successfully (DO-015, DA-195, TE-030). Of the analytical methods used, DSC appears to offer the greatest ease of operation coupled with a rapid turn-around time. A Dupont 990 thermal analysis system consisting of a 990 programming and recording console and a 990 system cell base with standard DSC cell were used in our laboratory.

DSC THEORY OF OPERATION AND APPLICATION

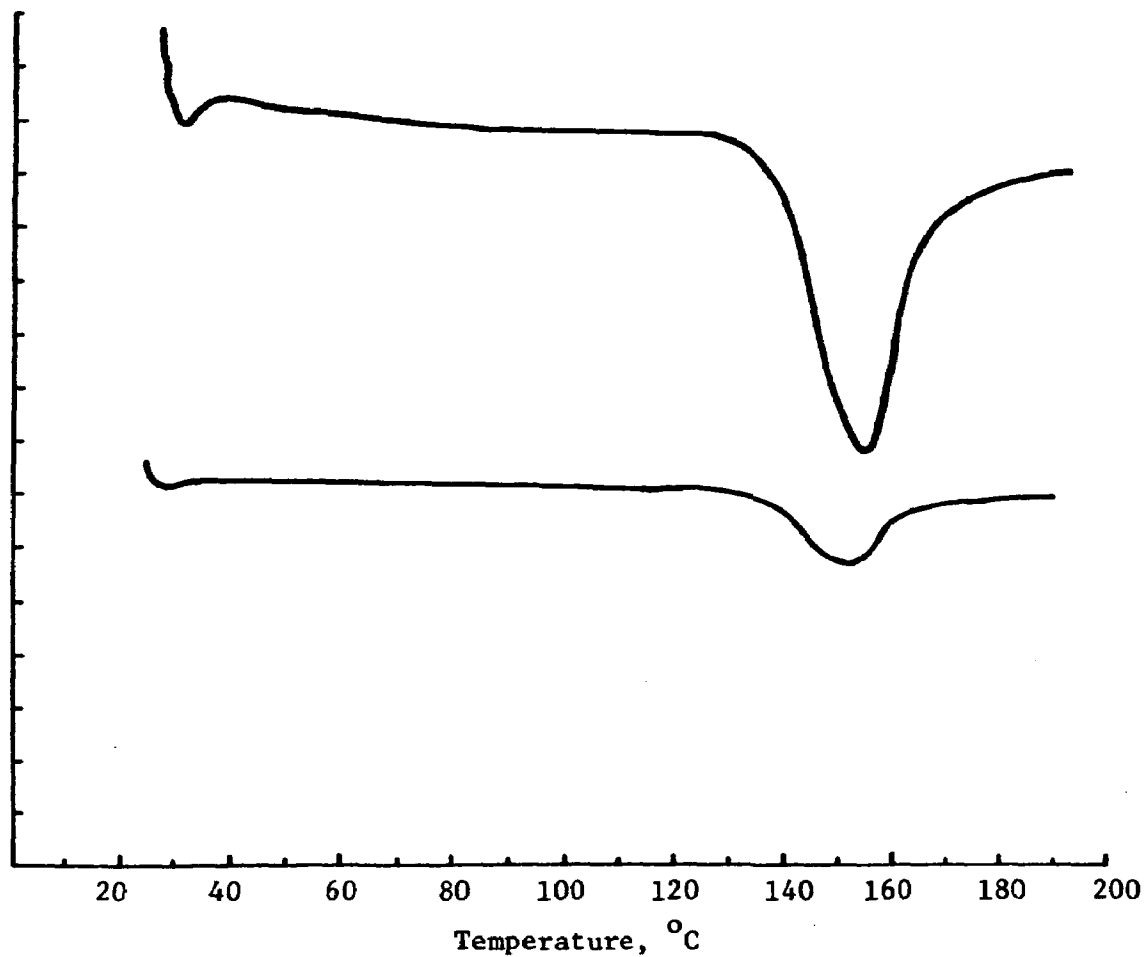
In the DSC mode, the Dupont System 990 gave very accurate results. Two identical aluminum pans, one containing the sample to be analyzed, the other the reference, are placed on the DSC cell. The cell is then covered and sealed to form an insulated environment. A programmed heating rate and maximum temperature limit are then selected on the 990 program and recording console. The system is then operator balanced to adjust the electronics to the temperature indicated inside the sample chamber by the thermocouples. The system is then placed in operation and allowed to heat at its programmed rate. As the sample and reference pans heat, the rate of energy absorption or evolution by the sample is recorded on a dual pen recorder as a function of temperature vs. change. To perform kinetic studies, the displacement of the curve from some predetermined or predrawn baseline is measured.

In the DSC thermogram of $\text{MgSO}_3 \cdot 3\text{H}_2\text{O}$, shown in Figure 4-1, only one endothermic transition was observed, starting at 120°C with a peak at 155°C . In the DSC scan of $\text{MgSO}_3 \cdot 6\text{H}_2\text{O}$, shown in Figure 4-2, it is significant to note that only one endothermic transition was observed starting at 45°C with a peak maximum near 90°C . These results are consistent with the studies of Dauerman (DA-195).

In a further refinement of the DSC studies, the area of the peaks generated for both pure $\text{MgSO}_3 \cdot 6\text{H}_2\text{O}$ and $\text{MgSO}_3 \cdot 3\text{H}_2\text{O}$ of various weight ranges were determined. From this a correlation factor was empirically determined. This correlation factor times the area of the peaks gave a very good approximation (within a few hundredths of a mg) of the actual amount in mg of each hydrate present.

The correlation factors for both $\text{MgSO}_3 \cdot 6\text{H}_2\text{O}$ and $\text{MgSO}_3 \cdot 3\text{H}_2\text{O}$ were determined by an area approximation technique of curves generated by pure samples. DSC scans were made of pure samples of either $\text{MgSO}_3 \cdot 6\text{H}_2\text{O}$ or $\text{MgSO}_3 \cdot 3\text{H}_2\text{O}$ which had been weighed on an analytical balance. The area of the peak generated by each species was calculated by multiplying the peak height in inches by the peak width at one-half the peak height. This was then divided into the total sample weight to determine the factor in mg/in^2 . Typical results are shown in Table 4-1.

This approach was tried with synthetic mixtures of pure $\text{MgSO}_3 \cdot 6\text{H}_2\text{O}$ and $\text{MgSO}_3 \cdot 3\text{H}_2\text{O}$. Typical scans such as Figure 4-3 were produced for these mixtures. By applying the aforementioned techniques, it is possible to determine the amounts of hexa- and tri-crystals in a mixture to within a total accuracy of a few percent.



Run No: 6
Date: 3-17-76
Operator: RES
Sample: P.S. Sample
Composite Sample Dried Solid
1/7/76

DTA-DSC
Scale, °C/in: 10
Weight, mg: .00536 gr
Reference: Empty Pan

Figure 4-1. DSC Scan of $\text{MgSO}_3 \cdot 3\text{H}_2\text{O}$

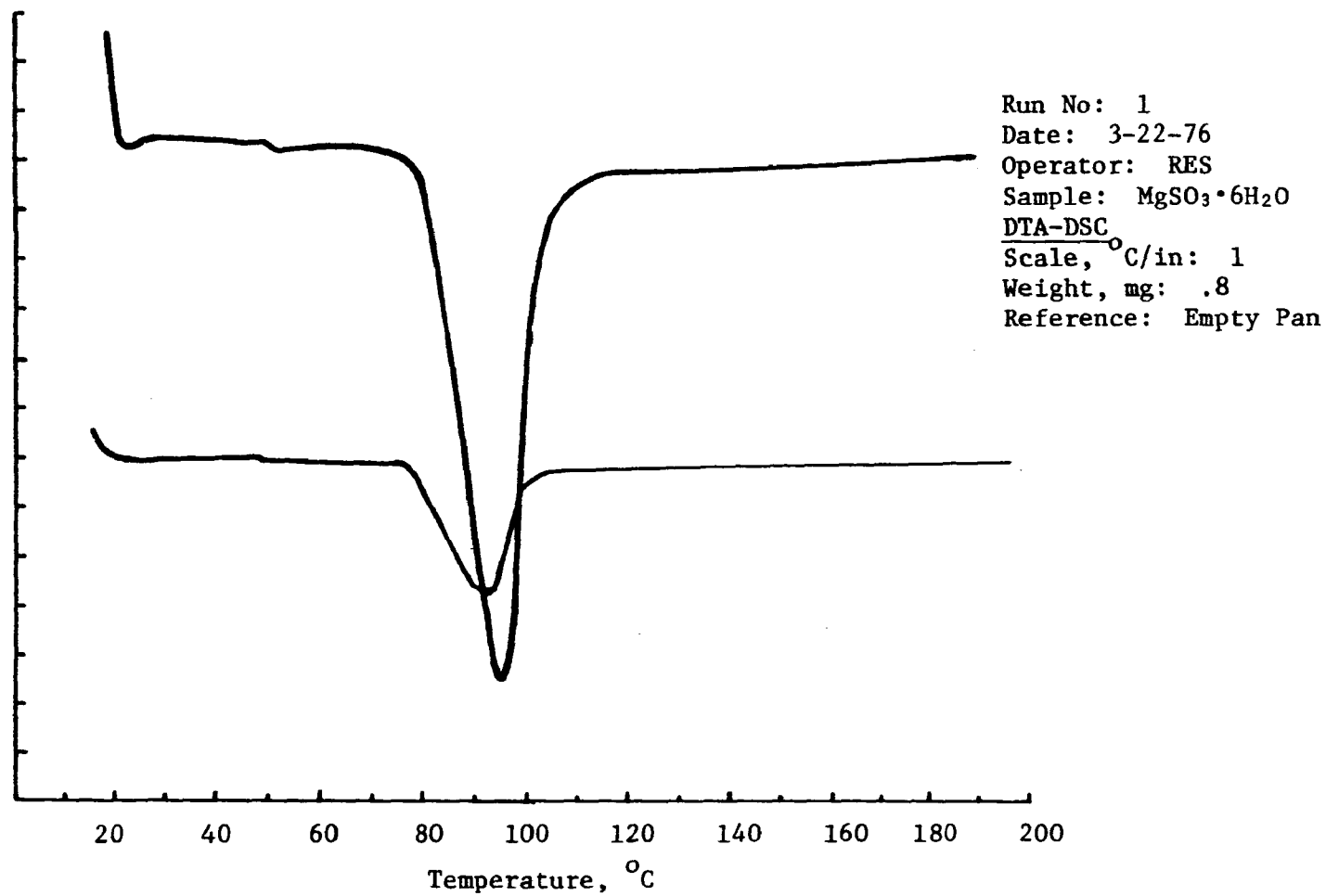


Figure 4-2. DSC Scan of $\text{MgSO}_3 \cdot 6\text{H}_2\text{O}$

TABLE 4-1.

Species	Sample Weight in mg.	÷	Peak Area in sq. in.	= mg/in ²
MgSO ₃ · 6H ₂ O	.80		3.6	.22
MgSO ₃ · 6H ₂ O	2.36		9.13	.26
MgSO ₃ · 6H ₂ O	.46		1.8	.26
MgSO ₃ · 6H ₂ O	.58		2.3	<u>.25</u>
Average				.25
MgSO ₃ · 3H ₂ O	.85		2.4	.35
MgSO ₃ · 3H ₂ O	.63		2.1	.30
MgSO ₃ · 3H ₂ O	.63		1.9	.33
MgSO ₃ · 3H ₂ O	1.11		3.2	<u>.34</u>
Average				.33

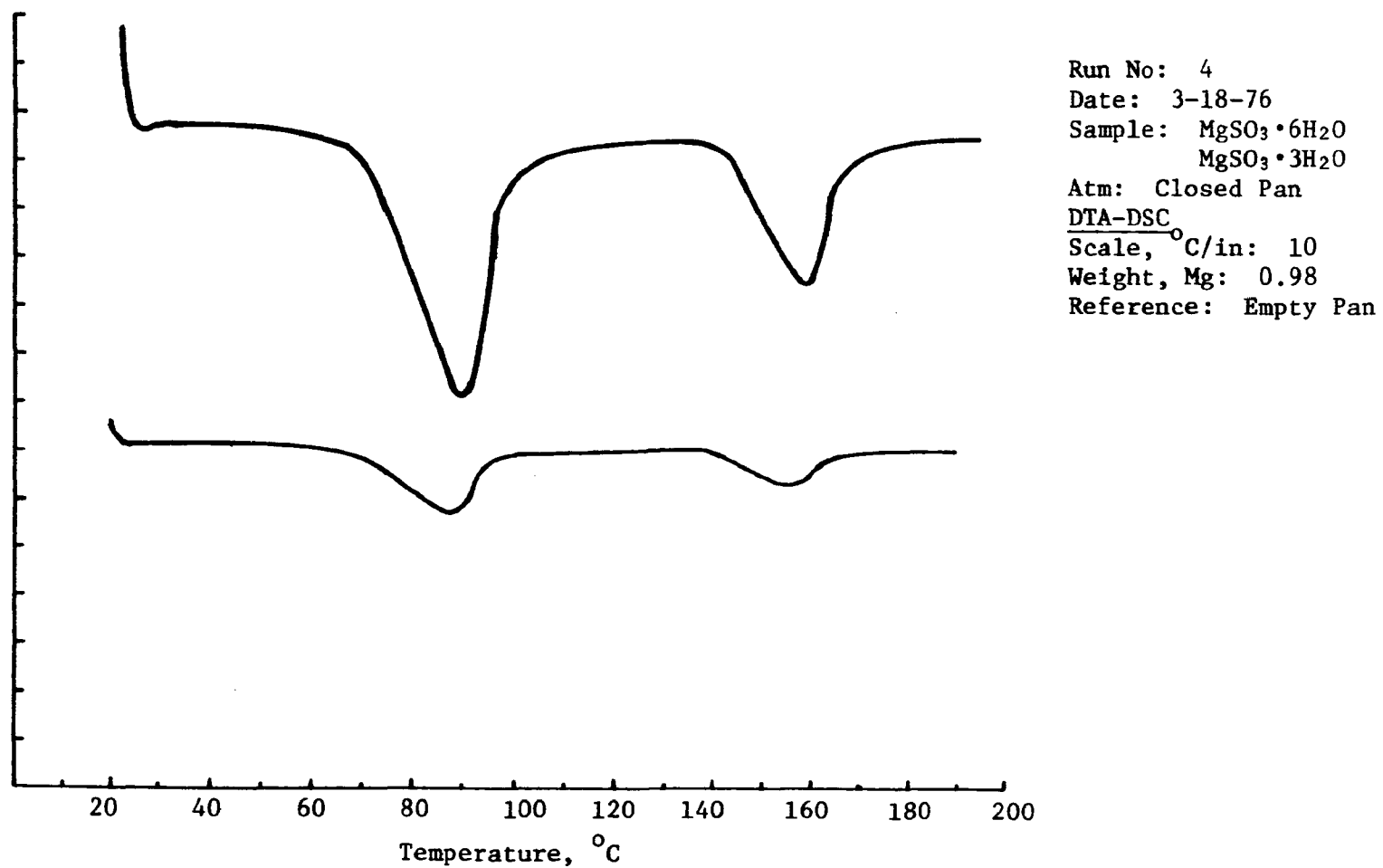


Figure 4-3. DSC Scan of $\text{MgSO}_3 \cdot 6\text{H}_2\text{O}$ and $\text{MgSO}_3 \cdot 3\text{H}_2\text{O}$

THEORY AND APPLICATION OF TGA ANALYSIS

Another analytical technique which is useful in quantifying mixtures of the tri- and hexahydrates is thermogravimetric analysis. A Dupont 990 thermal analyzer control and recording console was used in conjunction with a Dupont 951 thermogravimetric analyzer (TGA). The heart of the TGA system consists of a precision microbalance and counterweighting system which can be insulated from the surrounding environment. A sample of up to 1 gram is placed on the balance pan and is coarsely counterbalanced on the balance arm by applying counterweights. The entire system is then isolated from the surrounding environment. A "fine tune" balance is then accomplished by means of electronic counterbalancing. A constant heating rate is then applied to the sample in the balance pan. The 990 control unit will record weight loss or gain as a function of temperature.

The accuracy of the method was investigated by analyzing the thermograms of synthetic mixtures of the hexahydrate and tri-hydrate phases ranging from 10-90% in composition. From these thermograms, the water content and the magnesium sulfite content can be calculated. First, the water content calculations will be considered and compared to the theoretical values.

The water content of each hydrate in a mixture can be obtained from the TGA thermogram (a typical thermogram is shown in Figure 4-4) by taking into account the fact that the weight loss in the first dehydration step at 100°C represents the first three moles of water in $\text{MgSO}_3 \cdot 6\text{H}_2\text{O}$, i.e., 50% of the water content of the hexa form. The water loss beginning at 180°C is the remainder of the hexahydrate water plus all of the trihydrate water.

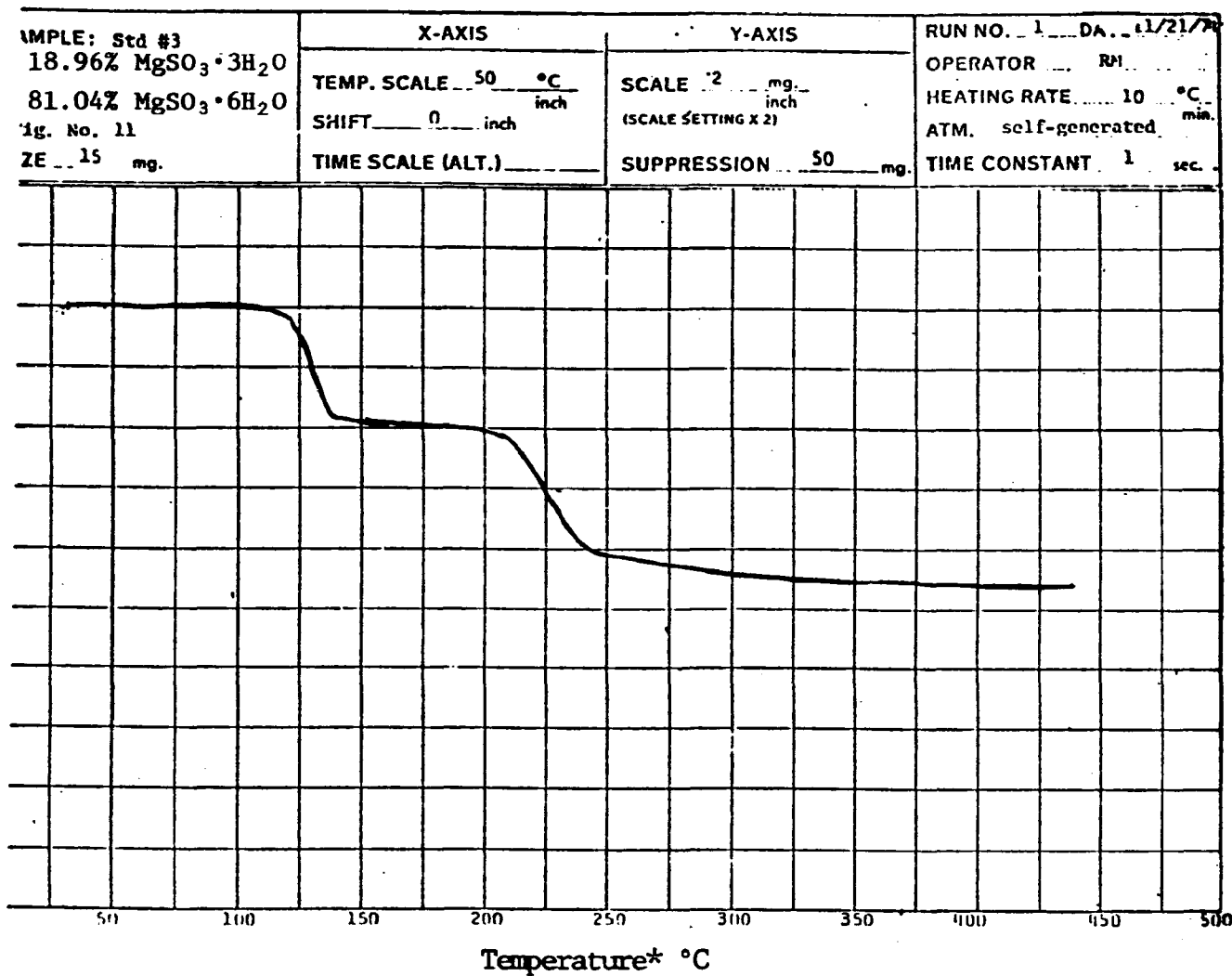


Figure 4-4. TGA of $\text{MgSO}_3 \cdot 6\text{H}_2\text{O}$ and $\text{MgSO}_3 \cdot 3\text{H}_2\text{O}$ Mixture

The amount of each hydrate may be calculated as follows:

% H₂O in MgSO₃·6H₂O in a mixture = (% weight loss in the first step to 175°C) x (2)

% H₂O in MgSO₃·3H₂O in a mixture = (% weight loss in the second step to 400°C) - (% weight loss in the first step to 175°C)

The theoretical values of the water content are calculated as follows:

% H₂O in MgSO₃·6H₂O in a mixture = % MgSO₃·6H₂O in the mixture

$$\times \frac{6H_2O}{MgSO_3 \cdot 6H_2O}$$

= % MgSO₃·6H₂O in the mixture

$$\times \frac{108}{212.3}$$

= % MgSO₃·6H₂O in the mixture

$$\times .509$$

% H₂O in MgSO₃·3H₂O in a mixture = % MgSO₃·3H₂O in the mixture

$$\times \frac{3H_2O}{MgSO_3 \cdot 3H_2O}$$

= % MgSO₃·3H₂O in the mixture

$$\times \frac{54}{158.3}$$

= % $\text{MgSO}_3 \cdot 3\text{H}_2\text{O}$ in the mixture

x 0.341

The magnesium sulfite content of a sample can be calculated from the TGA thermograms by performing a similar procedure as the water content calculations, and by taking into account that 6 moles of water represent 50.9% by weight of $\text{MgSO}_3 \cdot 6\text{H}_2\text{O}$ and 3 moles of water represent 34.1 % by weight of $\text{MgSO}_3 \cdot 3\text{H}_2\text{O}$. Thus the percentage of each hydrate in a mixture is calculated as follows:

% $\text{MgSO}_3 \cdot 6\text{H}_2\text{O}$ in a mixture = % weight loss at 175°C x
2/0.509

% $\text{MgSO}_3 \cdot 3\text{H}_2\text{O}$ in a mixture = (% weight loss between 175°
and 400°C - % weight loss at 175°C)/34.1

DESSICATOR TGA

While both DSC and TGA offer excellent analytical means for determining the compositions of mixtures of hexahydrate and trihydrate, neither method is well suited for field determinations. The DSC system is moderately expensive ($\approx \$10,000$) and not well suited for analyzing a large number of samples since it takes approximately 30 minutes for a single analysis. The TGA analysis while slightly more accurate is also more prone to operator error. The micro-balance system would also not adapt easily to a field environment, and the time required for a single analysis is longer than with DSC. Therefore, a modified field TGA method was developed.

A large glass vacuum desiccator was fitted with a heating mantle controlled by a Variac. All desiccant was removed and a thermometer was placed on the desiccator plate. The Variac setting was adjusted until the thermometer inside registered between 110-110°C. According to Dauerman (DA-195), when $\text{MgSO}_3 \cdot 6\text{H}_2\text{O}$ is heated in a self-generated atmosphere, two transition steps are observed: $\text{MgSO}_3 \cdot 6\text{H}_2\text{O} \rightarrow \text{MgSO}_3 \cdot 3\text{H}_2\text{O}$ starting at 100°C, then $\text{MgSO}_3 \cdot 3\text{H}_2\text{O} \rightarrow \text{MgSO}_3$ anhydrous starting at 175°C. Therefore, by adjusting the inside desiccator temperature to 100-110°C, the hexahydrate form should convert to trihydrate, but the trihydrate should remain unchanged.

A number of oven-dried glass vials were labeled and weighed on an analytical balance. To each vial, approximately 0.6 grams of pure hexahydrate or trihydrate was added. The exact weight added was determined by difference on the analytical balance. A glass wool plug was then inserted into each vial to maintain a self-generated atmosphere. The samples were then reweighed and placed into the heated glass desiccator. After 4 hours, all the samples were removed and cooled in an argon purged desiccator. The samples were then reweighed. The average weight loss was approximately 25% for hexahydrate samples and less than 1% for trihydrate samples (Table 4-2). The theoretical weight loss for the hexahydrate is 25.4%. Results for both tests are shown in Figure 4-5.

There are a number of advantages to the desiccator TGA method. A large number of samples can be processed at the same time, since approximately 20 samples can be placed in the desiccator. The weighing time for each sample is less than 10 minutes. Only an analytical balance and several desiccators are required for the analysis. A disadvantage, however, is that the technique is insensitive to contamination from inert species; that is, material that cannot be removed from the MgSO_3 hydrate

TABLE 4-2. DESSICCATOR TGA RESULTS @ 100°C

<u>Sample, wt%</u>		<u>Grams</u>		<u>Wt. Loss, %</u>	
Hexa	Tri	Sample Wt.	Wt. Loss	Observed	Theoretical
100	0	0.599	0.152	25.4	25.4
100	0	0.602	0.153	25.4	25.4
0	100	0.602	0.0018	0.29	0.0
0	100	0.600	0.0005	0.08	0.0
60	40	0.600	0.093	15.4	15.2
60	40	0.603	0.092	15.3	15.2
80	20	0.602	0.120	19.8	20.3
80	20	0.535	0.105	17.5	20.3

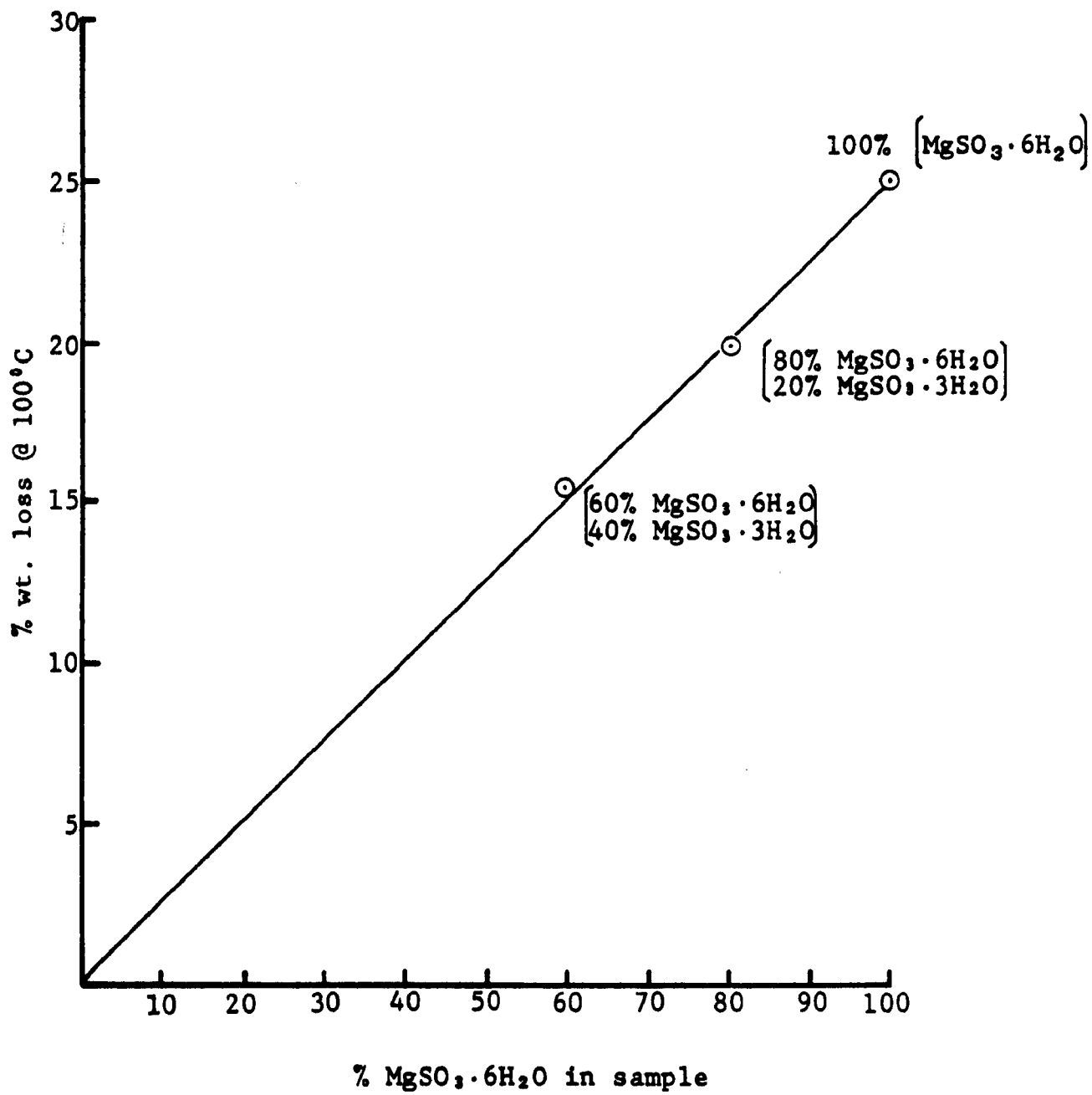


Figure 4-5. $\text{MgSO}_3 \cdot 6\text{H}_2\text{O}$ Wt. Loss vs. % Composition @ 100°C
(self generated atmosphere)

sample by such techniques as alcohol/water washing. An accurate estimate of the amount of contamination can be determined by wet chemical analyses.

BIBLIOGRAPHY

- DA-195 Dauerman, Leonard, Sulfur Oxide Removal From Power Plant Stack Gas. Magnesia Scrubbing-Regeneration: Production of Sulfuric Acid. Newark, New Jersey, New Jersey Institute of Technology, Feb. 1975.
- DO-015 Downs, W. and A. J. Kubasco, Magnesia Base Wet Scrubbing of Pulverized Coal Generated Flue Gas -- Pilot Demonstration. PB 198 074 Alliance, Ohio, Babcock and Wilcox Co., 1979.
- TE-030 Tennessee Valley Authority, Removal of Sulfur Dioxide from Stack Gases. Thermal Decomposition of Magnesium Sulfite. Muscle Shoals, Ala., Feb. 1971, #38.

TECHNICAL NOTE 200-045-54-03a

PRECIPITATION KINETICS OF MgSO_3
HYDRATES IN SCRUBBER-LIKE MEDIA

Prepared by:

J. L. Skloss
T. B. Parsons
P. S. Lowell

CONTENTS

1. Introduction.	240
2. Experimental Approach	241
3. Data Analysis Methods	243
4. Results and Discussion.	248
Experiment 3-2, Trihydrate Seed	
Crystals.	261
Experiment 3-3, Hexahydrate Seed	
Crystals.	263
Experiment 3-4, Trihydrate Seed	
Crystals.	263
Experiment 3-5, Hexahydrate Seed	
Crystals.	266
Experiment 3-6, Mixed Tri- and Hexa- hydrate Seed Crystals	268
Experiment 3-7, Mixed Tri- and Hexa- hydrate Seed Crystals	268
5. Conclusions	271
Appendix A	272

FIGURES

<u>Number</u>		<u>Page</u>
4-1	Results of DSC Analysis of a Pure Sample of MgSO ₃ •6H ₂ O	255
4-2	Results of DSC Analysis of a Pure Sample of MgSO ₃ •3H ₂ O	256
4-3	Results of DSC Analysis of Solids Precipitated After 470 Minutes in Experiment No. 3-5.	257
4-4	Electron Micrograph of Pure MgSO ₃ •6H ₂ O at 300X Magnification.	258
4-5	Electron Micrograph of Pure MgSO ₃ •3H ₂ O at 1000X Magnification.	259
4-6	Electron Micrograph of Solids from Experiment No. 3-5 at 1000X Magnification Showing Trihydrate Crystals.	260
4-7	Results of MgSO ₃ Hydrate Precipitation Rate Experiment 3-2 Employing Trihydrate Seed Crystals	262
4-8	Results of MgSO ₃ Hydrate Precipitation Rate Experiment 3-3 Employing Hexahydrate Seed Crystals	264
4-9	Results of MgSO ₃ Hydrate Precipitation Rate Experiment 3-4 Employing Trihydrate Seed Crystals	265

FIGURES (Continued)

<u>Number</u>	<u>Page</u>
4-10 Results of MgSO_3 Hydrate Precipitation Rate Experiment 3-5 Employing Hexahydrate Seed Crystals	267
4-11 Results of MgSO_3 Hydrate Precipitation Rate Experiment 3-6 Employing a Mixture of Tri- and Hexahydrate Seed Crystals.	269
4-12 Results of MgSO_3 Hydrate Precipitation Rate Experiment 3-7 Employing a Mixture of Tri- and Hexahydrate Seed Crystals.	270
A-1 Results of DSC Analysis of Solid Sample Taken at 60 Minutes in Experiment 3-2.	273
A-2 Results of DSC Analysis of Solid Sample Taken at 3150 Minutes in Experiment 3-2.	274
A-3 Results of DSC Analysis of Solid Sample Taken at 10 Minutes in Experiment 3-3.	275
A-4 Results of DSC Analysis of Solid Sample Taken at 20 Minutes in Experiment 3-3.	276
A-5 Results of DSC Analysis of Solid Sample Taken at 60 Minutes in Experiment 3-3.	277
A-6 Results of DSC Analysis of Solid Sample Taken at 150 Minutes in Experiment 3-3	278

FIGURES (Continued)

<u>Number</u>	<u>Page</u>
A-7 Results of DSC Analysis of Solid Sample Taken at 200 Minutes in Experiment 3-3.	279
A-8 Results of DSC Analysis of Solid Sample Taken at 60 Minutes in Experiment 3-4	280
A-9 Results of DSC Analysis of Solid Sample Taken at 1260 Minutes in Experiment 3-4	281
A-10 Results of DSC Analysis of Solid Sample Taken at 20 Minutes in Experiment 3-5	282
A-11 Results of DSC Analysis of Solid Sample Taken at 60 Minutes in Experiment 3-5	283
A-12 Results of DSC Analysis of Solid Sample Taken at 100 Minutes in Experiment 3-5.	284
A-13 Results of DSC Analysis of Solid Sample Taken at 120 Minutes in Experiment 3-5.	285
A-14 Results of DSC Analysis of Solid Sample Taken at 150 Minutes in Experiment 3-5.	286
A-15 Results of DSC Analysis of Solid Sample Taken at 180 Minutes in Experiment 3-5.	287
A-16 Results of DSC Analysis of Solid Sample Taken at 270 Minutes in Experiment 3-5.	288

FIGURES (Continued)

<u>Number</u>	<u>Page</u>
A-17 Results of DSC Analysis of Solid Sample Taken at 330 Minutes in Experiment 3-5.	289
A-18 Results of DSC Analysis of Solid Sample Taken at 390 Minutes in Experiment 3-5.	290
A-19 Results of DSC Analysis of Solid Sample Taken at 470 Minutes in Experiment 3-5.	291
A-20 Results of DSC Analysis of Solid Sample Taken at 1400 Minutes in Experiment 3-5	292
A-21 Results of DSC Analysis of Solid Sample Taken at 3200 Minutes in Experiment 3-5	293
A-22 Results of DSC Analysis of Solid Sample Taken at 20 Minutes in Experiment 3-6	294
A-23 Results of DSC Analysis of Solid Sample Taken at 50 Minutes in Experiment 3-6	295
A-24 Results of DSC Analysis of Solid Sample Taken at 60 Minutes in Experiment 3-6	296
A-25 Results of DSC Analysis of Solid Sample Taken at 180 Minutes in Experiment 3-6.	297
A-26 Results of DSC Analysis of Solid Sample Taken at 300 Minutes in Experiment 3-6.	298

FIGURE (Continued)

<u>Number</u>		<u>Page</u>
A-27	Results of DSC Analysis of Solid Sample Taken at 390 Minutes in Experiment 3-6.	299
A-28	Results of DSC Analysis of Solid Sample Taken at 4260 Minutes in Experiment 3-6	300
A-29	Results of DSC Analysis of Solid Sample Taken at 10 Minutes in Experiment 3-7	301
A-30	Results of DSC Analysis of Solid Sample Taken at 30 Minutes in Experiment 3-7	302
A-31	Results of DSC Analysis of Solid Sample Taken at 40 Minutes in Experiment 3-7	303
A-32	Results of DSC Analysis of Solid Sample Taken at 80 Minutes in Experiment 3-7	304
A-33	Results of DSC Analysis of Solid Sample Taken at 150 Minutes in Experiment 3-7.	305
A-34	Results of DSC Analysis of Solid Sample Taken at 240 Minutes in Experiment 3-7.	306
A-35	Results of DSC Analysis of Solid Sample Taken at 320 Minutes in Experiment 3-7.	307
A-36	Results of DSC Analysis of Solid Sample Taken at 1400 Minutes in Experiment 3-7	308

TABLES

<u>Number</u>		<u>Page</u>
2-1	Summary of Experimental Conditions in Tests of Magnesium Sulfite Hydrate Precipitation from Scrubber-Like Media.	242
4-1	Results of Magnesium Sulfite Hydrate Precipita- tion Experiment No. 3-2.	249
4-2	Results of Magnesium Sulfite Hydrate Precipita- tion Experiment No. 3-3.	250
4-3	Results of Magnesium Sulfite Hydrate Precipita- tion Experiment No. 3-4.	251
4-4	Results of Magnesium Sulfite Hydrate Precipita- tion Experiment No. 3-5.	252
4-5	Results of Magnesium Sulfite Hydrate Precipita- tion Experiment No. 3-6.	253
4-6	Results of Magnesium Sulfite Hydrate Precipita- tion Experiment No. 3-7.	254

SECTION 1

INTRODUCTION

The work described in this technical note is part of a study of the physical chemistry of the precipitation of magnesium sulfite hydrates. This chemical phenomenon is important in the design of magnesium-based SO_2 wet scrubbing processes. Field tests of the magnesium oxide processes have shown that both MgSO_3 trihydrate and hexahydrate precipitate from scrubbing solutions. The laboratory tests described here were done to investigate the rates of precipitation of the two hydrates from slurries characteristic of those in the magnesium oxide process. Precipitation rate studies in dilute solutions and experiments to study nucleation rates have also been performed and are described in Technical Notes 200-045-36-03, -54-04, 05 and 06.

SECTION 2

EXPERIMENTAL APPROACH

The equipment and experimental procedure employed in the precipitation rate studies are described in Technical Note 200-045-36-05, which gives the results of identical precipitation rate experiments in dilute solutions. A 4-liter pyrex reaction vessel was employed. The well-stirred reactor was situated in a constant temperature bath. All tests were done at 55°C. Batch addition of MgSO_4 and Na_2SO_3 feedstock solutions and MgSO_3 seed crystals was employed. The reactant solutions were composed of approximately 20 wt percent (2.08 molal) MgSO_4 and were supersaturated with respect to magnesium sulfite. The initial sulfite concentration was varied from about 0.3 to 0.5 gmole/l by varying of the concentration of the Na_2SO_3 feed solution. Precipitation was initiated by the addition of 1 gram of $\text{MgSO}_3 \cdot 6\text{H}_2\text{O}$ or $\text{MgSO}_3 \cdot 3\text{H}_2\text{O}$ seed crystals. In some experiments a mixture of 0.5 grams of each hydrate was employed. The experimental conditions of 55°C, pH 6, and 20 wt % MgSO_4 solutions are characteristic of solutions in operating magnesium oxide processes (scrubber-like media).

Reactor contents were sampled before addition of seed crystals and periodically thereafter. Tests were conducted for periods of 1,100 to 11,000 minutes. Analyses were performed to measure sodium, magnesium, total sulfur, sulfite, and sulfate (by difference) concentrations in the liquor; weight percent solids in the slurry; pH and temperature. Sulfate determinations indicated that the amount of sulfite oxidation to sulfate was negligible. The wet analytical chemistry methods listed in section 2.3 of Technical Note 200-045-36-05 were employed. In addition, microscopic examination and differential scanning

calorimetric (DSC) analyses of solids were performed. These methods are described in Technical Note 200-045-54-02.

It was found that measurement of the weight of solids produced was not a reliable indicator of the reaction rate. The results of chemical analyses of sulfite in the solution were used to calculate the number of moles of MgSO_3 solids precipitated. DSC analyses and microscopic examination provided semiquantitative information on the identification of the solid products.

Table 2-1 is a summary of the experiments conducted.

TABLE 2-1. SUMMARY OF EXPERIMENTAL CONDITIONS IN TESTS OF MAGNESIUM SULFITE HYDRATE PRECIPITATION FROM SCRUBBER-LIKE MEDIA¹.

Test No.	Initial Sulfite Concentration (gmole/l)	Composition of 1 gram of Seed Crystals
3-2	0.316	$\text{MgSO}_3 \cdot 3\text{H}_2\text{O}$
3-3	0.475	$\text{MgSO}_3 \cdot 6\text{H}_2\text{O}$
3-4	0.316	$\text{MgSO}_3 \cdot 3\text{H}_2\text{O}$
3-5	0.367	$\text{MgSO}_3 \cdot 6\text{H}_2\text{O}$
3-6	0.374	$\text{MgSO}_3 \cdot 3\text{H}_2\text{O}$ (0.5g) and $\text{MgSO}_3 \cdot 6\text{H}_2\text{O}$ (0.5g)
3-7	0.358	$\text{MgSO}_3 \cdot 3\text{H}_2\text{O}$ (0.5g) and $\text{MgSO}_3 \cdot 6\text{H}_2\text{O}$ (0.5)

- ¹. Tests were done at 55 °C and pH 6 in solutions containing approximately 20 wt % MgSO_4 . Initial magnesium concentration varied from 2.01 to 2.04 gmole/l.

SECTION 3

DATA ANALYSIS METHODS

For batch-solid/batch-liquid kinetics experiments, the precipitation rate can be calculated from the amount of solid material produced as a function of the time. The total number of moles of solids produced is plotted versus reaction time. The precipitation rate can be obtained from the slope of the resulting curve. The precipitation rate, R , at time t is expressed in equation 3-1.

$$R(t) = \lim_{\Delta t \rightarrow 0} \left(\frac{\Delta N}{\Delta t} \right) | t = \left(\frac{dN}{dt} \right) | t \quad (3-1)$$

where,

N = moles of solids produced

t = duration of the run in minutes, and

R = precipitation rate in mMoles/min at time t

The amount of precipitating material produced at time t can be determined from the change of concentration of ions in solution. That is, the change in the solution magnesium or sulfite ion concentration with time as determined by analytical means must be equivalent to the number of moles of magnesium or sulfite reacted to form the $MgSO_3$ hydrate product. The amount of precipitated material produced at time t was calculated from the following equation:

$$N(t) - N(t_0) = ([ION]_{t_0} - [Ion]_t) Vol_{Reactor} \quad (3-2)$$

where,

[Ion] = initial magnesium or sulfite ion concentration in solution in moles/l, and

Vol_{Reactor} = total reaction solution volume in liters.

Since the magnesium concentration was much greater than the sulfite concentration, the change in sulfite concentration was used to calculate the amount of precipitating material.

It is useful to describe precipitation rates with an equation which expresses the rate as a function of the important variables which determine it. This correlation of experimentally determined rate data is useful because it provides a means of calculating the rate in other systems. Using appropriate values for the variables, a precipitation rate can be predicted for design purposes. Equipment sizes and residence times can thus be established. Equation 3-3 shows an appropriate form for a rate correlation.

$$\text{rate} = \left\{ \begin{matrix} \text{kinetic} \\ \text{factor} \end{matrix} \right\} \left\{ \begin{matrix} \text{crystal} \\ \text{surface} \\ \text{area} \end{matrix} \right\} \left\{ \begin{matrix} \text{driving} \\ \text{force} \end{matrix} \right\} \quad (3-3a)$$

$$\frac{dW}{dt} = k \cdot A_s \cdot f_d \quad (3-3b)$$

This correlation form is based upon the idea that the precipitation rate is proportional to the crystal surface area and a driving force. If no nuclei are being formed and the McCabe ΔL law holds, the first two terms may be combined.

$$k = k^*B \quad (3-4)$$

$$k^*A_s = k^*W_o B (W/W_o)^{2/3} \quad (3-5a)$$

$$k^*A_s = kW_o (W/W_o)^{2/3} \quad (3-5b)$$

In equation 3-5, W is moles of solids formed, and B is the surface area factor in units of cm² crystal surface area per mole of initial seed.

The driving force is a function of the activities of ions in solution. It takes into account the difference between the activities at equilibrium and those at actual conditions. It may be expressed in terms of the relative saturation, r.

$$r_6 = \frac{a_{Mg^{++}} a_{SO_3} a_{H_2O}^6}{Ksp_6} \quad (3-6a)$$

$$= ap_6 / Ksp_6 \quad (3-6b)$$

$$r_3 = ap_3 / Ksp_3 \quad (3-7)$$

The moles of solids formed are normalized by dividing by the initial number of moles of seed, W_o.

$$\psi = W/W_o \quad (3-8)$$

Equation 3-3 may be rewritten in terms of the new variables, ψ and $f_d(r)$.

$$\frac{1}{\psi^{2/3}} \frac{d\psi}{dt} = kf_d(r) \quad (3-9)$$

Simplifying the derivative terms gives equation 3-10.

$$\frac{d(\psi^{1/3})}{dt} - \frac{1}{3}k_f d(r) \quad (3-10)$$

Equation 3-10 shows that rates should be calculated based on a graph of $\psi^{1/3}$ versus reaction time.

The time scale for the reaction is such that it is not convenient to use a linear abscissa. A convenient logarithmic scale defined such that the time origin is nonzero is given in equation 3-11.

$$\theta = \ln(t+10) \quad (3-11)$$

The time derivative indicated in equation 3-11 can be obtained in terms of θ by the following relationship:

$$\frac{d}{dt} = \frac{\partial \theta}{\partial t} \frac{d}{d\theta} \quad (3-12a)$$

$$= \frac{1}{(t+10)} \frac{d}{d\theta} \quad (3-12b)$$

In an effort to determine a driving force term, activity calculations were made using the Radian equilibrium model. Based upon the solution composition data, the relative saturations of the tri- and hexahydrates of MgSO_3 were calculated. These calculations indicated that the system was approaching a steady state relative saturation of about 2.5 rather than 1.0 as required by theory. Equilibrium solubility experiments at high ionic strength confirm this order of magnitude discrepancy between experimental and calculated values.

These results indicate that the equilibrium calculations made in these high ionic strength solutions are not accurate enough to correlate the data generated in this work. An update of either the theoretical basis of the calculations or the parameters used is indicated.

Since the equilibrium model could not be used as an analytical tool, it was not possible to calculate accurate driving force expressions for use in the rate data correlation. As a result, no attempt was made to calculate the rate constant for the correlation form shown in equation 3-3. The correlation form does show which variables are important in determining precipitation rates. And it indicates the proper form in which to plot rate data.

SECTION 4

RESULTS AND DISCUSSION

The results of the precipitation rate experiments are presented in Tables 4-1 through 4-6. The results of chemical analyses of slurry liquor samples were used to calculate moles solids precipitated. The calculation was based on the decrease in sulfite concentration in the solution, since the change in magnesium concentration was small compared to the total concentration. The total measured decrease in moles of Mg^{++} ion was approximately equal to that of the $\text{SO}_3^{=}$ ion within experimental error. The tables also give values for $\psi^{1/3}$ as defined in Section 3. Examples of the results of DSC analyses of solid samples are given in Figures 4-1 through 4-3. Figure 4-1 shows the DSC scan for a pure sample of magnesium sulfite hexahydrate and Figure 4-2 shows the DSC scan for a pure sample of the trihydrate. As indicated in the figures, the hexahydrate peak has a maximum at about 110°C and the trihydrate maximum occurs at about 170°C. Figure 4-3 shows an example from the DSC analysis of solids precipitated during Experiment No. 3-5. The solid sample was collected after 470 minutes. Figure 4-3 indicates that both the hexahydrate and the trihydrate are present in the solid sample.

Examples of electron micrographs of pure hydrates and the same sample from experiment 3-5 are shown in Figures 4-4 through 4-6. Figure 4-4 shows rhombic hexahydrate crystals at 300X magnification. The much smaller trihydrate crystals are shown in Figure 4-5 at 1000X magnification. The electron micrograph, in Figure 4-6, obtained at 1000X shows small trihydrate crystals growing on the surface of the much larger hexahydrate crystals.

TABLE 4.1. RESULTS OF MAGNESIUM SULFITE HYDRATE
PRECIPITATION EXPERIMENT NO. 3-2*

Sample Time (Min)	Results of Chemical Analyses of Slurry Liquor at Indicated Sample Time					** Moles Solids Precipitated	*** $\psi^{1/3}$
	Mg ⁺⁺		SO ₃ ⁼		pH		
	<u>gmole</u> ℓ	<u>gmole</u> kg water	<u>gmole</u> ℓ	<u>gmole</u> kg water			
0	2.02	2.07	0.316	0.324	6.4	0	1.00
60	1.94	1.99	0.303	0.310	6.4	0.037	1.92
180	1.94	1.99	0.304	0.311	6.4	0.034	1.88
260	1.90	1.94	0.295	0.301	6.4	0.058	2.20
1260	1.88	1.92	0.278	0.283	6.4	0.104	2.62
1700	1.91	1.95	0.275	0.281	6.4	0.110	2.67
3150	1.96	2.00	0.271	0.277	6.4	0.119	2.74
7000	1.95	1.99	0.248	0.253	6.4	0.176	3.10
8860	1.93	1.96	0.230	0.234	6.4	0.220	3.33
11500	1.93	1.92	0.228	0.232	6.4	0.221	3.34

* Experiment was conducted at 55°C using 1 gram of magnesium sulfite trihydrate seed crystals. The initial sodium ion concentration was 0.648 gmole/kg water and the initial sulfate ion concentration was 2.1 gmoles/kg water. The density of the liquid was 1.260g/ml.

** The moles solids precipitated were calculated from the number of moles of sulfite leaving solution.

*** $\psi \equiv \frac{\text{total moles of solids}}{\text{initial moles of seed crystals}}$

TABLE 4-2. RESULTS OF MAGNESIUM SULFITE HYDRATE
PRECIPITATION EXPERIMENT NO. 3-3*

Sample Time (Min)	Results of Chemical Analyses of Slurry Liquor at Indicated Sample Time					Moles** Solids Precipitated	ψ^{***}
	Mg^{++}		SO_3^-		pH		
	$\frac{gmole}{l}$	$\frac{gmole}{kg\ water}$	$\frac{gmole}{l}$	$\frac{gmole}{kg\ water}$			
0	2.04	2.14	0.475	0.498	6.41	0	1.00
10	1.98	2.06	0.432	0.450	6.48	0.128	3.04
20	1.93	2.00	0.401	0.416	6.40	0.218	3.62
30	1.95	2.02	0.398	0.413	6.36	0.224	3.64
40	1.93	2.00	0.384	0.398	6.30	0.260	3.83
60	1.88	1.94	0.366	0.378	6.25	0.306	4.04
150	1.87	1.93	0.355	0.367	6.27	0.332	4.14
200	1.88	1.94	0.358	0.370	6.30	0.318	4.09
1140	1.90	1.96	0.348	0.359	6.30	0.339	4.18

* Experiment was conducted at 55°C using 1 gram of magnesium sulfite hexahydrate seed crystals. The initial sodium ion concentration was 0.996 gmole/kg H₂O and the initial sulfate ion concentration was 2.17 gmole/kg H₂O. The density of the liquid was 1.260 g/ml.

** The moles solids precipitated were calculated from the number of moles of sulfite leaving solution.

*** $\psi = \frac{\text{total moles of solids}}{\text{initial moles of seed crystals}}$

TABLE 4-3. RESULTS OF MAGNESIUM SULFITE HYDRATE
PRECIPITATION EXPERIMENT NO. 3-4*

Sample Time (Min)	Results of Chemical Analyses of Slurry Liquor at Indicated Sample Time					Moles** Solids Precipitated	ψ ^{***} 1/3
	Mg ⁺⁺		SO ₃ ⁼		pH		
	$\frac{\text{gmole}}{\ell}$	$\frac{\text{gmole}}{\text{kg water}}$	$\frac{\text{gmole}}{\ell}$	$\frac{\text{gmole}}{\text{kg water}}$			
0	2.02	2.07	0.316	0.324	6.4	0	1.00
10	2.02	2.07	0.313	0.321	6.4	0.009	1.43
20	2.02	2.07	0.313	0.321	6.4	0.009	1.43
40	1.98	2.03	0.305	0.312	6.4	0.032	1.98
60	1.87	1.91	0.291	0.297	6.4	0.072	2.53
150	1.84	1.87	0.280	0.285	6.4	0.101	2.82
280	1.80	1.83	0.275	0.280	6.4	0.113	2.92
1260	1.81	1.83	0.216	0.219	6.4	0.271	3.88
1740	1.82	1.84	0.196	0.198	6.4	0.319	4.10
3150	1.86	1.88	0.166	0.168	6.4	0.392	4.38
7000	1.87	1.89	0.161	0.163	6.4	0.397	4.40
8860	1.87	1.89	0.165	0.167	6.4	0.379	4.33

* Experiment was conducted at 55°C using 1 gram of magnesium sulfite trihydrate seed crystals. The initial sodium ion concentration was 0.648 gmole/kg H₂O and the initial sulfate ion concentration was 2.10 gmole/kg H₂O. The density of the liquid was 1.260 g/ml.

** The moles solids precipitated were calculated from the number of moles of sulfite leaving solution.

*** $\psi = \frac{\text{total moles of solids}}{\text{initial moles of seed crystals}}$

TABLE 4-4. RESULTS OF MAGNESIUM SULFITE HYDRATE
PRECIPITATION EXPERIMENT NO. 3-5*

Sample Time (Min)	Results of Chemical Analyses of Slurry Liquor at Indicated Sample Time					Moles** Solids Precipitated	ψ ^{***} 173
	Mg ⁺⁺		SO ₃ ⁼		pH		
	$\frac{\text{gmole}}{\text{l}}$	$\frac{\text{gmole}}{\text{kg water}}$	$\frac{\text{gmole}}{\text{l}}$	$\frac{\text{gmole}}{\text{kg water}}$			
0	2.01	2.07	0.367	0.378	6.2	0	1.00
10	2.01	2.07	0.349	0.359	6.2	0.054	2.31
20	1.99	2.05	0.350	0.360	6.2	0.050	2.26
30	1.99	2.05	0.349	0.359	6.2	0.052	2.29
40	1.97	2.03	0.347	0.357	6.2	0.057	2.36
60	1.99	2.05	0.351	0.361	6.2	0.045	2.19
80	1.99	2.05	0.346	0.356	6.2	0.058	2.36
100	1.90	1.95	0.327	0.335	6.2	0.108	2.88
120	1.97	2.02	0.342	0.352	6.2	0.066	2.47
150	1.92	1.97	0.332	0.341	6.2	0.092	2.73
180	1.91	1.96	0.340	0.349	6.2	0.069	2.50
270	2.00	2.06	0.344	0.354	6.2	0.058	2.36
330	1.93	1.98	0.324	0.332	6.2	0.106	2.86
390	1.93	1.98	0.324	0.332	6.2	0.103	2.84
470	1.98	2.03	0.330	0.339	6.2	0.087	2.69
1400	1.86	1.89	0.246	0.250	6.2	0.277	3.91
3200	1.83	1.85	0.180	0.182	6.2	0.417	4.47

* Experiment was conducted at 55°C using 1 gram of magnesium sulfite hexahydrate seed crystals. The initial sodium ion concentration was 0.756 gmole/kg H₂O and the initial sulfate ion concentration was 2.10 gmole/kg H₂O. The density of the liquid was 1.260 g/ml.

** The moles solids precipitated were calculated from the number of moles of sulfite leaving solution.

*** $\psi = \frac{\text{total moles of solids}}{\text{initial moles of seed crystals}}$

TABLE 4-5. RESULTS OF MAGNESIUM SULFITE HYDRATE
PRECIPITATION EXPERIMENT NO. 3-6*

Sample Time (Min)	Results of Chemical Analyses of Slurry Liquor at Indicated Sample Time					Moles Solids Precipitated	ψ ^{***} 1/3
	Mg ⁺⁺		SO ₃ ⁼		pH		
	<u>gmole</u> l	<u>gmole</u> kg water	<u>gmole</u> l	<u>gmole</u> kg water			
0	2.01	2.08	0.374	0.386	5.9	0	1.00
10	1.94	2.00	0.364	0.375	5.9	0.030	1.86
20	1.98	2.04	0.375	0.387	5.9	0.001	-
30	1.96	2.02	0.363	0.374	5.9	0.033	1.91
40	1.94	2.00	0.358	0.369	5.9	0.048	2.13
50	1.95	2.01	0.360	0.371	5.9	0.042	2.04
60	2.00	2.06	0.370	0.382	5.9	0.012	1.46
80	1.99	2.05	0.367	0.379	5.9	0.021	1.69
100	1.99	2.05	0.365	0.377	5.9	0.027	1.81
120	1.99	2.05	0.363	0.374	5.9	0.033	1.91
180	1.98	2.04	0.358	0.369	5.9	0.048	2.13
240	1.95	2.01	0.354	0.365	5.9	0.060	2.28
300	1.95	2.01	0.357	0.368	5.9	0.051	2.17
390	1.95	2.01	0.345	0.355	5.9	0.087	2.56
4260	1.90	1.93	0.204	0.207	5.9	0.510	4.54

* Experiment was conducted at 55°C using 0.5g each of magnesium sulfite trihydrate and hexahydrate seed crystals. The initial sodium ion concentration was 0.772 gmole/kg H₂O and the initial sulfate ion concentration was 2.11 gmole/kg H₂O. The density of the liquid was 1.260 g/ml.

** The moles solids precipitated were calculated from the number of moles of sulfite leaving solution.

*** $\psi = \frac{\text{total moles of solids}}{\text{initial moles of seed crystals}}$

TABLE 4-6. RESULTS OF MAGNESIUM SULFITE HYDRATE PRECIPITATION EXPERIMENT NO. 3-7*

Sample Time Time (Min)	Results of Chemical Analyses of Slurry Liquor at Indicated Sample Time						
	Mg ⁺⁺		SO ₃ ⁼		pH		
	<u>gmole</u> ℓ	<u>gmole</u> kg water	<u>gmole</u> ℓ	<u>gmole</u> kg water		Moles ^{**} Solids Precipitated	*** ψ1/3
0	2.03	2.10	0.358	0.370	6.0	0.000	1.00
10	1.88	1.93	0.340	0.349	6.0	0.054	2.21
20	2.00	2.06	0.337	0.347	6.0	0.063	2.32
30	1.94	1.99	0.332	0.341	6.0	0.078	2.47
40	1.91	1.96	0.322	0.330	6.0	0.108	2.74
60	1.89	1.94	0.313	0.321	6.0	0.135	2.94
80	1.93	1.98	0.316	0.324	6.0	0.126	2.88
100	1.93	1.98	0.321	0.330	6.0	0.111	2.76
120	1.87	1.92	0.316	0.324	6.0	0.126	2.88
150	1.93	1.98	0.318	0.326	6.0	0.120	2.83
180	1.96	2.01	0.326	0.335	6.0	0.096	2.64
240	1.99	2.05	0.320	0.329	6.0	0.114	2.79
320	2.00	2.06	0.330	0.340	6.0	0.084	2.53
380	1.91	1.96	0.317	0.325	6.0	0.123	2.86
1400	1.95	1.99	0.272	0.278	6.0	0.258	3.63

* Experiment was conducted at 55°C using 0.5g each of magnesium sulfite trihydrate and hexahydrate seed crystals. The initial sodium ion concentration was 0.740 gmole/kg H₂O and the initial sulfate ion concentration was 2.13 gmole/kg H₂O. The density of the liquid was 1.260 g/ml.

** The moles solids precipitated were calculated from the number of moles of sulfite leaving solution.

*** $\psi = \frac{\text{total moles of solids}}{\text{initial moles of seed crystals}}$

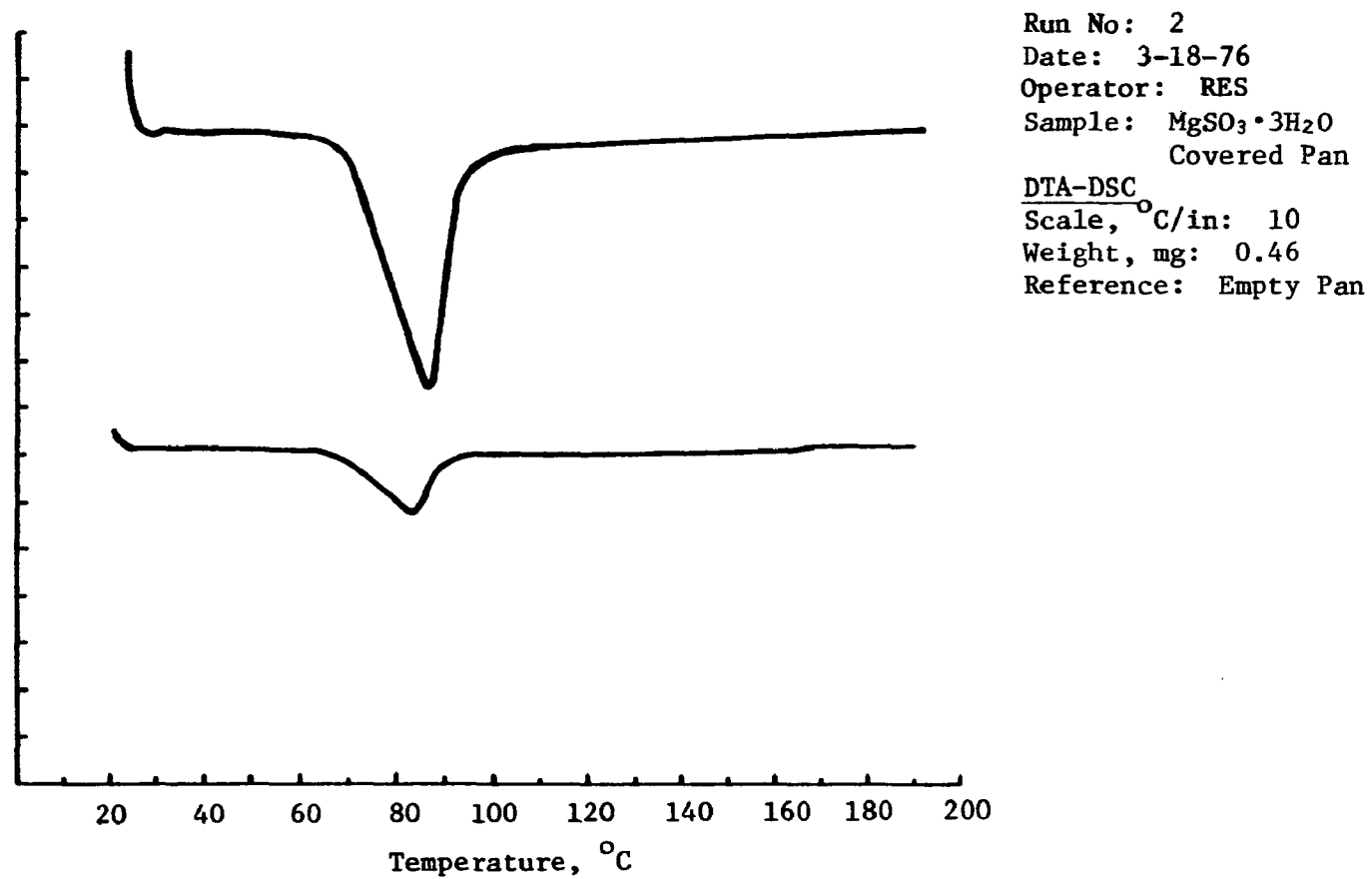
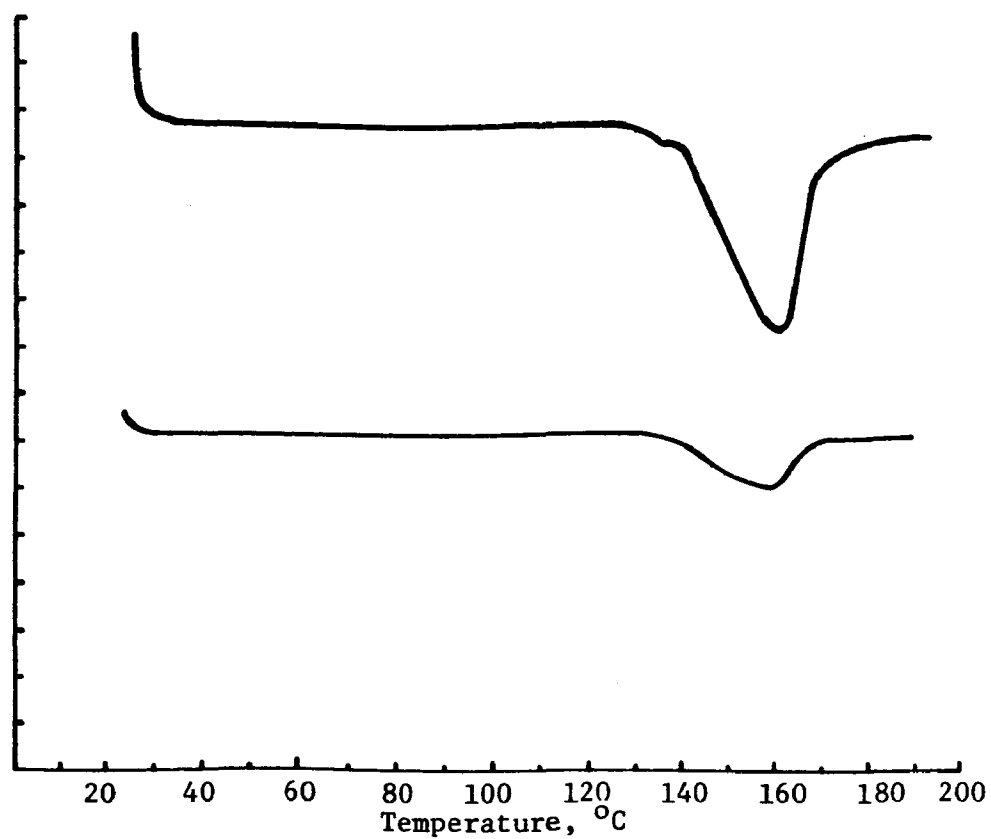


Figure 4-1. Results of DSC Analysis of a Pure Sample of $\text{MgSO}_3 \cdot 3\text{H}_2\text{O}$



Run No: 3
Date: 3-18-76
Operator: RES
Sample: $\text{MgSO}_3 \cdot 3\text{H}_2\text{O}$
Covered Pan
Flow Rate: Start 27°C
DTA-DSC
Scale, °C/in: 10
Weight, mg: 0.83
Reference: Empty Pan

Figure 4-2. Results of DSC Analysis of a Pure Sample of $\text{MgSO}_3 \cdot 3\text{H}_2\text{O}$

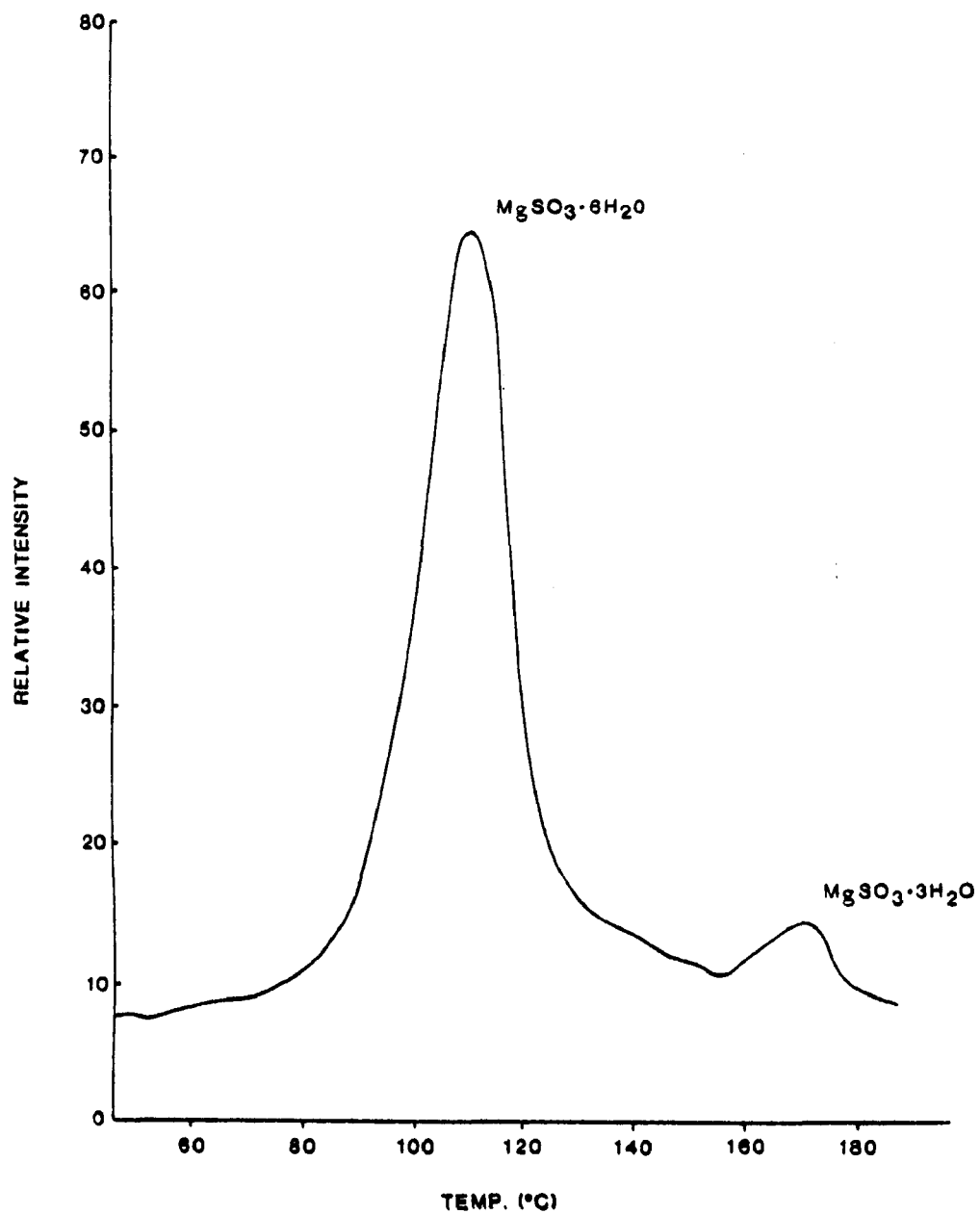


Figure 4-3. Results of DSC Analysis of Solids Precipitated After 470 Minutes in Experiment No. 3-5.

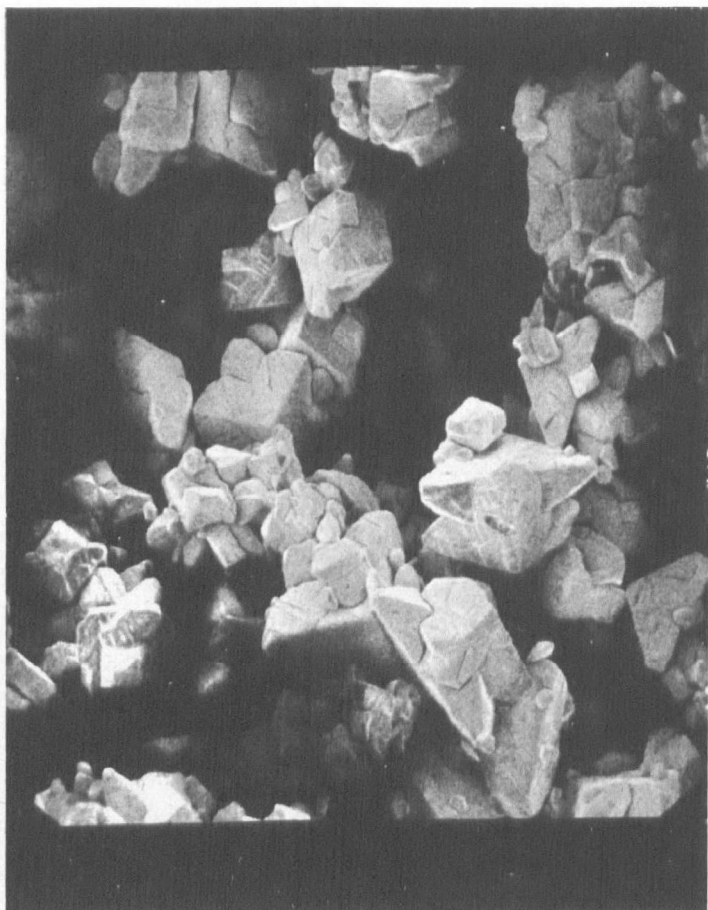


FIGURE 4-4.
ELECTRON MICROGRAPH 300X
OF $\text{MgSO}_3 \cdot 6\text{H}_2\text{O}$ CRYSTALS (RHOMBIC)
NUCLEATED AT 28°C

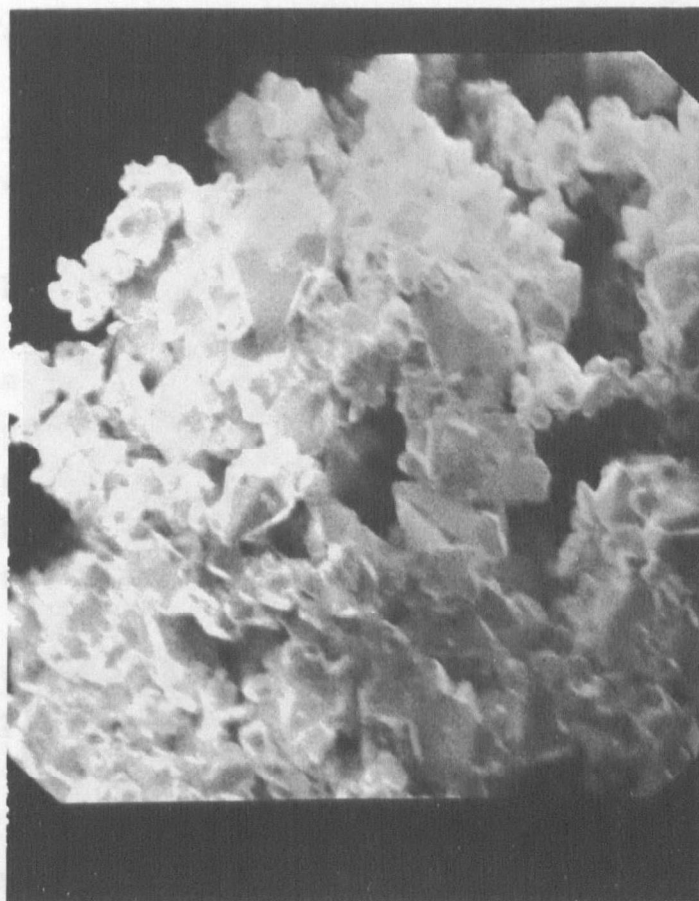


FIGURE 4-5.
ELECTRON MICROGRAPH 1000X OF
 $\text{MgSO}_3 \cdot 3\text{H}_2\text{O}$ CRYSTALS NUCLEATED
AND GROWN OVERNIGHT AT 65°C

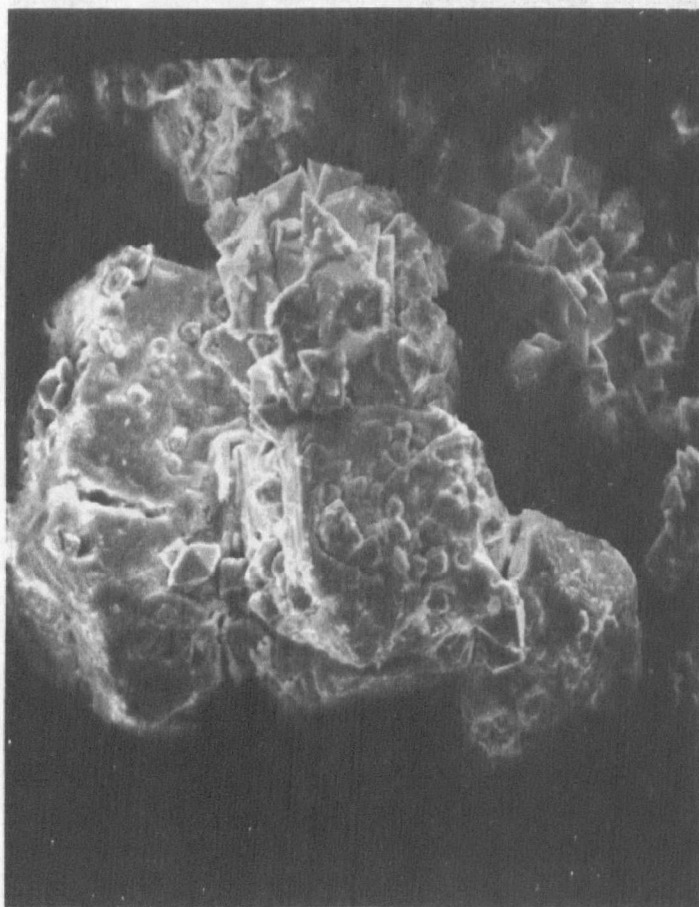


FIGURE 4-6.
ELECTRON MICROGRAPH (1000X)
FROM R3-5 AT T= 470 MINS
TRI CRYSTALS GROWING ON
LARGER HEXA CRYSTALS.

DSC scans for solid samples obtained during the experiments described in Tables 4-1 through 4-6 are included in the appendix. These analyses, and the results of microscopic analyses, were used for qualitative identification of the solids produced during each precipitation experiment.

The precipitation rate data from each experiment are plotted in the form $\psi^{1/3}$ versus θ in Figures 4-7 through 4-12. These figures also indicate the composition of the solid products. The approximate fraction of trihydrate present at each sample point is shown at the top of the graphs. Observations and comments about what occurred during each experiment are summarized in the following paragraphs.

Experiment 3-2, Trihydrate Seed Crystals

(Table 4-1, Figure 4-7, Figures A-1 and A-2)

The solid products from this experiment consisted solely of the trihydrate. At the experimental conditions of 0.316 gmole/l initial sulfite concentration and trihydrate seed crystals it is apparent that nucleation of the hexahydrate did not occur. Primary nucleation of hexahydrate was observed at 55°C in 20 wt % MgSO_4 solutions at a sulfite concentration of about 0.55 gmole/kg H_2O . In secondary nucleation experiments with trihydrate seed crystals at 55°C hexahydrate nucleation was not observed.

The trihydrate exhibited a constant precipitation rate. Since a dramatic increase in the initial crystal growth rate was not observed it appears as if secondary trihydrate nucleation did not occur. This observation is consistent with the results of secondary nucleation experiments reported in Technical Note 200-045-54-05.

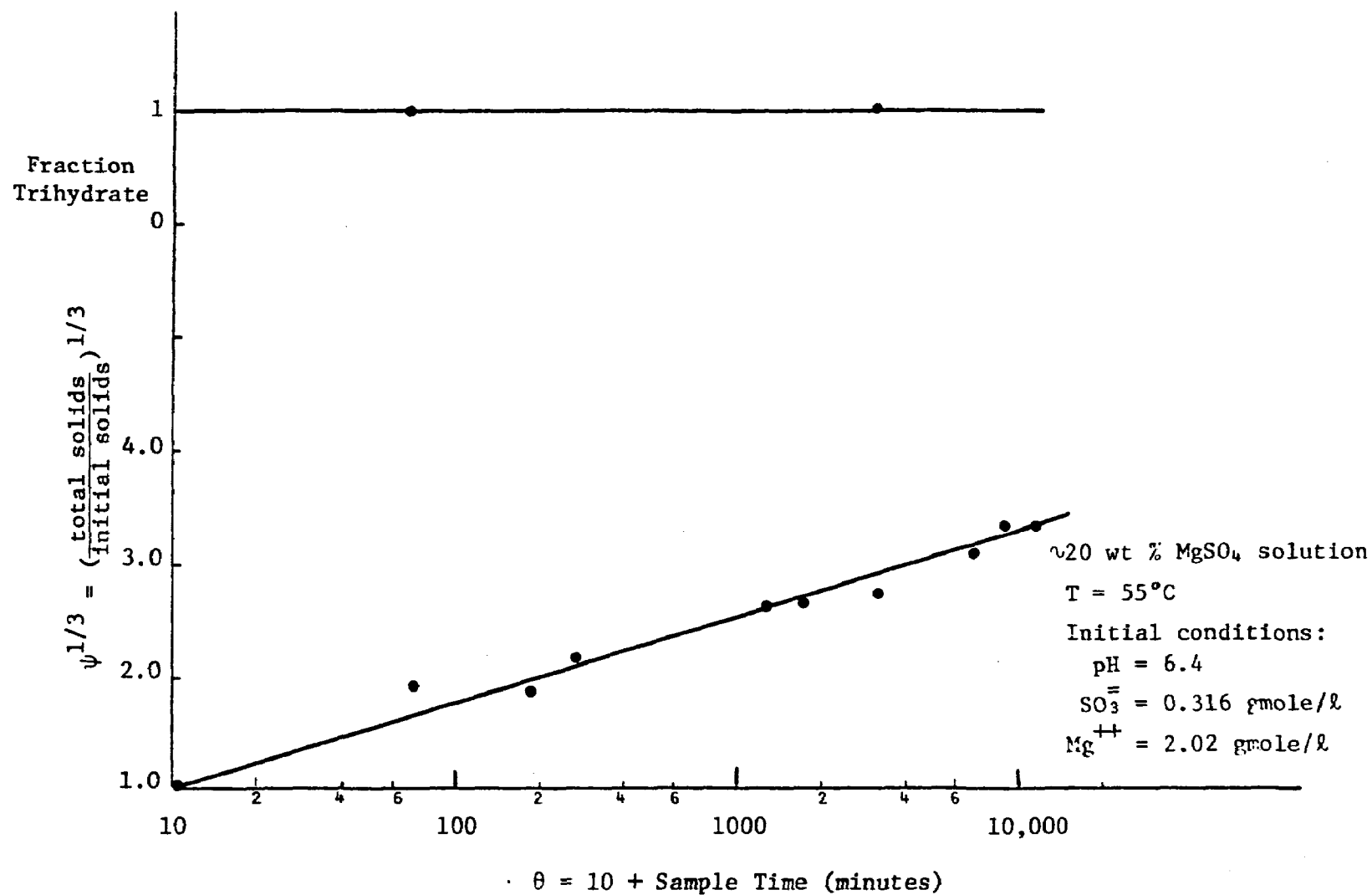


Figure 4-7. Results of MgSO_3 Hydrate Precipitation Rate Experiment 3-2 Employing Trihydrate Seed Crystals

Experiment 3-3, Hexahydrate Seed Crystals

(Table 4-2, Figure 4-8, Figures A-3 through A-7)

A high initial sulfite concentration of 0.475 gmole/l was employed in this experiment. Hexahydrate nucleation was observed visually in the first 20 minutes. These results occurred at approximately the same solution conditions as those reported in previous secondary nucleation experiments at 59.2°C. (Technical Note 2-0-045-54-05). In addition, the graph of $\psi^{1/3}$ vs. θ in Figure 4-8 shows an initial high rate of solids growth which is consistent with the observation of nucleation. The results of DSC analysis indicated the product was pure hexahydrate at the end of 200 minutes. Formation of trihydrate crystals was not observed.

Experiment 3-4, Trihydrate Seed Crystals

(Table 4-3, Figure 4-9, Figures A-8 and A-9)

This test was done under the same conditions as experiment 3-2. Again the products consisted solely of the trihydrate and a relatively constant growth rate occurred. The precipitation rate was faster than that in Run 3-2, although the same initial sulfite concentration was employed and the driving forces should be the same in the two experiments. The faster growth rate could be the result of seed crystal surface area effects. Smaller seed crystals provide a larger surface area per volume. The seed crystal preparation method employed could have resulted in some variations in crystal size.

It is apparent from Figure 4-9 that the system approached equilibrium at about 10,000 minutes.

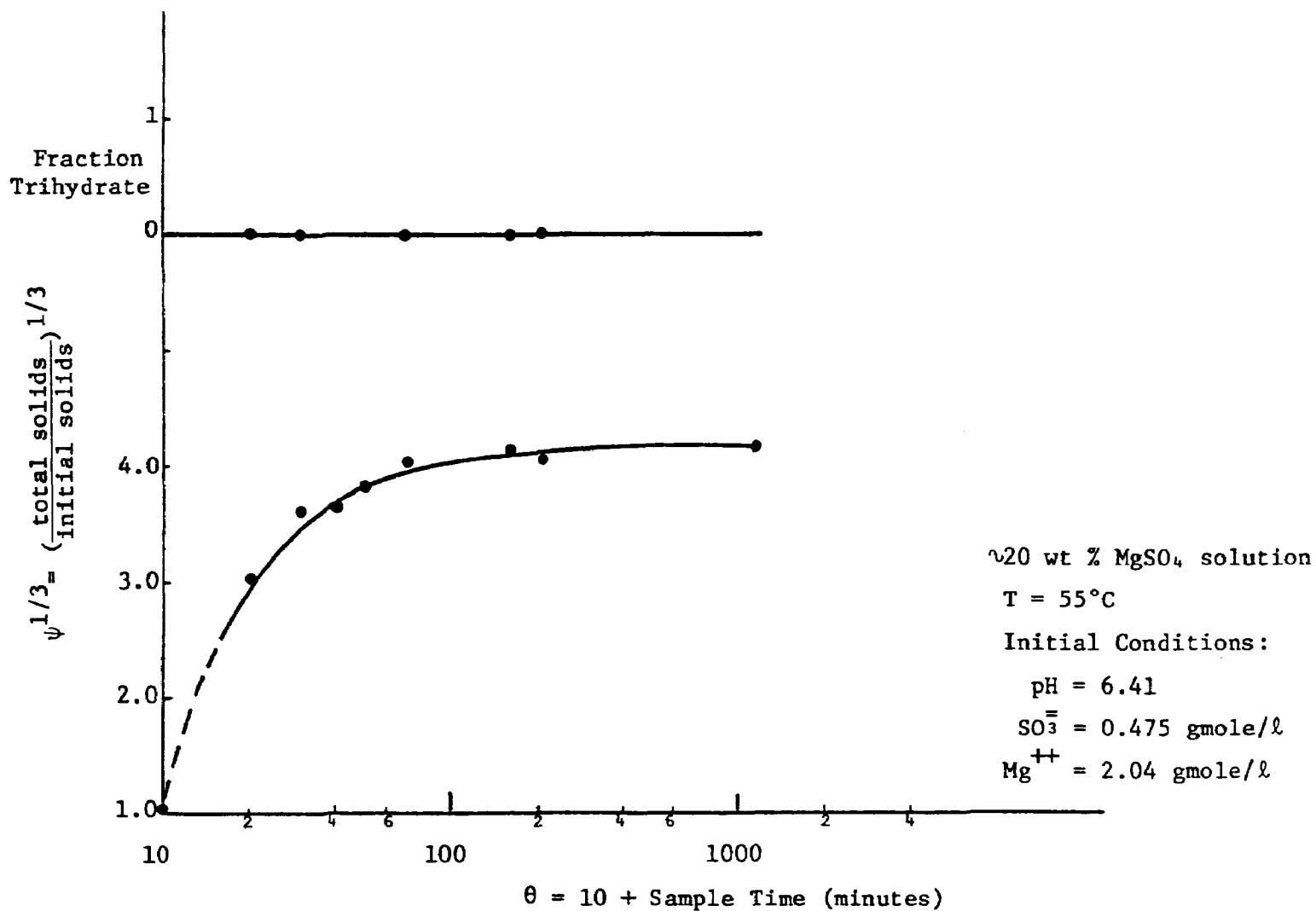


Figure 4-8. Results of MgSO_3 Hydrate Precipitation Rate
Experiment 3-3 Employing Hexahydrate Seed Crystals

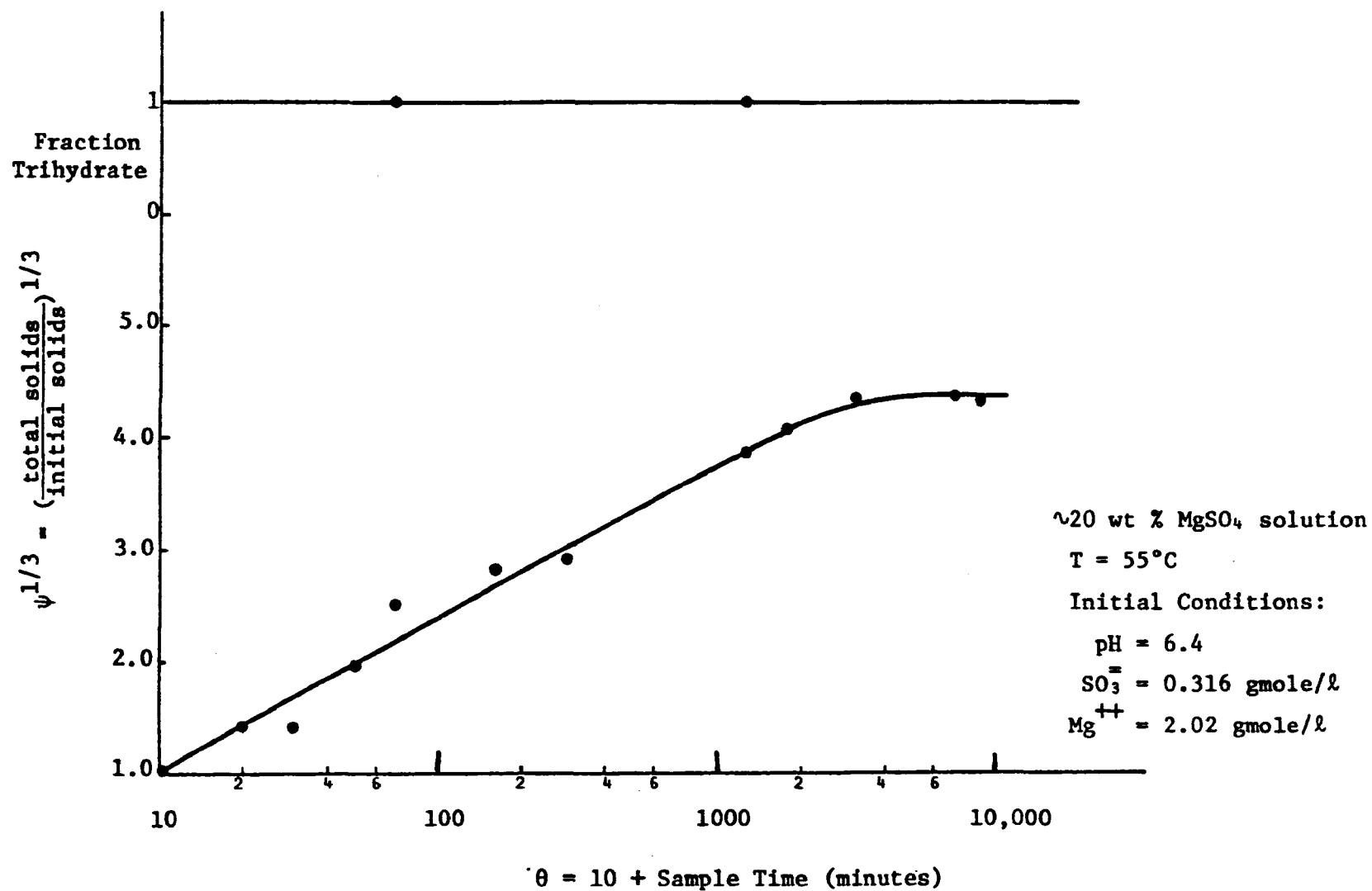


Figure 4-9. Results of MgSO_3 Hydrate Precipitation Rate
 Experiment 3-4 Employing Trihydrate Seed Crystals

Experiment 3-5, Hexahydrate Seed Crystals

(Table 4-4, Figure 4-10, Figures A-10 through A-21)

This experiment employed a lower initial sulfite concentration than experiment 3-3, which also employed hexahydrate seed crystals. Hexahydrate nucleation was not apparent from visual observations, and it is not clearly indicated in Figure 4-10.

The results of DSC analyses of solid samples indicated initial formation of the hexahydrate followed by complete conversion to the trihydrate. In the first part of the run, an increase in total solids occurred which is attributed to the precipitation of hexahydrate. This is confirmed by DSC analyses which show almost pure hexahydrate up to about 300 minutes. It is probable that at the end of 100 minutes the solution is saturated with respect to hexahydrate precipitation. In the intermediate period up to 500 minutes the amount of solids present changes relatively little while the fraction of trihydrate is increasing. These results indicate that the hexahydrate is dissolving and the trihydrate is precipitating. After about 400 minutes an increase in the fraction of trihydrate occurs. The trihydrate precipitation rate is initially slow because there is very little trihydrate crystal surface area available. As the trihydrate surface area increases, an increase in the rate of trihydrate precipitation is observed. This increase is apparent after 400 minutes in Figure 4-10.

Trihydrate crystals could have occurred as a result of nucleation, since the solution was supersaturated with respect to trihydrate for some period of time. However, clear evidence of secondary trihydrate nucleation has not been obtained in previous experiments. It is also possible that the occurrence

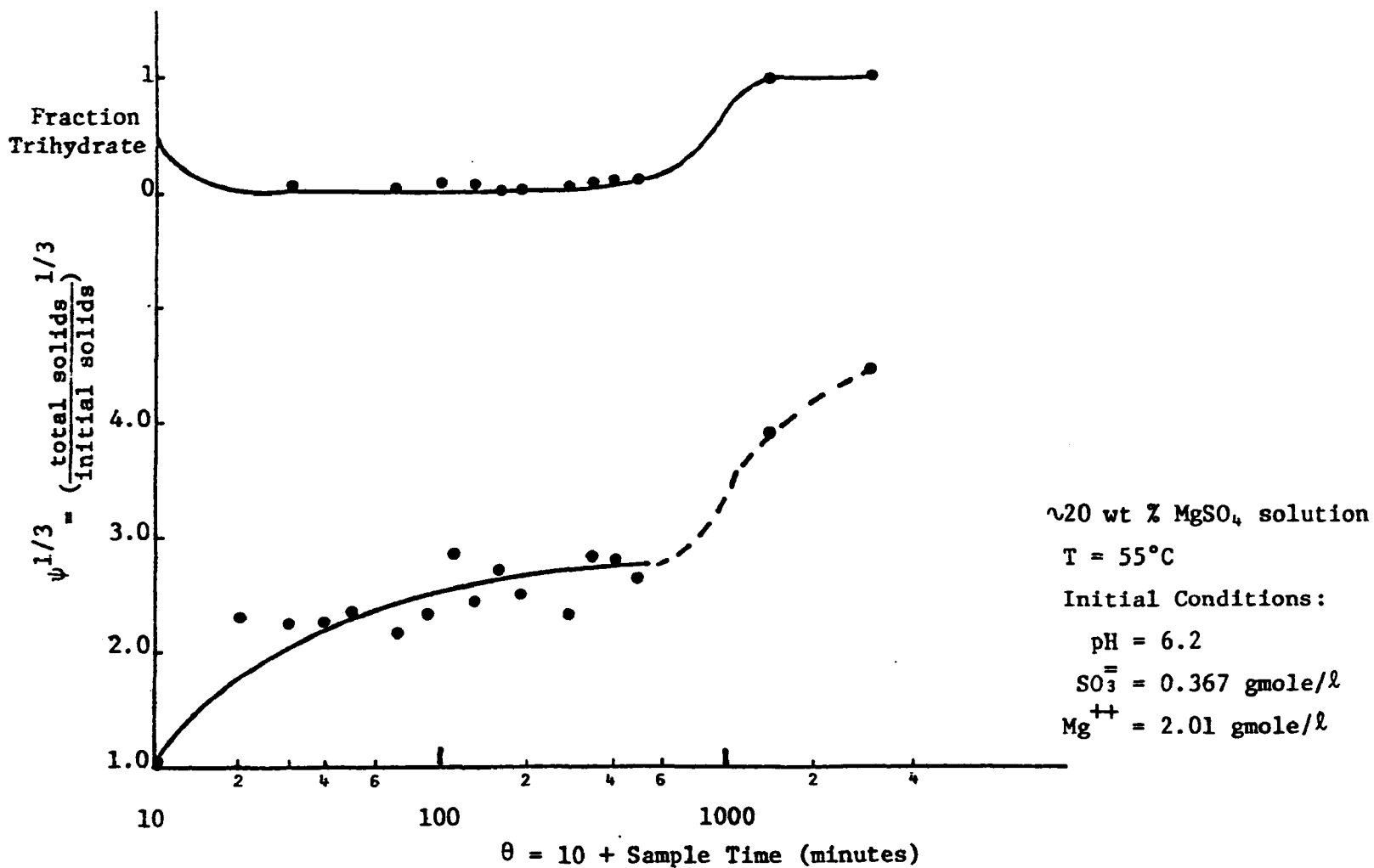


Figure 4-10. Results of MgSO_3 Hydrate Precipitation Rate
Experiment 3-5 Employing Hexahydrate
Seed Crystals

of trihydrate crystals can be attributed to seed crystal characteristics. Growth of trihydrate crystals on the surface of hexahydrate crystals was observed as was shown in Figure 4-6. Crystal surface imprefections or the presence of small amounts of trihydrate seeds could account for initiation of trihydrate precipitation. DSC scans of samples taken very early in the test showed very small amounts of trihydrate crystals. It is not clear from the experimental results what initiated the formation of trihydrate crystals in tests employing hexahydrate seed crystals.

Experiment 3-6, Mixed Tri- and Hexahydrate Seed Crystals
(Table 4-5, Figure 4-11, Figures A-22 through A-28)

The results of this mixed seed crystal test at an initial sulfite concentration of 0.374 gmole/l can be explained on the same basis as those of experiment 3-5. Again, immediate precipitation of the hexahydrate followed by hexahydrate dissolution and trihydrate precipitation were observed. At the end of 4000 minutes all the hexahydrate had dissolved and the solid product was pure trihydrate.

Experiment 3-7, Mixed Tri- and Hexahydrate Seed Crystals
(Table 4-6, Figure 4-12, Figures A-29 through A-36)

This experiment was done under the same conditions as experiment 3-6, except the initial sulfite and magnesium concentrations were slightly different. The same qualitative results were observed, but the initial rate of solids production was higher. The difference in precipitation rate can be attributed to either seed crystal surface area effects or a difference in driving force terms.

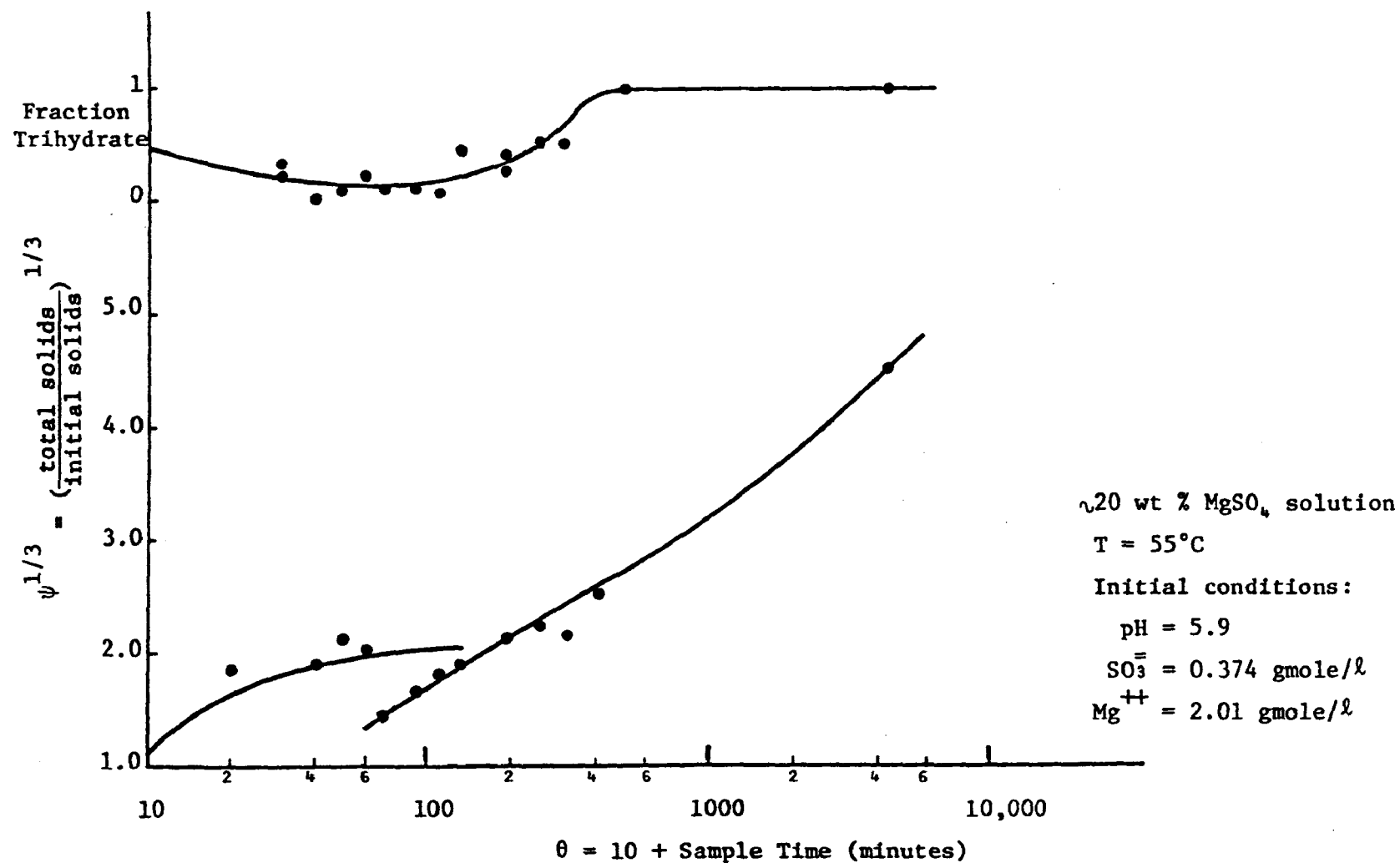


Figure 4-11. Results of MgSO_3 Hydrate Precipitation Rate: Experiment 3-6 Employing a Mixture of Tri- and Hexahydrate Seed Crystals

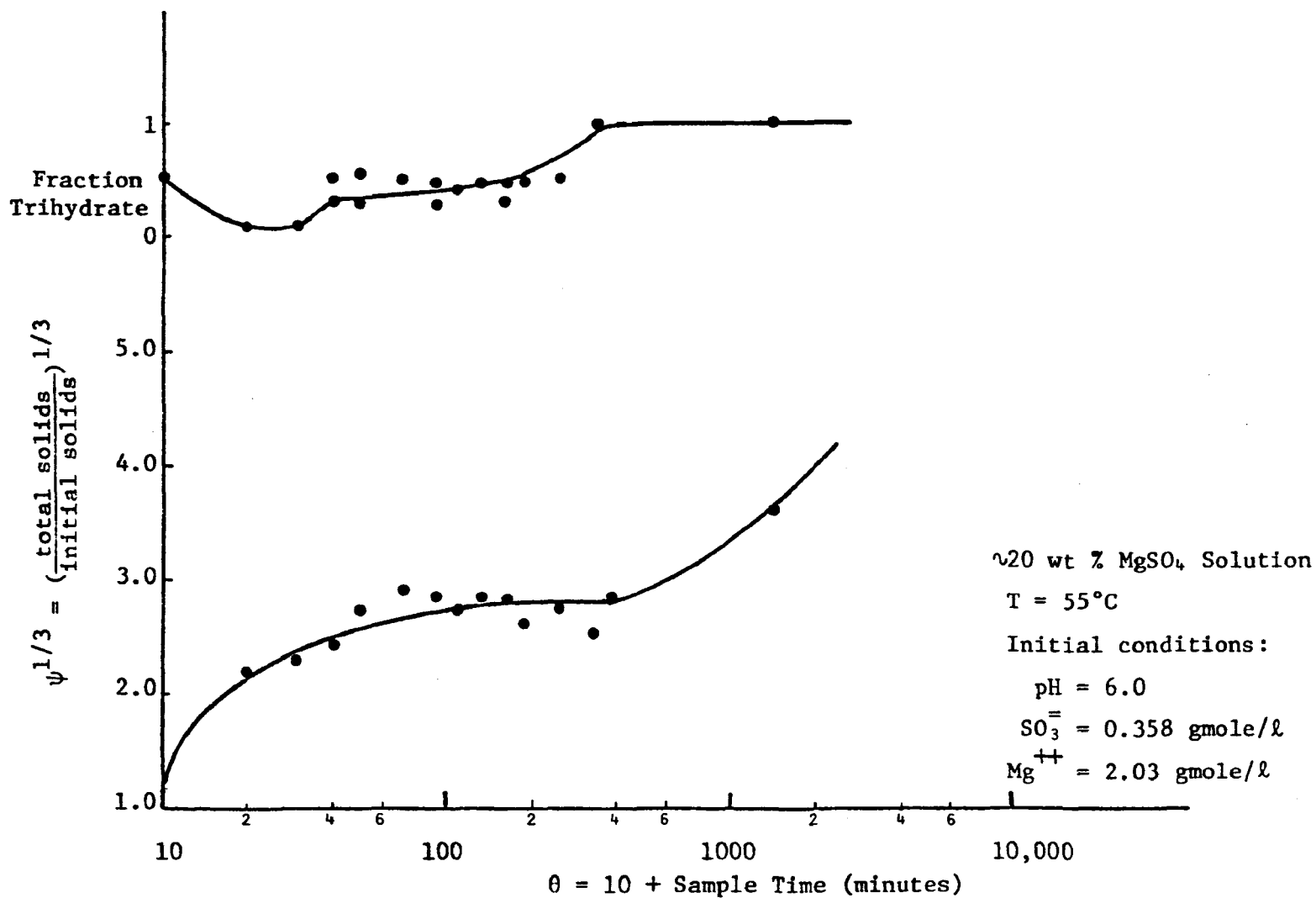


Figure 4-12. Results of MgSO_3 Hydrate Precipitation Rate Experiment 3-7 Employing a Mixture of Tri- and Hexahydrate Seed Crystals

SECTION 5

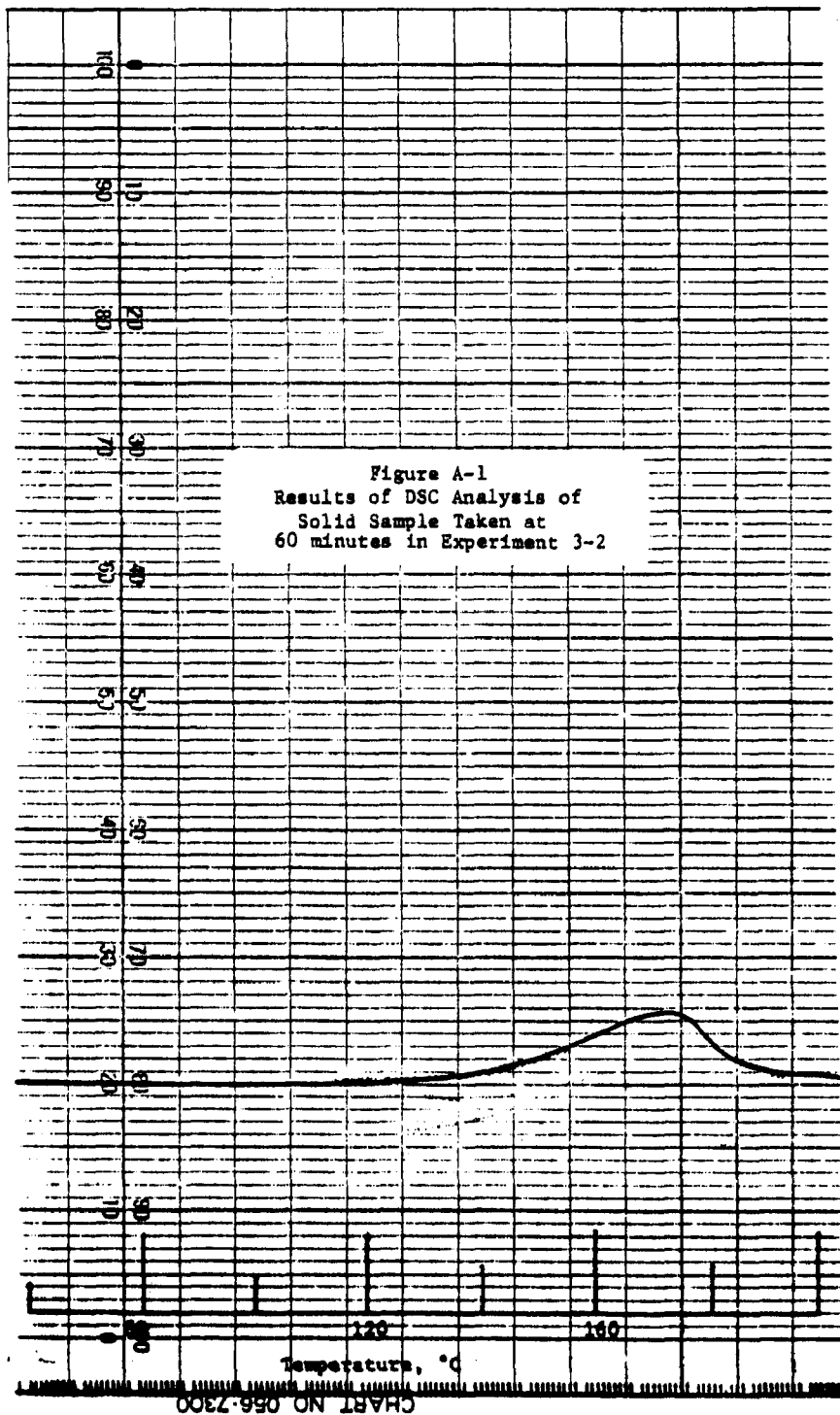
CONCLUSIONS

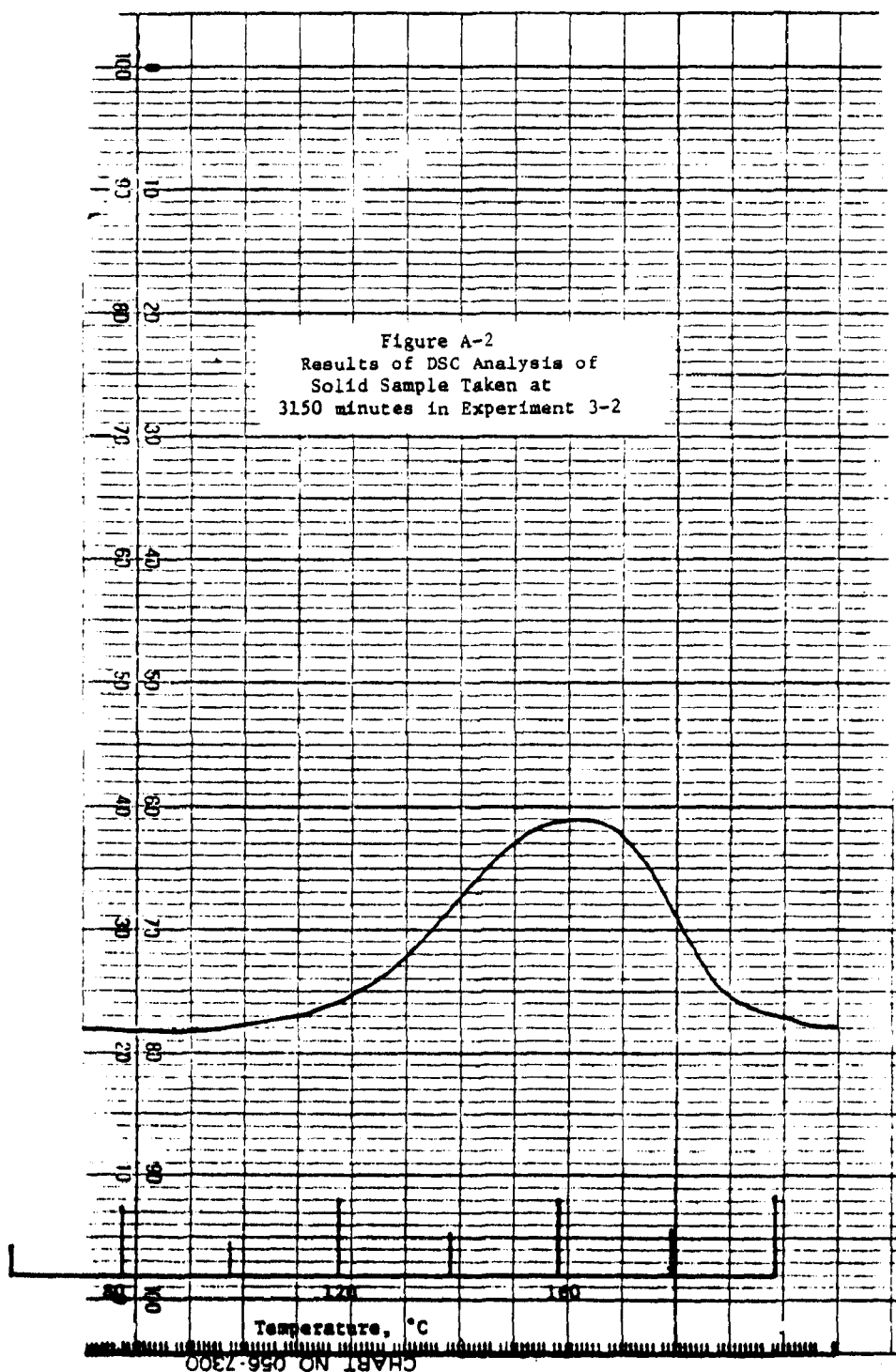
The results of these precipitation rate studies provide an accurate qualitative explanation of what occurs during MgSO_3 hydrate precipitation under conditions characteristic of the magnesium oxide wet scrubbing process. Data are available for obtaining a quantitative rate correlation; however, some refinement of computational tools will be required in order to calculate accurate driving force terms.

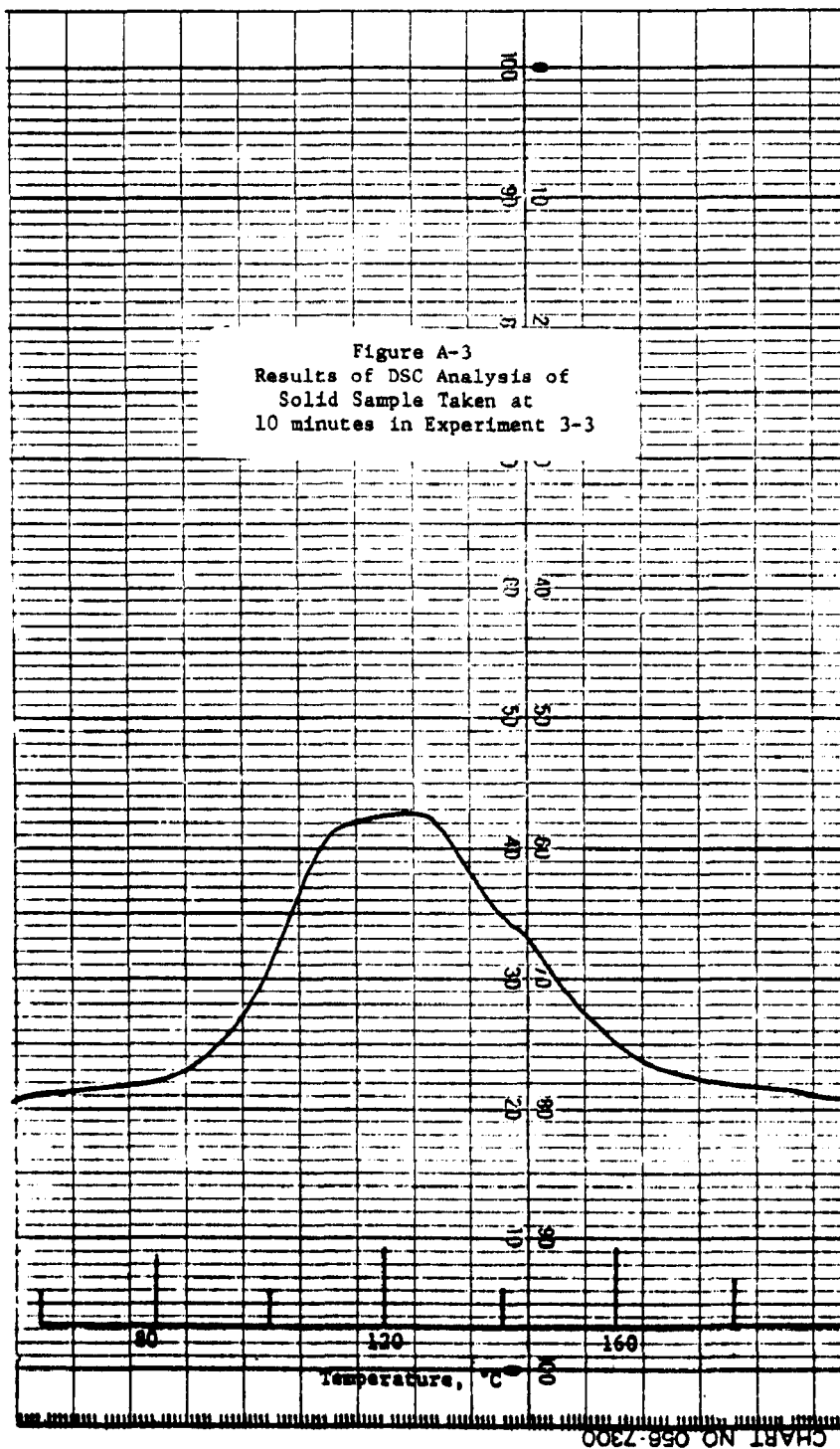
The results for mixed hydrate precipitation in scrubber-like media are consistent with those for precipitation of individual hydrates in dilute solutions and with tests of primary and secondary nucleation in scrubber-like media. Hexahydrate nucleation and precipitation rates are faster than those of the trihydrate. The trihydrate is the thermodynamically stable form. Clear evidence of trihydrate nucleation is not apparent. These results provide an adequate basis for the design of a system to produce either hydrate as a solid product.

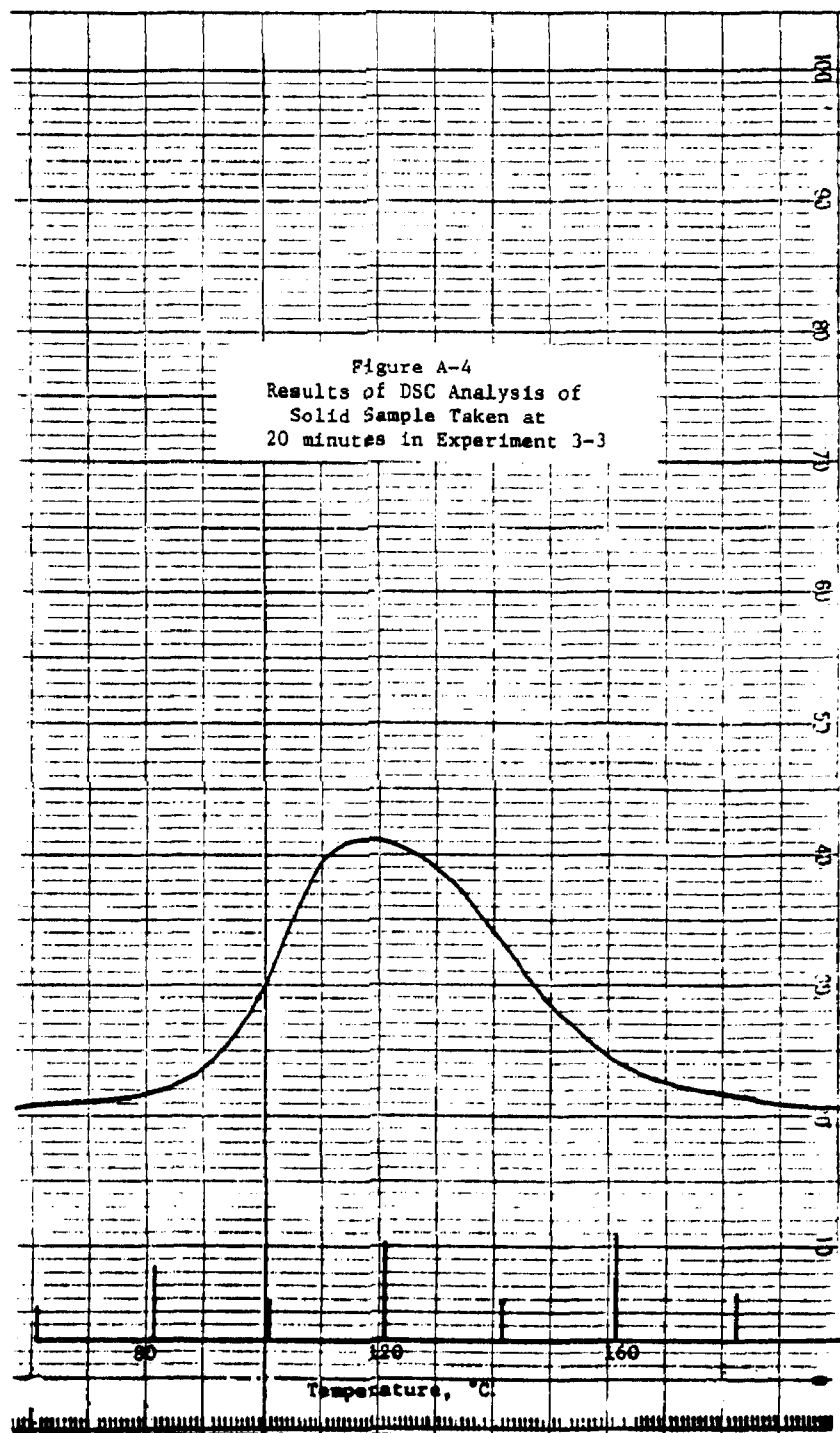
APPENDIX A
TO TECHNICAL NOTE
200-045-54-03a
FIGURES A-1 THROUGH A-36

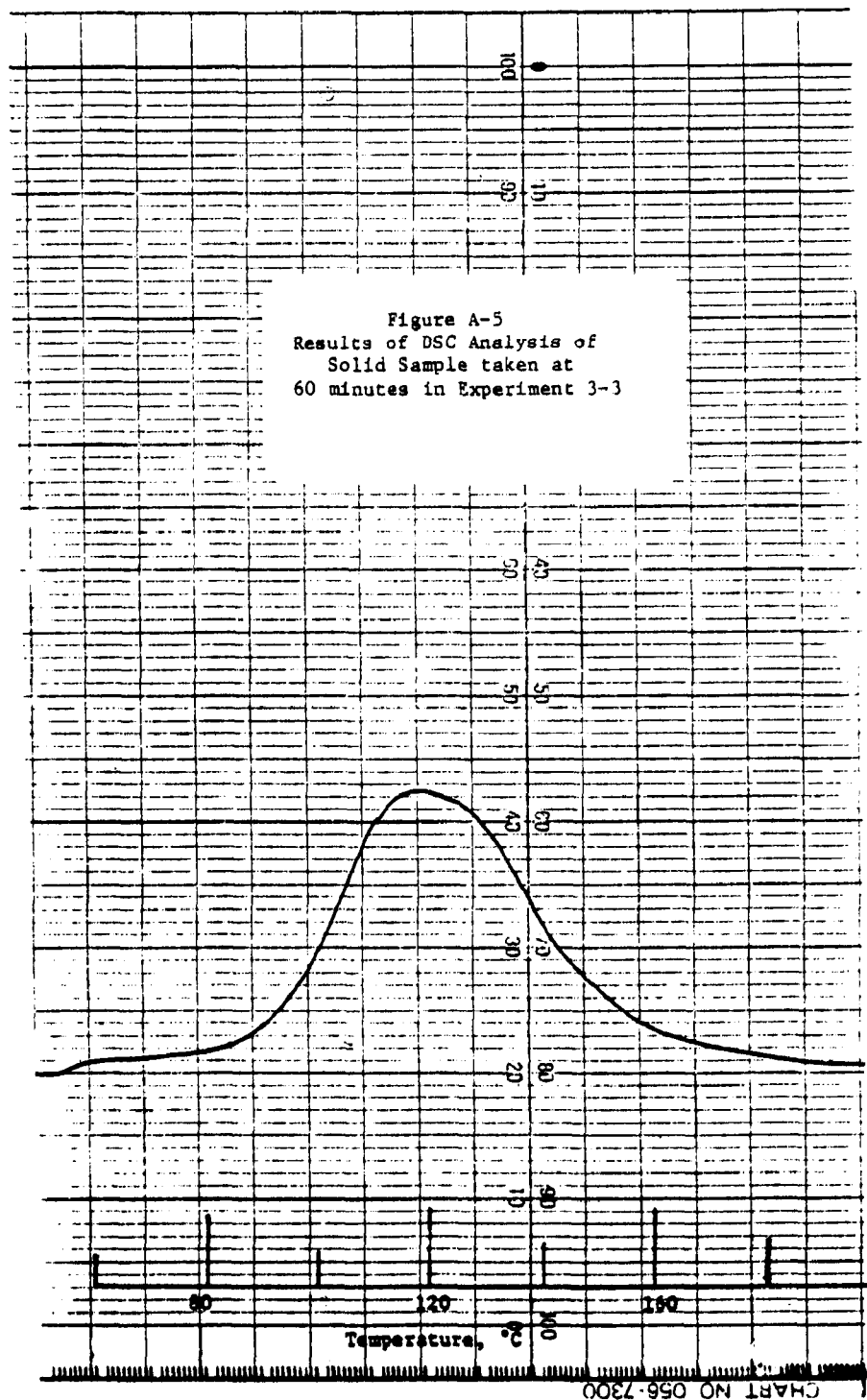
RESULTS OF DSC ANALYSIS OF
SOLID SAMPLES FROM PRECIPITATION
RATE EXPERIMENTS IN SCRUBBER-LIKE MEDIA

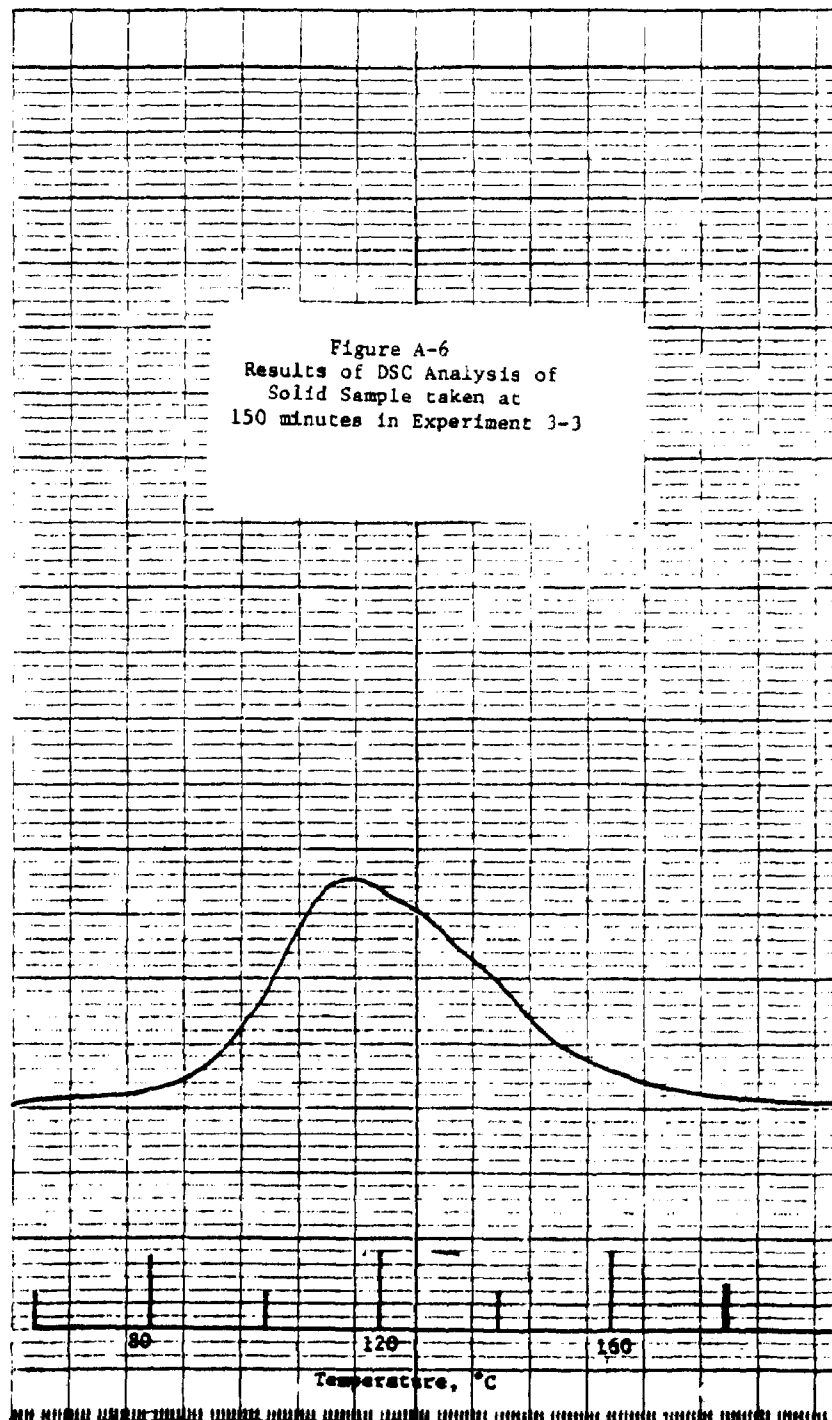












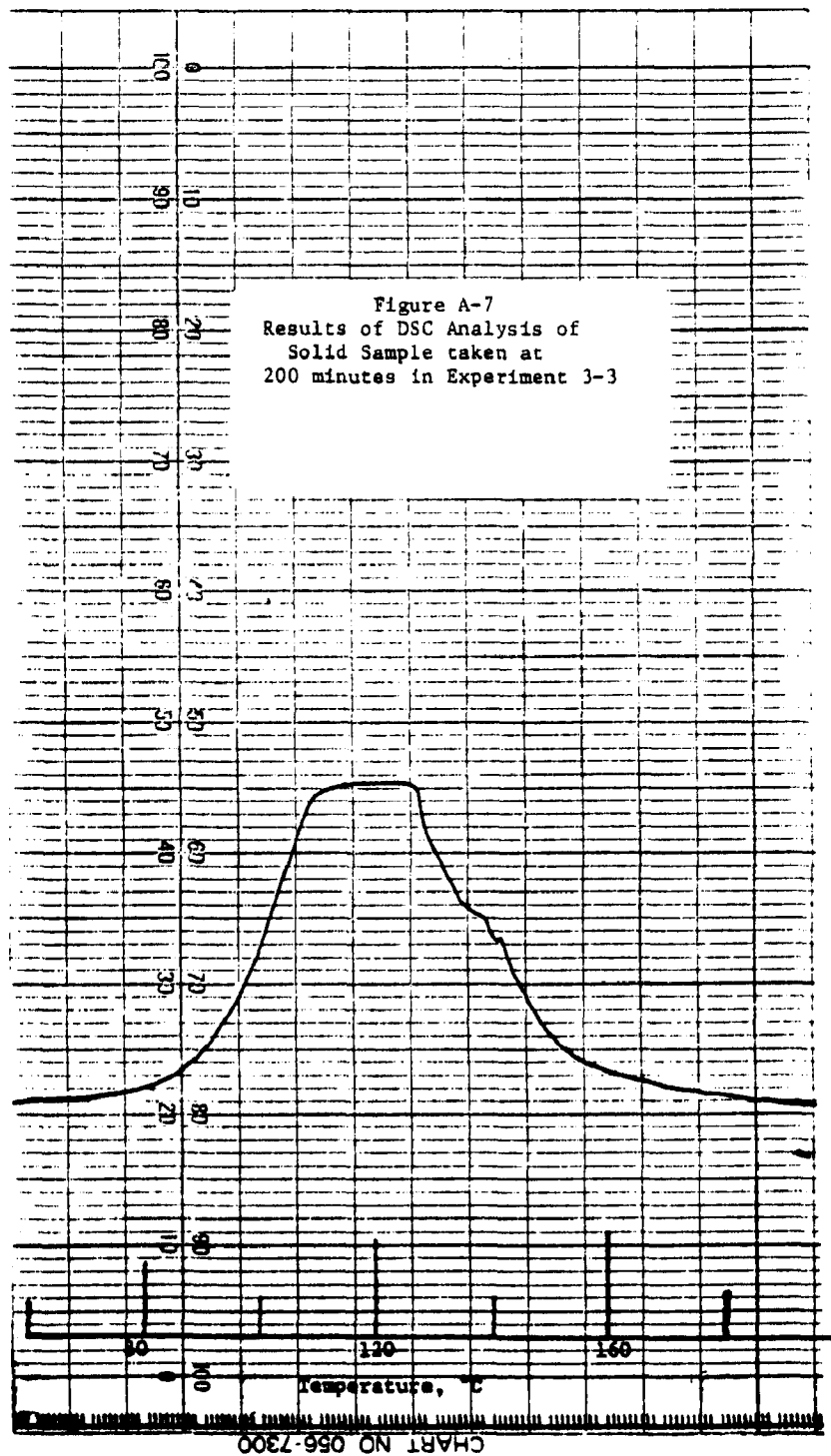


Figure A-8
Results of DSC Analysis of
Solid Sample taken at
60 minutes in Experiment 3-4

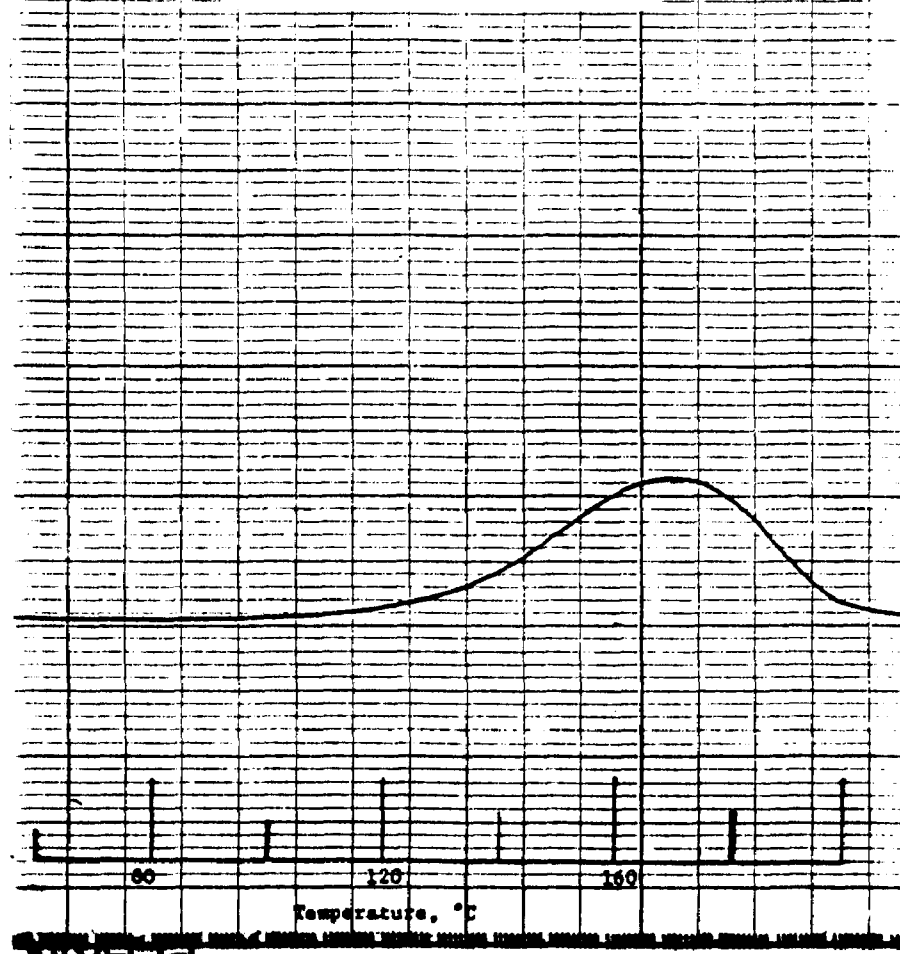


Figure A-9
Results of DSC Analysis of
Solid Sample taken at
1260 minutes in Experiment 3-4

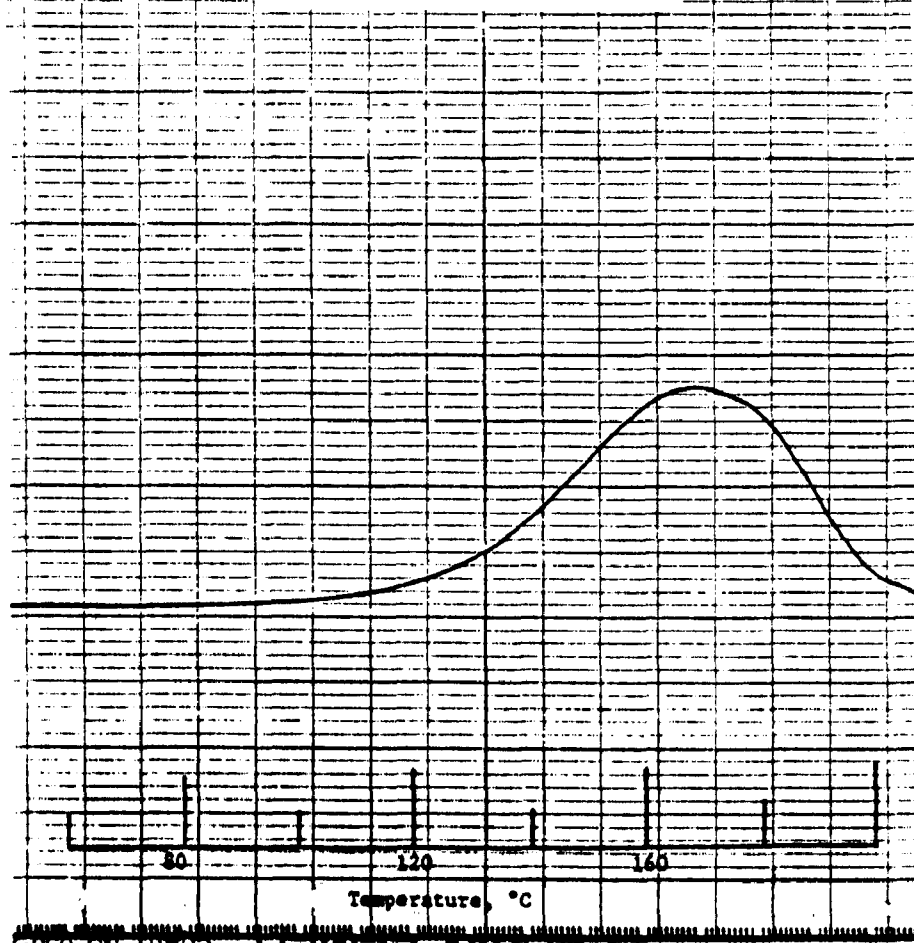
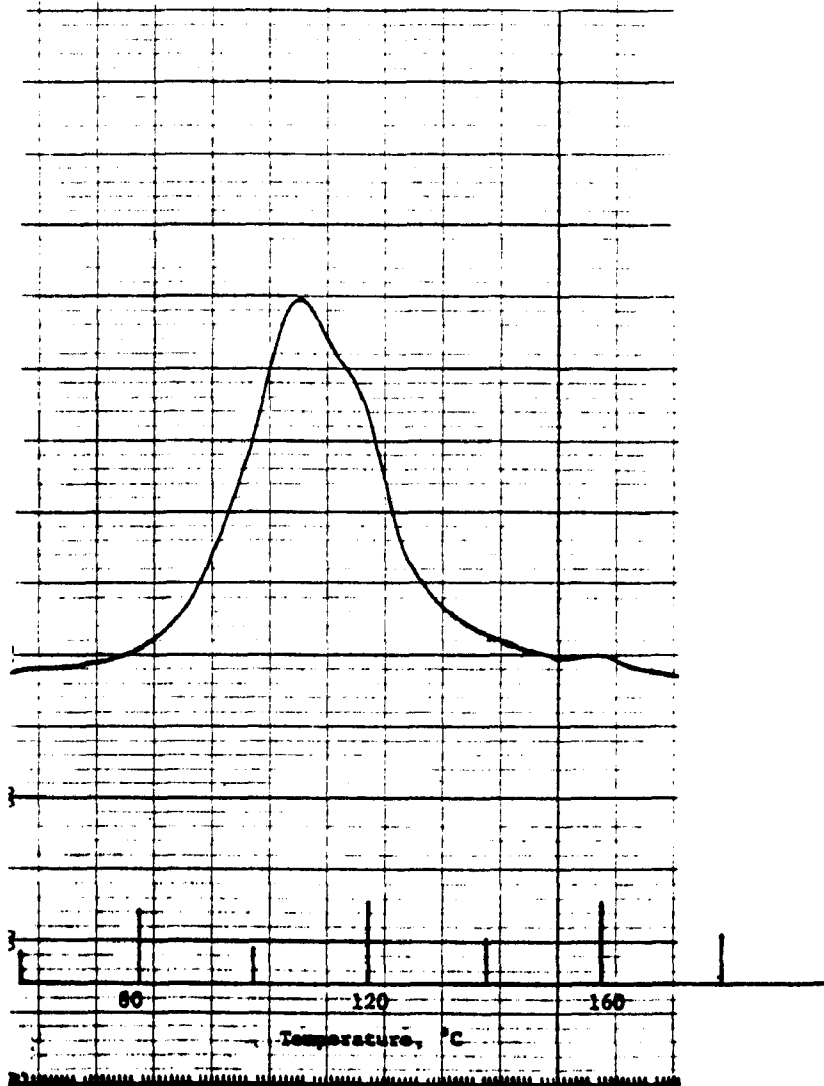


Figure A-10
Results of DSC Analysis of
Solid Sample taken at
20 minutes in Experiment 3-5



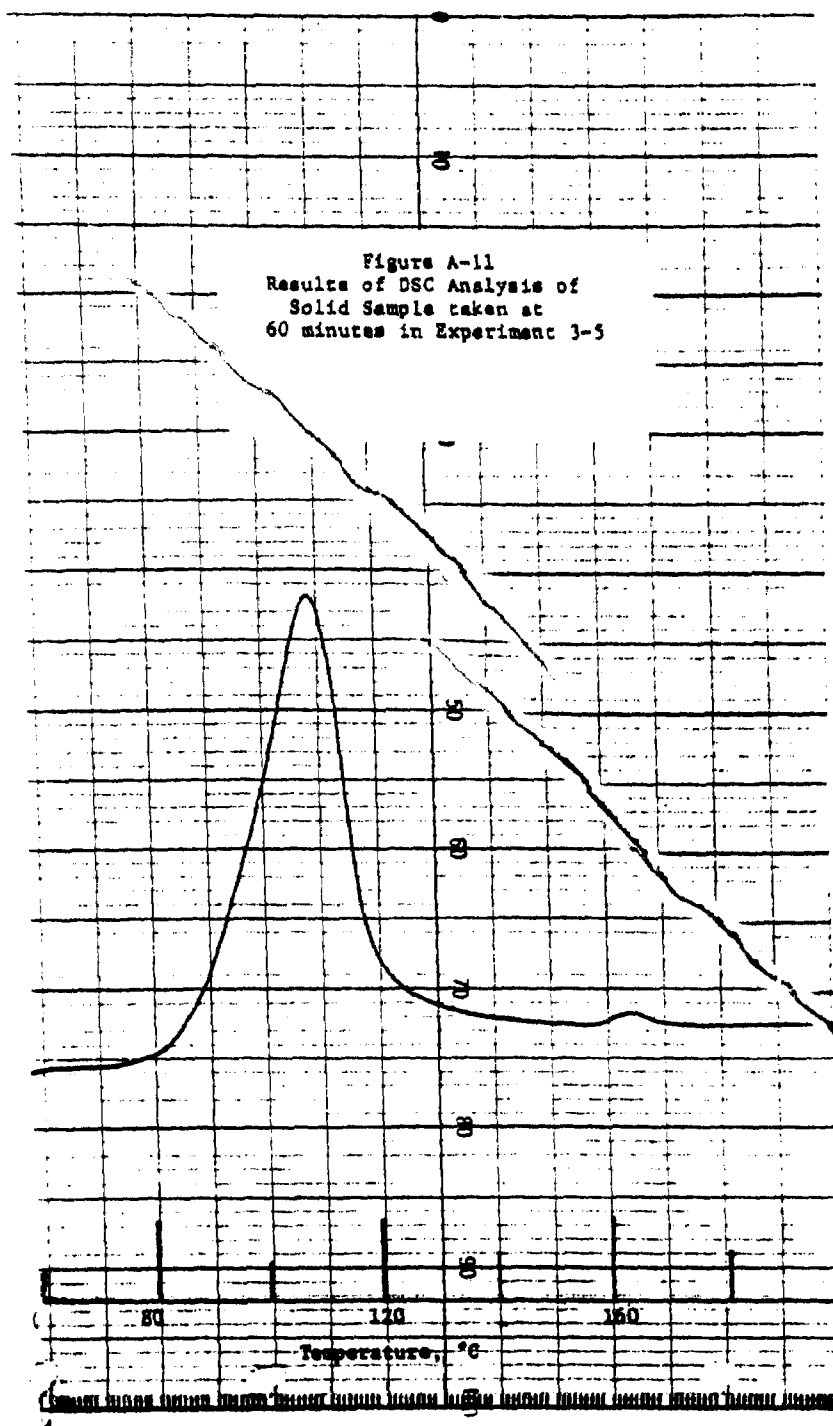


Figure A-12
Results of DSC Analysis of
Solid Sample taken at
100 minutes in Experiment 3-5

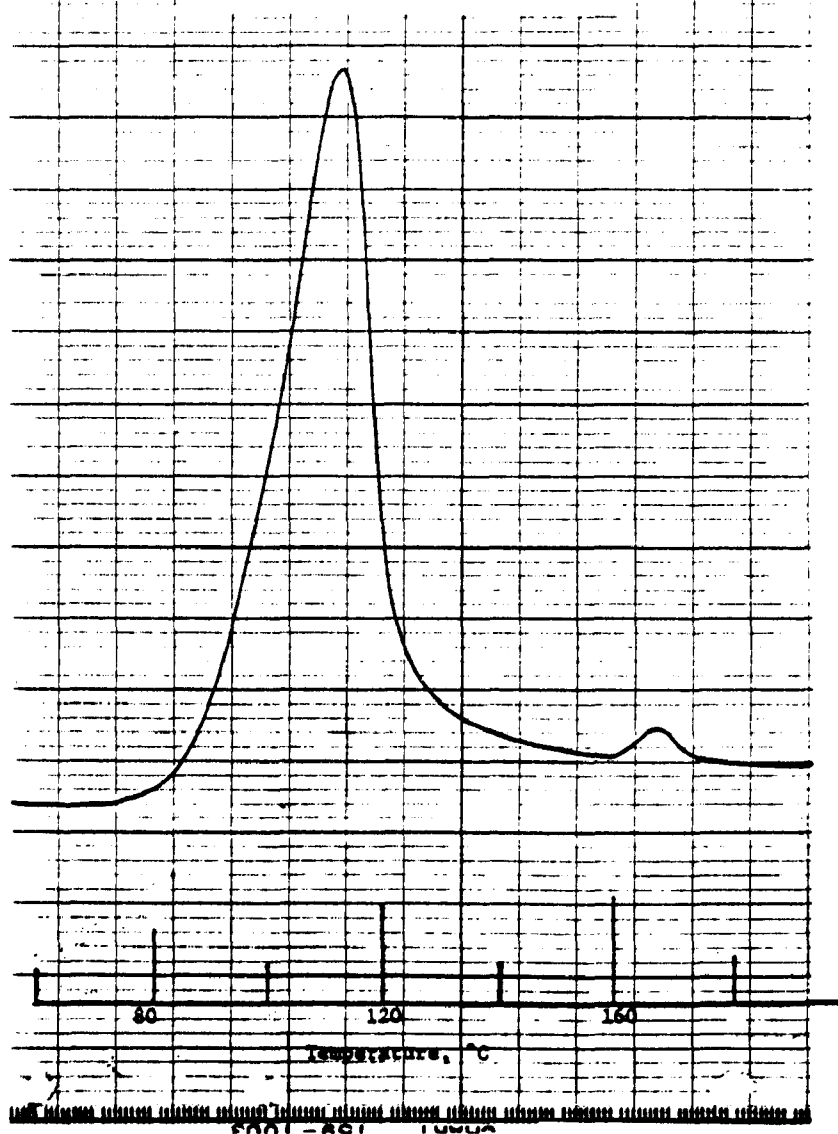


Figure A-13
Results of DSC Analysis of
Solid Sample taken at
120 minutes in Experiment 3-5

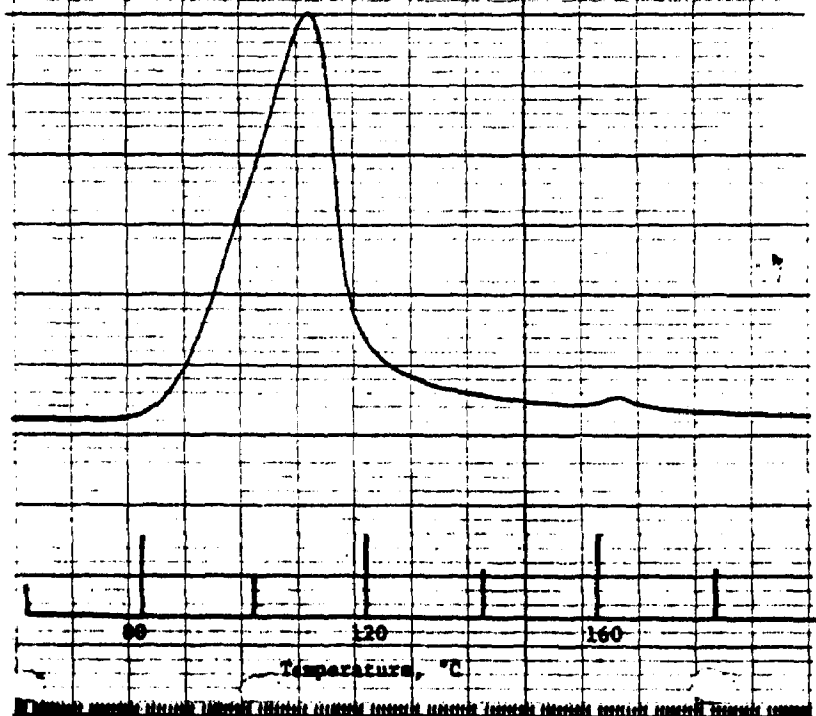


Figure A-14
Results of DSC Analysis of
Solid Sample taken at
150 minutes in Experiment 3-5

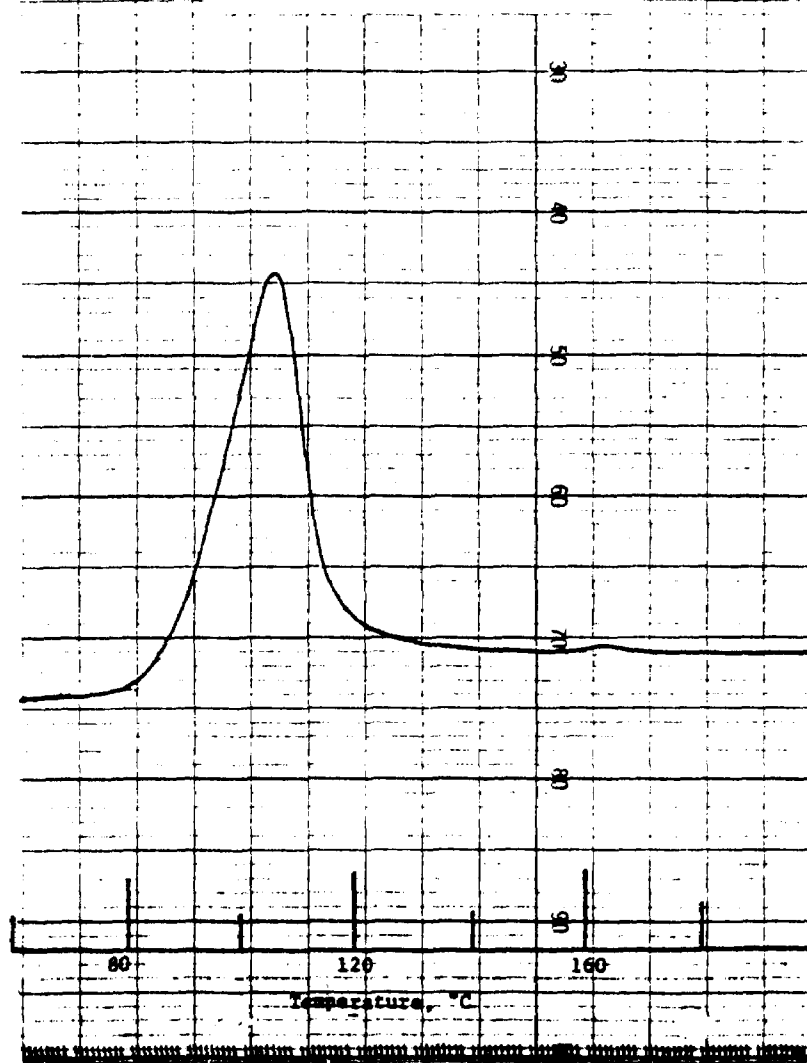


Figure A-15
Results of DSC Analysis of
Solid Sample taken at
180 minutes in Experiment 3-5

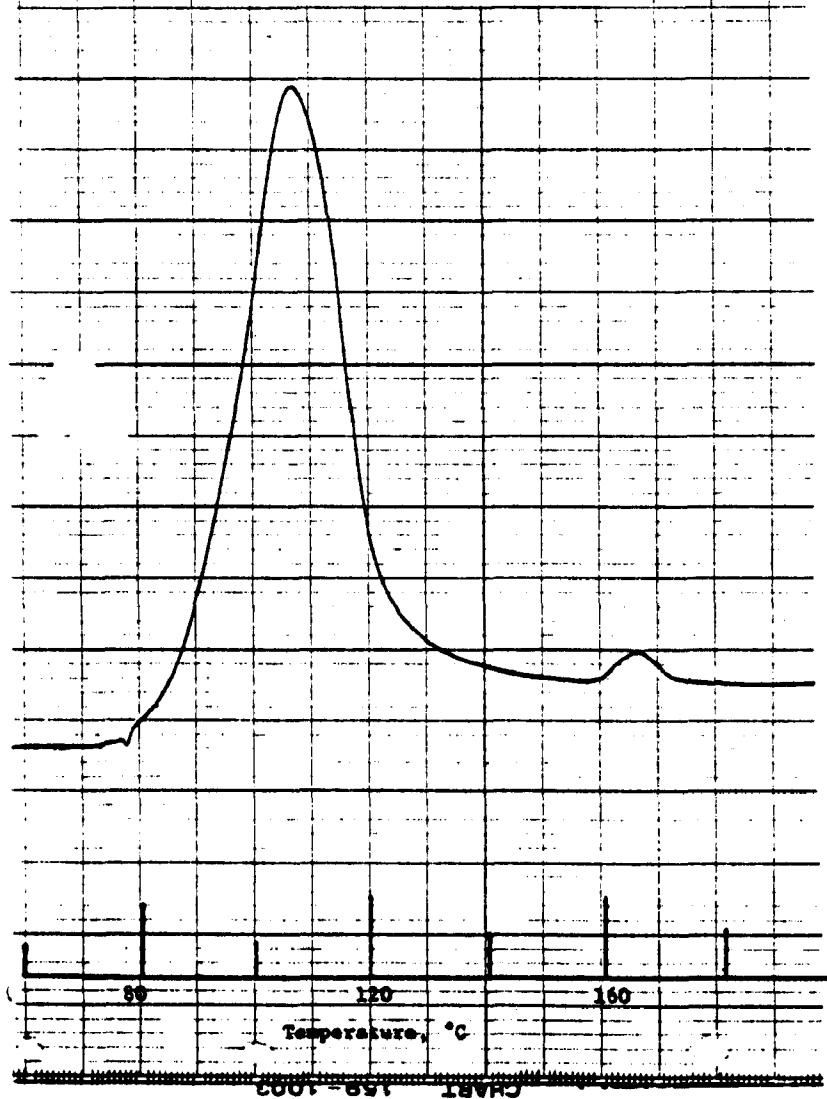


Figure A-16
Results of DSC Analysis of
Solid Sample taken at
270 minutes in Experiment 3-5

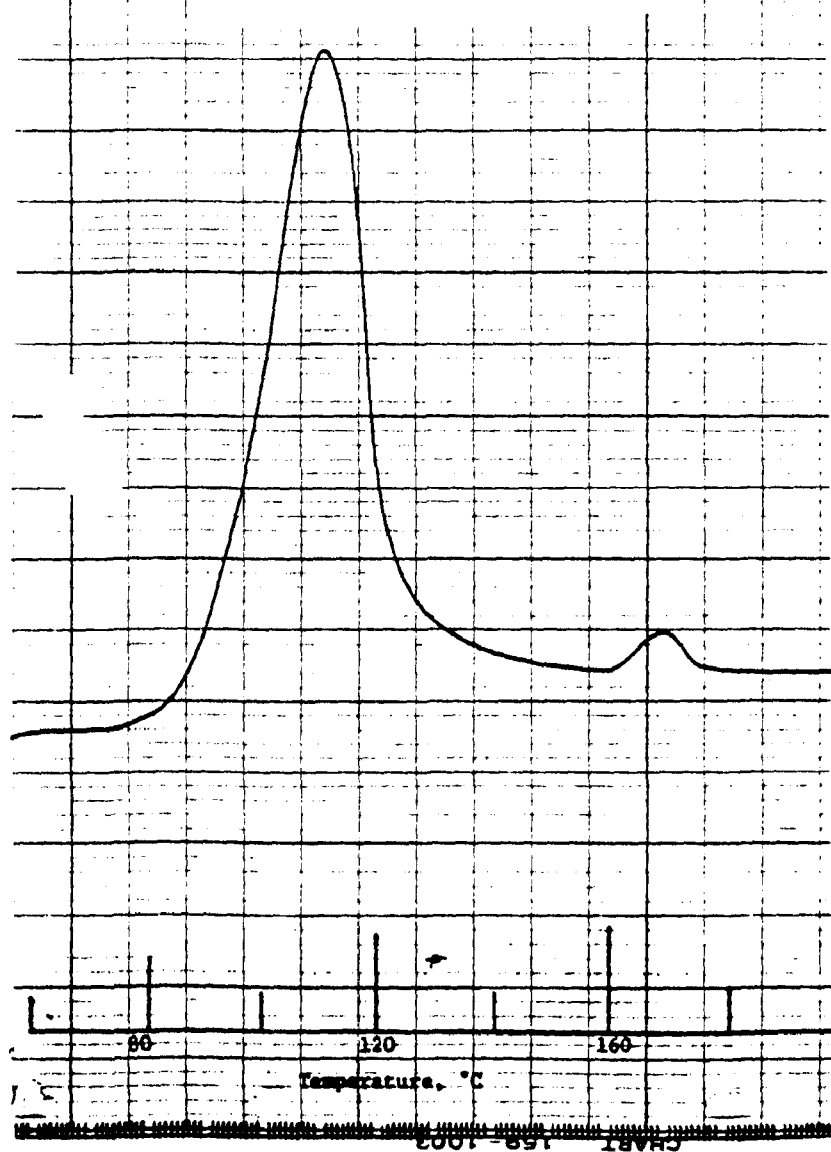


Figure A-17
Results of DSC Analysis of
Solid Sample Taken at
330 minutes in Experiment 3-5

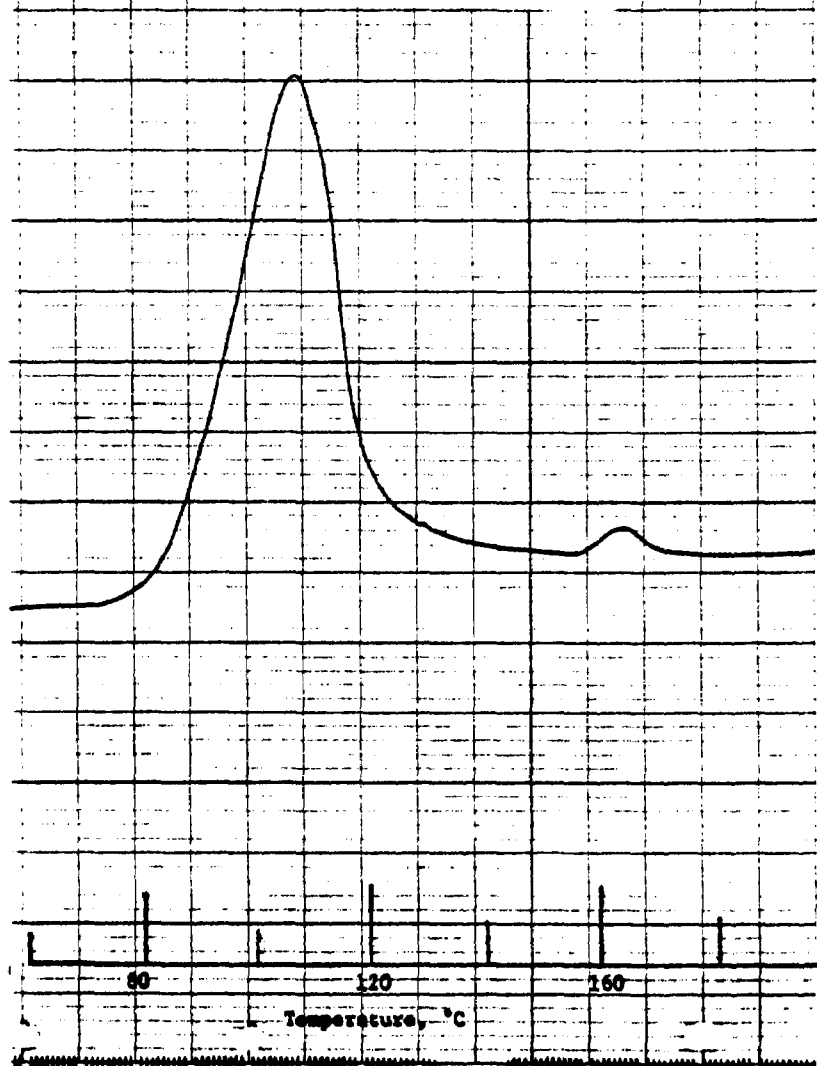


Figure A-18
Results of DSC Analysis of
Solid Sample Taken at
390 minutes in Experiment 3-5

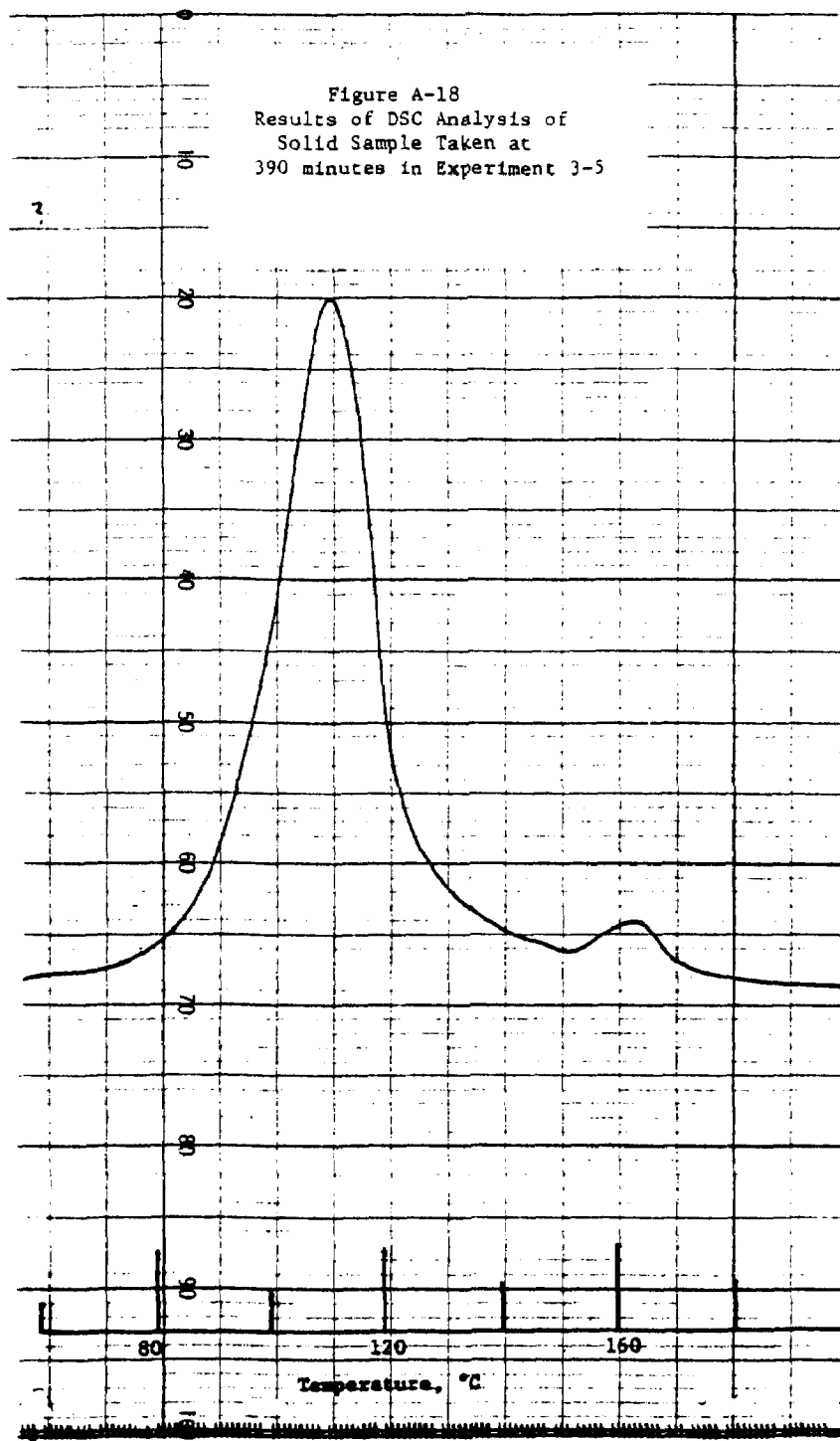
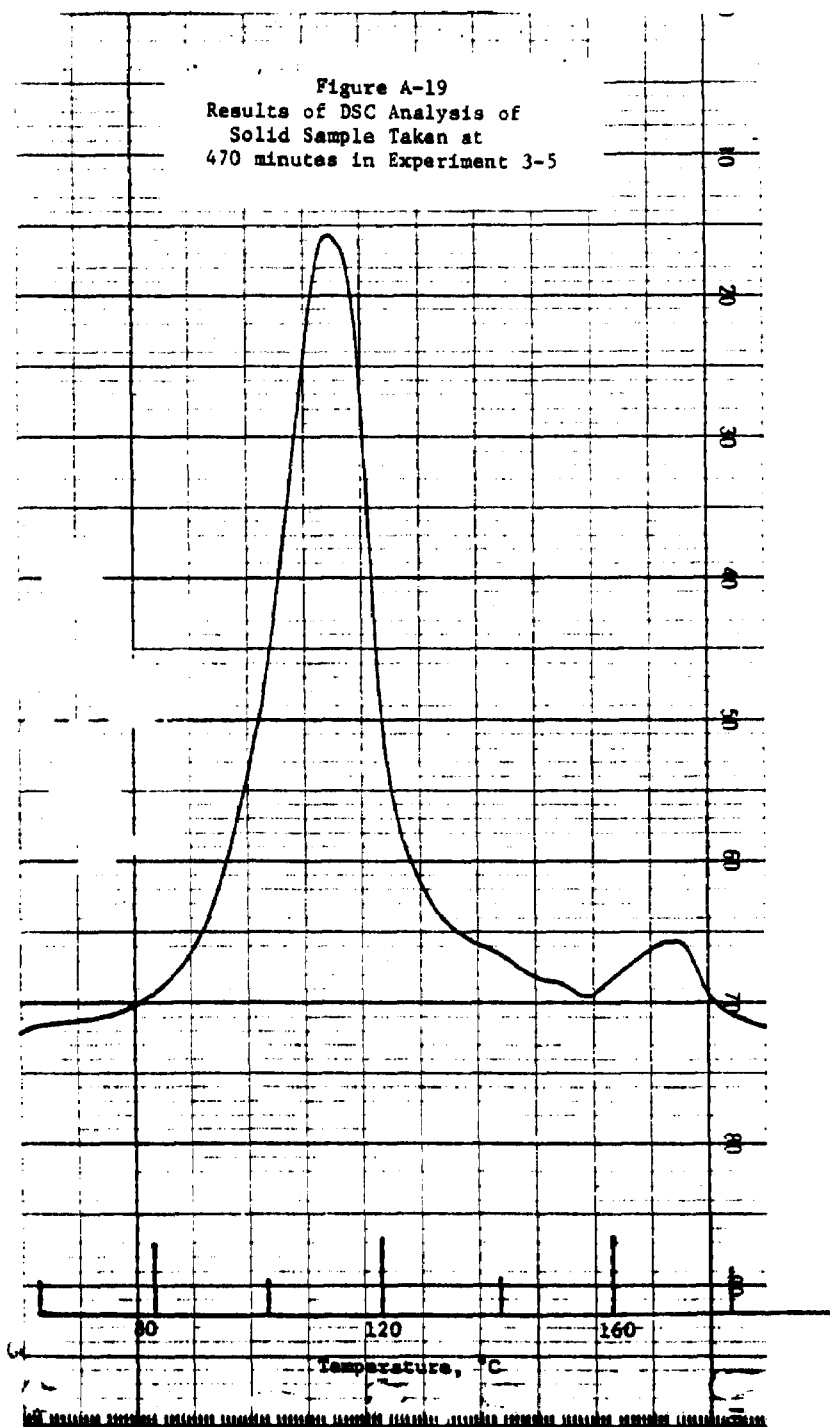


Figure A-19
Results of DSC Analysis of
Solid Sample Taken at
470 minutes in Experiment 3-5



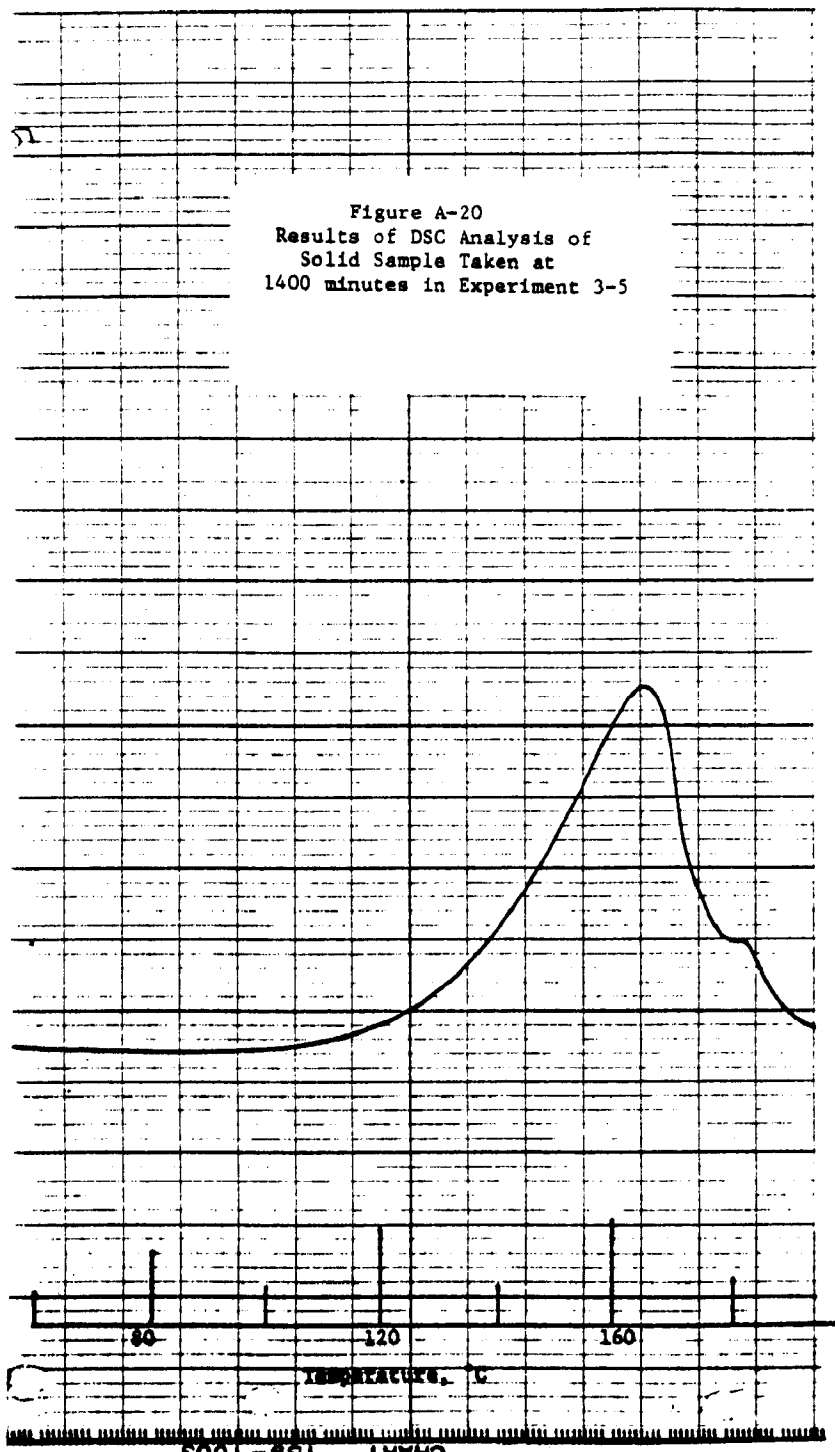
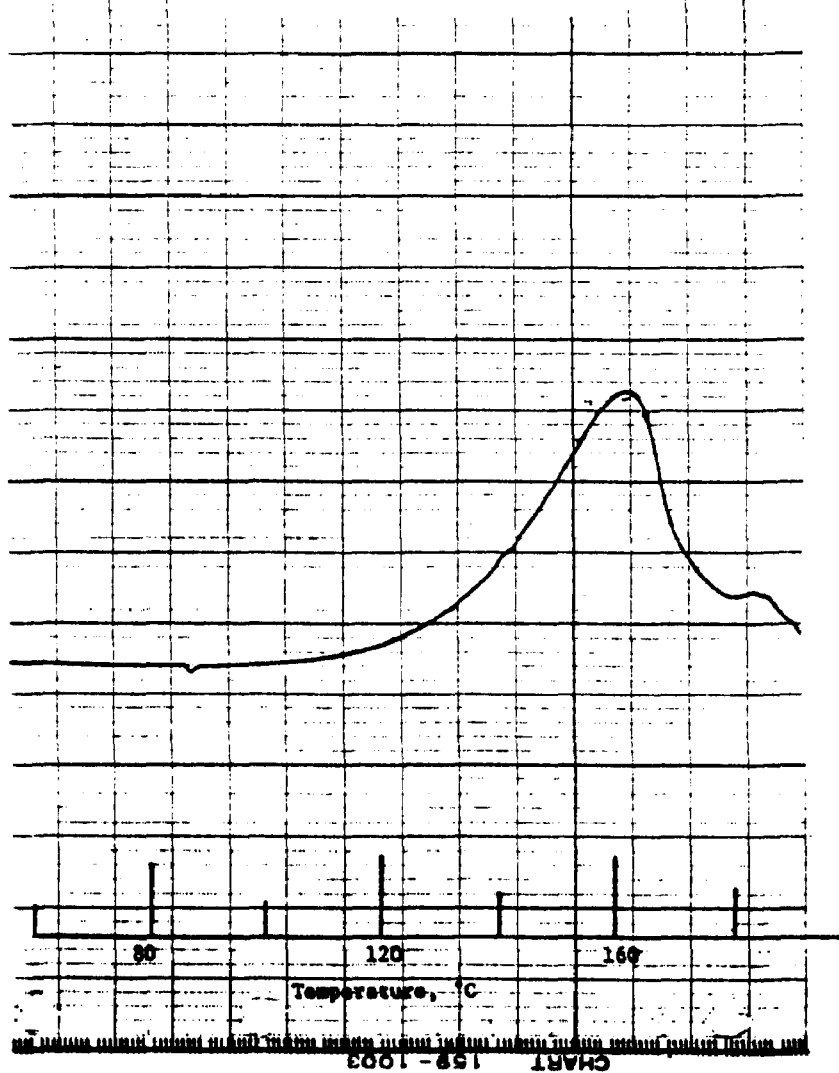


Figure A-21
Results of DSC Analysis of
Solid Sample taken at
3200 minutes in Experiment 3-5



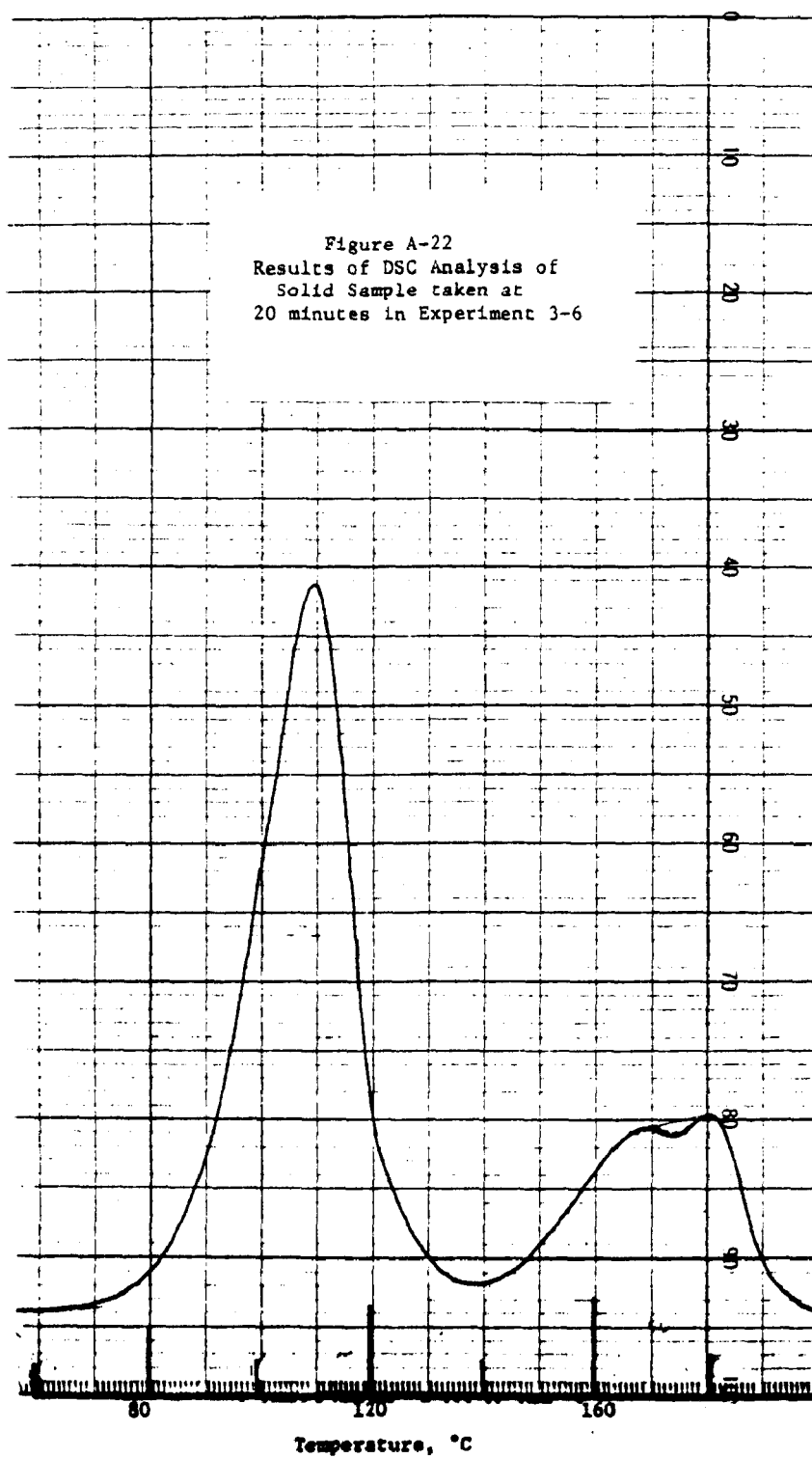


Figure A-23
Results of DSC Analysis of
Solid Sample taken at
50 minutes in Experiment 3-6

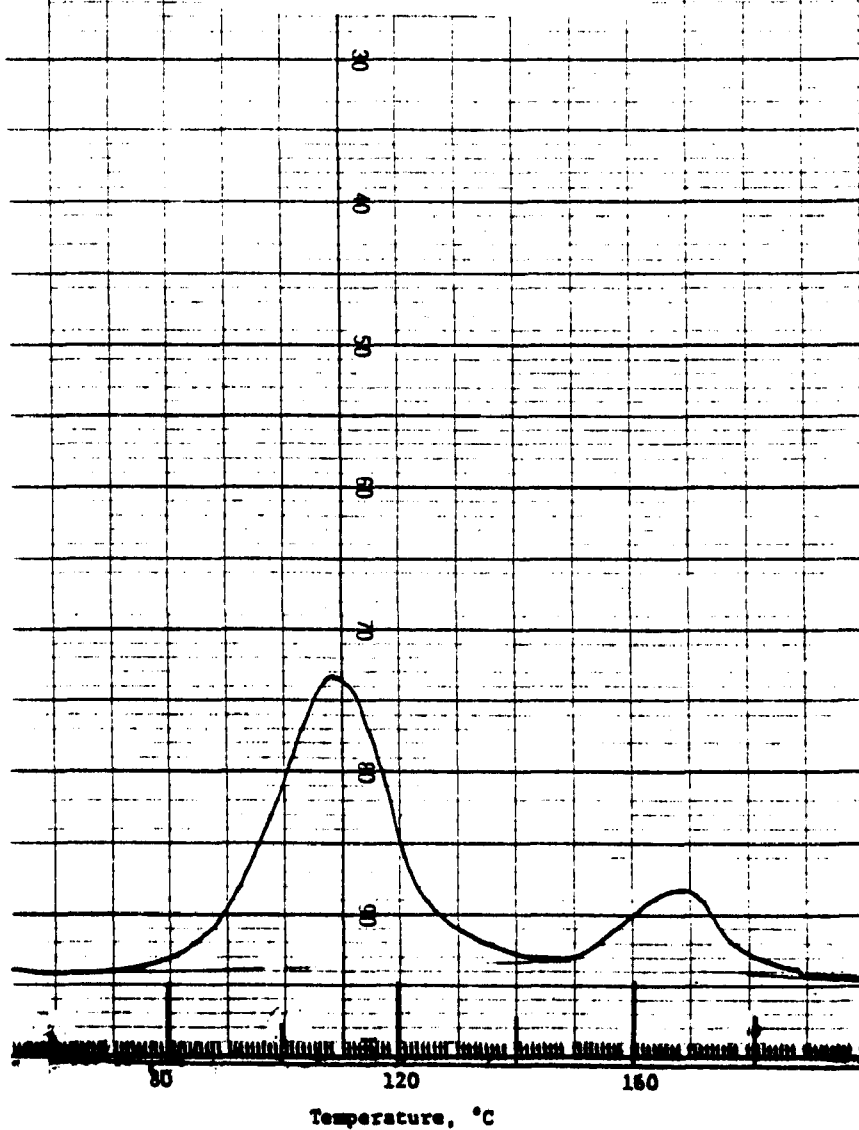


Figure A-24
Results of DSC Analysis of
Solid Sample taken at
60 minutes in Experiment 3-6

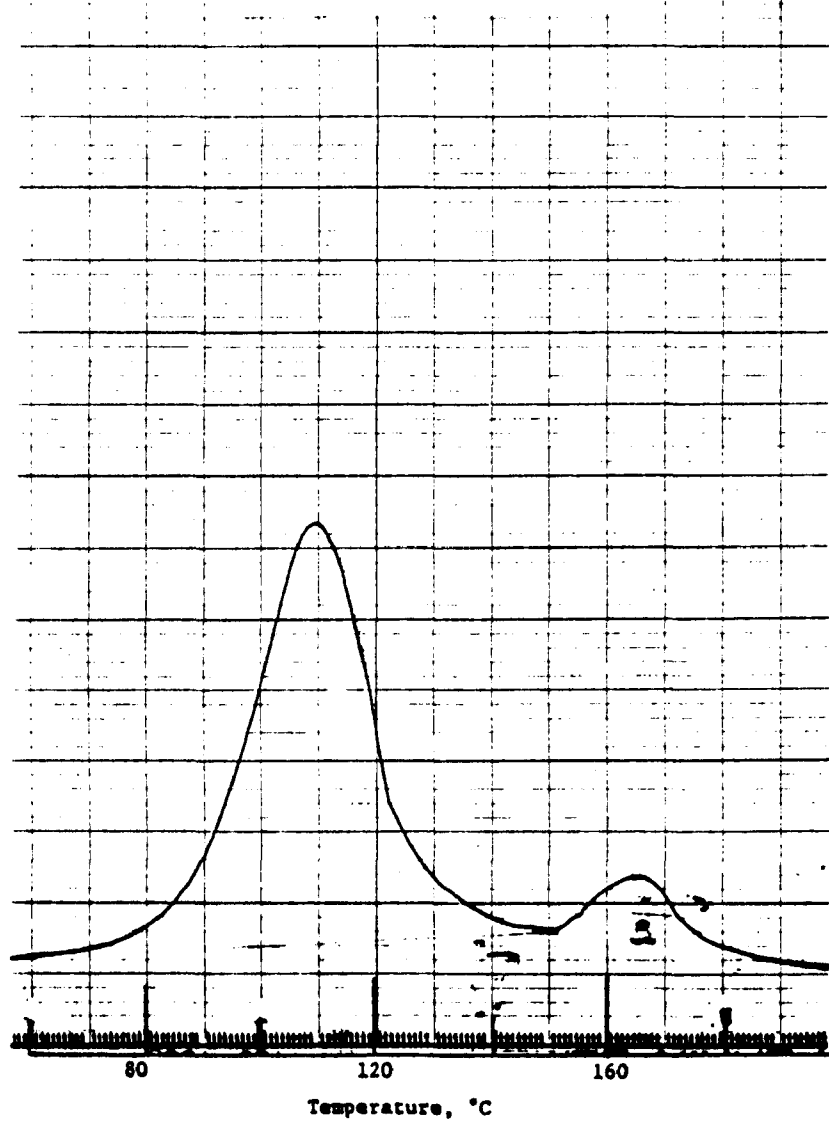


Figure A-25
Results of DSC Analysis of
Solid Sample Taken at
180 minutes in Experiment 3-6

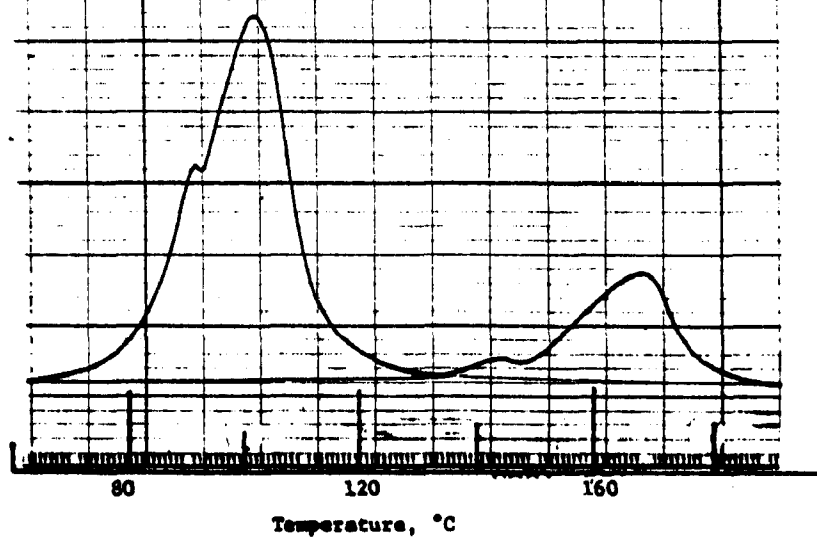


Figure A-26
Results of DSC Analysis of
Solid Sample Taken at
300 minutes in Experiment 3-6

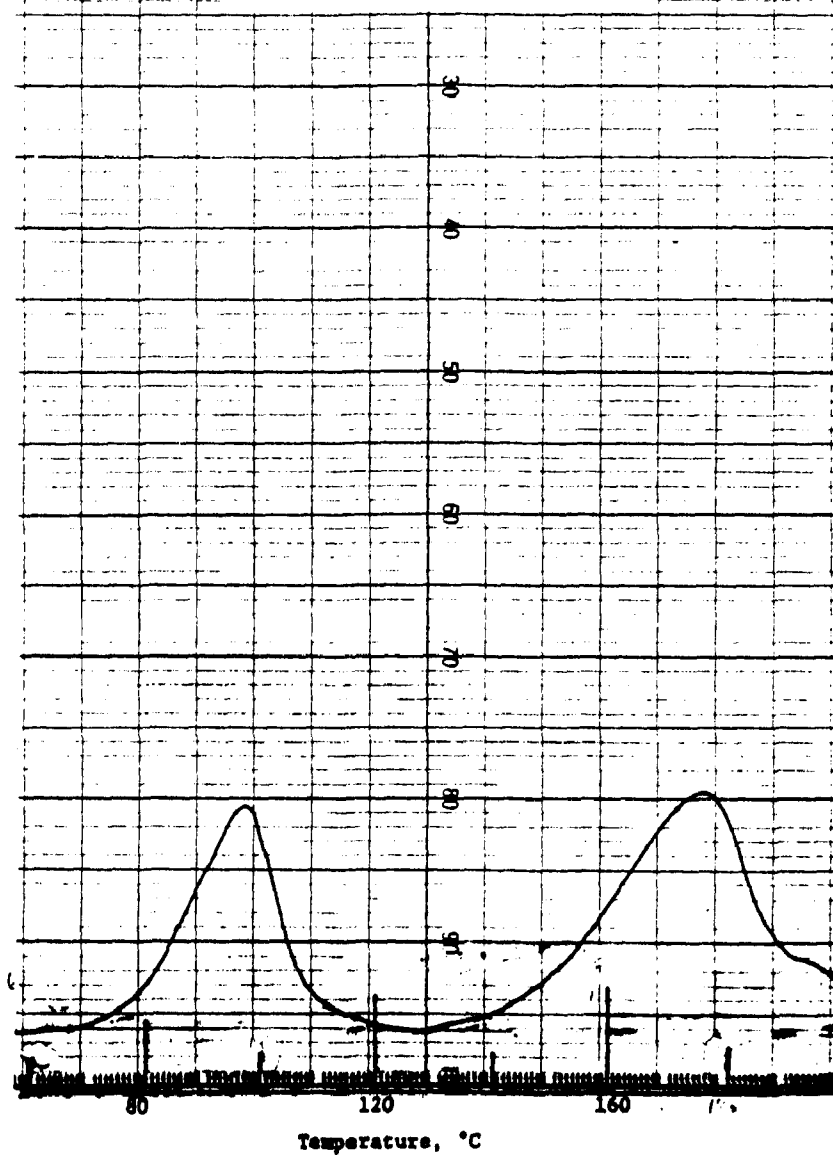
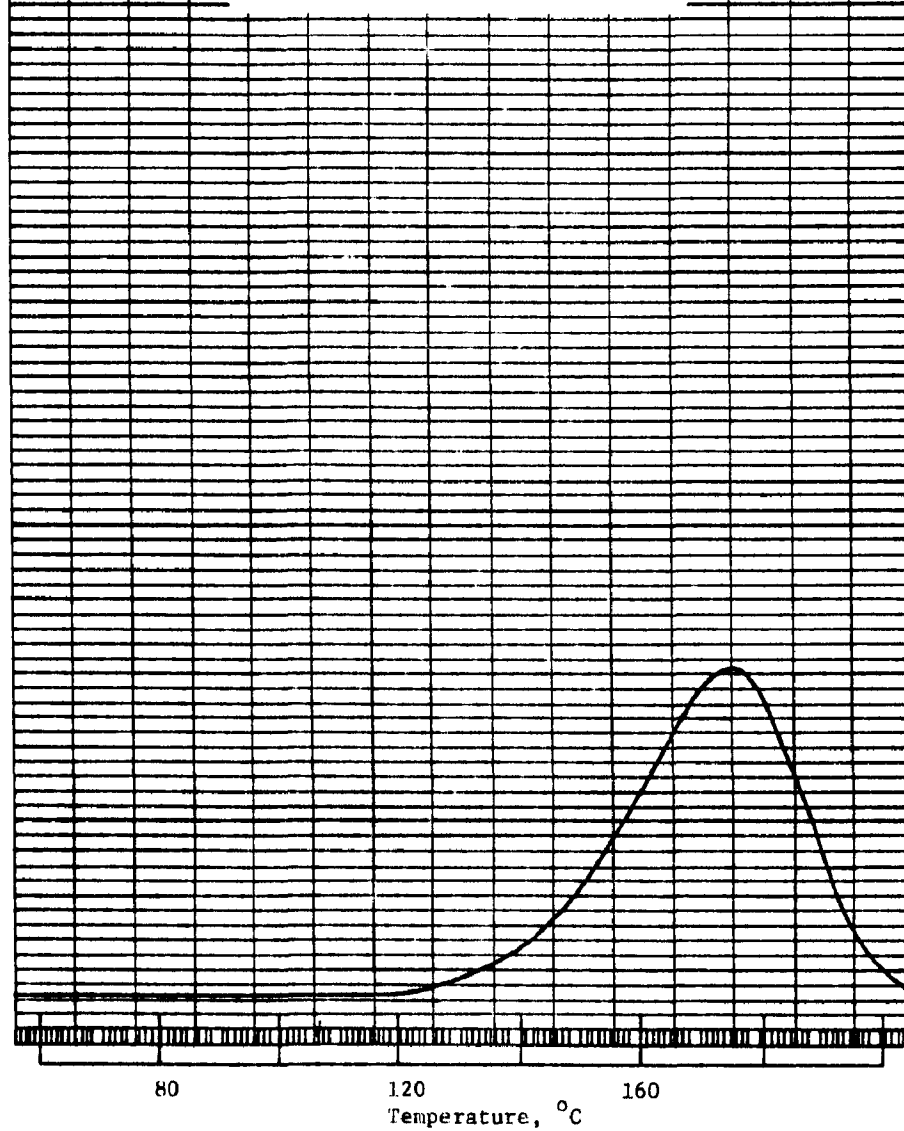
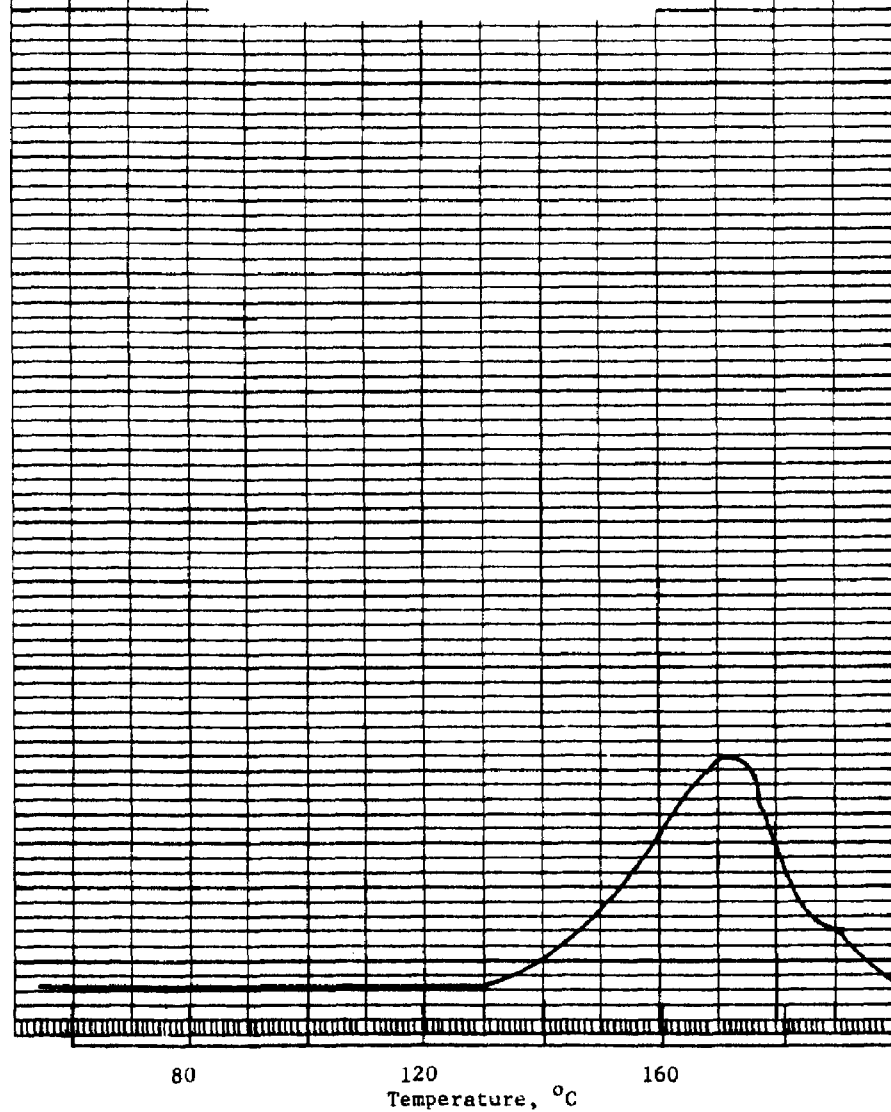


Figure A-27
Results of DSC Analysis of
Solid Sample Taken at
390 minutes in Experiment 3-6



02-2308-

Figure A-28
Results of DSC Analysis of
Solid Sample Taken at
4260 minutes in Experiment 3-6



02-2307-1

Figure A-29
Results of DSC Analysis of
Solid Sample Taken at
10 minutes in Experiment 3-7

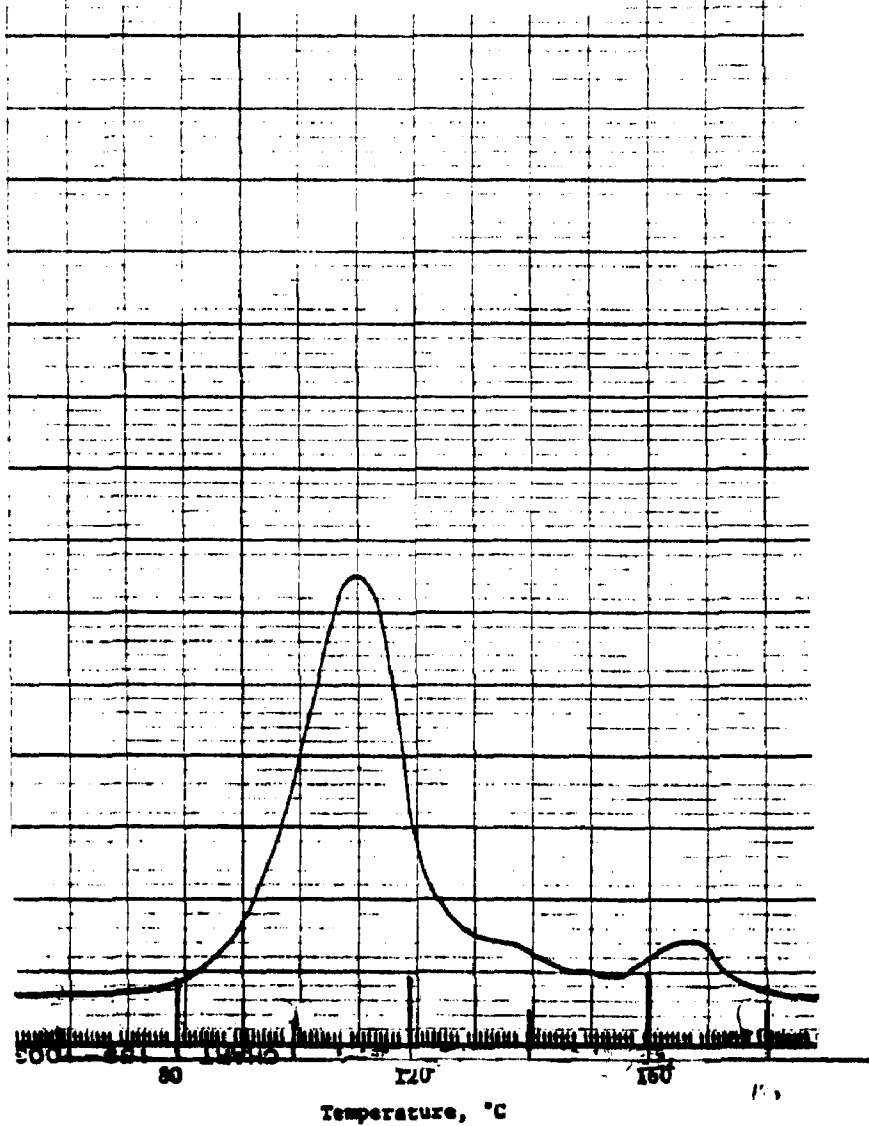


Figure A-30
Results of DSC Analysis of
Solid Sample Taken at
30 minutes in Experiment 3-7

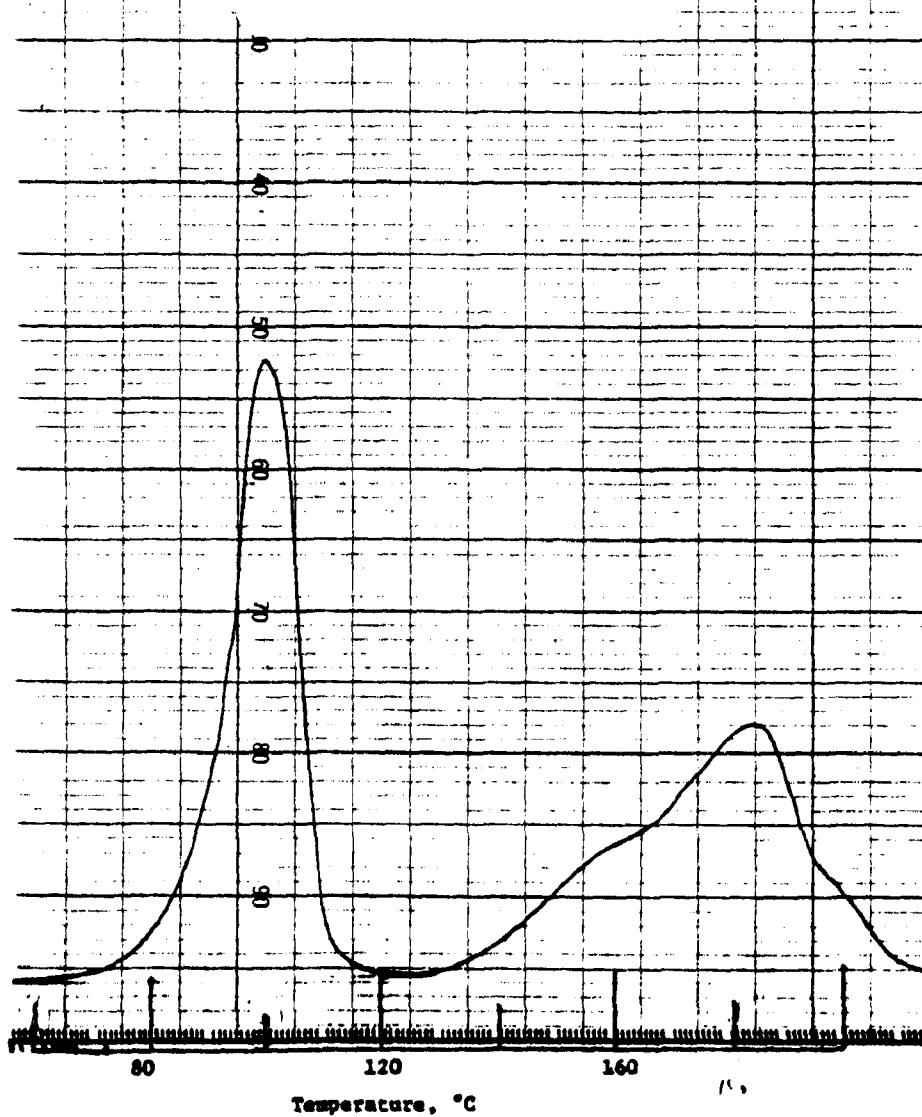


Figure A-31
Results of DSC Analysis of
Solid Sample Taken at
40 minutes in Experiment 3-7

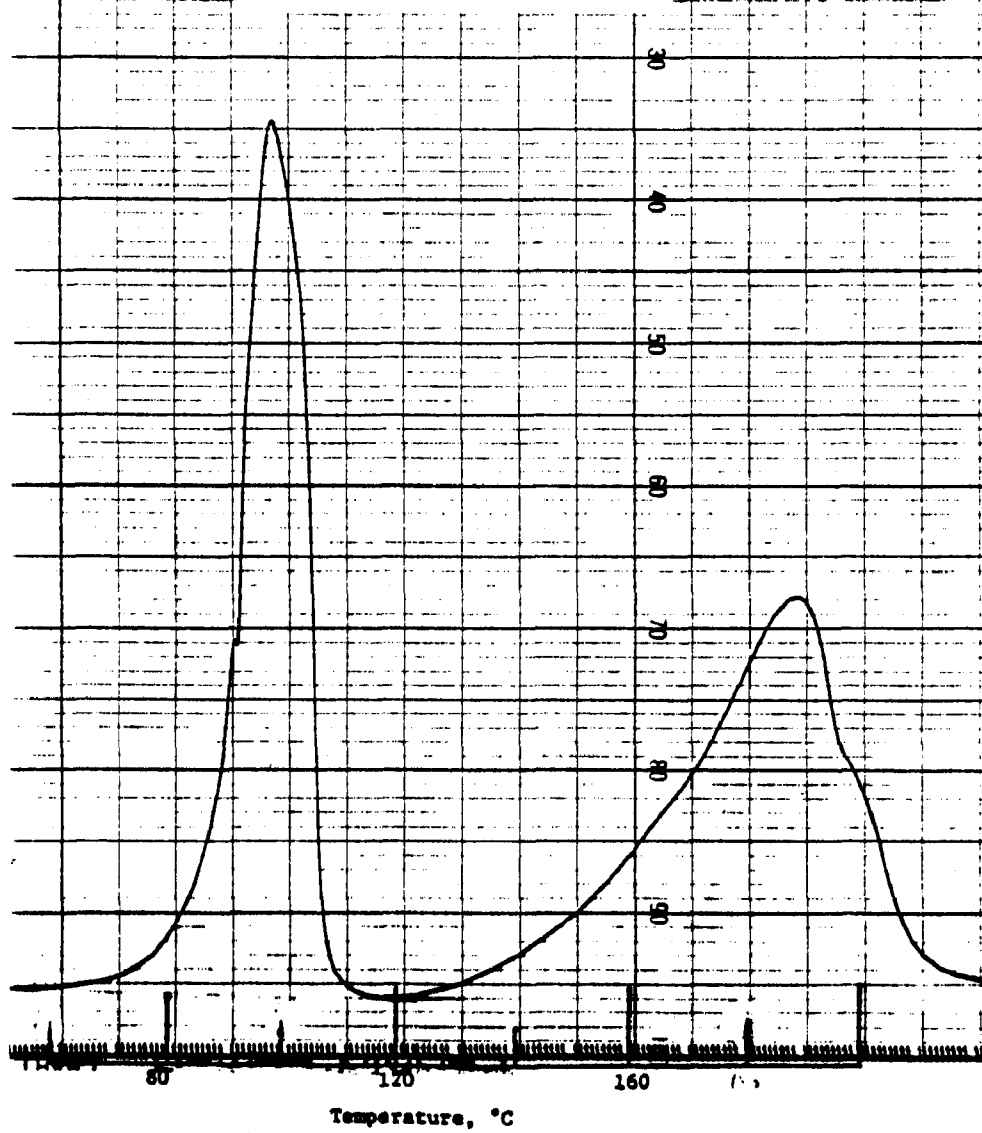


Figure A-32
Results of DSC Analysis of
Solid Sample Taken at
80 minutes in Experiment 3-7

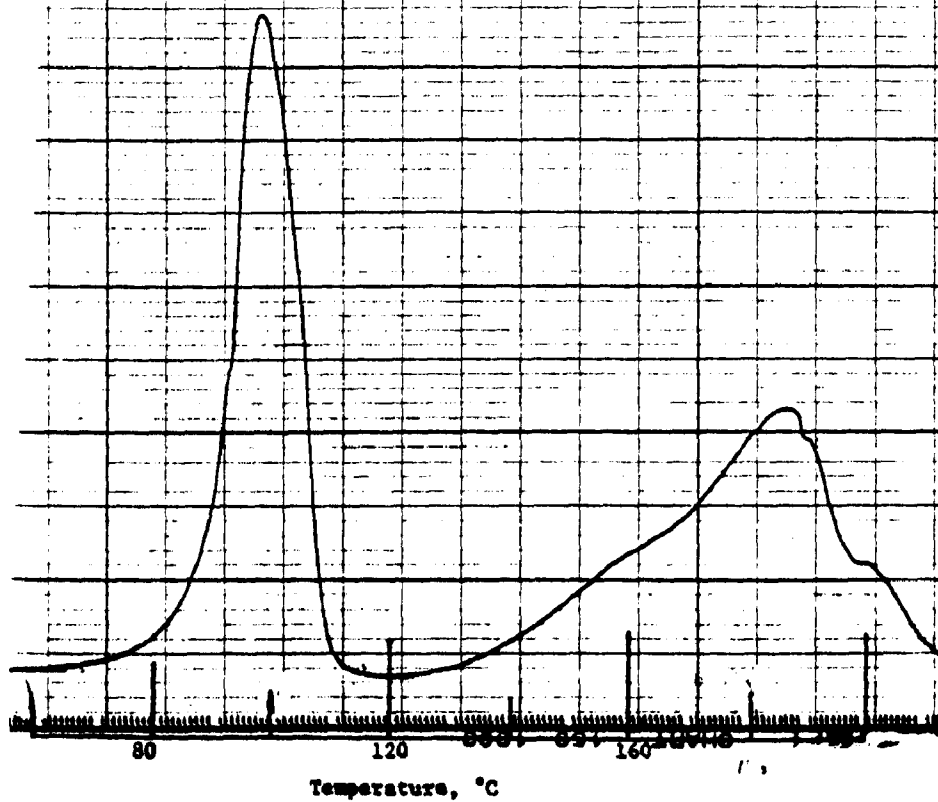


Figure A-33
Results of DSC Analysis of Solid
Sample Taken at
150 minutes in Experiment 3-7

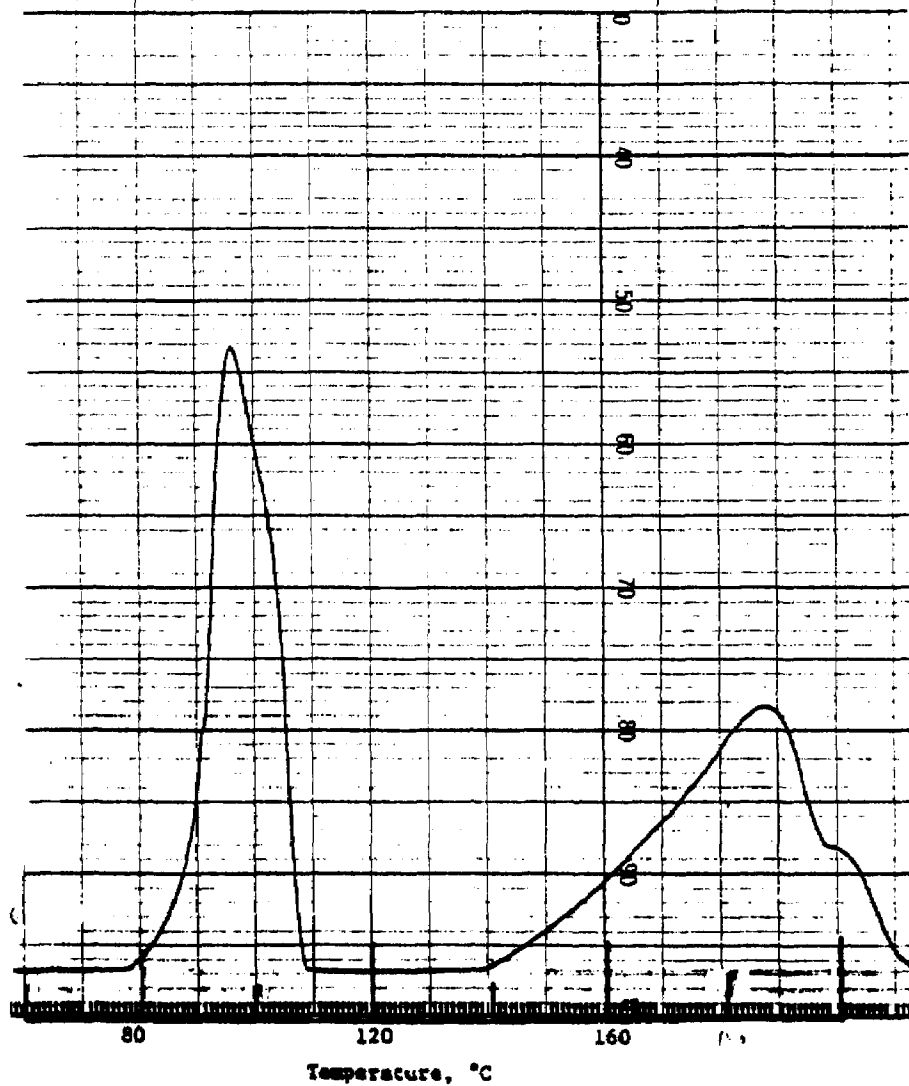


Figure A-34
Results of DSC Analysis of Solid
Sample Taken at
240 minutes in Experiment 3-7

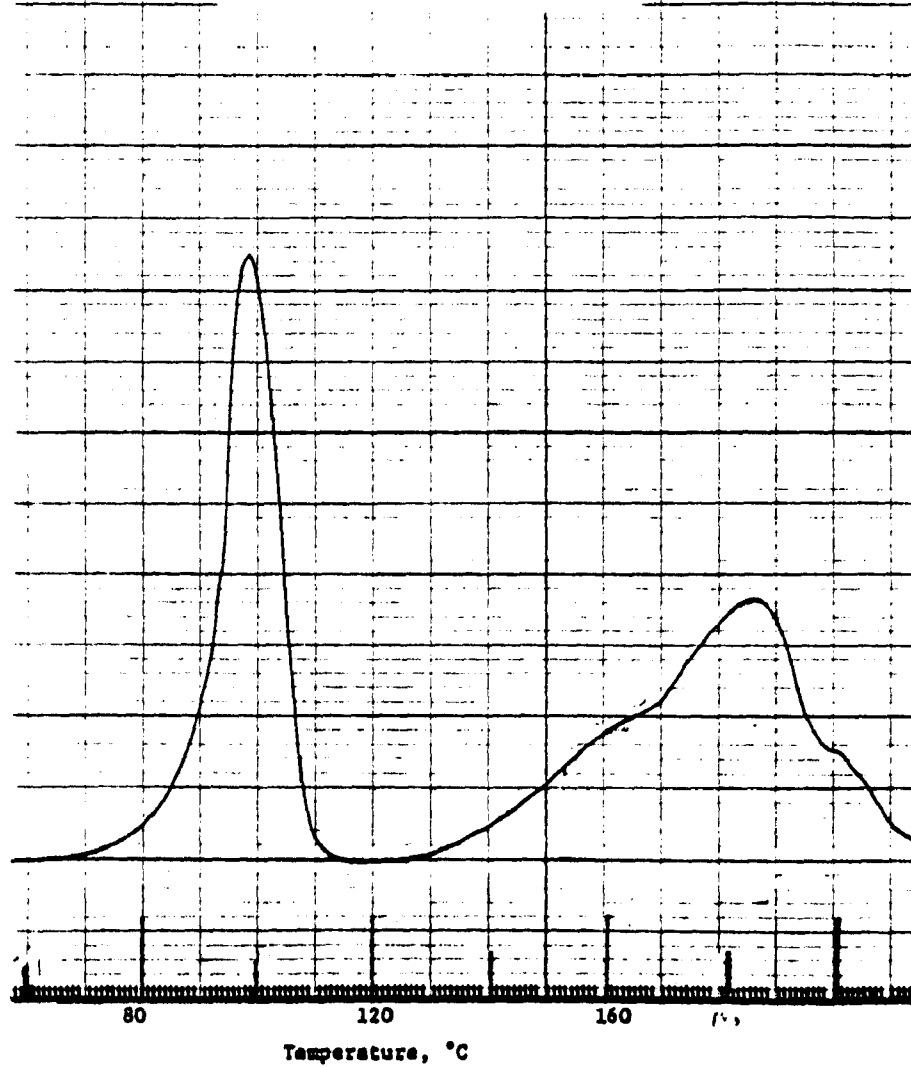


Figure A-35
Results of DSC Analysis of Solid
Sample Taken at
320 minutes in Experiment 3-7

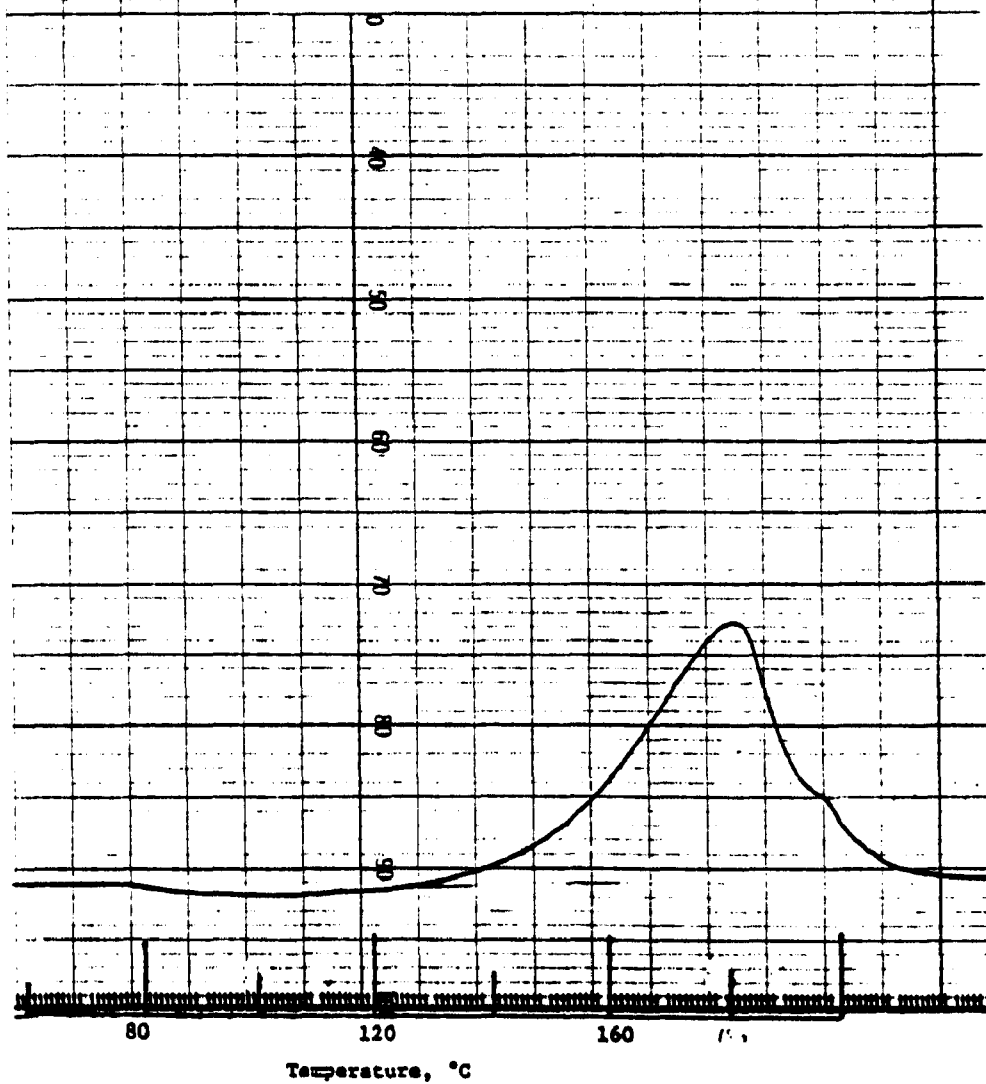
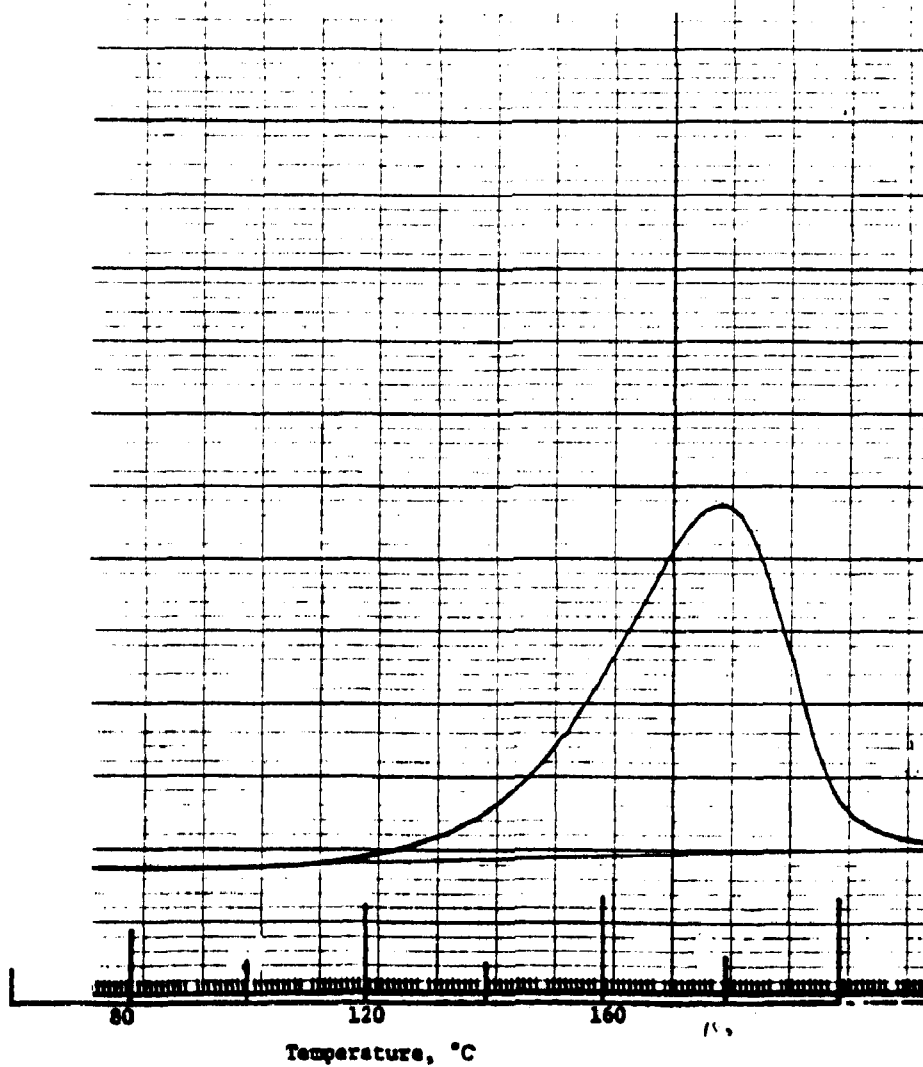


Figure A-36
Results of DSC Analysis of Solid
Sample Taken at
1400 minutes in Experiment 3-7



Technical Note 200-045-54-04

HOMOGENEOUS NUCLEATION OF
 MgSO_3 HYDRATES IN SCRUBBER-LIKE
MEDIA

Prepared by:

J. L. Skloss

CONTENTS

1. Introduction.	312
2. Experimental Method for Homogeneous Nucleation. . .	313
3. Results	315
4. Discussion.	320
5. Conclusion.	335

FIGURES

<u>Number</u>	<u>Page</u>
3-1 DSC Scans of Magnesium Sulfite Solids Nucleated in Scrubber-Like Media at Various Temperatures	317
3-2 Homogeneous Nucleation from 20% MgSO_4 Solutions and pH 6.	319
4-1 X-Ray Diffraction Pattern of $\text{MgSO}_3 \cdot 6\text{H}_2\text{O}$ Crystals Nucleated at 28°C	321
4-2 X-Ray Diffraction Pattern of $\text{MgSO}_3 \cdot 6\text{H}_2\text{O}$ Crystals Nucleated at 50°C	321
4-3 X-Ray Diffraction Pattern of $\text{MgSO}_3 \cdot 3\text{H}_2\text{O}$ Crystals Nucleated at 69°C	323
4-4 Photomicrograph 125x of $\text{MgSO}_3 \cdot 6\text{H}_2\text{O}$ Crystals (Rhombic) Nucleated at 28°C	325
4-5 Photomicrograph 125x of $\text{MgSO}_3 \cdot 6\text{H}_2\text{O}$ Crystals (Hexagonal) Nucleated at 50°C	326
4-6 Photomicrograph 250x of $\text{MgSO}_3 \cdot 3\text{H}_2\text{O}$ Crystals Nucleated and Grown Overnight at 65°C	327
4-7 Electron Micrograph 300x of $\text{MgSO}_3 \cdot 6\text{H}_2\text{O}$ Crystals (Rhombic) Nucleated at 28°C	328
4-8 Electron Micrograph 100x of $\text{MgSO}_3 \cdot 6\text{H}_2\text{O}$ Crystals (Hexagonal) Nucleated at 50°C	329
4-9 Electron Micrograph 1000x of $\text{MgSO}_3 \cdot 3\text{H}_2\text{O}$ Crystals Nucleated at 69°C	330

FIGURES (Continued)

<u>Number</u>	<u>Page</u>
4-10 Electron Micrograph 1000x of $\text{MgSO}_3 \cdot 3\text{H}_2\text{O}$ Crystals Nucleated and Grown Overnight at 65°C.331
4-11 Infrared Spectra of Magnesium Sulfite Nucleated at 50°C and 69°C334

TABLES

<u>Number</u>	<u>Page</u>
3-1 Solution Compositions Observed to Produce Homogeneous Nucleation at Various Temperatures.316
4-1 X-Ray Diffraction Data for $\text{MgSO}_3 \cdot 6\text{H}_2\text{O}$322
4-2 X-Ray Diffraction Data for $\text{MgSO}_3 \cdot 3\text{H}_2\text{O}$324

SECTION 1

INTRODUCTION

The magnesium oxide process removes sulfur dioxide from the flue gas by the precipitation of magnesium sulfite solids. This precipitation occurs whenever the solubility product of magnesium sulfite is exceeded if seed crystals are present. In the absence of nuclei, metastable solutions of magnesium sulfite can be formed. Supersaturation can be increased only to the limit whereby the magnesium sulfite solids are precipitated spontaneously. In clear solutions this induced precipitation is called primary nucleation. The purpose of this study was to determine the compositions required to spontaneously nucleate magnesium sulfite solids from scrubber type solutions at various temperatures. It was also important to determine which hydrate species are nucleated at the various temperatures and whether any hydrate mixtures are obtained.

SECTION 2

EXPERIMENTAL METHOD FOR HOMOGENEOUS NUCLEATION

Concentrated sodium sulfite solutions were added to aliquots of a concentrated magnesium sulfate solution at various temperatures until nucleation was visually observed. The final compositions of the mixed solutions were comparable to the magnesium oxide scrubber conditions: 20% magnesium sulfate (2.08 molal) and pH 6. The temperature range investigated was 28 to 80°C.

EXPERIMENTAL DETAILS

A stock solution of reagent grade magnesium sulfate was prepared and analyzed to contain 2.63 molal (or 2.53 molar) magnesium and total sulfate. The pH at room temperature was 2.9. Insoluble traces which otherwise might have interfered with the nucleation process were allowed to settle to the bottom of the stock solution for one week, and aliquots were withdrawn by pipet from the center of the solution.

Nucleation runs were started by transferring 100g of magnesium sulfate stock solution into a 125-ml erlenmeyer flask containing a teflon coated magnetic stir bar. The flask was stoppered and placed into a 0.5 l glass-lined water bath maintained at the desired temperature within $\pm 1^\circ\text{C}$. Solution stirring, the rate of which was constant from run to run, was achieved by the use of a magnetic stirrer located under the water bath. Sodium sulfite salt was added and dissolved in the magnesium sulfate solution to the saturation limit. Depending upon the temperature, 0.6 to 2g of sodium sulfite was required. The pH of the magnesium sulfate solution increased from 2.9 to approximately 6. A separate sodium sulfite solution was then

prepared by dissolving 6g of sodium sulfite in 22g of 0.6 molar sulfuric acid solution. This solution (pH = 7.5) was saturated with respect to sodium sulfite at 25°C and was subsaturated at the higher temperatures.

After temperature stabilization was obtained, the sodium sulfite solution was added dropwise to the magnesium sulfate solution at the rate of 4-5 ml per minute. At the first visual sign of nucleation, the pH was measured with a temperature-compensated Orion 701 meter and the samples were diluted and analyzed. The elapsed time from start to finish of each nucleation experiment was generally less than seven minutes. After nucleation, the slurry was immediately filtered, and the solids were washed with 50% ethanol and oven-dried at 45°C for 30 minutes. The oxidation of sulfite ion was negligible because of the short time required to perform these nucleation runs. The analytical methods used were:

Magnesium - Colorimetric titration with an EDTA standard solution.

Sodium Sulfite - Iodine-buffer preparation and back-titration with a thio-sulfate standard solution.

Sulfate - Peroxide oxidation of sulfite, hydrogen ion exchange, controlled evaporation leaving quantitative residue of sulfuric acid, and titration with a hydroxide standard solution. Sulfate = total sulfur minus sulfite.

SECTION 3

RESULTS

Primary nucleation runs were made at 28, 40, 50, 69, and 80°C in 20% magnesium sulfate media. These data are shown in Table 3-1. The magnesium, sodium, sulfite, and sulfate concentrations are expressed in molality units.

Identification of the nucleated solids was made by differential scanning calorimetry (DSC) using the Perkin Elmer DSC-2 instrument. The waters of hydration of magnesium sulfite hexahydrate or trihydrate are released in one step by using a steady stream of nitrogen across the sample. The loss of water is recorded in the DSC thermogram by measuring the surge of energy required to maintain a steady temperature rise. The DSC thermograms of the various nucleated solids are shown in Figure 3-1. Two patterns are observed: the loss of the waters of hydration at 100-110°C or at 160-170°C, conforming, respectively, to the properties of pure $\text{MgSO}_3 \cdot 6\text{H}_2\text{O}$ or pure $\text{MgSO}_3 \cdot 3\text{H}_2\text{O}$.

Chemical analyses showed that the magnesium sulfite content of the nucleated solids was either 4.7 or 6.3 mole/g, which is, respectively, the theoretical value for $\text{MgSO}_3 \cdot 6\text{H}_2\text{O}$ or $\text{MgSO}_3 \cdot 3\text{H}_2\text{O}$. These results and the DSC thermograms above showed that pure $\text{MgSO}_3 \cdot 3\text{H}_2\text{O}$ is nucleated at 69 and 80°C. No hydrate mixtures were observed.

The activity products

$$a_{\text{Mg}^{++}} \cdot a_{\text{SO}_3^{=}} \cdot a^3_{\text{H}_2\text{O}} = a_{\text{p}_3}$$

were calculated by the Radian equilibrium program using the data from Table 3-1. The a_{p_3} values versus nucleation

TABLE 3-1. SOLUTION COMPOSITIONS OBSERVED TO PRODUCE
HOMOGENEOUS NUCLEATION AT VARIOUS TEMPERATURES

Temperature °C±1°C	pH	{Mg ⁺² }	{Na ₂ SO ₃ }	{SO ₄ ⁻² }	Species Nucleated	ap ₃ ×10 ⁵
28	5.7	2.220	0.381	2.240	MgSO ₃ ·6H ₂ O*	30.5
40	6.0	2.190	0.393	2.206	MgSO ₃ ·6H ₂ O**	31.6
50	6.1	2.028	0.519	2.053	MgSO ₃ ·6H ₂ O**	35.9
60	6.2	2.091	0.602	2.112	MgSO ₃ ·6H ₂ O**	37.1
69	6.2	2.040	0.678	2.065	MgSO ₃ ·3H ₂ O	35.3
80	6.3	2.257	0.602	2.273	MgSO ₃ ·3H ₂ O	28.8

Note Solution concentrations are expressed in molality units. Density was 1.260 g/ml at room temperature.

* Rhombic crystal habit

** Hexagonal crystal habit

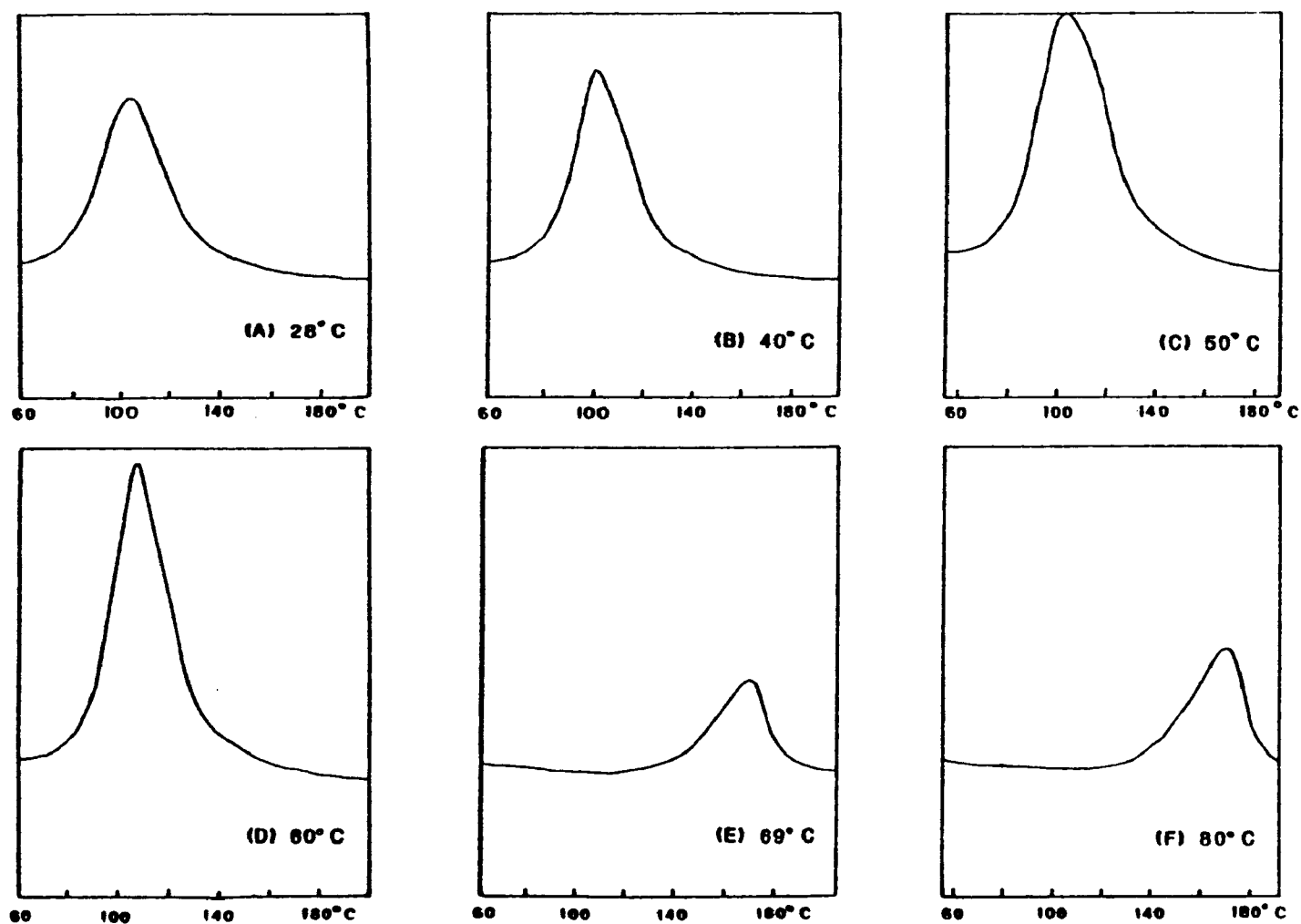


Figure 3-1. DSC Scans of Magnesium Sulfite Solids Nucleated in Scrubber-Like Media at Various Temperatures

temperatures are plotted in Figure 3-2, and curves have been drawn to represent the boundary for the onset of homogeneous nucleation for the hexahydrate and trihydrate phases of magnesium sulfite. Also included for comparison are the saturated solution activity products of $\text{MgSO}_3 \cdot 6\text{H}_2\text{O}$ and $\text{MgSO}_3 \cdot 3\text{H}_2\text{O}$ as a function of temperature. At the start of nucleation the relative saturation of $\text{MgSO}_3 \cdot 6\text{H}_2\text{O}$, defined as a_{p_6}/K_{sp_6} , was approximately four at 28°C and approximately three at 60°C , where

$$a_{p_6} = a_{p_3} \cdot a_{\text{H}_2\text{O}}^3.$$

At 69 and 80°C , the relative saturation of $\text{MgSO}_3 \cdot 3\text{H}_2\text{O}$, defined as a_{p_6}/K_{sp_3} , was approximately twelve when nucleation occurred.

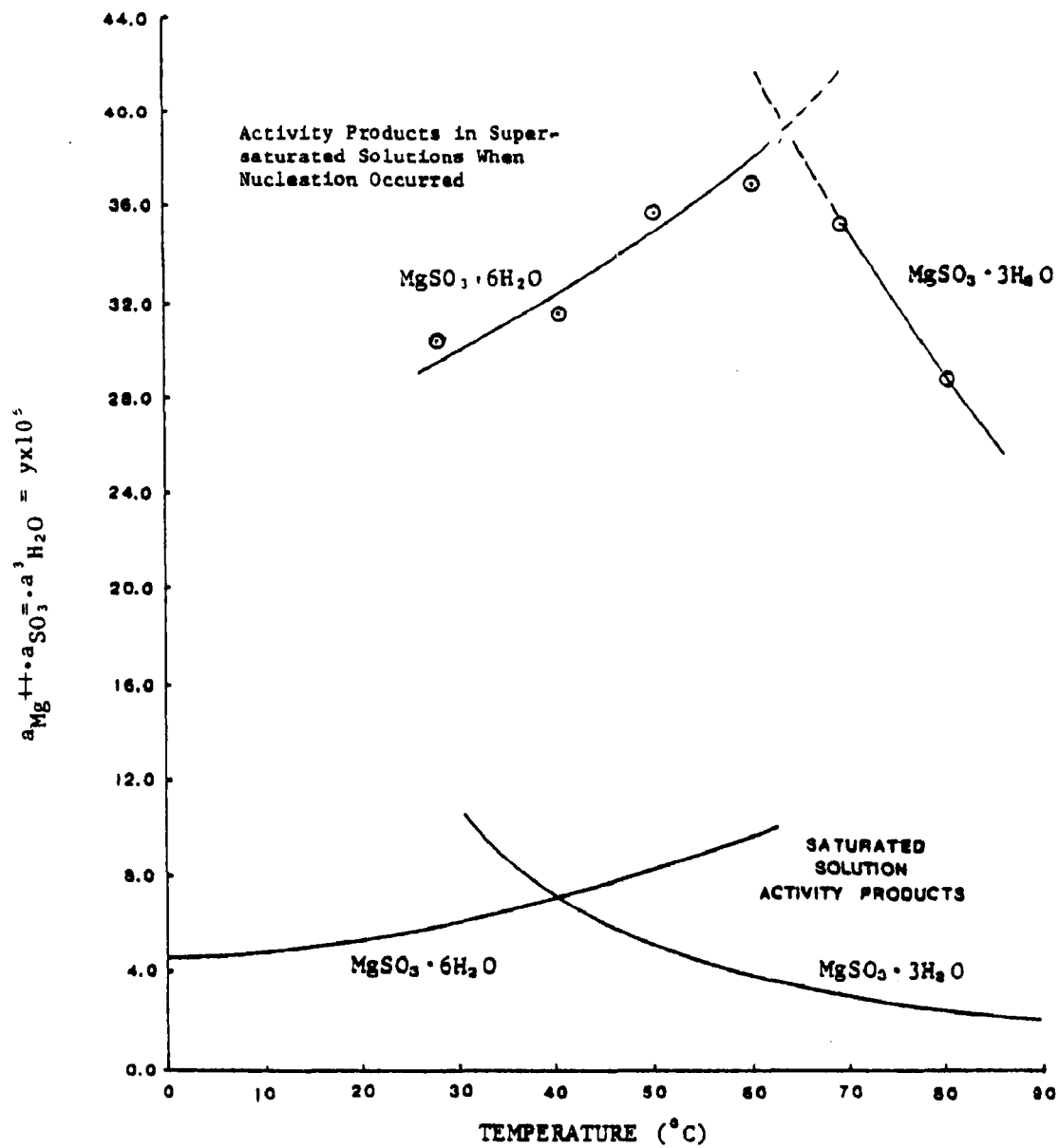


Figure 3-2. Homogeneous Nucleation from 20% $MgSO_4$ Solutions and pH 6

SECTION 4

DISCUSSION

Magnesium sulfite trihydrate is predicted by thermodynamics to be the stable phase in 20% magnesium sulfate solutions at 40, 50 and 60°C. However, from Section 3 it was shown that pure magnesium sulfite hexahydrate was nucleated at these temperatures. Only at temperatures above 65°C was the trihydrate phase observed to nucleate. This indicates that a kinetic effect is definitely involved in the nucleation process.

The shape of the hexahydrate crystals nucleated at 28°C was different from that of hexahydrate crystals obtained at the higher temperatures. However, the x-ray diffraction patterns of the solids nucleated at 28 and 50°C were virtually the same and confirm that these crystals are pure $\text{MgSO}_3 \cdot 6\text{H}_2\text{O}$ (see Figures 4-1 and 4-2). The two patterns compare well with each other and with the literature values for $\text{MgSO}_3 \cdot 6\text{H}_2\text{O}$ listed in Table 4-1. The relative intensities, I/I_1 , of the peaks depend somewhat on the packing of the crystals in the sample holder but are mostly a function of the atomic spacings in the crystal lattice. Positive identification of crystals is possible by this method.

The x-ray diffraction pattern (Figure 4-3) of the solids nucleated at 60°C was also obtained and it was found to agree with the literature data for $\text{MgSO}_3 \cdot 3\text{H}_2\text{O}$ (Table 4-2). This comparison confirms that magnesium sulfite was nucleated as the pure trihydrate phase at 69°C.

Microscopic examination revealed the characteristic shapes and sizes of the various types of nucleated crystals. Four samples are discussed here:

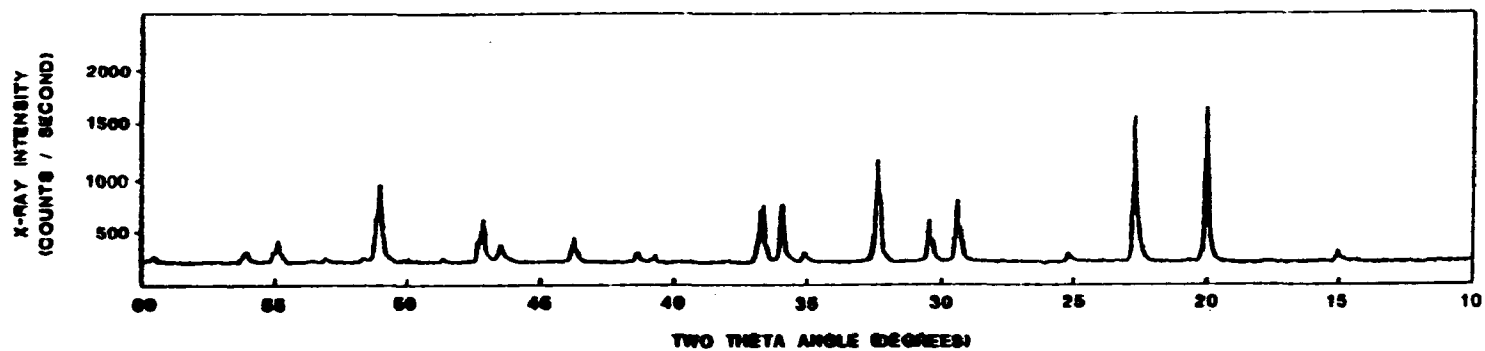


Figure 4-1. X-Ray Diffraction Pattern of $\text{MgSO}_3 \cdot 6\text{H}_2\text{O}$
Crystals Nucleated at 28°C

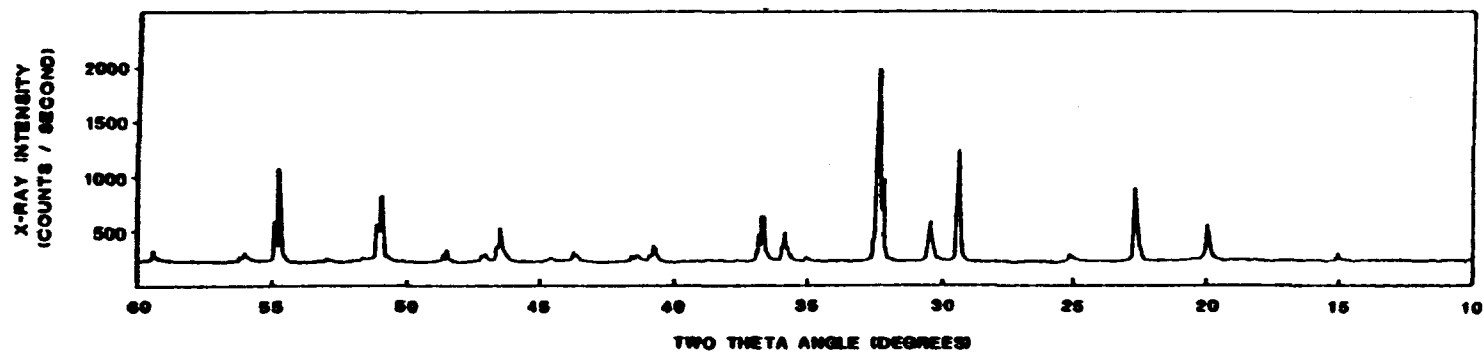


Figure 4-2. X-Ray Diffraction Pattern of $\text{MgSO}_3 \cdot 6\text{H}_2\text{O}$
Crystals Nucleated at 50°C

TABLE 4-1. X-RAY DIFFRACTION DATA FOR
MgSO₃•6H₂O

d(A°)	I/I ₁	2θ for CuKα ₁ (degrees)
5.7	4	15.5
4.40	80	20.2
3.87	100	23.0
3.01	32	29.6
2.90	32	30.8
2.74	100	32.6
2.42	60	37.1
2.05	12	44.1
1.91	32	47.6
1.77	70	51.6
1.71	4	53.6
1.66	32	55.3
1.63	4	56.4
1.54	8	60.0

ASTM X-Ray Powder Diffraction Pattern Data File, Card
No. 1-0473.

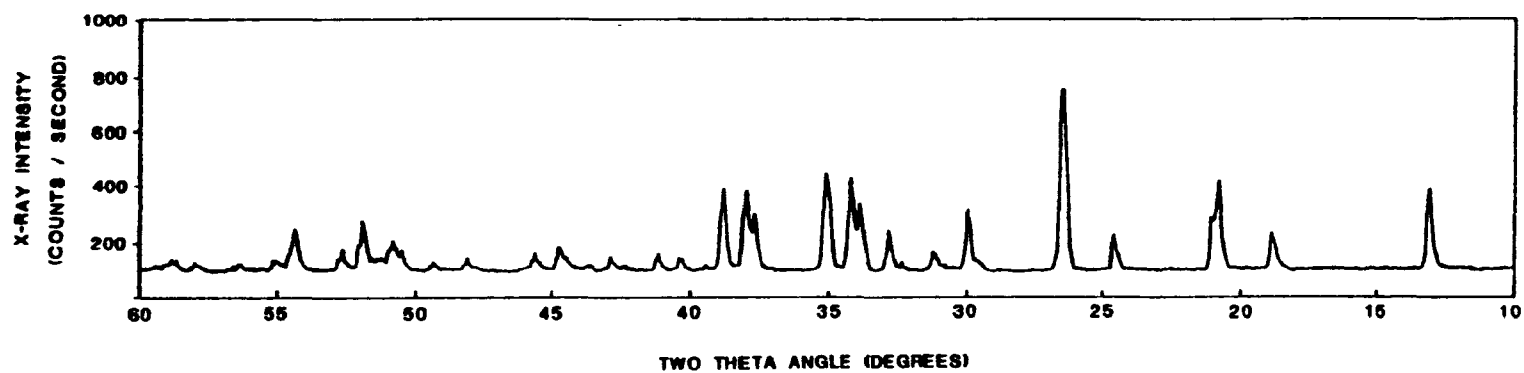


Figure 4-3. X-Ray Diffraction Pattern of $\text{MgSO}_3 \cdot 3\text{H}_2\text{O}$
Crystals Nucleated at 69°C

TABLE 4-2. X-RAY DIFFRACTION DATA FOR $\text{MgSO}_3 \cdot 3\text{H}_2\text{O}$

d(A°)	I/I	2 θ CuK α_1 degrees	d(A°)	I/I	2 θ CuK α_1 degrees
6.71	80	13.2	2.23	8	40.4
4.70	30	18.9	2.20	6	41.0
4.27	60	20.8	2.11	6	42.8
3.62	20	24.6	2.08	4	43.5
3.35	100	26.6	2.02	14	44.8
3.02	8	29.6	1.99	6	45.6
2.98	30	30.0	1.89	4	48.0
2.87	10	31.1	1.84	4	49.5
2.77	6	32.3	1.81	6	50.5
2.72	20	32.9	1.80	14	50.8
2.65	30	33.8	1.78	8	51.3
2.62	45	34.2	1.76	30	51.9
2.56	50	35.0	1.74	8	52.6
2.39	20	37.6	1.69	20	54.3
2.37	40	37.9	1.67	6	55.0
2.32	40	38.8	1.63	4	56.4
			1.56	4	59.0

ASTM X-Ray Powder Diffraction Pattern Data File, Card No. 11-239

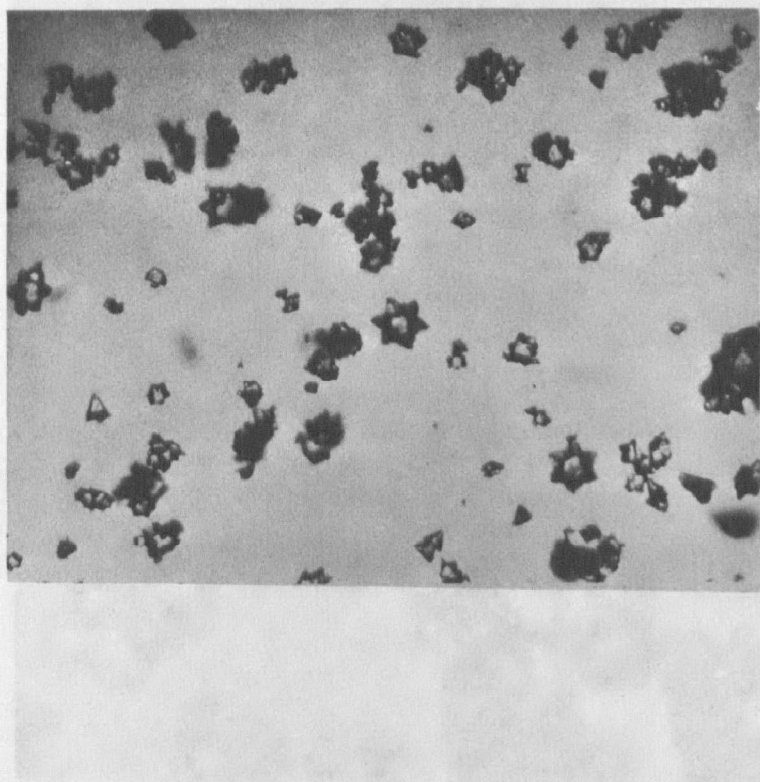


FIGURE 4-4.

PHOTOMICROGRAPH 125X
OF $\text{MgSO}_3 \cdot 6\text{H}_2\text{O}$ CRYSTALS (RHOMBIC)
NUCLEATED AT 28°C

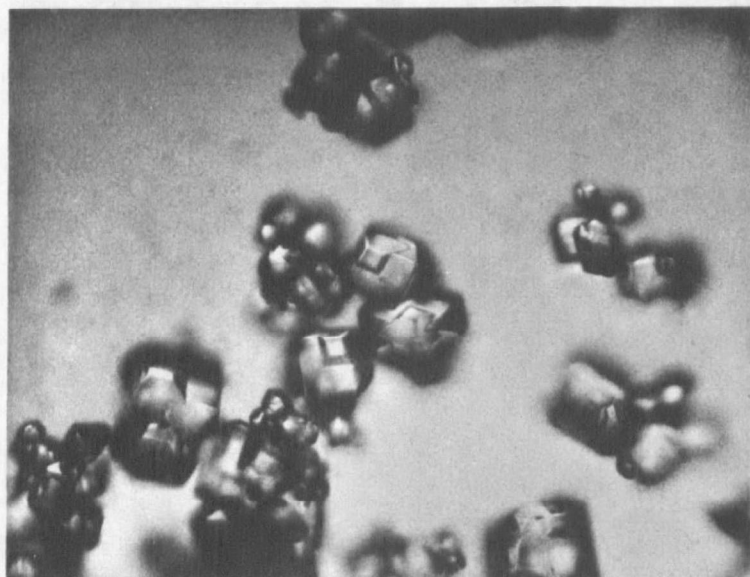


FIGURE 4-5.
 PHOTOMICROGRAPH 125X
 OF $\text{MgSO}_3 \cdot 6\text{H}_2\text{O}$ CRYSTALS (HEXAGONAL)
 NUCLEATED AT 50°C

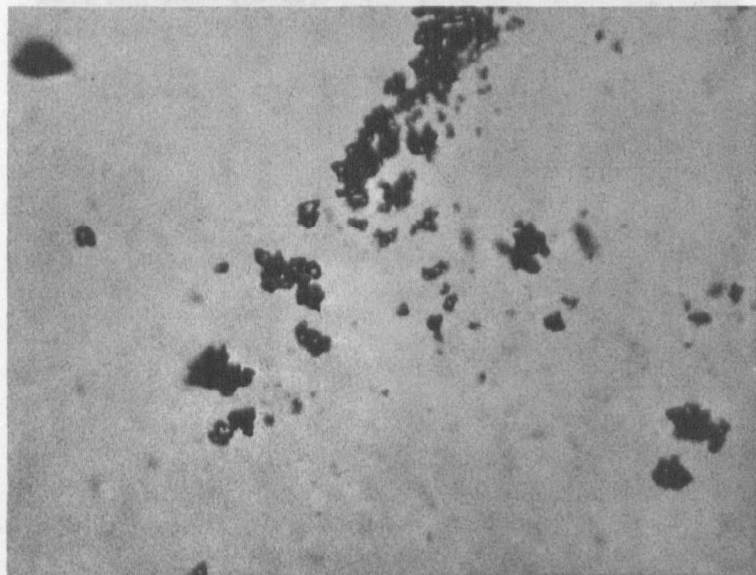


FIGURE 4-6.

PHOTOMICROGRAPH 250X
OF $\text{MgSO}_3 \cdot 3\text{H}_2\text{O}$ CRYSTALS NUCLEATED
AND GROWN OVERNIGHT AT 65°C

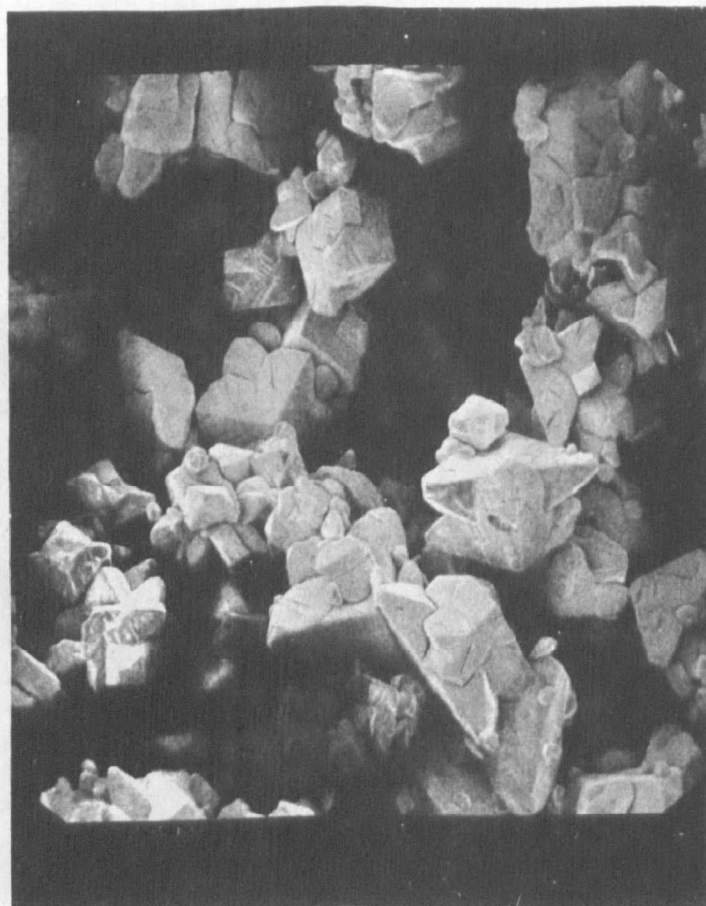


FIGURE 4-7
ELECTRON MICROGRAPH 300X
OF $\text{MgSO}_3 \cdot 6\text{H}_2\text{O}$ CRYSTALS (RHOMBIC)
NUCLEATED AT 28°C

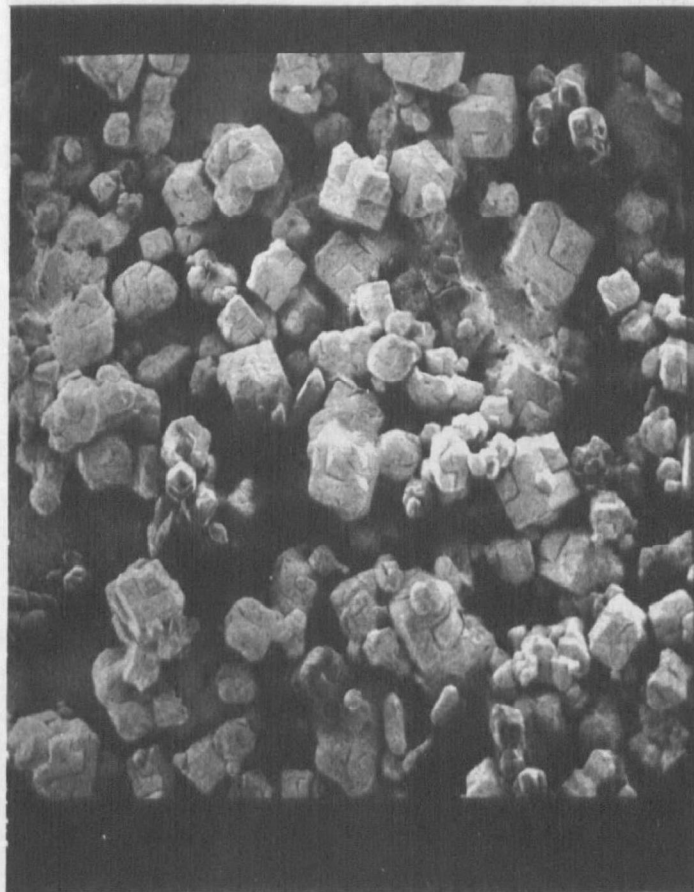


FIGURE 4-8.
ELECTRON MICROGRAPH 100X
OF $\text{MgSO}_3 \cdot 6\text{H}_2\text{O}$ CRYSTALS (HEXAGONAL)
NUCLEATED AT 50°C

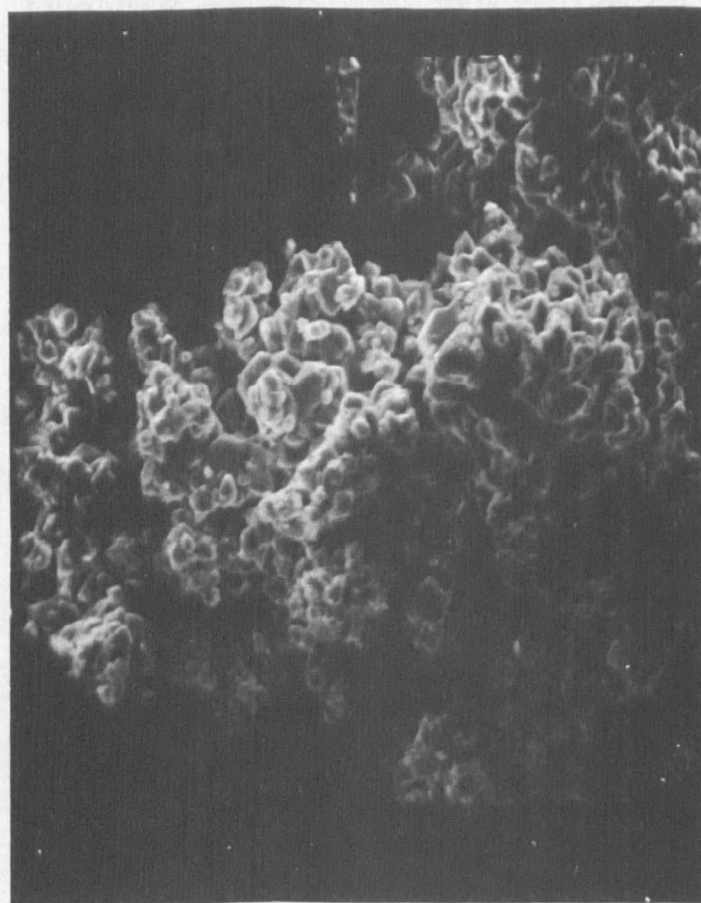


FIGURE 4-9.

ELECTRON MICROGRAPH 1000X
OF $\text{MgSO}_3 \cdot 3\text{H}_2\text{O}$ CRYSTALS
NUCLEATED AT 69°C

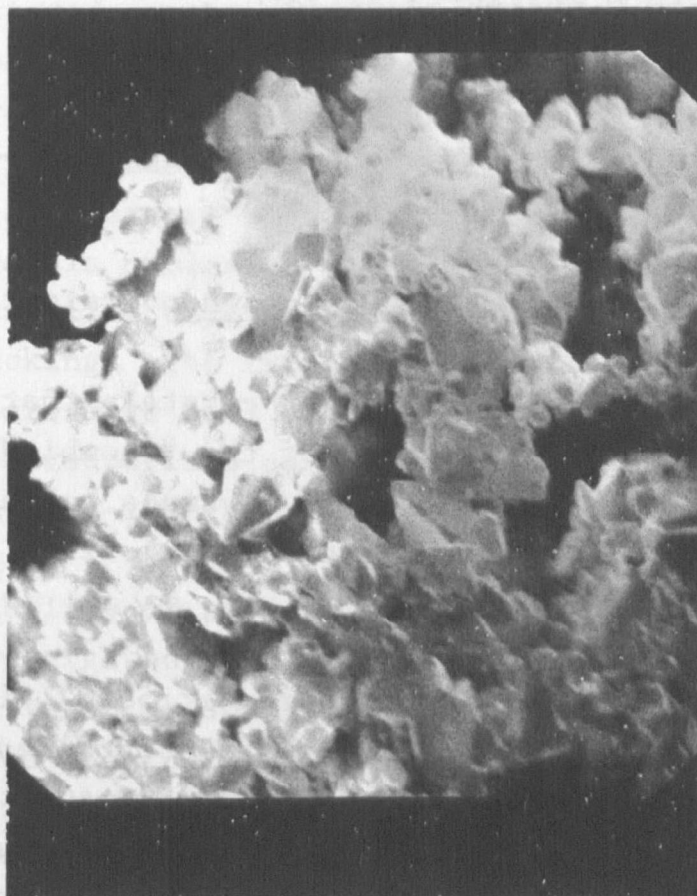


FIGURE 4-10

ELECTRON MICROGRAPH 1000X OF
 $\text{MgSO}_3 \cdot 3\text{H}_2\text{O}$ CRYSTALS NUCLEATED
AND GROWN OVERNIGHT AT 65°C

- (1) $\text{MgSO}_3 \cdot 6\text{H}_2\text{O}$ nucleated at 28°C
- (2) $\text{MgSO}_3 \cdot 6\text{H}_2\text{O}$ nucleated at 50°C
- (3) $\text{MgSO}_3 \cdot 3\text{H}_2\text{O}$ nucleated at 69°C
- (4) $\text{MgSO}_3 \cdot 3\text{H}_2\text{O}$ nucleated and grown overnight at 65°C .

Figure 4-4 shows the $\text{MgSO}_3 \cdot 6\text{H}_2\text{O}$ crystals that were nucleated at 28°C . These crystals are of the "rhombic" habit and are characterized as pyramid shaped crystals having triangular faces and sharp points. Individual crystal sizes vary from 10 to 100 microns.

The $\text{MgSO}_3 \cdot 6\text{H}_2\text{O}$ crystals nucleated at 50°C (Figure 4-5) are typical of the other hexahydrate crystals obtained by nucleation in 20% magnesium sulfate solutions at 40 and 60°C . These crystals are of the "hexagonal" habit and are characterized as box-shaped crystals with raised flat surfaces at the corners. Size variation was 10-100 microns.

The $\text{MgSO}_3 \cdot 3\text{H}_2\text{O}$ crystals nucleated at 69°C were visible only at 400x magnification and no photomicrograph is included here. Larger trihydrate crystals, which were prepared in a separate test by nucleation and overnight growth in a 20% magnesium sulfate solution at 65°C , are shown in Figure 4-6. These crystals (10 microns) are barely distinguishable in this photo.

Electron micrographs of the four samples listed above were also made (Figures 4-7 through 4-10). These film exposures have the advantage of providing a greater depth of field. Some deterioration of the crystals such as a loss of waters of hydration was caused by the electron bombardment and the high vacuum conditions. Gold plating of the crystal samples was performed

in an effort to reduce these effects. Figures 4-7 and 4-8 provide a comparison of the $\text{MgSO}_3 \cdot 6\text{H}_2\text{O}$ crystals nucleated at 28 and 50°C, respectively. Unfortunately, in the case of the "hexagonal" crystal habit, some detail is lost by the rounding of some edges and corners of the box-shaped crystals. The $\text{MgSO}_3 \cdot 3\text{H}_2\text{O}$ crystals nucleated at 69°C are shown in Figure 4-9. Individual micro-sized crystals are noticeable even though the details are lacking. The trihydrate crystals nucleated and grown at 65°C are more well defined. See Figure 4-10. These crystals are characterized as bipyramid shaped crystals with size variation of 1-10 microns in length.

The possibility of sulfate inclusion in the nucleated solids was investigated. In spite of the high magnesium sulfate concentrations, no sulfate content in the crystals was found. Infrared spectra of nucleated magnesium sulfite hexahydrate and trihydrate crystals are shown in Figure 4-11. Sulfate, which would absorb at 1100 cm^{-1} , is absent from these spectra.

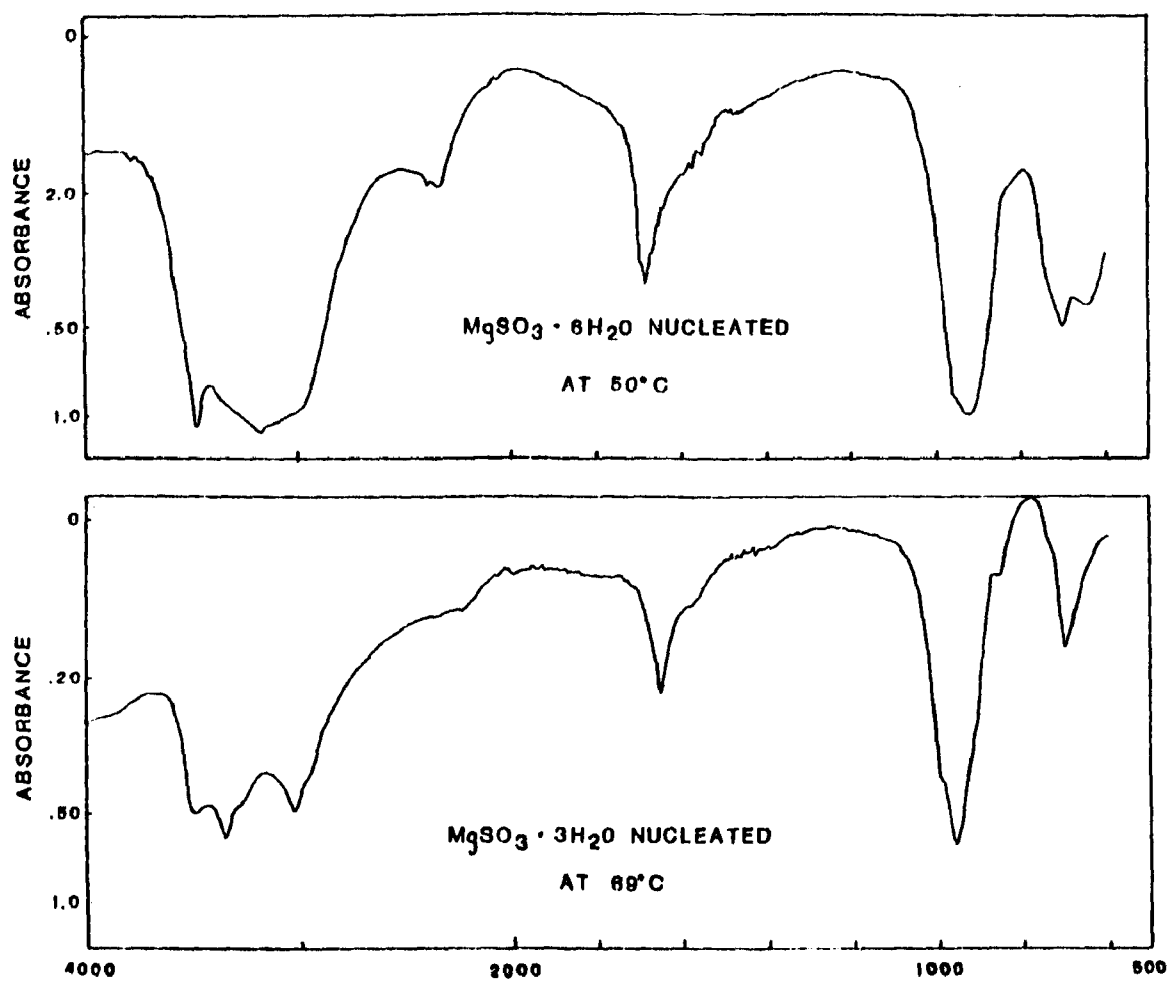


Figure 4-11. Infrared Spectra of Magnesium Sulfite Nucleated at 50°C and 69°C

SECTION 5

CONCLUSION

The magnesium sulfite solids that nucleated from the 20% magnesium sulfate pH 6 solutions consisted of pure $\text{MgSO}_3 \cdot 6\text{H}_2\text{O}$ at 28, 40, 50, and 60°C and pure $\text{MgSO}_3 \cdot 3\text{H}_2\text{O}$ at 69 and 70°C. No hydrate mixtures were observed. The relative saturation values required to cause homogeneous nucleation were approximately 3-4 for $\text{MgSO}_3 \cdot 6\text{H}_2\text{O}$ and approximately 12 for $\text{MgSO}_3 \cdot 3\text{H}_2\text{O}$. Sizes of the nucleated crystals ranged from 1-10 microns for the trihydrate phase and 10-100 microns for the hexahydrate phase of magnesium sulfite.

TECHNICAL NOTE 200-045-54-05

SECONDARY NUCLEATION OF MgSO_3
HYDRATES IN SCRUBBER-LIKE MEDIA

Prepared by:

L. A. Rohlack
R. E. Pyle

CONTENTS

1.	Introduction.	338
2.	Experimental approach	339
	Secondary Nucleation Apparatus	339
	Operational Procedure.	346
	Analytical Methods	348
3.	Experimental Results.	350
	Data Processing.	350
	Results.	352
4.	Discussion of Results	356

FIGURES

<u>Number</u>		<u>Page</u>
2-1	Secondary Nucleation Apparatus	340
2-2	Plexi-Glas Reactor	342
2-3	Continuous pH Monitor.	345
3-1	MgSO ₃ ·6H ₂ O Secondary Nucleation Run #4-3B.	351
3-2	Primary and Secondary Nucleation from 20% MgSO ₄ Solutions and pH 6	355

TABLES

<u>Number</u>		<u>Page</u>
3-1	Secondary Nucleation Experimental Run Data	353
3-2	Secondary Nucleation Experimental Run Data	354

SECTION 1

INTRODUCTION

Radian Corporation has conducted an experimental study to identify, measure, and characterize the formation of magnesium sulfite trihydrate and hexahydrate solids by the phenomenon of secondary nucleation. This study is essential in order to accurately predict conditions necessary for the preferential production of either hydrated phase of MgSO_3 . It was therefore, the objective of this study to:

- determine the onset of secondary nucleation for the trihydrate and hexahydrate phases of MgSO_3 , and
- characterize the influence of temperature and stirring rate on the threshold or onset for secondary nucleation.

This Technical Note presents in detail the experimental approach used and the experimental data obtained from the secondary nucleation kinetics studies on the hexahydrate and trihydrate crystalline phases of MgSO_3 .

SECTION 2

EXPERIMENTAL APPROACH

An experimental secondary nucleation apparatus utilizing a continuous liquid feed, batch-solid system was specially designed and constructed to perform the experimental segment of this study. During one phase of the secondary nucleation of magnesium sulfite trihydrate experiments, a slurry recycle loop was incorporated into the kinetics apparatus. Along with the design of the kinetics apparatus, special consideration was given to both the operational and analytical procedures used during this study in order to ensure that consistent and accurate measurement of all pertinent parameters could be obtained.

Secondary Nucleation Apparatus

The secondary nucleation apparatus used during this study is a crystallization kinetics device from which quantitative measurements can be obtained for correlating the variables of concentration, temperature, and stirrer speed with the secondary nucleation of insoluble solids. With this apparatus, experimental conditions such as reactor temperature, stirring speed, feed stream composition and flowrate can be controlled and varied independently to achieve conditions required for the onset of secondary nucleation.

A schematic diagram of the apparatus is shown in Figure 2-1. The essential components are:

- continuous liquor feed system,
- reactor, and

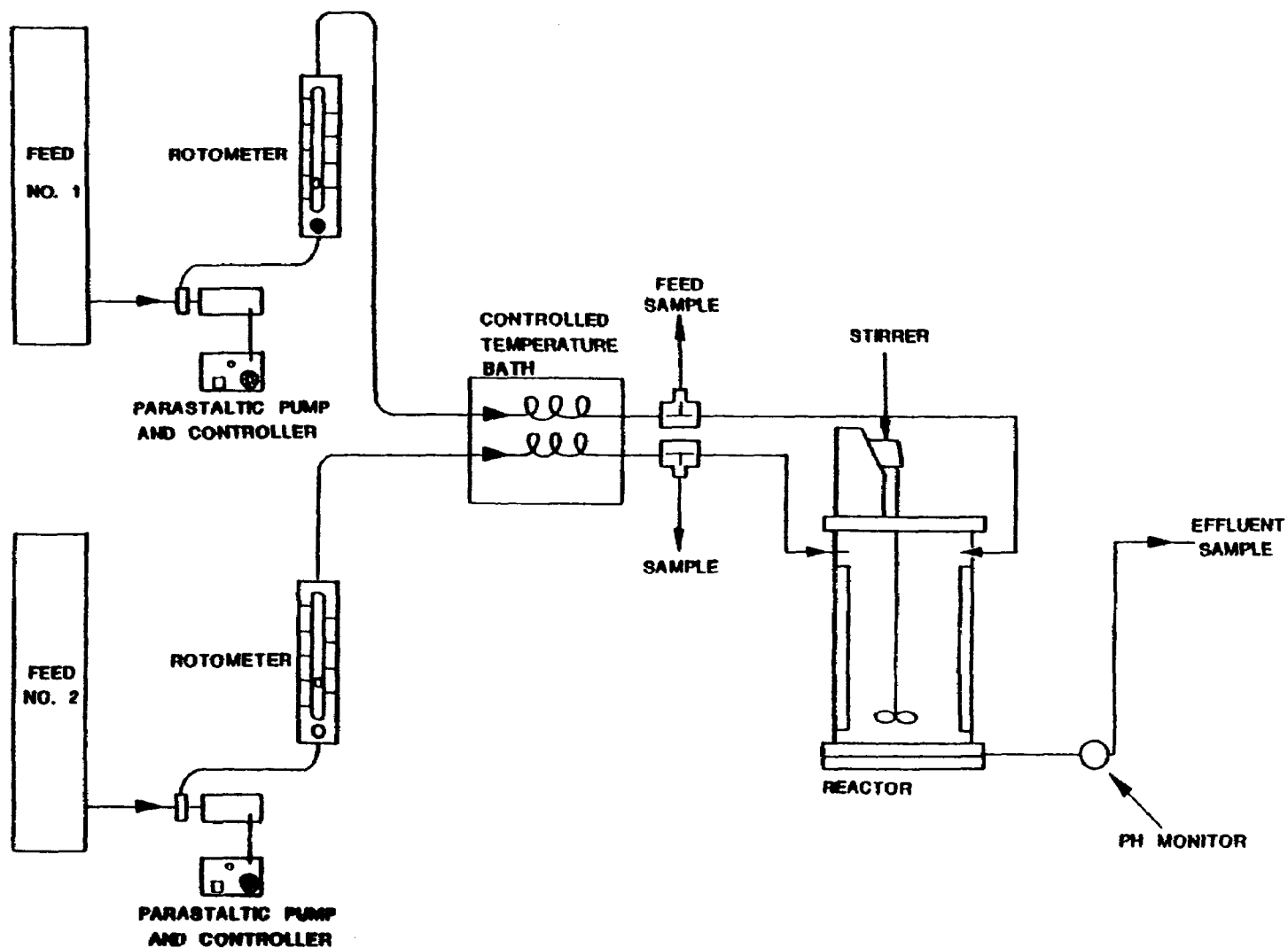


Figure 2-1. Secondary Nucleation Apparatus

- pH monitor.

Continuous Liquor Feed System

The continuous liquid feed system supplies the reactor with two well defined feed streams. Parameters such as liquor composition, flowrate, and temperature can be varied and accurately controlled. Two 60-liter linear polyethylene containers were used to mix and store the feed stream solutions. Peristaltic pumps and controllers were used in transferring the feed streams from the feed tanks to the reactor at accurately controlled flowrates which were easily monitored by an inline rotameter. Before entering the reactor, the feed streams passed through a constant temperature water bath so that the reactor temperature could be varied as desired from 30°C to 68°C. When reactor temperatures in excess of 40°C were desired, the reactor was placed in the temperature-controlled bath to minimize heat loss to the atmosphere. Upon leaving the constant temperature bath the feed streams passed through a three-way stopcock. At this point the feed streams could either go to the reactor or could be diverted to the feed stream sampling points.

Plexiglas Reactor

A specially designed 2750 ml plexiglas reactor, as shown in Figure 2-2, served as the reaction vessel for precipitation and incipient secondary nucleation. The feed streams were input to the reactor at an angle of 180 degrees to each other and directed toward a propeller to insure rapid and thorough mixing of the feed streams. A second propeller near the bottom of the reactor was used to suspend the solids while baffles broke up the circular motion of the liquor to enhance mixing. Oxygen free nitrogen gas could be forced into the top of the reactor to either purge the system of oxygen or force liquor out of the

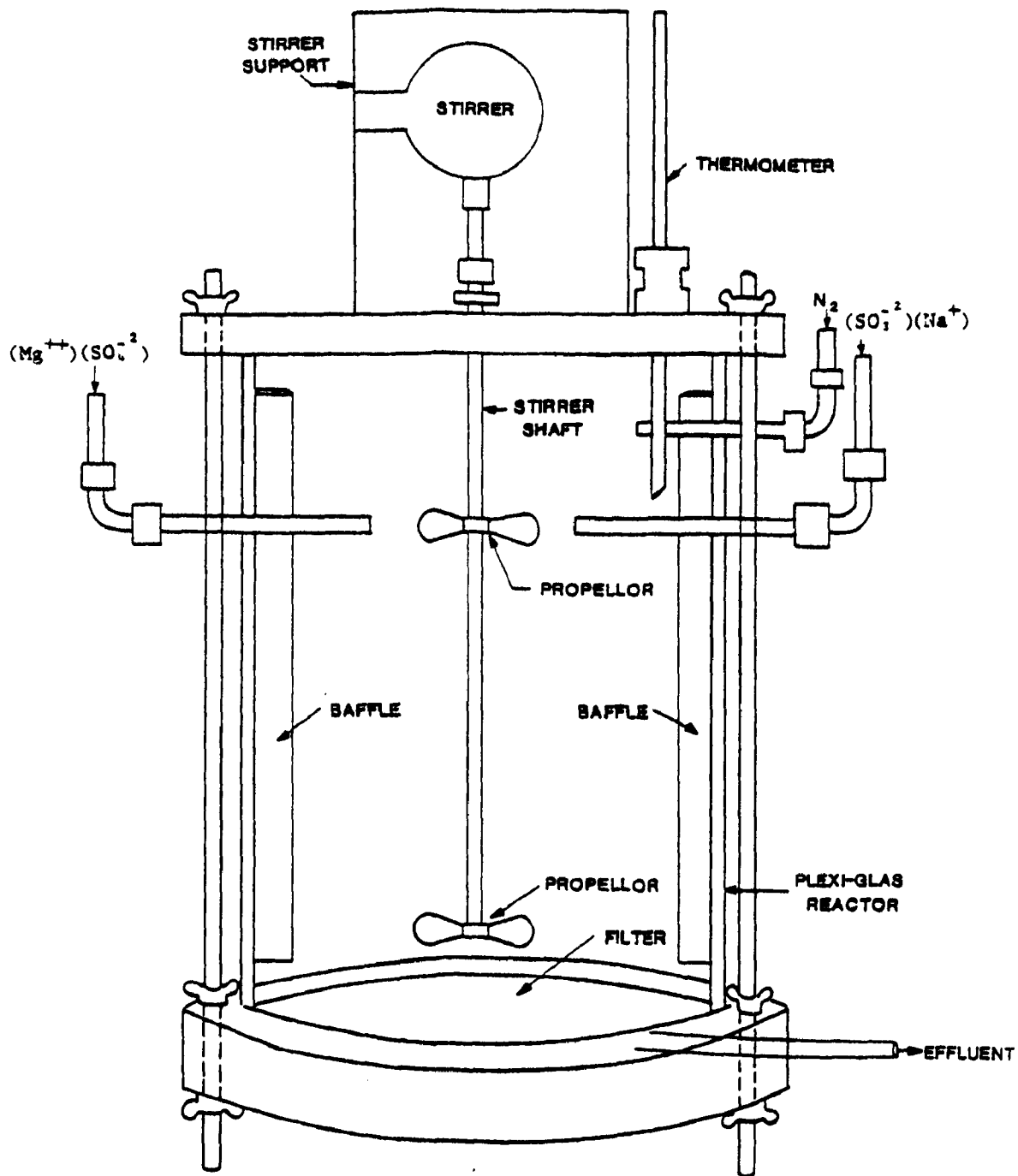


Figure 2-2. Plexi-Glas Reactor

reactor. The reactor liquor temperature was monitored by a thermometer mounted in the top of the reactor. In order to separate the liquor from the solids, a 142 millimeter filter was positioned in the bottom of the reactor. Liquor passing through the filter exited the reactor through a plexiglas tube where it could then be discarded or collected for analysis or storage.

In an attempt to characterize the secondary nucleation of magnesium sulfite trihydrate, a slurry recycle loop was incorporated into the reactor. Slurry was removed from the bottom of the reactor through a plexiglas tube by means of a peristaltic pump. Upon leaving the pump, the slurry was forced through a quick disconnect and then returned to the top portion of the reactor. By incorporating this slurry recycle device, a representative weight percent solids sample could be obtained quickly and easily by collecting a known small volume of slurry at the quick disconnect.

pH Monitor

As the effluent stream left the reactor, its pH was monitored either continuously or intermittently depending upon the characteristics of the liquor. During preliminary magnesium sulfite hexahydrate ($\text{MgSO}_3 \cdot 6\text{H}_2\text{O}$) secondary nucleation runs, in which the reactor temperature was less than 40° Centigrade, a continuous pH monitoring system was used to closely monitor the pH of the effluent stream. This type of pH monitoring system proved to be an efficient means of obtaining accurate effluent pH values at low sample temperatures.

During runs made at temperatures greater than 40° Centigrade an intermittent pH sampling system was used. The intermittent system proved suitable for obtaining accurate pH values at higher reaction temperatures.

Continuous pH Monitor

The continuous pH monitor, Figure 2-3, was designed to provide a means for obtaining accurate pH values with minimal operator effort. Effluent liquor entered the top of a 100 milliliter three-necked flask by means of a glass tube which extended down into the flask to just above the stirrer. A small magnetic stirring bar was used to thoroughly mix the liquor assuring a homogeneous sample was being monitored. pH electrodes were tightly fitted in both of the side ports of the flask and the electrodes extended below the surface of the liquor, insuring proper liquor to electrode contact. Liquor left the monitor by means of a glass tube which extended only slightly down into the flask. The pH meter could be left on for continuous monitoring of the effluent or the pH meter could be turned on and off for occasional monitoring of the pH.

Intermittent pH Monitor

Whenever the reactor temperature was less than 40° Centigrade, the above pH monitoring system was used because the reactor temperature and pH monitor sample temperature were essentially the same. When reactor temperatures above 40°C were required, the continuous pH monitor proved to be an unsuitable means for sample pH measurement because of temperature differences from reactor to sample. Therefore, an intermittent pH monitor was used to give accurate pH measurements of reactor solutions at temperatures above 40° Centigrade. A small 50 milliliter beaker served as the collection device. In the bottom of the beaker a small stirring bar maintained a homogeneous solution while two pH electrodes submerged in the liquor monitored the pH. Because of the small size of the collection device, the time required to obtain an accurate pH value was minimal, allowing little or no temperature change in the effluent temperature during pH monitoring. During a run, pH values were generally obtained during the collection of

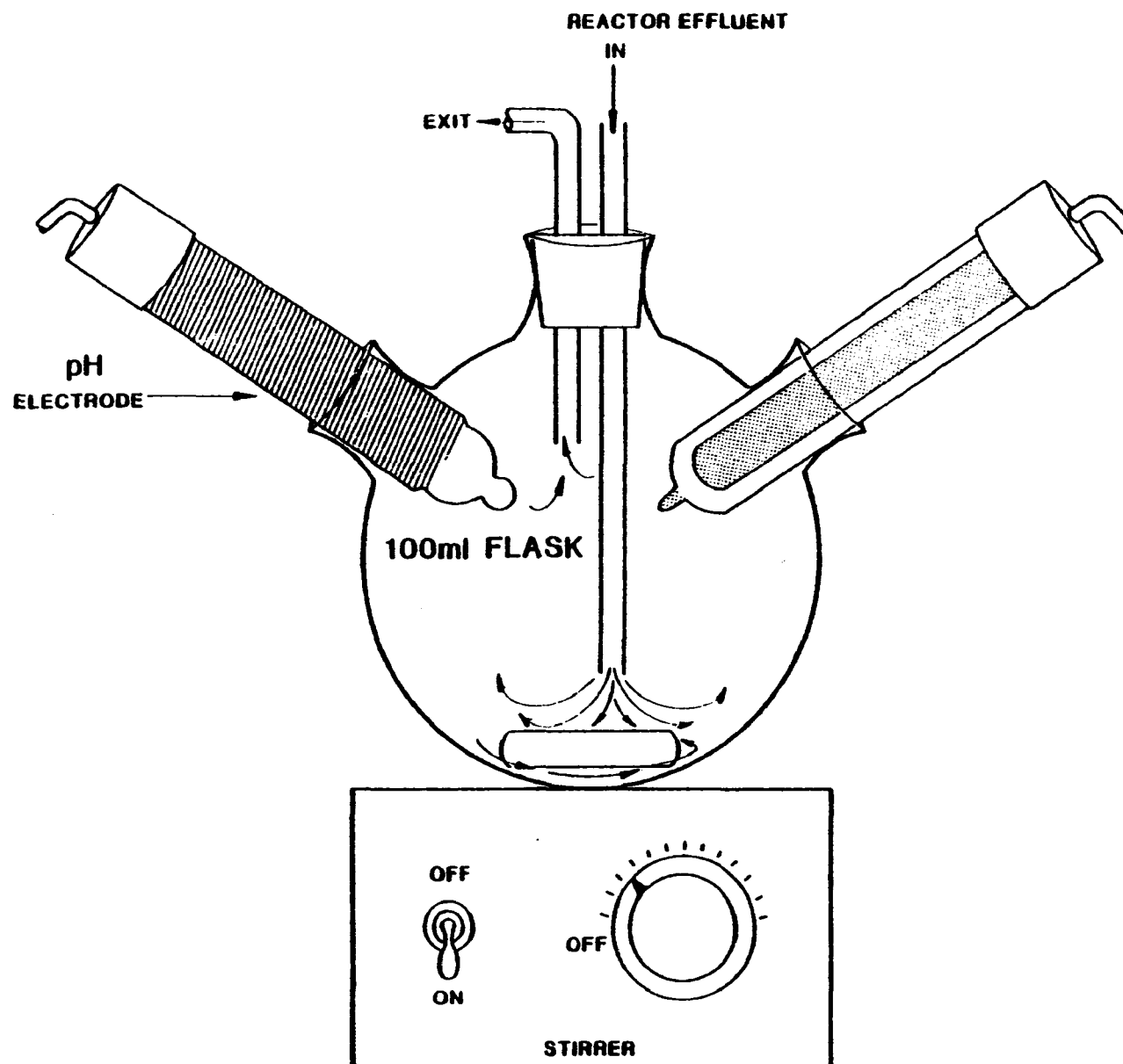


Figure 2-3. Continuous pH Monitor

aqueous sulfite samples.

OPERATIONAL PROCEDURE

In this section the operational procedures used in performing the secondary nucleation experiments for both the hexahydrate and trihydrate forms of magnesium sulfite are discussed. All of the operational procedures used during this segment of the program were developed to minimize undesirable changes in either the solid or liquid phases within the feed tanks, transfer lines, or reactor. Steps were also taken to ensure maximum ease of operation during the kinetics run to enable the operator to concentrate on the progress of the experiment. For a given set of operating conditions, the following operational procedures were developed to fulfill the objectives of the run.

Initially, the temperature bath was turned on and the proper temperature setting selected. Then the two feed tanks were thoroughly cleaned and filled with the appropriate quantity of deionized water. In order to minimize oxidation during a run, oxygen free nitrogen gas was bubbled through the feed tanks, thus purging any dissolved oxygen from the deionized water and forming a blanket of inert nitrogen gas above the water. This protective blanket of nitrogen gas also minimized the chances of air to liquid contact when the liquid level decreased during the run.

During the purging with nitrogen gas, there was sufficient time to thoroughly clean the reactor. All foreign material was removed by first rinsing the reactor with a dilute HCl solution which helped loosen and dissolve any scale which may have formed during the previous run. After sufficient HCl solution had been rinsed through the reactor, a sufficient amount of deionized water was used to finish cleaning out the reactor. After rinsing, the reactor was examined for physical abnormalities which were

corrected before final assembly of the unit. Oxygen-free nitrogen gas was used to purge any oxygen in the reactor prior to the run. After final inspection of the reactor, the proper quantities of chemicals were added to the already purged feed tanks. Then, depending on the amount of agitation required to completely dissolve the chemicals in the feed tanks, either manual stirring or a laboratory stirrer was used to agitate the liquor. A flotation lid was used whenever possible to minimize liquid-air contact and a plexiglas lid was kept on top of the feed tanks at all times in order to keep out foreign particles and also minimize any air turbulence above the flotation lid.

After the feed tanks were properly prepared and the reactor was ready for use, feed stream flow rates were set and feed stream samples were taken. The peristaltic pumps used to control the flowrates of the two feed streams were turned on and flow was diverted to the sample ports. Rotameters gave an accurate indication of the flowrate and were used to maintain a constant feed stream flow throughout the course of the run. By adjusting the peristaltic pump controller, the flowrate could be adjusted and controlled. The rotameters were calibrated routinely prior to each run by collecting a certain volume of sample in a specified time. After a certain feed stream flowrate was obtained, feed stream samples were collected in the proper collection medium for storage or analysis.

Next, the magnesium sulfate flow was diverted back into the reactor and the reactor was allowed to fill approximately 80% full with the magnesium sulfate feed. The reactor stirrer was turned on and a stirring rate set by adjusting the variac. For the majority of the runs the stirring rate was maximum (~ 1200 RPM), allowing for optimum agitation of reactor contents. A stirring speed of ~ 1000 RPM (variac set at 85) was used during

those runs designed to study the effect of stirring speed on secondary nucleation. Next, a solution containing approximately 0.5 molar sodium sulfite was added to the reactor in order to obtain an initial reactor sulfite concentration of .1 molar. Just before the reactor was completely filled, a known quantity of seed crystals was added to the agitated liquor. For most of the runs one gram of seed crystals was used, but during some of the magnesium sulfite trihydrate runs 10 grams of seed crystals were used in order to help clarify secondary nucleation of the trihydrate phase. After the seed crystals were added, the thermometer was positioned. As soon as the reactor was filled with the .5 molar sulfite solution, the stirrer fitting was tightened and the feed streams were diverted into the reactor. At this time the run was officially started.

During all of the runs, several operational variables were monitored in order to maintain a constant set of working conditions. Feed stream flowrates were kept at a constant rate by a visual check of the flowrate as indicated by the rotameter. A thermometer in the top of the reactor allowed for the continuous monitoring of reactor temperature. Adjustments in reactor temperature could be made by adjusting the reactor bath temperature, but after several runs the temperature bath setting required for a certain reactor temperature was accurately known. For the most part, adjustments were seldom required in either the feed stream flowrate or the reactor temperature during a run. This ease of operation allowed the operator to more closely monitor the approach and occurrence of secondary nucleation.

ANALYTICAL METHODS

In this section, a brief outline of the analytical methods used in the MgSO_3 hydrate secondary nucleation studies is given.

- Magnesium - colorimetric titration with Na_2EDTA or dilution preparation and atomic absorption determination;
- Sulfite - iodine-buffer preparation and back titration with standard arsenite or thiosulfate;
- Sulfate - peroxide oxidation of sulfite, hydrogen ion exchange, and titration with standard sodium hydroxide. Sulfate is calculated as the difference between total sulfur and sulfite sulfur;
- Sodium - dilution preparation and atomic absorption determination; and
- Chloride - potentiometric titration with standard silver nitrate.

SECTION 3

EXPERIMENTAL RESULTS

DATA PROCESSING

The onset of secondary nucleation of magnesium sulfite hexahydrate is relatively easy to detect by monitoring the effluent sulfite concentration. Also, because of the substantial increase in the particle number density that accompanies secondary nucleation, a visual change in reactor opacity indicates to the operator that secondary nucleation of the hexahydrate crystalline phase has occurred. Because of the substantially slower growth rate of the magnesium sulfite trihydrate phase the detection of secondary nucleation of this phase by either monitoring the sulfite concentration or by visual means was not possible.

Detection of Secondary Nucleation of Magnesium Sulfite Hexahydrate

By closely monitoring the effluent sulfite concentration during an experimental run, one can determine accurately the onset of secondary nucleation of magnesium sulfite hexahydrate. By plotting the effluent sulfite concentration versus time one can accurately determine the sulfite concentration and thus the complete reactor solution composition at the onset of secondary nucleation.

Figure 3-1 shows a typical plot of effluent sulfite concentration versus time for a MgSO_3 hexahydrate secondary nucleation run. The onset of a secondary nucleation is taken at the maximum experimental sulfite concentration.

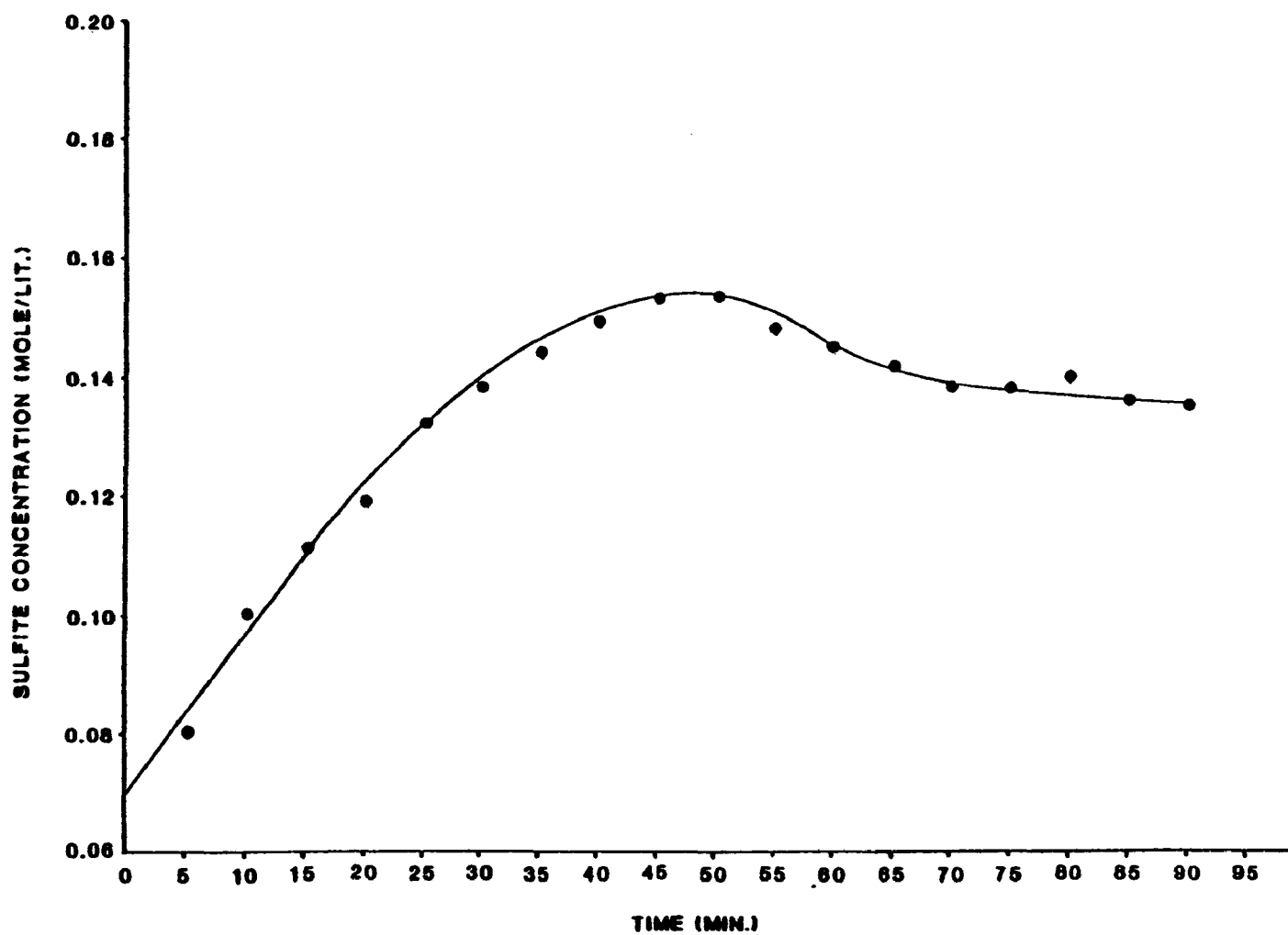


Figure 3-1. $\text{MgSO}_3 \cdot 6\text{H}_2\text{O}$ Secondary Nucleation Run # 4-3B

Detection of Secondary Nucleation of Magnesium Sulfite Trihydrate

Because of the substantially slower growth rate of the magnesium sulfite trihydrate phase, the detection of the onset of secondary nucleation by this batch solid-flow through liquid experimental technique was not possible. Other experimental techniques were tried in an effort to characterize trihydrate secondary nucleation as a function of temperature. A variable temperature batch-solid - batch-liquid experimental method was tried, as well as experiments using the batch-solid flow through liquid crystallizer with added slurry recycle loop. Both techniques rely on a change in the system weight percent solids as a function of time or temperature as a means of detecting the onset of secondary nucleation of trihydrate. These techniques, however, also proved unsuccessful.

RESULTS

Experimental results for the secondary nucleation kinetics studies on $\text{MgSO}_3 \cdot 6\text{H}_2\text{O}$ have been summarized in Tables 3-1 and 3-2. The activity products were calculated by inputting the pertinent reaction solution information such as concentrations of magnesium, sodium, sulfite, and sulfate; pH and temperature into the Radian chemical equilibrium computer program.

In Figure 3-2, a plot of y , where $y = a \cdot p \cdot 6 / a^3 \text{H}_2\text{O}$, is shown versus temperature. The secondary nucleation data for hexahydrate is plotted along with the primary nucleation data obtained previously for MgSO_3 hexahydrate and trihydrate (see Technical Note #200-045-54-04). The results of reduced stirrer speed hexahydrate kinetics runs are also plotted in Figure 3-2.

TABLE 3-1. SECONDARY NUCLEATION EXPERIMENTAL RUN DATA*

Run	Type Seed	Stirring Speed (RPM)	Temp. (°C)	pH	[Mg ⁺²]	[Na ⁺]	[SO ₄ ⁻²]	[SO ₃ ⁻²]
4-3B	MgSO ₃ •6H ₂ O	1200	30.0	6.03	2.07	.390	2.10	.195
4-4B	MgSO ₃ •6H ₂ O	1200	44.4	6.03	2.11	.690	2.14	.345
4-7B	MgSO ₃ •6H ₂ O	1200	46.0	6.0	2.04	.678	2.07	.339
4-8B	MgSO ₃ •6H ₂ O	1200	45.0	5.96	1.97	.704	2.00	.352
4-9B	MgSO ₃ •6H ₂ O	1200	33.6	5.75	1.96	.554	1.99	.277
4-10B	MgSO ₃ •6H ₂ O	1000	32.6	6.10	1.93	.514	1.96	.257
4-11B	MgSO ₃ •6H ₂ O	1000	32.5	6.13	1.97	.526	2.00	.263
4-12B	MgSO ₃ •6H ₂ O	1200	60.5	6.25	1.91	1.136	1.94	.568
4-12B	MgSO ₃ •6H ₂ O	1200	60.5	6.25	1.91	1.060	1.94	.530
4-12B	MgSO ₃ •6H ₂ O	1200	60.5	6.25	2.07	1.154	2.10	.577
4-12B	MgSO ₃ •6H ₂ O	1200	60.5	6.25	2.07	1.076	2.10	.538
4-13B	MgSO ₃ •6H ₂ O	1200	59.2	6.27	2.02	1.038	2.05	.519
4-14B	MgSO ₃ •6H ₂ O	1000	58.3	6.28	1.96	1.062	1.99	.531

* All analyses are reported in millimoles/liter.

TABLE 3-2. SECONDARY NUCLEATION EXPERIMENTAL RUN DATA*

Run No.	a Mg ⁺²	a SO ₃ ⁻²	a H ₂ O	K sp ₆	ap ₆	Rel. Sat. ₆	y
4-3B	3.349-01	7.276-04	0.939	6.124-05	1.670-04	2.727	2.019-04
4-4B	3.182-01	1.012-03	0.9312	7.62-05	2.100-04	2.756	2.600-04
4-7B	2.955-01	1.322-03	0.9339	7.86-05	2.59-04	3.295	3.18-04
4-8B	2.900-01	1.021-03	0.9345	7.735-05	1.97-04	2.547	2.417-04
4-9B	3.034-01	7.898-04	0.9380	6.45-05	1.632-04	2.530	1.978-04
4-10B	2.935-01	1.053-03	0.9401	6.35-05	2.13-04	3.354	2.568-04
4-11B	3.006-01	1.087-03	0.9388	6.34-05	2.24-04	3.533	2.702-04
4-12B	2.498-01	1.754-03	0.9263	9.78-05	2.77-04	2.83	3.489-04
4-12B	2.531-01	1.612-03	0.9281	9.78-05	2.61-04	2.669	3.262-04
4-12B	2.798-01	1.657-03	0.9215	9.78-05	2.838-04	2.902	3.627-04
4-12B	2.833-01	1.521-03	0.9234	9.78-05	2.67-04	2.730	3.393-04
4-13B	2.749-01	1.544-03	0.9257	9.60-05	2.67-04	2.781	3.368-04
4-14B	2.621-01	1.670-03	0.9268	9.48-05	2.77-04	2.922	3.484-04

* All analyses are reported in millimoles/liter.

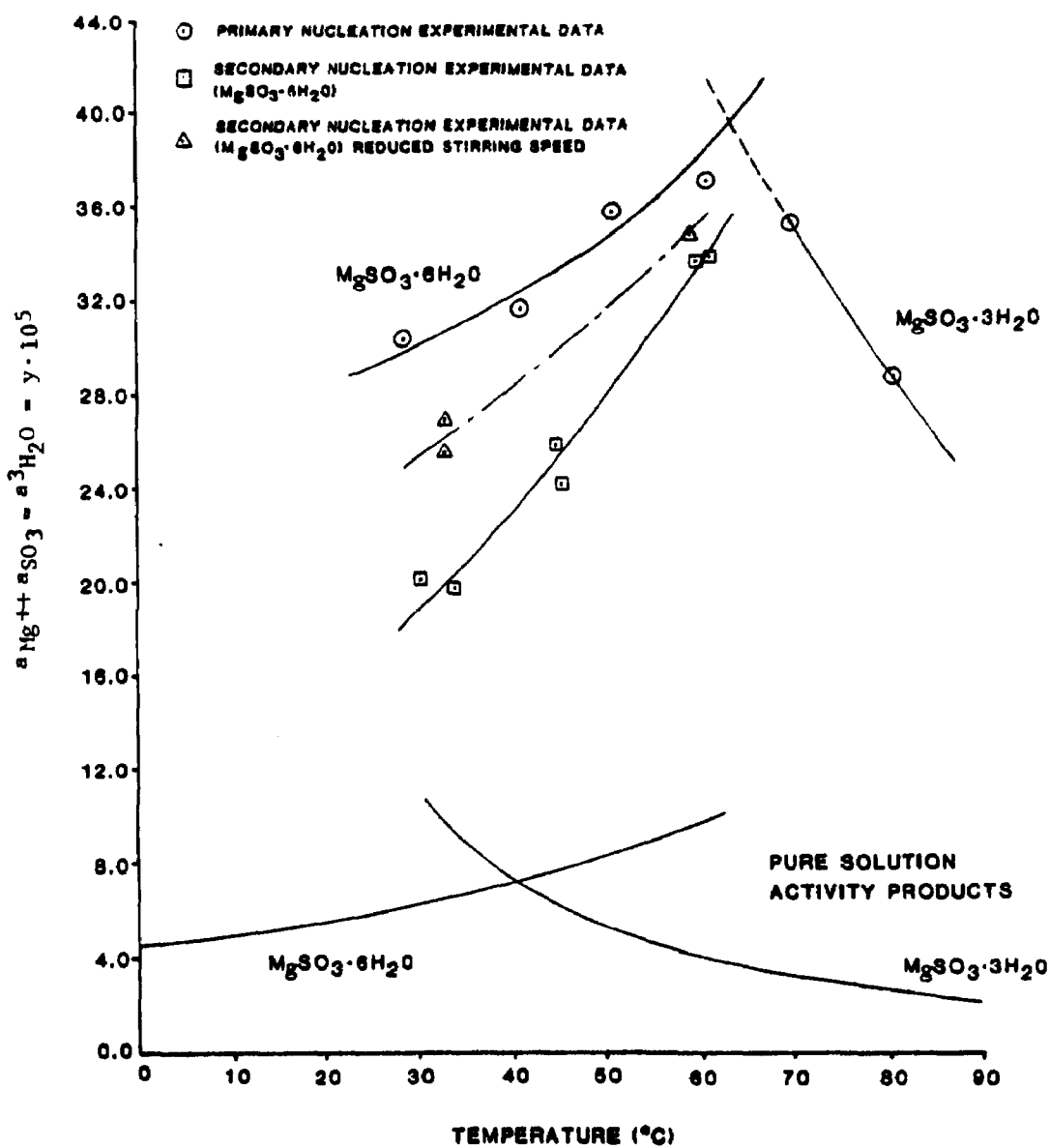


Figure 3-2. Primary and Secondary Nucleation From 20% MgSO_4 Solutions and pH 6

02-2296-1

SECTION 4

DISCUSSION OF RESULTS

As can be seen from Figure 3-2, a stirring speed effect was observed in the hexahydrate secondary nucleation kinetics results. The slower stirring speed means that a lower impact energy is imparted to the crystals, and thus a higher solution supersaturation (i.e., larger activity product) is required to reach the onset of secondary nucleation. In the limit of zero stirring speed, the onset of secondary nucleation will be coincident with the onset of primary nucleation.

TECHNICAL NOTE 200-045-54-06

ADDITIVE EXPERIMENTS ON TRIHYDRATE
KINETICS

Prepared by:

J. L. Skloss

CONTENTS

1. Introduction.	359
2. Experimental.	360
3. Experimental Results.	361
Bibliography	367

TABLES

<u>Number</u>		<u>Page</u>
1	Effect of 50 ppm Additive of the Nucleation and Precipitation of $\text{MgSO}_3 \cdot 3\text{H}_2\text{O}$ at 55°C and pH 8.5 . .	363
2	Effect of 50 ppm Additive on the Nucleation and Precipitation of $\text{MgSO}_3 \cdot 3\text{H}_2\text{O}$ in High Sulfite Solutions at 55°C and pH 6.1	364
3	Effect of 50 ppm Additive on the Precipitation of $\text{MgSO}_3 \cdot 3\text{H}_2\text{O}$ at 55°C and pH 8.2 Using Seed	365
4	Effect of 50 ppm Additive on the Precipitation of $\text{MgSO}_3 \cdot 3\text{H}_2\text{O}$ in 20% MgSO_4 Solution at 55°C and pH 6.1 Using Seed	366

SECTION 1

INTRODUCTION

The removal of sulfur dioxide from flue gases involves the precipitation of magnesium sulfite hydrate solids in the magnesium oxide system. Typical scrubber solutions are supersaturated with respect to magnesium sulfite at the normal operating temperature of 55°C. $\text{MgSO}_3 \cdot 3\text{H}_2\text{O}$ is the stable phase under these conditions, and any enhancement of the normally slow precipitation rate of $\text{MgSO}_3 \cdot 3\text{H}_2\text{O}$ would be an advantage to the scrubber operation.

One method of potentially modifying the precipitation rate is the use of metal cations of high ionic charge as additives (SH-021). The purpose of this study is to investigate the effect of these various additives on the precipitation and nucleation kinetics of $\text{MgSO}_3 \cdot 3\text{H}_2\text{O}$. This Technical Note reports the experimental results of this study.

SECTION 2

EXPERIMENTAL

Separate 55°C solutions of magnesium chloride or magnesium sulfate and sodium sulfite were prepared and were mixed together. 500-ml portions were transferred into erlenmeyer flasks, and the flasks were immersed in a common 55°C water bath. Magnesium, sulfite, and pH measurements were made. To study additive effects on precipitation rate, 0.16g of pure $\text{MgSO}_3 \cdot 3\text{H}_2\text{O}$ seed was added to each flask. Then 50 ppm of various additives were added to the test flasks, and the effects were compared with the control flask which contained no additive. Each flask contained a magnetic stir bar which was powered by a separate magnetic stirrer located below the water bath. The flasks were sealed with rubber stoppers, and the solutions were stirred continuously for 48 hours. The solutions were supersaturated with respect to magnesium sulfite at 55°C, and $\text{MgSO}_3 \cdot 3\text{H}_2\text{O}$ solids were nucleated or precipitated during this period. The slurries were filtered, and the solids were washed, dried, and weighed.

SECTION 3

EXPERIMENTAL RESULTS

The results of the additive experiments are presented in Tables 1-4.

Table 1

The precipitated solids were slightly colored by the additive agents, but the chemical analyses showed that the solids were nearly pure $\text{MgSO}_3 \cdot 3\text{H}_2\text{O}$. No substantial change of the additive in the solution was found. Urea addition had no effect.

Table 2

PH lowered to 6.1.

Table 3

Additive agents had no effect, except for Co which caused some of the seed crystals to dissolve. The Co complex with SO_3^{-2} is probable.

Table 4

Scrubber condition of 20% MgSO_4 and pH 6. Additives had no effect except for Co which caused a negative effect on the precipitation of $\text{MgSO}_3 \cdot 3\text{H}_2\text{O}$.

It is observed that all of the additives except urea appear to enhance the rate of growth of $\text{MgSO}_3 \cdot 3\text{H}_2\text{O}$ in those experiments

without the addition of seed material; that is, nucleation. The additives appear to have no enhancement effect on the precipitation rate of $\text{MgSO}_3 \cdot 3\text{H}_2\text{O}$.

TABLE 1. EFFECT OF 50 PPM ADDITIVE OF THE NUCLEATION AND
PRECIPITATION OF $\text{MgSO}_3 \cdot 3\text{H}_2\text{O}$ AT 55°C AND pH 8.5.

Initial Mg^{++} mole/l	Initial $\text{SO}_3^{=}$ mole/l	50 ppm Additive used	$\text{MgSO}_3 \cdot 3\text{H}_2\text{O}$ ppt'd, g/l
0.134	0.135	Al^{+3} as AlCl_3	4.2
0.147	0.124	Cr^{+6} as CrO_3	2.0
0.145	0.132	Cr^{+3} as $\text{Cr}_2(\text{SO}_4)_3$	1.3
0.147	0.133	Co^{++} as CoCl_2	3.2
0.145	0.137	urea	0.10
0.135	0.137	none	0.10

$$\text{Rel. Sat.} = a.p._3 / K_{sp_3} = 1.5$$

TABLE 2. EFFECT OF 50 PPM ADDITIVE ON THE NUCLEATION AND
PRECIPITATION OF $\text{MgSO}_3 \cdot 3\text{H}_2\text{O}$ IN HIGH SULFITE
SOLUTIONS AT 55°C AND pH 6.1.

Initial Mg^{++} mole/l	Initial $\text{SO}_3^{=}$ mole/l	50 ppm Additive used	$\text{MgSO}_3 \cdot 3\text{H}_2\text{O}$ ppt'd, g/l
0.174	1.48	Al^{+3} as AlCl_3	0.2
0.174	1.48	Cr^{+6} as CrO_3	1.0
0.174	1.48	Cr^{+3} as $\text{Cr}_2(\text{SO}_4)_3$	0.4
0.174	1.48	Co^{++} as CoCl_2	0.2
0.174	1.48	none	0.05
Rel. Sat. = 2.3			

TABLE 3. EFFECT OF 50 PPM ADDITIVE ON THE PRECIPITATION
OF $\text{MgSO}_3 \cdot 3\text{H}_2\text{O}$ AT 55°C AND pH 8.2 USING SEED.

Initial Mg^{++} mole/l	Initial SO_3^- mole/l	50 ppm Additive used	$\text{MgSO}_3 \cdot 3\text{H}_2\text{O}$ ppt'd, g/l
0.139	0.130	Al^{+3} as AlCl_3	0.76
0.140	0.135	Cr^{+6} as CrO_3	0.77
0.132	0.132	Cr^{+3} as $\text{Cr}_2(\text{SO}_4)_3$	0.81
0.137	0.137	Co^{++} as CoCl_2	0
0.132	0.132	urea	0.69
0.141	0.132	none	0.76

Rel. Sat = 1.5

Amount of seed used was 0.32 g $\text{MgSO}_3 \cdot 3\text{H}_2\text{O}$ per l. g/l $\text{MgSO}_3 \cdot 3\text{H}_2\text{O}$ precipitated are in excess of the seed.

TABLE 4. EFFECT OF 50 PPM ADDITIVE ON THE PRECIPITATION
OF $\text{MgSO}_3 \cdot 3\text{H}_2\text{O}$ IN 20% MgSO_4 SOLUTION AT 55°C
AND pH 6.1 USING SEED.

Initial Mg^{++} mole/l	Initial SO_3^{--} mole/l	50 ppm Additive used	$\text{MgSO}_3 \cdot 3\text{H}_2\text{O}$ ppt'd, g/l
2.2	0.30	Cr^{+6} as $\text{K}_2\text{Cr}_2\text{O}_7$	17.8
2.2	0.30	Co^{++} as CoCl_2	4.1
2.2	0.30	Ni^{++} as NiCl_2	22.8
2.2	0.30	Cu^{++} as CuCl_2	19.1
2.2	0.30	Zn^{++} as ZnSO_4	21.8
2.2	0.30	none	22.2

Amount of seed used was 0.32g $\text{MgSO}_3 \cdot 3\text{H}_2\text{O}$ per l. g/l $\text{MgSO}_3 \cdot 3\text{H}_2\text{O}$
precipitated are in excess of the seed.

BIBLIOGRAPHY

- SH-021 Shor, Steven M., Effects of Surfactants and Inorganic Additives on Nucleation Kinetics in Mixed Suspension Crystallization. PhD. Thesis, Iowa State University, 1970.

TECHNICAL REPORT DATA
(Please read Instructions on the reverse before completing)

1. REPORT NO. EPA-600/7-77-109		2.		3. RECIPIENT'S ACCESSION NO.	
4. TITLE AND SUBTITLE Precipitation Chemistry of Magnesium Sulfite Hydrates in Magnesium Oxide Scrubbing				5. REPORT DATE September 1977	
				6. PERFORMING ORGANIZATION CODE	
7. AUTHOR(S) Philip S. Lowell, Frank B. Meserole, and Terry B. Parsons				8. PERFORMING ORGANIZATION REPORT NO.	
9. PERFORMING ORGANIZATION NAME AND ADDRESS Radian Corporation 8500 Shoal Creek Boulevard Austin, Texas 78766				10. PROGRAM ELEMENT NO. EHE528	
				11. CONTRACT/GRANT NO. 68-02-1319, Tasks 36 and 54	
12. SPONSORING AGENCY NAME AND ADDRESS EPA, Office of Research and Development Industrial Environmental Research Laboratory Research Triangle Park, NC 27711				13. TYPE OF REPORT AND PERIOD COVERED Task Final; 7/75-12/76	
				14. SPONSORING AGENCY CODE EPA/600/13	
15. SUPPLEMENTARY NOTES IERL-RTP Task Officer for this report is Charles J. Chatlyne, Mail Drop 61, 919/541-2915.					
16. ABSTRACT The report gives results of laboratory studies defining the precipitation chemistry of MgSO₃ hydrates. The results apply to the design of Mg-based scrubbing processes for SO₂ removal from combustion flue gas. In Mg-based scrubbing processes, MgSO₃ precipitates as either trihydrate or hexahydrate. The hydrate formed depends on equipment design and operating conditions. Theoretical prediction, verified experimentally, indicated that MgSO₃ trihydrate is the thermodynamically stable hydrate formed at scrubbing process conditions. MgSO₃ hexahydrate is formed as a metastable solid due to kinetic phenomena. Nucleation and crystal growth rates are much faster for hexahydrate than for trihydrate. The time scales observed in kinetic experiments at scrubbing process conditions are: hexahydrate precipitation (10's of minutes), hexahydrate dissolution and trihydrate precipitation (100's of minutes), and attainment of trihydrate equilibrium (1000's of minutes). Nucleation plays a dominant role in the formation of trihydrate solids. These results indicate that Mg-based scrubbing process can be designed to precipitate a majority of either hydrate form. Important design variables include scrubbing liquor composition and temperature, seed crystal composition, slurry volume, equipment residence times, and energy inputs to the slurry that influence nucleation.					
17. KEY WORDS AND DOCUMENT ANALYSIS					
a. DESCRIPTORS		b. IDENTIFIERS/OPEN ENDED TERMS		c. COSATI Field/Group	
Air Pollution Magnesium Oxides Scrubbers Magnesium Inorganic Compounds Hydrates		Precipitation (Chemistry) Desulfurization Flue Gases Combustion Nucleation		Air Pollution Control Stationary Sources Magnesium Sulfite Hydrates	
				13B 07B 07A 07D 21B	
18. DISTRIBUTION STATEMENT Unlimited		19. SECURITY CLASS (This Report) Unclassified		21. NO. OF PAGES 374	
		20. SECURITY CLASS (This page) Unclassified		22. PRICE	